THE NATIONAL ACADEMIES PRESS

SHARE   f   t   in   ✉

Nondestructive Testing to Identify Delaminations Between HMA Layers, Volume 4 - Uncontrolled Evaluation Reports

DETAILS

BUY THIS BOOK

FIND RELATED TITLES

AUTHORS

Heitzman, Michae;l Maser, Kenneth; Tran, Nam H.; Brown, Ray; Bell, Haley; Holland, Steve; Ceylan, Halil; Belli, Kimberly; and Hiltunen, Dennis

Visit the National Academies Press at **NAP.edu** and login or register to get:

– Access to free PDF downloads of thousands of scientific reports
– 10% off the price of print titles
– Email or social media notifications of new titles related to your interests
– Special offers and discounts

The Second
STRATEGIC HIGHWAY RESEARCH PROGRAM

SHRP 2 REPORT S2-R06D-RW-4

Nondestructive Testing to Identify Delaminations Between HMA Layers

Volume 4

MICHAEL HEITZMAN

KENNETH MASER

NAM H. TRAN

RAY BROWN

HALEY BELL

STEVE HOLLAND

HALIL CEYLAN

KIMBERLY BELLI

DENNIS HILTUNEN

National Center for Asphalt Technology at Auburn University
Alabama

TRANSPORTATION RESEARCH BOARD

Subscriber Categories

Construction
Highways
Maintenance and Preservation
Pavements

The Second Strategic Highway Research Program

America's highway system is critical to meeting the mobility and economic needs of local communities, regions, and the nation. Developments in research and technology—such as advanced materials, communications technology, new data collection technologies, and human factors science—offer a new opportunity to improve the safety and reliability of this important national resource. Breakthrough resolution of significant transportation problems, however, requires concentrated resources over a short time frame. Reflecting this need, the second Strategic Highway Research Program (SHRP 2) has an intense, large-scale focus, integrates multiple fields of research and technology, and is fundamentally different from the broad, mission-oriented, discipline-based research programs that have been the mainstay of the highway research industry for half a century.

The need for SHRP 2 was identified in *TRB Special Report 260: Strategic Highway Research: Saving Lives, Reducing Congestion, Improving Quality of Life,* published in 2001 and based on a study sponsored by Congress through the Transportation Equity Act for the 21st Century (TEA-21). SHRP 2, modeled after the first Strategic Highway Research Program, is a focused, time-constrained, management-driven program designed to complement existing highway research programs. SHRP 2 focuses on applied research in four areas: Safety, to prevent or reduce the severity of highway crashes by understanding driver behavior; Renewal, to address the aging infrastructure through rapid design and construction methods that cause minimal disruptions and produce lasting facilities; Reliability, to reduce congestion through incident reduction, management, response, and mitigation; and Capacity, to integrate mobility, economic, environmental, and community needs in the planning and designing of new transportation capacity.

SHRP 2 was authorized in August 2005 as part of the Safe, Accountable, Flexible, Efficient Transportation Equity Act: A Legacy for Users (SAFETEA-LU). The program is managed by the Transportation Research Board (TRB) on behalf of the National Research Council (NRC). SHRP 2 is conducted under a memorandum of understanding among the American Association of State Highway and Transportation Officials (AASHTO), the Federal Highway Administration (FHWA), and the National Academy of Sciences, parent organization of TRB and NRC. The program provides for competitive, merit-based selection of research contractors; independent research project oversight; and dissemination of research results.

Copyright Information

Notice

SHRP 2 Reports

THE NATIONAL ACADEMIES
Advisers to the Nation on Science, Engineering, and Medicine

The **National Academy of Sciences** is a private, nonprofit, self-perpetuating society of distinguished scholars engaged in scientific and engineering research, dedicated to the furtherance of science and technology and to their use for the general welfare. On the authority of the charter granted to it by Congress in 1863, the Academy has a mandate that requires it to advise the federal government on scientific and technical matters. Dr. Ralph J. Cicerone is president of the National Academy of Sciences.

The **National Academy of Engineering** was established in 1964, under the charter of the National Academy of Sciences, as a parallel organization of outstanding engineers. It is autonomous in its administration and in the selection of its members, sharing with the National Academy of Sciences the responsibility for advising the federal government. The National Academy of Engineering also sponsors engineering programs aimed at meeting national needs, encourages education and research, and recognizes the superior achievements of engineers. Dr. Charles M. Vest is president of the National Academy of Engineering.

The **Institute of Medicine** was established in 1970 by the National Academy of Sciences to secure the services of eminent members of appropriate professions in the examination of policy matters pertaining to the health of the public. The Institute acts under the responsibility given to the National Academy of Sciences by its congressional charter to be an adviser to the federal government and, on its own initiative, to identify issues of medical care, research, and education. Dr. Harvey V. Fineberg is president of the Institute of Medicine.

The **National Research Council** was organized by the National Academy of Sciences in 1916 to associate the broad community of science and technology with the Academy's purposes of furthering knowledge and advising the federal government. Functioning in accordance with general policies determined by the Academy, the Council has become the principal operating agency of both the National Academy of Sciences and the National Academy of Engineering in providing services to the government, the public, and the scientific and engineering communities. The Council is administered jointly by both Academies and the Institute of Medicine. Dr. Ralph J. Cicerone and Dr. Charles M. Vest are chair and vice chair, respectively, of the National Research Council.

The **Transportation Research Board** is one of six major divisions of the National Research Council. The mission of the Transportation Research Board is to provide leadership in transportation innovation and progress through research and information exchange, conducted within a setting that is objective, interdisciplinary, and multimodal. The Board's varied activities annually engage about 7,000 engineers, scientists, and other transportation researchers and practitioners from the public and private sectors and academia, all of whom contribute their expertise in the public interest. The program is supported by state transportation departments, federal agencies including the component administrations of the U.S. Department of Transportation, and other organizations and individuals interested in the development of transportation. **www.TRB.org**

www.national-academies.org

SHRP 2 STAFF

ACKNOWLEDGMENTS

FOREWORD

Monica A. Starnes, Ph.D., *Senior Program Officer, Renewal*

Asphalt pavements with delamination problems experience considerable early damage because delaminations provide paths for moisture damage and the development of damage such as stripping, slippage cracks, and pavement deformation. Early detection of the existence, extent, and depth of delaminations in asphalt pavements is key for determining the appropriate rehabilitation strategy and thus extending the life of the given pavement.

This report presents the findings of the first two phases of SHRP 2 Renewal Project R06D, Nondestructive Testing to Identify Delaminations Between HMA Layers. The main objective of the project was to develop nondestructive testing (NDT) techniques capable of detecting and quantifying delaminations in HMA pavements. The NDT techniques should be applicable to construction, project design, and network-level assessments.

During Phase 1 of the project, the research team evaluated NDT methods that could potentially detect the most typical delaminations in asphalt pavements. Both laboratory and field testing were conducted during this task. Based on the findings from this testing, the manufacturers of two promising technologies conducted further development of their products to meet the goals of this project in Phase 2. The two technologies advanced in this research were ground penetrating radar (GPR) and impact echo/spectral analysis of surface waves (IE/SASW).

Additionally, the project developed guidelines and piloted both NDT technologies in collaboration with highway agencies. Once completed, the results from this additional scope of work will be published as an addendum to this report.

CONTENTS

CHAPTER 1

3d-Radar Report

System Description

This chapter was prepared by 3d-Radar and describes how the 3d-Radar system was improved for the field evaluation in Task 7. Figure 1.1 shows the improved system assembled behind a pickup truck before the uncontrolled field evaluation in Florida. The following sections briefly describe each component of the system in detail.

GeoScope

The 3d-Radar GeoScope emits a step frequency continuous waveform, which is a sine wave with constant amplitude and stepwise frequency variation. The waveform is specified by a start frequency, a stop frequency, a frequency step, and a dwell time (amount of time spent transmitting a sine wave at a given frequency). A laptop is necessary to set up the GeoScope and visualize the data stream, via an Ethernet connection, while preprocessing and data storage take place within the GeoScope. Data are displayed in the three dimensions (inline and crossline B-scans; C-scan) directly during the acquisition in navigable panels in real time.

Antenna Array

An array model B3231 was used for the acquisition. The system makes it possible to collect up to 31 parallel B-scans simultaneously, with a minimum spacing of 10 cm (approximately 4 in.). The array has an overall width of 3.2 m (approximately 10.5 ft) and is connected to the GeoScope through a single cable.

Vehicle Mount

A special tower mount has been designed to quickly shift between data acquisition and system transportation. The mount consists of a cylinder fixed to the hitch receiver of the vehicle, connected on top to a rotatable cylinder. The array is attached to a frame that can be raised and lowered along the main tower by an electrical hinge. During data acquisition, the array is lowered and perpendicular to the vehicle, covering most of a traffic lane. During transportation between survey sites, the array can be lifted and turned 90°, thus minimizing possible traffic safety issues.

System Settings

To determine the speed of the survey, the time required to perform a complete array scan, which is sending and receiving through all the active channels along with the inline sampling, needs to be calculated. 3d-Radar provides an Excel-based utility to assist with these calculations to define the maximum surveying speed during the acquisition. As summarized in Table 1.1, three different system configurations were tested, allowing for different maximum vehicle speeds.

The objective was to implement configurations to match the purposes of a routine control (high speed), a more careful evaluation (medium speed), and an in-depth assessment of the road substructure (slow speed).

For this phase of the testing, it was preferred to keep the same frequency characteristics of the signal in terms of bandwidth and sampling (frequency step), while decimating the spatial sampling moving from a slow-speed to a high-speed acquisition. The high-speed settings meet the minimum requirement of 1 sample per foot.

The bandwidth (BW) allows a resolution:

$$\frac{1}{BW} = 1.36 \text{ ns}$$

When a relative permittivity value of 5 as average for asphalts is used, the spatial resolution on the shallow subsurface of a road structure is approximately 2.39 cm (0.94 in.).

1

Figure 1.1. Antenna array and tower mount in position for data collection.

Real-Time Processing and Postprocessing

The real-time processing sequence consists of

- Inverse Fast Fourier Transform (including frequency filter);
- Background subtraction;
- Time windowing; and
- Range gain compensation.

These operations are performed on all active channels, with user-selectable parameters, and allow for a full 3-dimensional visualization of the data cube directly during the acquisition phase on the laptop that controls the GeoScope ground-penetrating radar (GPR) device.

The steps listed above are the basic steps necessary to provide a classical time domain visualization of the radar data. Because the GeoScope is a step-frequency GPR, it is natural to have data recorded in frequency domain, because what is measured is very similar to a frequency response of the subsurface.

Postprocessing through 3d-Radar Examiner touches the same processing steps as does the real time, plus some other tasks that can be fine-tuned to improve visualization or produce an output for specific applications (i.e., the delamination detection algorithm designed for this project).

Given the wide bandwidth that can be recorded with the system and the variety of scenarios that are faced in GPR survey work, data stored in frequency domain represents a versatile, raw starting point to build a solid, fine-tuned processing sequence to produce the time domain synthetic section that will be the basis for interpretation and analysis. Nonetheless, the user has an either-or option for storing the acquired data in time domain, exactly as captured during real-time processing. If confidence in the processing settings is high enough, this indicates a good way to save time in postprocessing. For this set of data captures, frequency domain data were collected in order to provide greater options during postprocessing.

Delamination Detection Algorithm

The delamination detection algorithm was prototyped on the basis of data collected at the National Center for Asphalt Technology (NCAT) facility during 2009 and 2010.

The algorithm was built to account for the fact that delamination can occur at a relatively wide range of depths and show a variety of amplitude characteristics in the recorded data. The approach we chose is based on isolating a subvolume where delamination is most likely to happen and performing an energy-based study of frequency intervals on the subvolume. The advantage is that considering frequencies, every sample will carry information about the whole depth range to be analyzed, while sorting the energetic

Table 1.1. System Configuration for Three Speeds

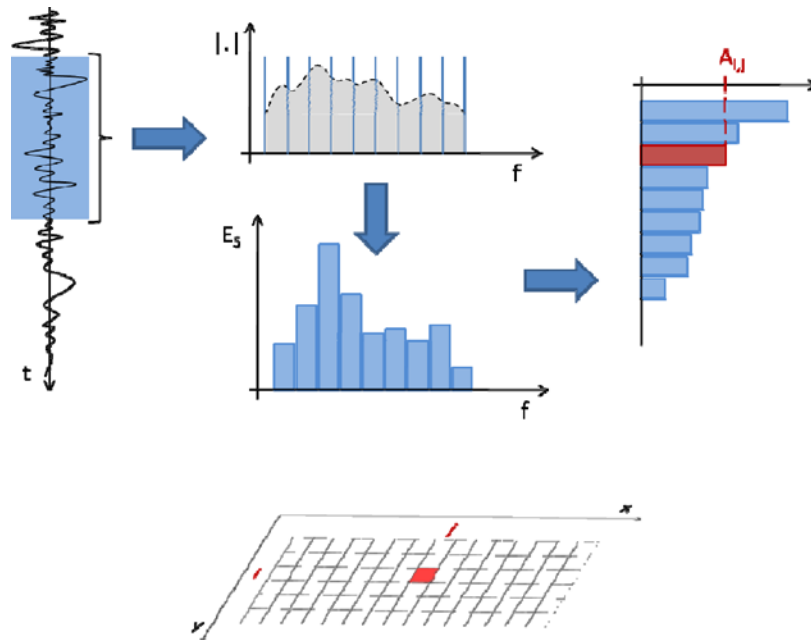|	**Slow Speed**	**Medium Speed**	**High Speed**
Frequency range	200 MHz–3 GHz	200 MHz–3 GHz	200 MHz–3 GHz
Frequency step	2.5 MHz	2.5 MHz	2.5 MHz
Dwell time	1 µs	0.6 µs	0.5 µs
Inline sampling	10 cm (~4 in.)	20 cm (~8 in.)	30 cm (~12 in.)
Crossline sampling	10 cm (~4 in.)	20 cm (~8 in.)	30 cm (~12 in.)
B-scans per swath	31	16	11
Maximum speed	~3.5 mph	~18 mph	~45 mph

Figure 1.2. Schematic representation of the delamination detection algorithm: operations on the trace in position x = j, y = i. E_s = user defined.

values takes care of the varying amplitudes of signatures due to delamination.

Schematically, the time window of interest is extracted from every trace and converted to frequency domain, where the spectrum is divided into frequency intervals, or "bins." The algorithm computes the energy contained in every bin and then sorts the obtained values. The value that will be finally extracted is relative to only one bin, which is selected by the user (Figure 1.2).

The user then defines a threshold value for E_s and the minimum size for an anomaly of interest to produce the final output (Figure 1.3).

Difficulties Encountered, Future Implementation, and Next Steps

The settings for data collection could potentially be modified to meet the needs of each department of transportation in terms of traffic flow and safety. Feedback from the operators during some of the field work indicated that sometimes slower speeds are safer because traffic flow is more controllable. Additionally, studying the data can allow fine-tuning of the waveform characteristics for the specific application, which can change the maximum possible speed without data loss.

The analysis of the data collected has also indicated that slow-speed measurements are affected by some sort of movement of the antenna, particularly visible close to the surface. Suspicions were that this behavior is due to the resonant frequency of the vehicle suspension; that is, the antenna vibrates together with the vehicle and produces small undulations in the data. Crosschecking typical values for resonance frequency of the suspensions with the variations in the data shows this to be the case. Future implementations will need to address this issue, directly in the hardware if possible, by either modifying the antenna mount, using an optional antenna trailer, or possibly in postprocessing software.

The size of the generated files is another issue. This issue is present when storing files, transferring files, and postprocessing. Modification of the Examiner software package to support optional routines for semiautomatic partitioning to allow fast processing and access of subsections is being implemented. Within future releases of Examiner, it will be possible
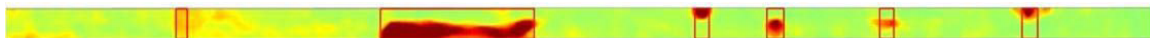

Figure 1.3. The red rectangles in the picture are the final output of the algorithm, a result of a statistical analysis based on parameters input by the user.

4

to divide the data into smaller portions, an operation now performed manually by the user.

The delamination detection algorithm has given reasonably good results for some of the data collected and lacked consistency for others. As the algorithm was developed on the basis of experience at the NCAT facility, where human-introduced simulated delamination provided solid and clean characteristics, this should be regarded as a fairly good first result. Further study of the data collected in real situations, combined with ground truth, will refine the signature given by a delamination both qualitatively and quantitatively. The next step for the detection algorithm is to increase its robustness based on the type of anomaly to be detected. Additionally, the algorithm will attempt to factor in characteristics of the road substructure where variation in depth of targeted layers and eventual lateral discontinuities are present. Finally, the current version of the algorithm requires multiple inputs from the user, which means that the data analyst should have a background in GPR data processing. A further refinement that includes a detailed and targeted analysis of the data and ground truths collected during this project should minimize the input required in future revisions, making it a more user-friendly tool for nonspecialist operators.

CHAPTER 2

Olson Engineering, Inc., Results

This chapter describes the results of Phase 2 subcontract research conducted by Olson Engineering, Inc., at the National Center for Asphalt Technology (NCAT), Auburn University, in Alabama, and at test sites in Gainesville, Florida, and Pittsburg, Kansas. The research examined nondestructive testing (NDT) and evaluation of the pavement at these sites with stress wave methods for debonded hot-mix asphalt (HMA) layers. The field portion of this investigation was performed in accordance with generally accepted testing procedures. Research team members were Patrick K. Miller, Yajai Tinkey, and Larry D. Olson.

Introduction

Phase 2 of the SHRP 2 R06D research project for stress wave detection of delaminated (debonded) asphalt pavement layers focused on the use of spectral analysis of surface waves and impact echo (SASW and IE) tests to determine the condition of asphalt pavements. Olson Engineering has added four transducer wheels to the Bridge Deck Scanner (BDS) to accelerate the testing. The new system with six transducer wheels was used again on the NCAT Pavement Test Track site to verify the accuracy of the test results from the new system. Then the BDS with six transducer wheels was used to determine the conditions of asphalt pavements in Florida and Kansas.

IE and SASW Test Setup

The same test setup was used in all three test sites. The two transducer wheels within the same pair were spaced 6 in. Only one solenoid was used to impact the asphalt so that the transducer wheel nearest to the solenoid impactor acquired the IE data and both transducer wheels acquired the data for SASW tests. Distances between each sensor wheel pair were varied between 2 and 3 ft.

IE and SASW Results from the NCAT Test Track

Test results from the NCAT test track with known, constructed delaminations are presented in the section on NCAT pavement. Summaries of findings from the NCAT test results are given below:

1. Results from the IE tests were able to identify debonding conditions with a depth of 5 in. However, the IE tests were not able to detect shallow delaminations (2-in.-deep delaminations). This result is most likely caused by the inability of the current system to excite the needed high frequencies and the fundamental difficulty to excite high frequencies in asphalt at above freezing temperatures because of asphalt's temperature-dependent elastic moduli. This outcome is in contrast to the BDS performance for IE tests on concrete pavements and decks that have higher elastic stiffness/moduli and are not temperature-dependent to any significant degree.
2. The SASW tests were successfully used to identify debonding conditions on the NCAT asphalt test track pavement. A sharp drop in the surface wave velocities appeared to correlate well with the depth of debonding, as shown in the section on test results from the SASW tests. Both shallow debonding (2 in.) and deeper debonding (5 in.) were detected by using the SASW tests, as sufficiently high frequencies were excited for SASW tests at the nominally 50°F and higher test temperatures.

SASW Test Results from the Florida Pavement

On the basis of test results from the NCAT test track, only SASW test results were processed from the Florida pavement. In general, the conditions of the 2,000-ft section of the tested Florida pavement were similar to those identified

5

with SASW tests of known delaminations at the NCAT track. The majority of test locations showed a sharp drop of surface wave velocity at wavelengths corresponding to depths between 0.2 and 0.4 ft. This drop was indicative of either possible debonding at these depths or an existence of a thin layer of lower stiffness/moduli material at these depths. In addition, the conditions of the pavement at the centerline of the lane seemed to be in better condition than did those of the wheelpaths. Finally, the general conditions of the pavement on the right wheelpath (0 to −5 ft) appeared to be in the worst condition, with slower velocity in comparison to the left wheelpath (0 to +5 ft).

SASW Test Results from the Kansas Pavement

On the basis of test results from the NCAT test track, only SASW test results were processed from the Kansas pavement, as well. Overall, the majority of the data from the Kansas test site had relatively high surface wave velocities near the pavement surface (<0.3 ft deep) and decreasing velocities with depth indicating weaker underlying materials. The team's interpretation of the data overall is that the road likely had a relatively new asphalt overlay of good condition with an older underlying pavement composed of weaker material with widely varying velocity/moduli conditions. Research by others on asphalt pavements has shown that decreases in surface wave velocity correlate well with aging/reduction of moduli in asphalt as pavements deteriorate with traffic loading and time.

Summary of Stress Wave Findings from Scanning IE and SASW Testing

IE scanning with the BDS system was able to detect 5-in.-deep delaminations, but not the 2-in.-deep delaminations at the NCAT test track. SASW testing was able to detect delaminations at depths of 2 in. and deeper. It was further found that there could be additional benefits from SASW scanning of asphalt in terms not only of debonding but also by providing data on the moduli of the pavement materials where it was not delaminated, as well. To the best of the team's knowledge, the application of slow rolling at 1 to 2 mph, contacting IE and SASW scanning for asphalt pavements, was done for the first time in this study.

Development of Bridge Deck Scanner Hardware

The initial IE and SASW testing performed as Phase 1 of the SHRP 2 research project at the NCAT Pavement Test Track in Opelika, Alabama, in October 2009 used a two-wheel rolling measurement system. The two-wheel pair system was developed under a National Cooperative Highway Research Program grant (NCHRP IDEAS Project No. 32—Vehicle Mounted Bridge Deck Scanner [BDS] by Tinkey, Olson, and Miller) awarded to the research team members. The NCHRP research involved performing scanning IE tests, surface waves tests, and other tests for mapping out reinforcing corrosion-induced bridge deck delaminations and general condition assessment evaluation of concrete bridge decks. The BDS system had already evolved through multiple prototype versions into a fairly mature two-wheeled device.

The basic BDS two-wheel system essentially consists of two transducer wheels made of high-density polyethylene (HDP) with six embedded Olson Instruments IE sensor heads around the circumference of the wheel at 6-in. intervals to allow for tests every 6 in. The sensor heads were paired with a small steel solenoid impactor. The wheels were coupled together with a rubber isolated axle that provided alignment of both displacement transducers for SASW testing or misalignment (offset 30°) of the two wheels in the case of IE testing to make impact at both wheels for IE tests only. The system had onboard signal conditioning and was controlled by an Olson Instruments Freedom Data PC. The Freedom Data PC performed all trigger and timing functions as well as the data acquisition and the data analysis and presentation. Figures 2.1 and 2.2 show photographs of the two-wheel pair IE/SASW scanner in use during Phase 1 testing at the test track.

After two separate rounds of testing at the NCAT test track, extensive analysis and comparison of the collected data to the known in-situ condition, and constructive feedback from the investigative team, a series of modifications of the IE/SASW scanning system were implemented before Phase 2 testing. The first testing round was in October 2009 on "warm" asphalt and the second testing round was in March 2010 on "cold" asphalt. The objective of these modifications was to improve
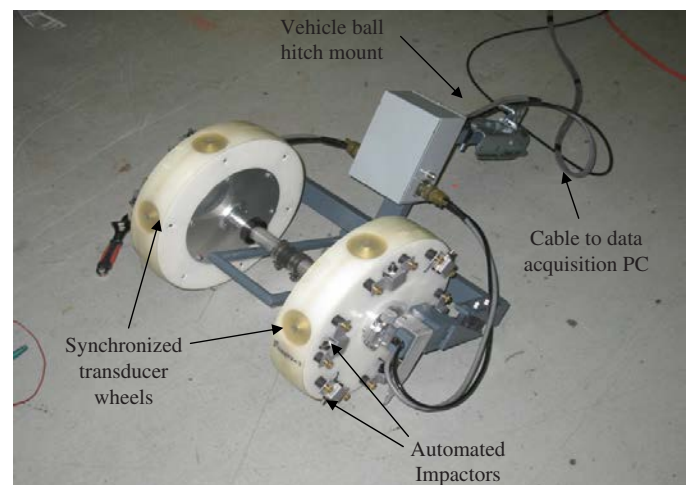

Figure 2.1. Photograph of the IE/SASW system used during Phase 1 testing.

Figure 2.2. Scanning IE/SASW testing performed during Phase 1 on the NCAT test track.

the ability of the system to detect near-surface delaminations (~2 in. deep) as well as to increase the number of test wheels to improve the test area coverage of a single pass and thus to reduce the required test time of a single lane.

In the initial Phase 1 study, a variety of NDT test methods was evaluated, and it was found that the IE test method provided the most consistent results in determining debonded asphalt conditions. However, the IE test method was not able to detect shallow debonding at a depth of approximately 2 in. It was suggested by the research team that the SASW test method may provide a better indication of debonding conditions, particularly shallow debonding. It was also discussed that the transducer spacing of 1 ft, while excellent for IE testing, was not ideal for SASW testing. The possibility of the solenoid impactor being too close to the first transducer and creating so-called near-field wave effects was also discussed with the research team. Therefore, a series of experiments was conducted in the team's laboratory on both concrete and asphalt specimens, in which the distance between the two transducers was varied, as well as the distance between the impactor and the first transducer. The results of these experiments found that a 6-in. spacing between transducers would most likely be optimal at locating debonding conditions at depths ranging from ~1 to 10 in. This depth fully covers typical asphalt pavement thicknesses. It was concluded that the original impactor to first transducer distance of 1.75 in. was not creating near field effects at a 6-in. transducer spacing but most likely was complicating the analysis at the previous transducer spacing of 12 in. Therefore, it was determined, on the basis of these experiments, to retain the impactor/first transducer spacing of 1.75 in. and to reduce the transducer/transducer spacing to 6 in. This test configuration was used on the NCAT test track in February 2011 to verify the ability of the scanning SASW system to locate shallow debonding condition, and excellent results were achieved, as discussed in the section on NCAT pavement.

On a related note regarding SASW testing, the alignment of a single pair of transducer wheels to allow for SASW testing is imperative. However, based on testing and experiments it was necessary to isolate the wheels from one another using rubber couplings to avoid excessive vibrations noise. Experiments were done with multiple different axle configurations incorporating rubber isolation, but there was trouble with wheel slippage at times, as had been the case at the Florida test site. The recent axle configuration used rubber isolated hubs attached to the wheel with steel shear pins and an aluminum axle, also with shear pins (see Figure 2.3). This configuration was used at the Kansas test site and experienced no slippage.

Axle hub ring, rubber mounted with 6 steel shear studs

Aluminum axle locked with metal pins
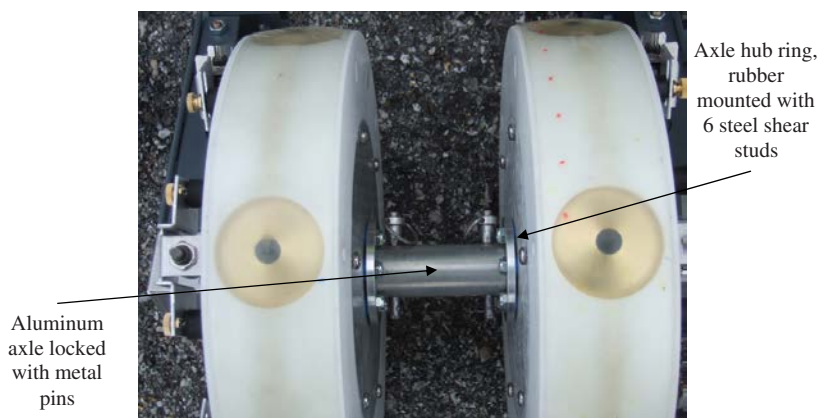
Figure 2.3. Current IE/SASW scanning system, showing new axle configuration and 6-in. transducer spacing shown inline for SASW testing (offset for alternating IE testing).

8

The major upgrade implemented to the IE/SASW scanning system was the expansion from a single pair of two wheels to three separate wheel pairs for a total of six wheels. The decision to expand to six measurement wheels was made when the testing plan was to perform IE testing on 2-ft spacings to cover a full 12-ft lane width in a single pass, leaving 1 ft of space on either side. However, as described above, through additional analysis, recommendations by the research team, and additional laboratory testing, the optimal test configuration for asphalt pavement delamination detection was determined to be IE/SASW with a 6-in. displacement transducer spacing, as shown in Figure 2.4. With a spacing of 2 ft between each pair of wheels, it would require five or six pairs of wheels to provide full coverage of a single 12-ft lane. Therefore, when testing was conducted at the Florida and Kansas test sites, two passes were performed to cover the full lane width. Additional expansion of the system could be completed in the future to eliminate the need for two passes.

The additional four measurement wheels (two pairs) were constructed to be nearly identical to the original pair of transducer wheels. This construction included six IE/SASW transducers per wheel evenly spaced around the circumference at 6-in. intervals, six impactor solenoids, and electronic circuitry for signal conditioning, solenoid firing, and data acquisition triggering. As the four new wheels were built, a few slight modifications were made to improve the design: a lip of the HDP wheel was added to secure the urethane tire (which previously had slowly rolled off the transducer wheel on long scans) and a variable attenuator circuit was added to the signal conditioning to allow the signal to be reduced in voltage amplitude to avoid clipping during data acquisition. Another major modification was the addition of trigger timing circuitry to synchronize the three independent transducer wheel pairs. This timing circuitry eliminated the possibility of multiple wheel pairs (or individual transducer wheels in the case of IE testing) firing at the same time, which would cause confusion in the propagated waves and data collection. The timing circuitry also forced the wheel pairs to fire sequentially (from left to right) to allow the data to be well organized in the software. The timing circuitry had two separate options, which allowed the scanning system to be run as three sets of SASW testing wheel pairs or as six individual IE testing wheels. The last major change necessary was the addition of an independent distance wheel to record the distance from the start of the scan to each data collection point with any of the transducer wheels or pairs. The distance wheel output 128 pulses per revolution, resulting in a distance measurement resolution of approximately 0.1 in.

Several other miscellaneous upgrades were also completed to improve the ease of use, ease of setup, and simplicity. For instance, the assembly of the wheel-pair carriage was simplified and redesigned to make it easier and quicker to assemble. The towing assembly mounted to the truck was also slightly altered, adding more pin (rather than bolted) connections to ease field assembly (see Figure 2.5). The attachment of the wheel pairs to the towing assembly was changed to a clamping attachment that could slide on the towing assembly bar, creating endless configuration possibilities. Lift bails were added to the towing assembly to allow the transducer wheels to be picked off the asphalt surface to back the system up or reposition the truck with greater ease (see Figure 2.6). The
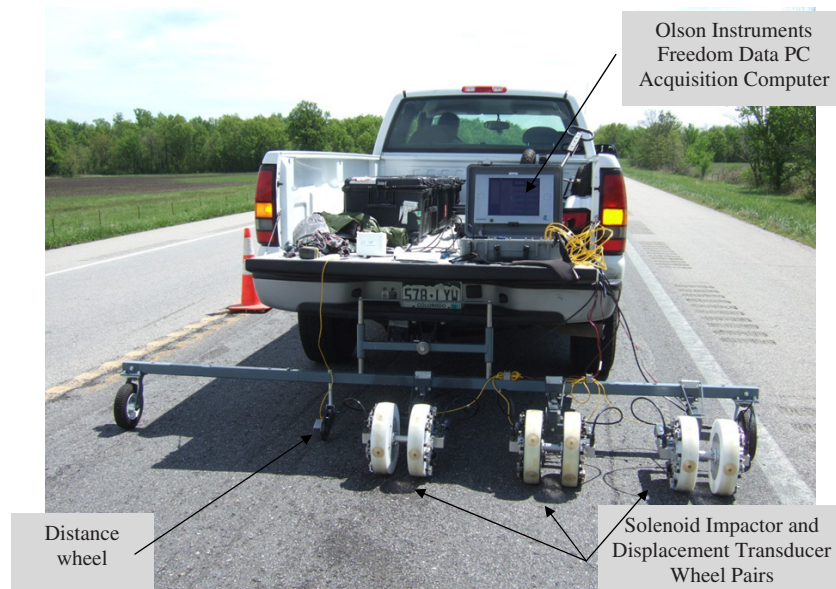
Source: Photograph from the Pittsburg, Kansas, test site.

Figure 2.4. Current IE/SASW scanning system, showing the SASW test setup of 6-in. transducer spacings with distance of 2 ft between pairs.
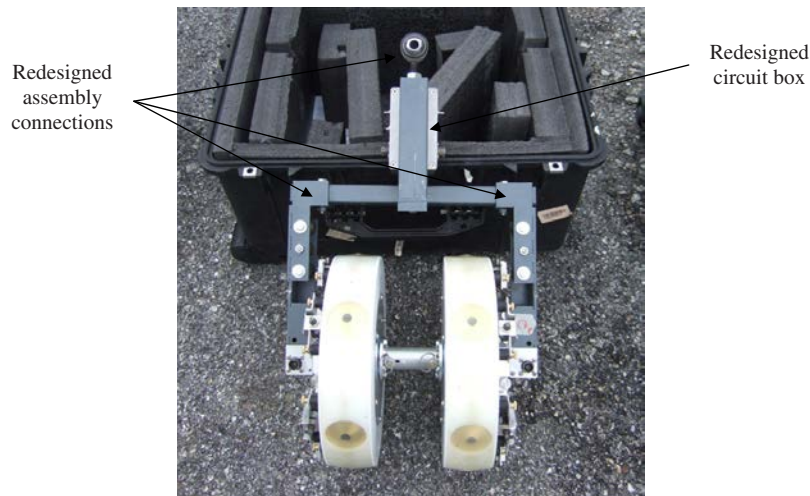
Figure 2.5. Current IE/SASW scanning system, showing simplified assembly connections and a smaller circuitry box.

wiring between the transducer wheels and the data acquisition computer was also simplified.

The system is still run with the Olson Instruments Freedom Data PC, which runs the acquisition software and provides all data acquisition. The solenoids are powered either with a 12-VDC battery or with a cigarette lighter car plug.

IE and SASW Method and Data Acquisition with Bridge Deck Scanner

The six-wheel BDS system was designed to perform either

1. IE testing on all 6 transducer wheels; or
2. IE testing on the transducer wheel near the impactor solenoid and SASW testing from adjacent pairs of transducer wheels.

The first type of testing (IE) is best applied to condition assessment of concrete bridge or garage deck slabs without an asphalt overlay. The later type of testing (IE and SASW) works well with asphalt material, either full depth or as an overlay. This project used the second test setup to perform primarily SASW testing; thus, only SASW will be discussed. The IE testing was also used at the NCAT test track and is discussed more in the section on NCAT pavement. To perform SASW testing, sensor elements in both transducer wheels (within a pair) were aligned and locked with a pin to prevent the slippage. The sensor elements were offset approximately 2 in. between each adjacent pair of transducer wheels. Figure 2.7 shows a typical test setup, including the transducer locations of all wheels for the SASW setup.

In this case, the system was set so that only the solenoids of the left transducer wheel (of the pair) are used for generating impacts. The solenoids of the right transducer wheel (of the

Figure 2.6. Current IE/SASW scanning system, showing the sliding connection system and lift bails.
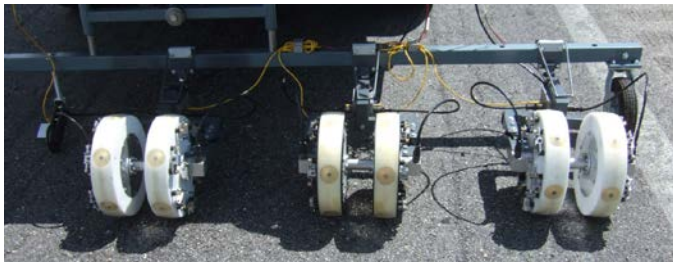
Figure 2.7. Typical SASW testing setup.

pair) are disabled for the duration of the testing. The impact sequence starts with firing the single solenoid used for the left pair of transducer wheels, followed by the solenoid for the middle pair of transducer wheels, and finally, the solenoid for the right pair of transducer wheels. The sequence is then repeated. Once one of the solenoids fires, data acquisition for all three pairs of transducer wheels (all six channels) is recorded simultaneously, but only the data from the pair of wheels where the solenoid is fired and impacts are analyzed. At each acquisition, two channels (one wheel pair) will actually have valid surface wave data. The other four channels (two pairs) acquire background noise. The postanalysis software scans through all the acquired data and pulls out only valid SASW data for further analysis.

Features in the postanalysis software include auto-windowing, dynamic masking/dispersion curve display, and composite velocity calculations. Plotting of the test results is performed in Golden Software Surfer software. Short discussions of the IE and SASW methods are presented below to explain and illustrate the methods that are discussed in other references, including Nondestructive Test Methods for Evaluation of Concrete in Structures by American Concrete Institutes Committee 228, Report ACI 228.2R-98.

IE Method

The IE method involves hitting the concrete surface with a small impactor (or impulse hammer) and identifying the reflected wave energy with a displacement (or accelerometer) receiver mounted on the surface near the impact point [ASTM Standard C-1383(07)]. After the impact, the resulting displacement or acceleration response of the receiver is recorded. Although the resonant echoes are usually not apparent in the time domain, they are more easily identified in the frequency domain (linear displacement spectrum). Consequently, the time domain test data are processed with a Fast Fourier Transform (FFT), which allows identification of frequency peaks (echoes). If the thickness of a slab is known, the compression wave velocity (Vp) can be determined by Equation 2.1:

$$Vp = 2 * d * f / \beta \tag{2.1}$$

where d = slab thickness and f = resonant frequency peak.

Equation 2.1 is modified by a beta factor of ~0.96 for concrete slabs and algebraically rewritten to calculate the echo depth thickness, d. An example result for one IE scan line from a new bridge with cracking/void concerns that was tested with the BDS system is shown in Figure 2.8. Thickness echo data shown on the left include an approach slab from 0 to 20 ft followed by 80 ft of the concrete bridge deck. The time domain signal is in the upper right, and its corresponding IE thickness echo of 8.05 in. in the linear displacement frequency spectra is in the lower right in Figure 2.8.

Shallow delaminations of less than a few inches may not produce a distinct echo peak response in an IE test if the necessary high frequencies cannot be generated, as often occurs for warm to hot asphalt. However, such a delamination has the potential to be identified by a low-frequency flexural response similar to that occurring in BDS-IE testing of concrete bridge decks. Shallow deck delaminations less than a depth of 3 to 4 in. are identified by an apparently much thicker echo depth due to the resonant flexing associated with a concrete delamination (due to reinforcing corrosion and expansion) parallel to the deck surface. However, unless the asphalt is tested at freezing and lower temperatures and, thus, the asphalt is almost concrete-like in terms of its modulus, then this flexural response may not be measured. In this study, all asphalt temperatures were above freezing at the NCAT test track, and there was no indication of the hoped-for low-frequency flexural response that might have indicated the presence of the shallow, 2-in.-deep delaminations. In Phase 1, some apparent, possible flexural responses indicative of shallow asphalt delamination were measured. These results likely indicate either one of two conditions. The first condition is that the material could be lacking consolidation or could be of low density, which causes a decrease in the resonant frequency of the slab, or could be lacking consolidation and low density. The second condition is that the area could have a near–surface, shallow delamination that has a strong low-frequency flexural resonance and the full-depth asphalt pavement slab resonance is not observed. If a delamination is present, the depth of the delamination cannot usually be determined through IE testing because the flexural resonance of the delamination would depend strongly on the delamination depth and area. In concrete, with special solenoid IE testing equipment, team members have been able to excite frequencies as high as 50 kHz and measure concrete thicknesses as thin as 1.5 in. (0.125 ft), with an Olson Instruments Impact Echo-1 Super Thin test head. However, because of the viscous, temperature-dependent stiffness/moduli of asphalt, it is difficult to excite such high frequencies in asphalt, particularly as temperatures increase. At low temperatures of freezing and below, asphalt is more concrete-like, and it is easier to excite high frequencies and measure echoes from thin asphalt pavements or shallow delamination depths. Because this is
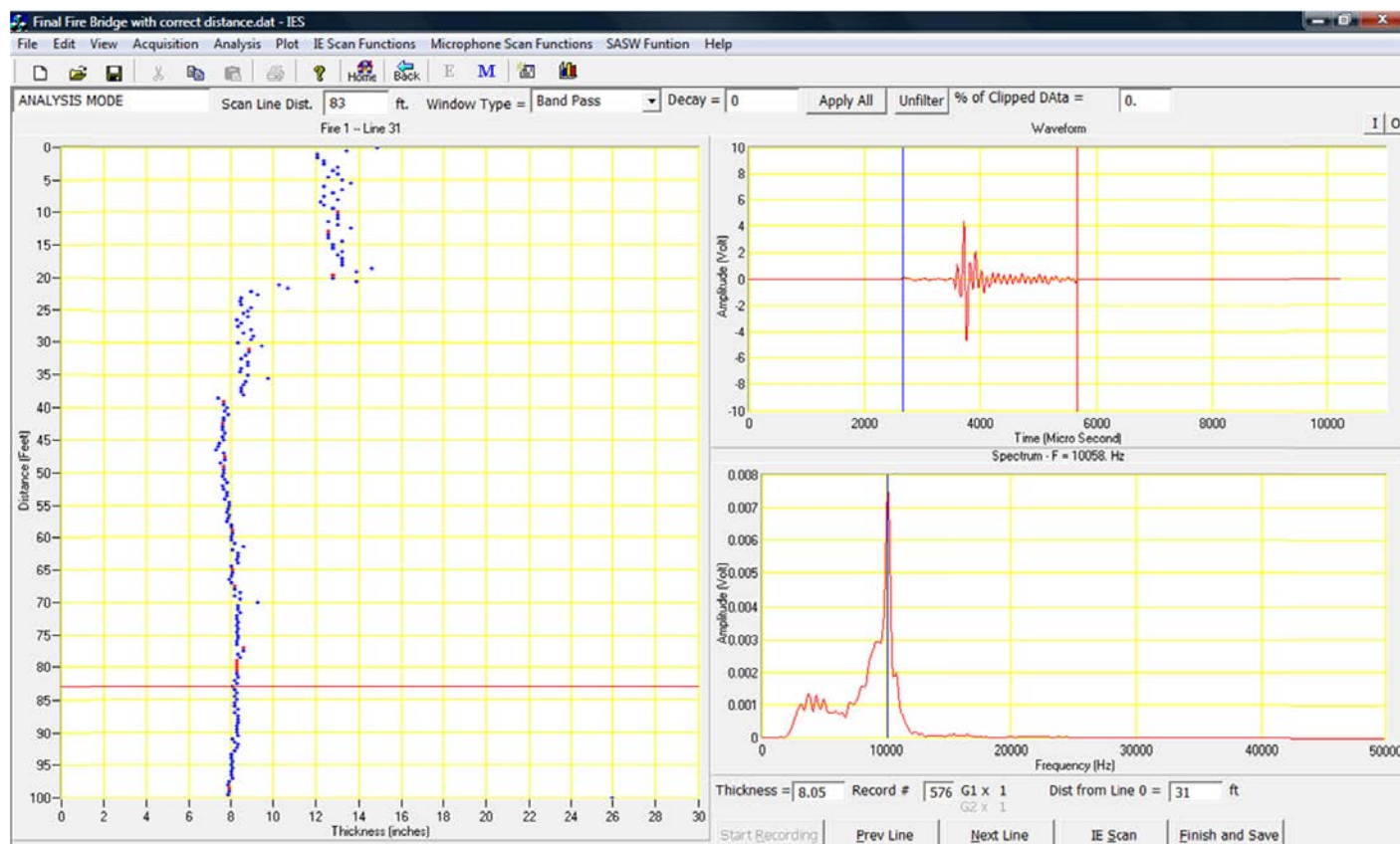
Figure 2.8. Example IE scanning results from the BDS-IE system on a new bridge.

generally not the case, the flexural response of a delamination that corresponds to an apparently greater thickness of asphalt was generally found to be the best indication of delaminations less than a depth of 5 in. in Phase 1 studies, but this condition was not consistently apparent in the IE results.

SASW Method

The SASW method uses the dispersive characteristics of surface waves to determine the variation of the surface wave velocity (stiffness) of layered systems with depth. Shear wave velocity profiles can be determined from the experimental dispersion curves (surface wave velocity versus wavelength) obtained from SASW measurements through a process called "forward modeling." Forward modeling is an iterative inversion process to match experimental and theoretical results. Materials that can be tested with the SASW method include concrete, asphalt, soil, rock, masonry, and wood. Applications of the SASW method include but are not limited to (1) determination of pavement system profiles, including the surface layer, base, and subgrade materials; (2) determination of seismic velocity profiles needed for dynamic loading analysis; (3) determination of abutment depths of bridge substructure; and (4) condition assessment of structural concrete. SASW

can also measure crack depths (for cracks perpendicular to the surface) in bridge decks. The SASW method uses the dispersive characteristics of surface waves to evaluate concrete integrity with increasing wavelength (depth). Open, unfilled cracks will result in slower surface wave velocities. Weak, fire-damaged, and poor-quality concrete (less stiff/lower elastic moduli) also produce slower surface wave velocities.

In the NCHRP IDEAS BDS research, SASW tests were conducted with two of the same microphones that were used as noncontacting transducers. The distance between the two microphones was 4 in. (10.1 cm), and a solenoid impactor was used as an impact source. The microphones were mounted 3 in. (7.6 cm) above the concrete slab, and the source was located between 8 and 18 in. (20.3 and 45.7 cm) away from the closest microphone. Good-quality SASW data (top trace in Figure 2.9) with a good coherence up to 10,000 Hz (second trace from top in Figure 2.9) was captured by both microphones. The SASW data shown in Figure 2.9 were exponentially windowed after the large amplitude surface wave pulse traveled by the data to eliminate other wave vibration modes. The surface wave velocity can be calculated from the phase plot (third trace from top in Figure 2.9) as a function of wavelength (velocity = frequency × wavelength). The surface wave velocity is calculated to be approximately
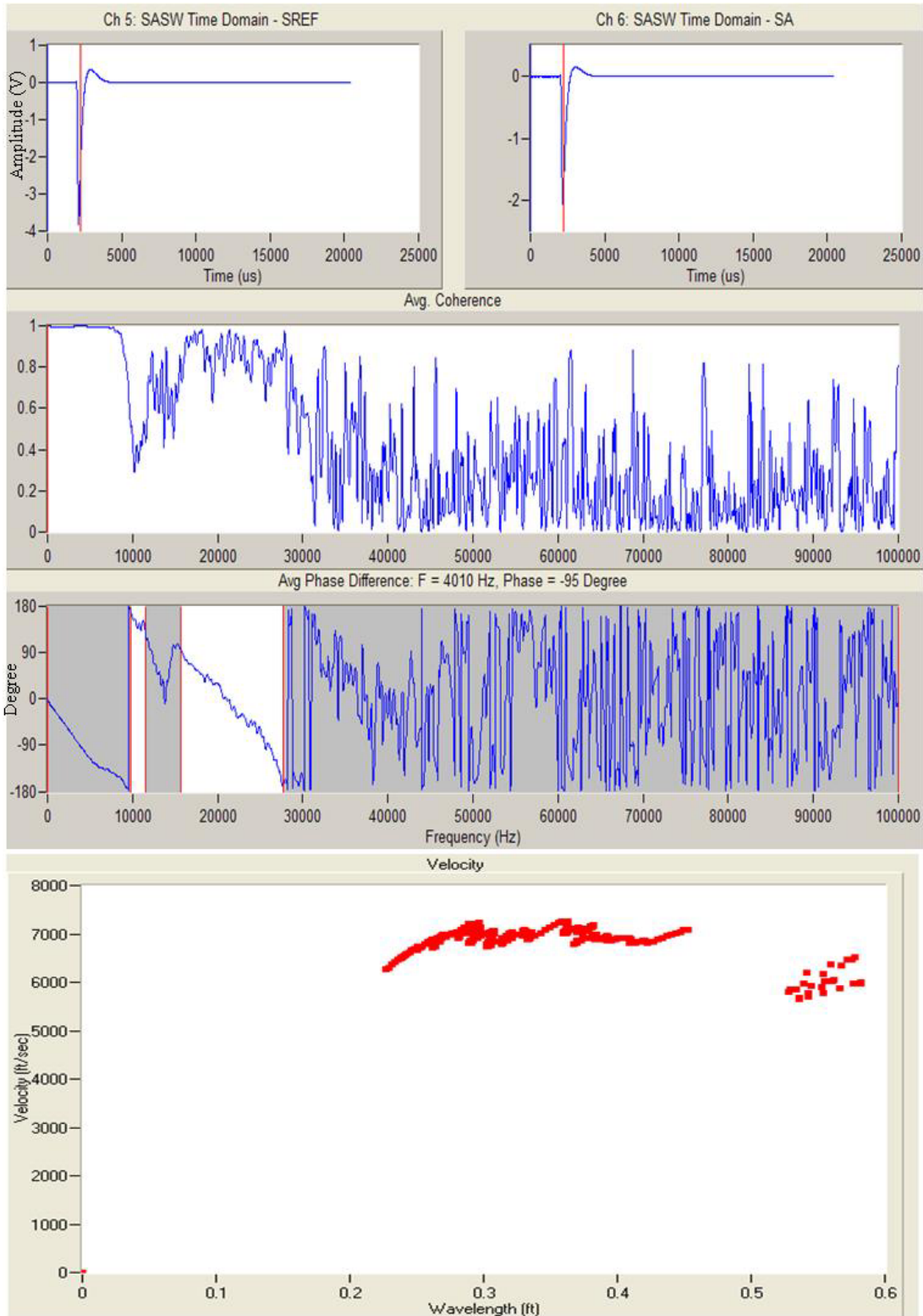
Figure 2.9. Example SASW data processing from noncontact microphones from NCHRP IDEAS BDS research.
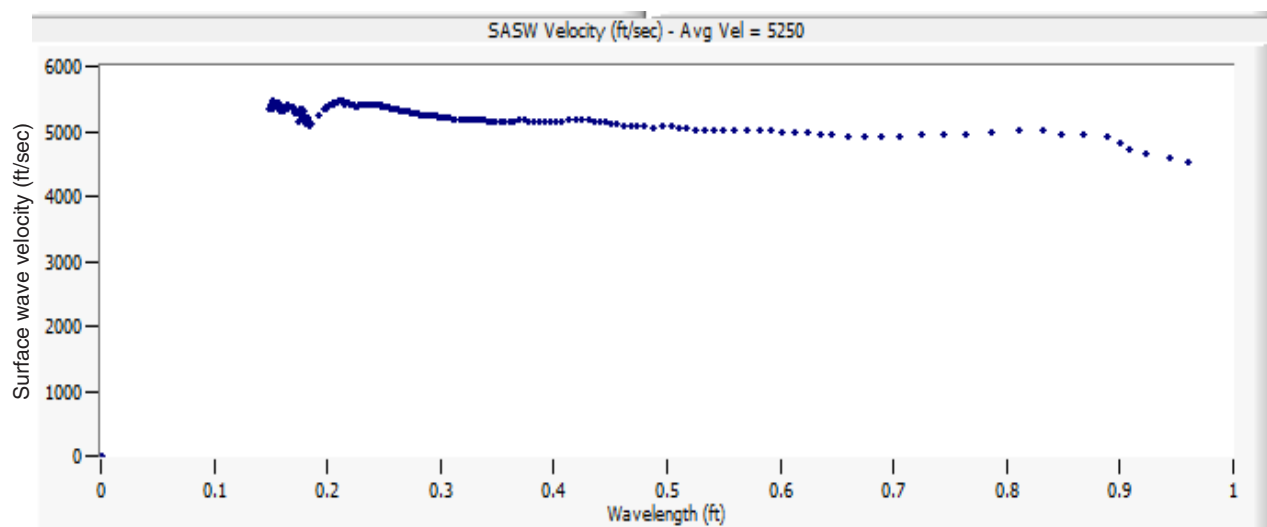
Figure 2.10. A dispersion curve from a sound location on NCAT pavement.

7,000 ft/s uniformly from wavelengths of 0.2 to 0.4 ft (6.1 to 12.1 cm), as seen in the last trace in Figure 2.9, which agreed well with the results from contacting displacement transducers. Coherence near 1.0 is high-quality data from two or more impacts. Thus, for the SASW tests conducted with the BDS system on asphalt pavement, the calculation of coherence was not possible since there was only one impact per test location during rolling.

At this time, microphones for SASW testing do not produce SASW results of as high quality as do the rolling, displacement transducers. Consequently, only the rolling sensor wheels were used in the R06D field testing program, which is reported.

Data Interpretation of SASW Test Results

Sound pavement yields a high and constant surface wave velocity shown as a flat and horizontal line in a dispersion curve throughout the depth of the pavement. A typical example is shown in Figure 2.10. It was found that the presence of a sharp drop in the surface wave velocity within the dispersion curve acted as a reliable indication of potential debonding within asphalt pavements. The location (wavelength) of the velocity drop related closely to the depth of the debonding. Figure 2.11 presents a dispersion curve (surface wave velocity versus wavelength) from a location from Section 1 from the NCAT site.
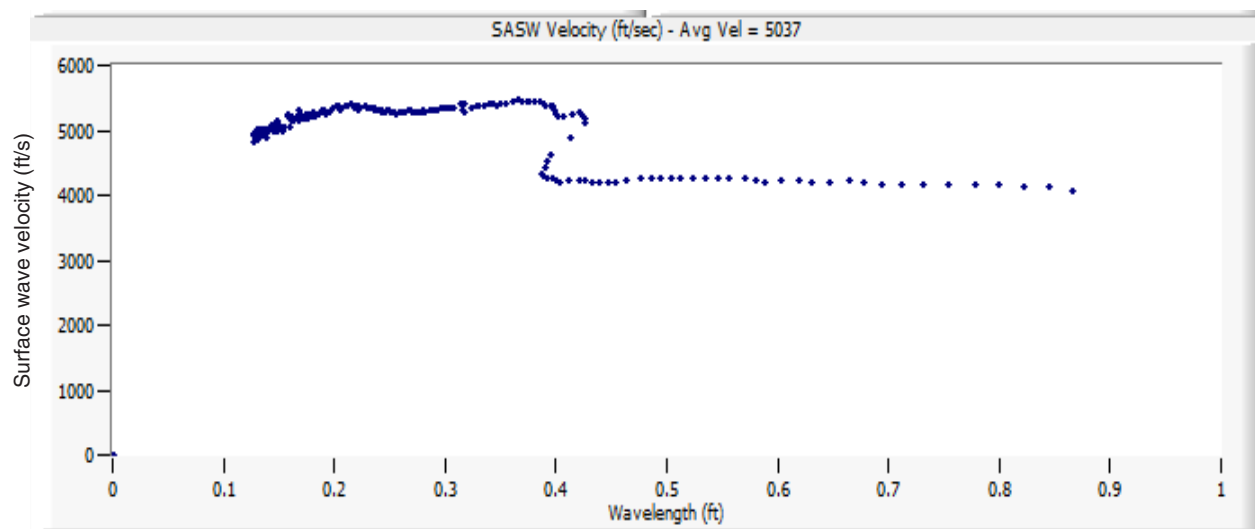
Figure 2.11. A dispersion curve from a location with debonding at a depth of 5 in.
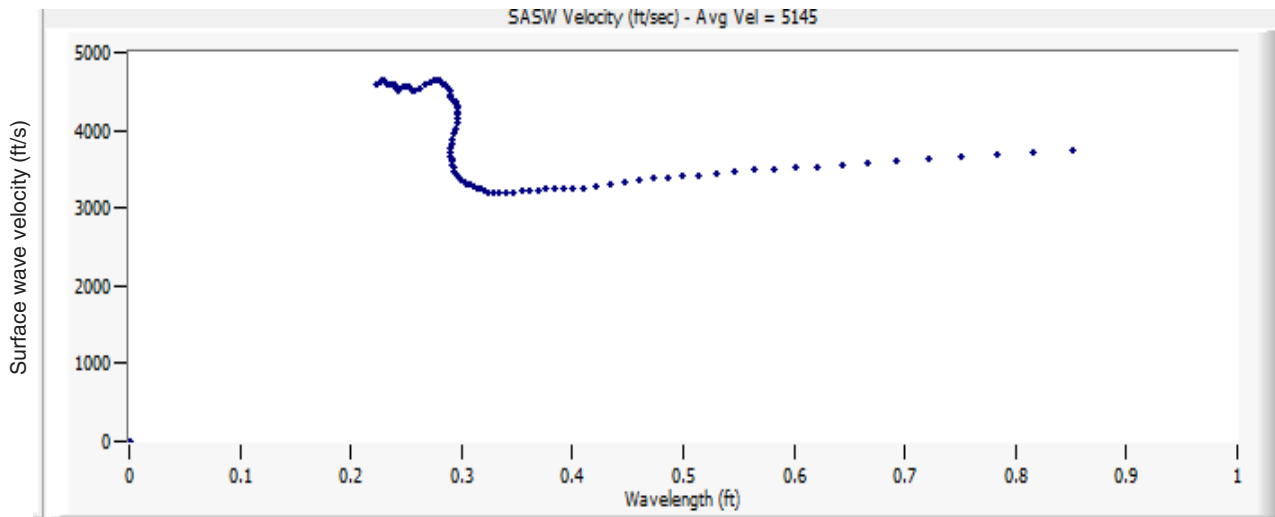
Figure 2.12. A dispersion curve from a location with debonding at a depth of 2 in.

The actual as-built plan showed baghouse dust at a depth of 5 in. to simulate debonding within the HMA. Review of Figure 2.12 shows a sharp drop in the surface wave velocity at a depth of 0.41 ft, or 4.9 in., which is indicative of the delamination depth. Figure 2.12 presents a dispersion curve from a location in Section 6 (HMA pavement with partial stripping) where the bottom of delamination is approximately 2 in. deep. Reviews of Figures 2.13 and 2.14 show 5-in.-deep delaminations for baghouse dust and thin paper, respectively.

NCAT Pavement Test Track SASW and IE Results

Test Setup

The BDS system with six wheels was connected onto a hitch of a vehicle, as shown in Figure 2.15. The IE and SASW scanning

tests were performed in two runs. For the first run, the centerlines of the left, middle, and right transducer wheels were located at Grid Lines 4.25 ft, 6.25 ft, and 10.25 ft, respectively. For the second run, the centerlines of the left, middle, and right transducer wheels were located at Grid Lines 5.25 ft, 7.25 ft, and 9.25 ft, respectively. Figure 2.16 shows the test locations from both runs.

Test Results from the SASW Scans

This section presents test results from the SASW scanning of the NCAT pavement. The test results are presented in surface wave velocity plots at different depths from 0.1 ft to 0.7 ft from the surface. Surface waves velocities are presented in a gray-scale ranging from 3,000 (shown in light gray) to 5,000 ft/s (shown in black). The higher the surface wave velocity, the better the condition of the asphalt pavement. Anomalies can
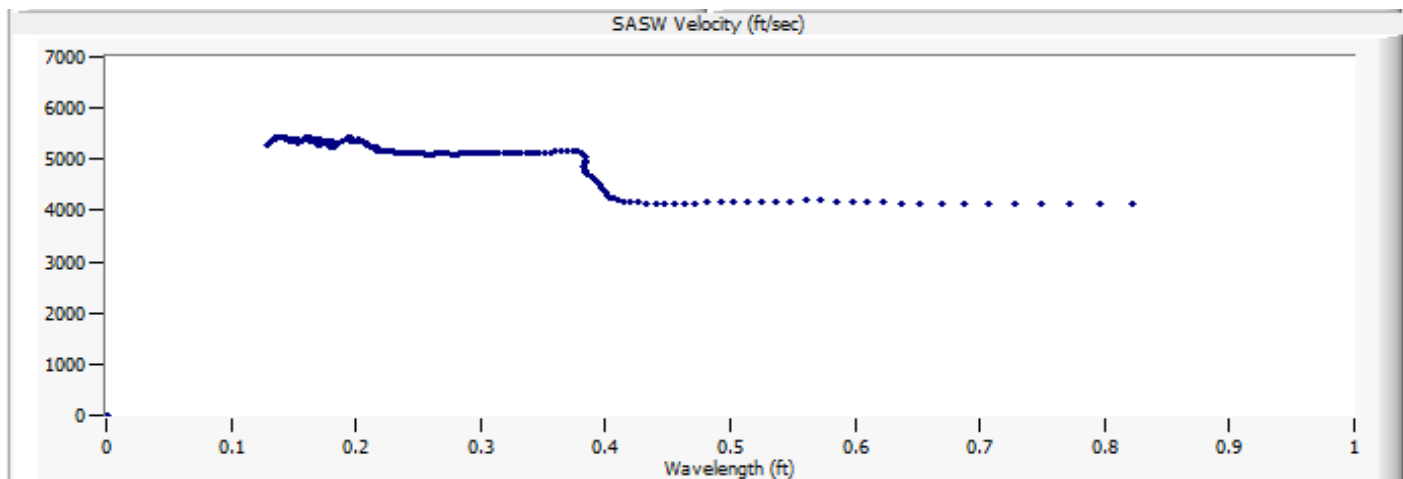
Note: Surface wave velocity decreases from ~5,200 ft/s (vertical scale) to ~4,300 ft/s at a wavelength of 0.4 ft (~5 in.) and indicates the presence of the delamination.

Figure 2.13. SASW dispersion curve example of baghouse dust delamination built at a depth of 5 in.
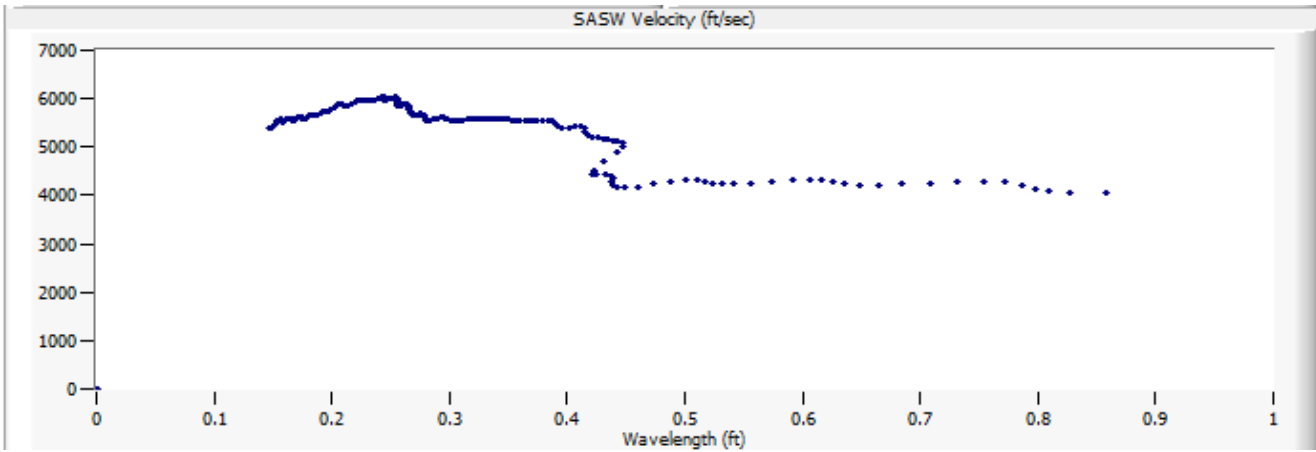
Note: Surface wave velocity decreases from ~5,300 ft/s (vertical scale) to ~4,300 ft/s at a wavelength of 0.43 ft (~5 in.) and indicates the presence of the delamination.

Figure 2.14. SASW dispersion curve example of thin paper delamination built at a depth of 5 in.

be seen as a light spot (zone) as the velocities are lower. Figures 2.17 to 2.26 present the surface wave velocity profiles from all 10 sections of the NCAT Pavement Test Track.

Reviews of Figure 2.17 (Section 1) show a drop of surface wave velocity between depths of 0.4 and 0.5 ft. Thus, the results show a likelihood of debonding between depths of 0.4 and 0.5 ft (4.8 and 6.0 in.). This interpretation of the SASW test results agrees well with the as-built condition.

Reviews of Figures 2.18 and 2.19 (Sections 2 and 3) show a sound pavement with high velocities consistently from top to bottom of the pavement. This interpretation of the SASW test results agrees well with the as-built condition.

Reviews of Figure 2.20 (Section 4) show lower velocities starting at depths of 0.3 to 0.4 ft from Grid Line 4 ft to 7 ft. This interpretation does not correlate well with the as-built condition.

Reviews of Figure 2.21 (Section 5) show that data from approximately 25% of the test locations have a drop in velocity

at depths of 0.2 to 0.3 ft. The majority of the test location shows a drop in velocity at depths of 0.3 to 0.4 ft.

Reviews of Figure 2.22 (Section 6) show low velocities from Grid Lines 9 and 10 at the shallow depth (0.1 to 0.2 ft). This low velocity indicates debonding at depths between 0.1 and 0.2 ft.

Reviews of Figure 2.23 (Section 7) show a sound pavement except at the lower-left corner (a few test locations), where the test results show a shallow delamination between 0.1 and 0.2 ft.

Reviews of Figure 2.24 (Section 8) show delamination below Grid Line 4 ft at depths between 0.4 and 0.5 ft (approximately 30% of the data points) and between depths of 0.5 and 0.6 ft (approximately 60% of the data points).

Reviews of Figure 2.25 (Section 9) show a sound pavement that does not agree with the as-built condition.

Figure 2.15. Test setup for IE and SASW at NCAT test track.

Centerline of the Transducer
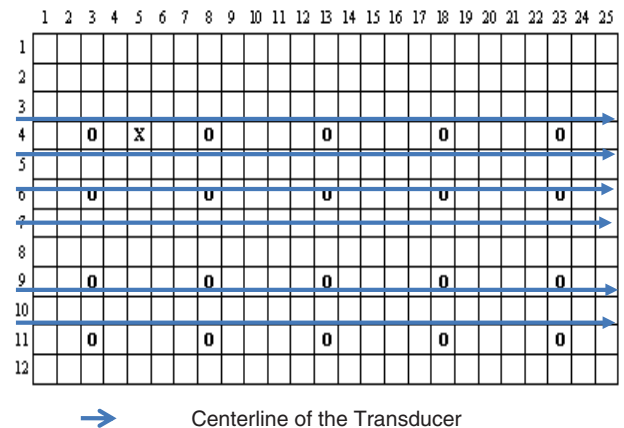
Figure 2.16. Test locations on any 25-ft sections of NCAT pavement test track.

Depth = 0.1 – 0.2 ft

Depth = 0.2 – 0.3 ft

Depth = 0.3 – 0.4 ft

Depth = 0.4 – 0.5 ft

Surface Wave
Velocity (ft/sec)

Depth = 0.5 – 0.6 ft

Depth = 0.6 – 0.7 ft
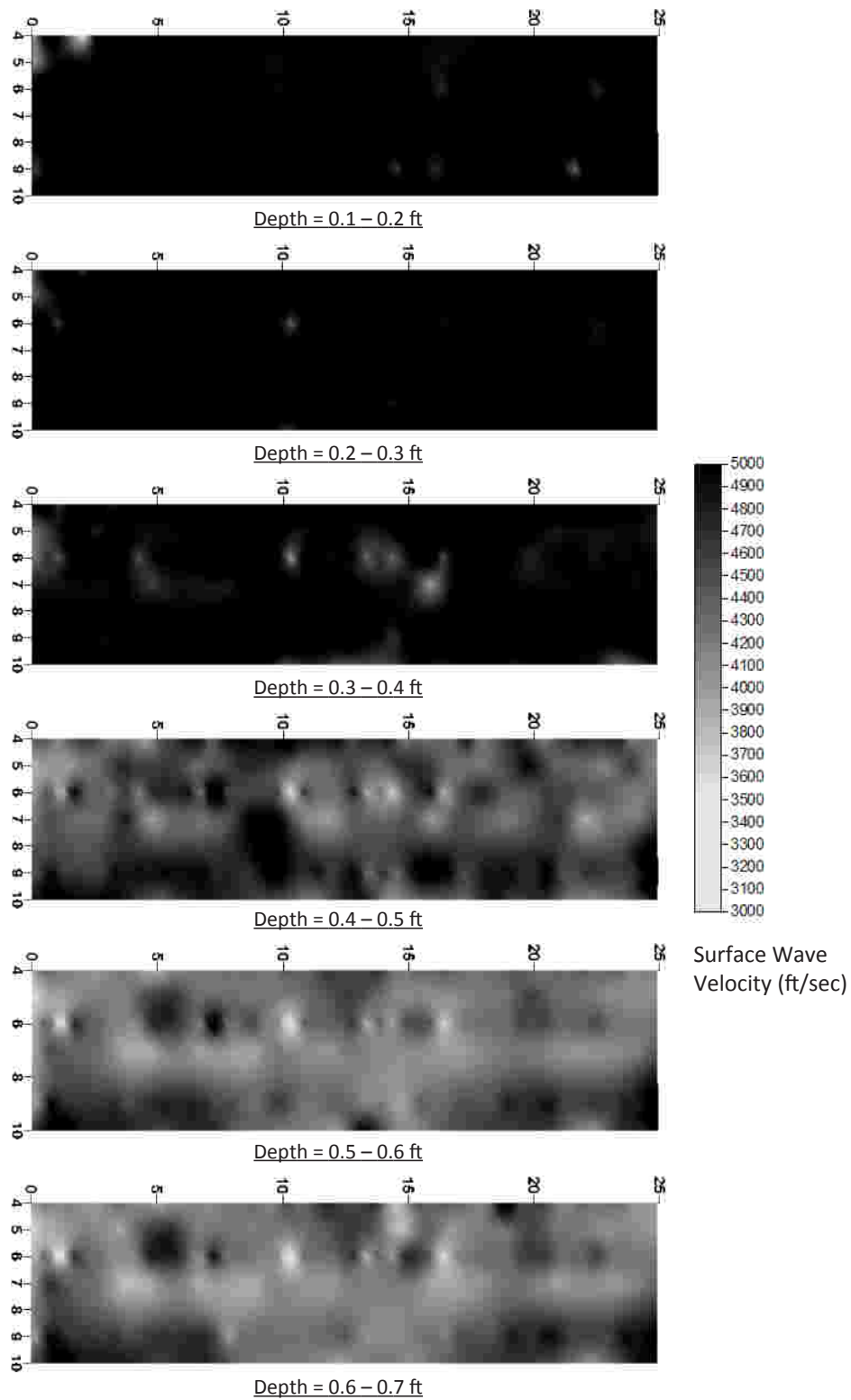
Note: Section 1 = 0 to 25 ft.

Figure 2.17. Profile plots of surface wave velocity.
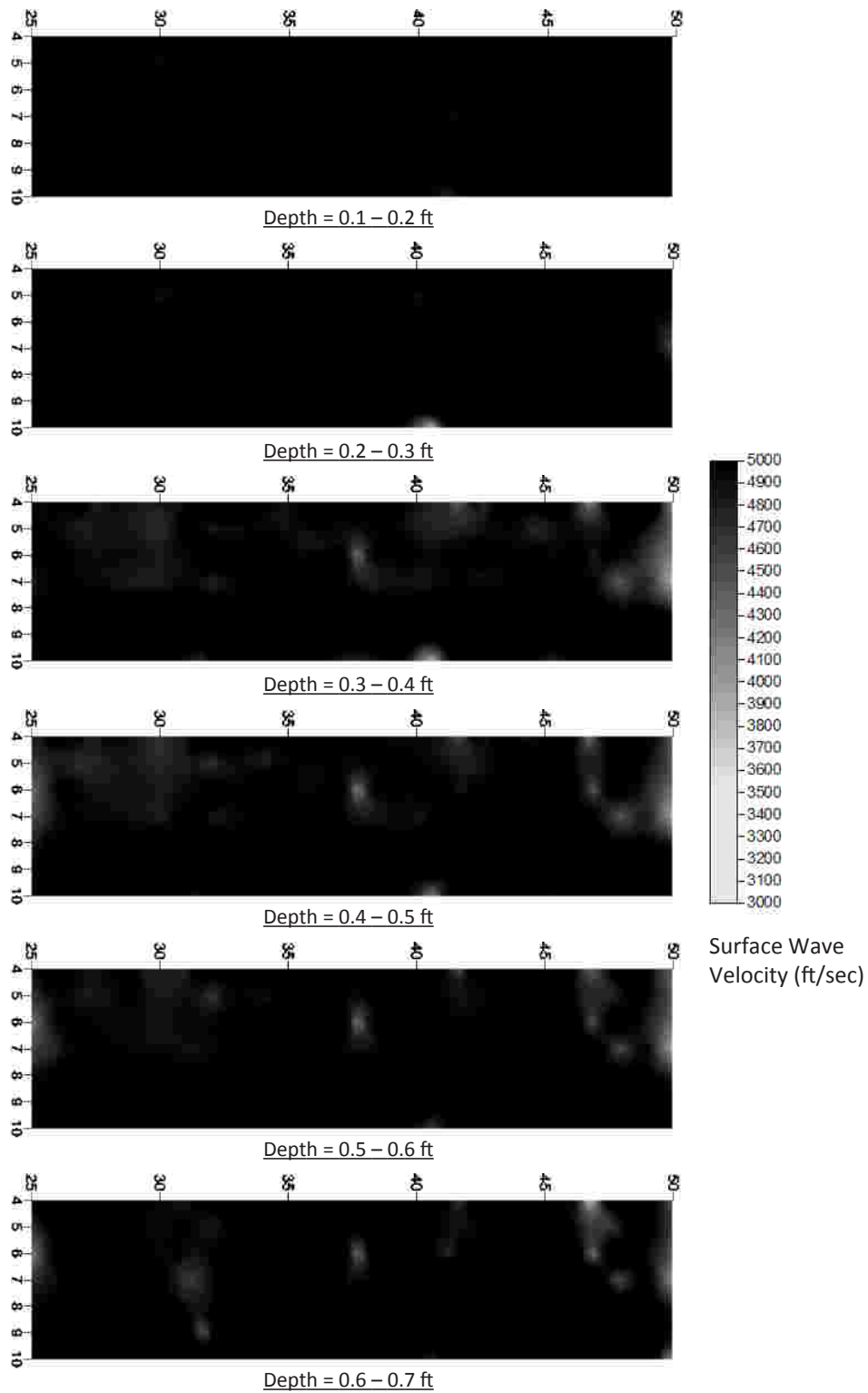
Note: Section 2 = 25 to 50 ft.

Figure 2.18. Profile plots of surface wave velocity.
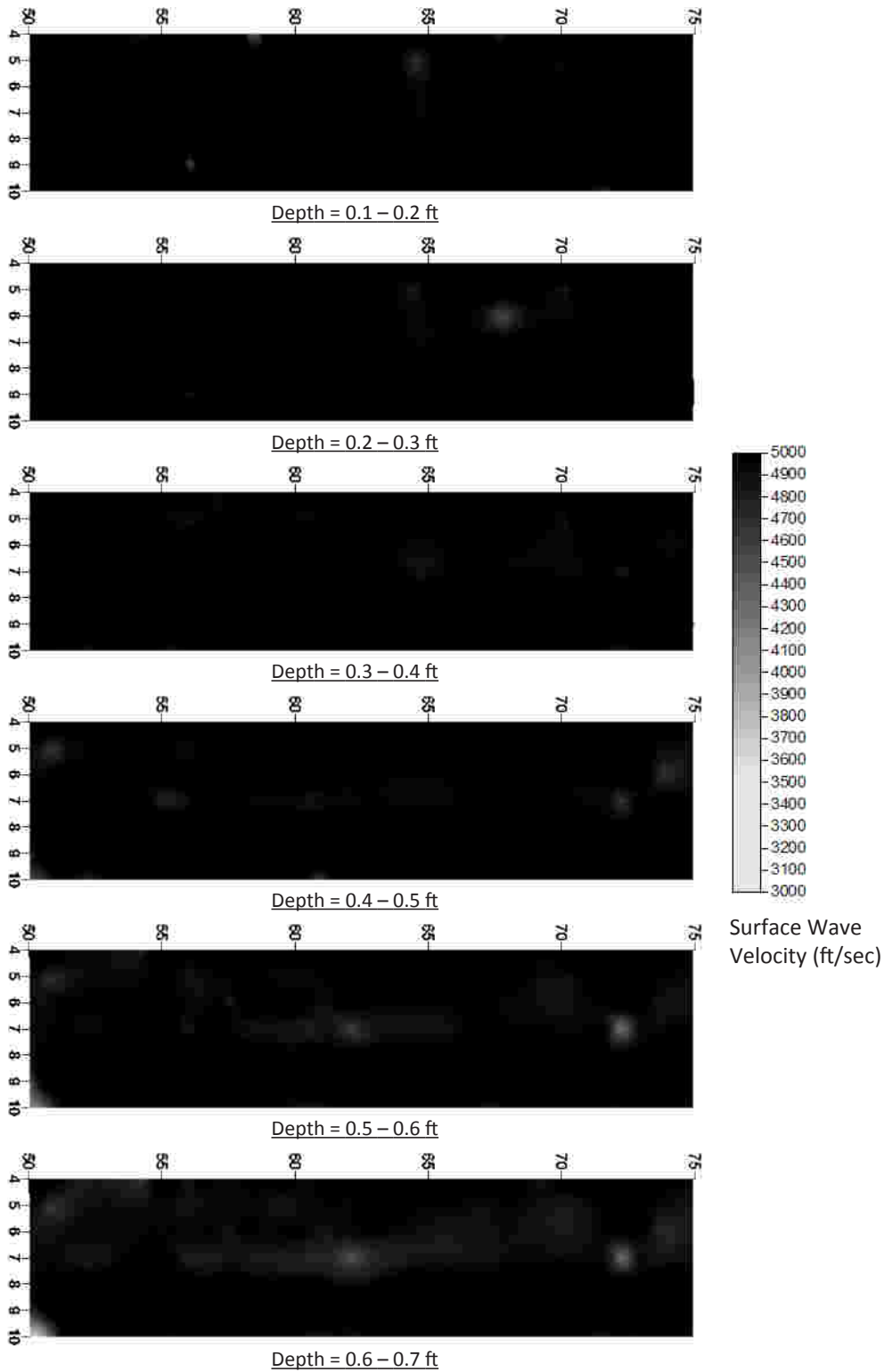
Note: Section 3 = 50 to 75 ft.

Figure 2.19. Profile plots of surface wave velocity.
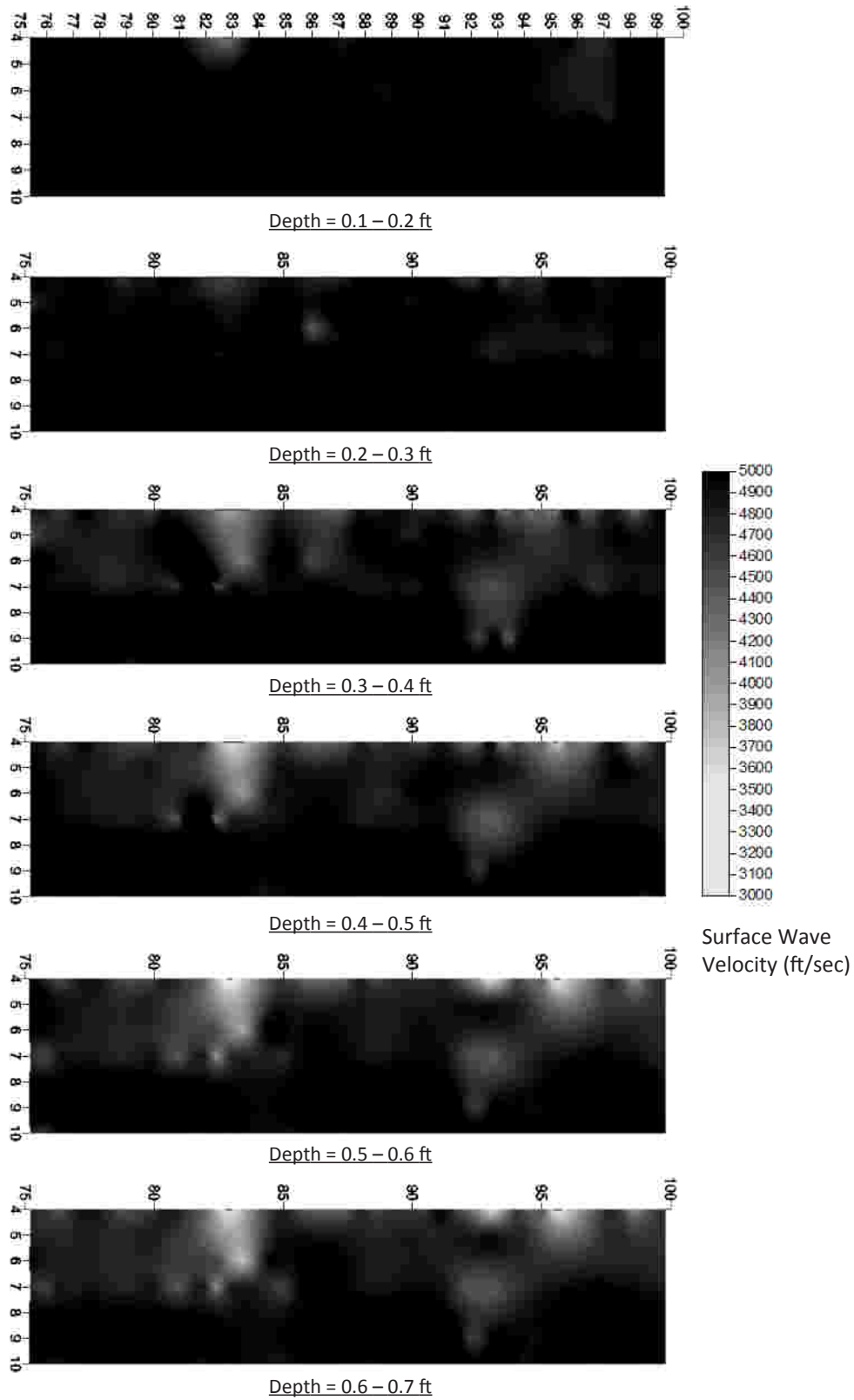
Note: Section 4 = 75 to 100 ft.

Figure 2.20. Profile plots of surface wave velocity.

Depth = 0.1 – 0.2 ft

Depth = 0.2 – 0.3 ft

Depth = 0.3 – 0.4 ft

Depth = 0.4 – 0.5 ft

Depth = 0.5 – 0.6 ft

Depth = 0.6 – 0.7 ft

Surface Wave Velocity (ft/sec)
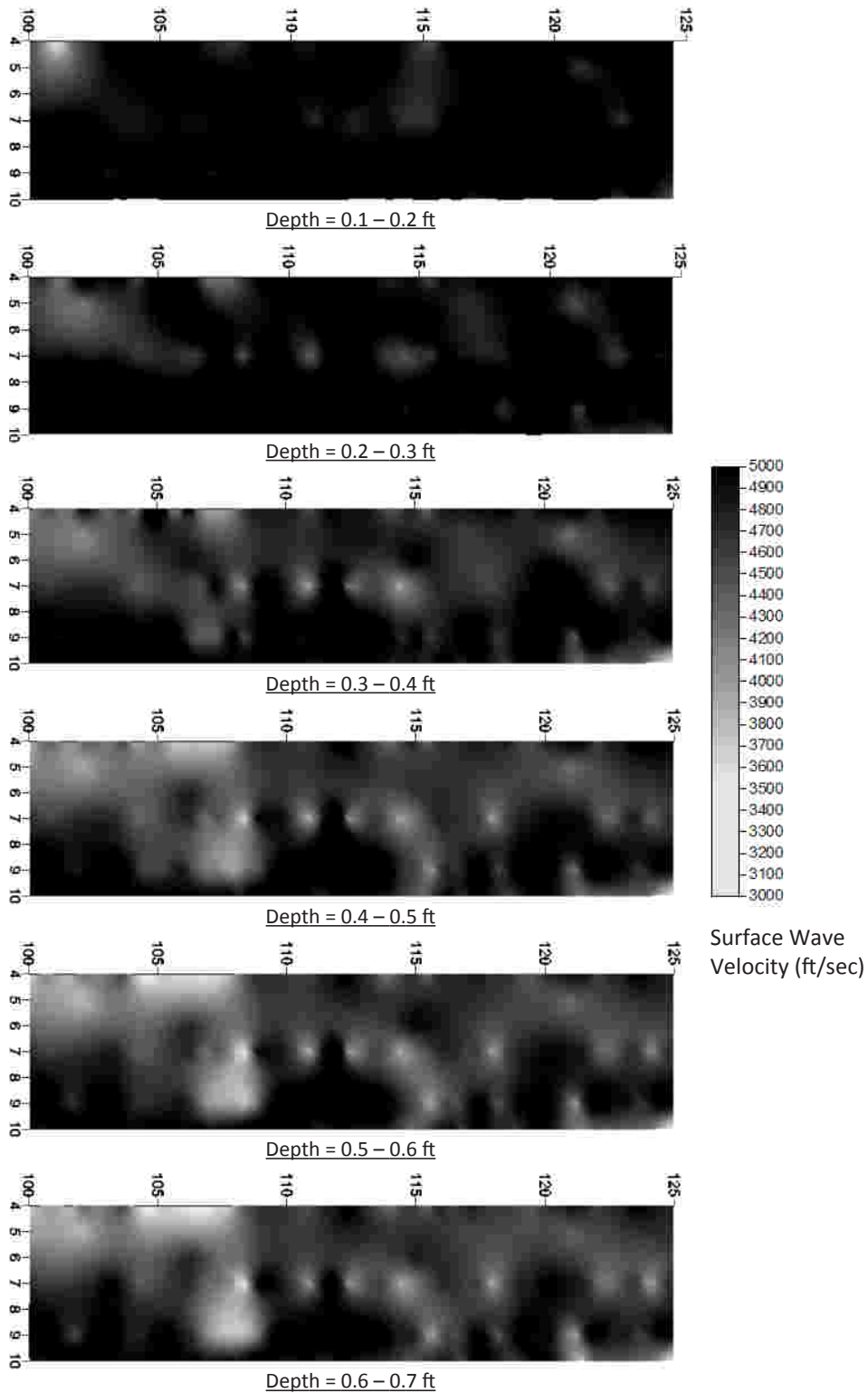
Note: Section 5 = 100 to 125 ft.

Figure 2.21. Profile plots of surface wave velocity.
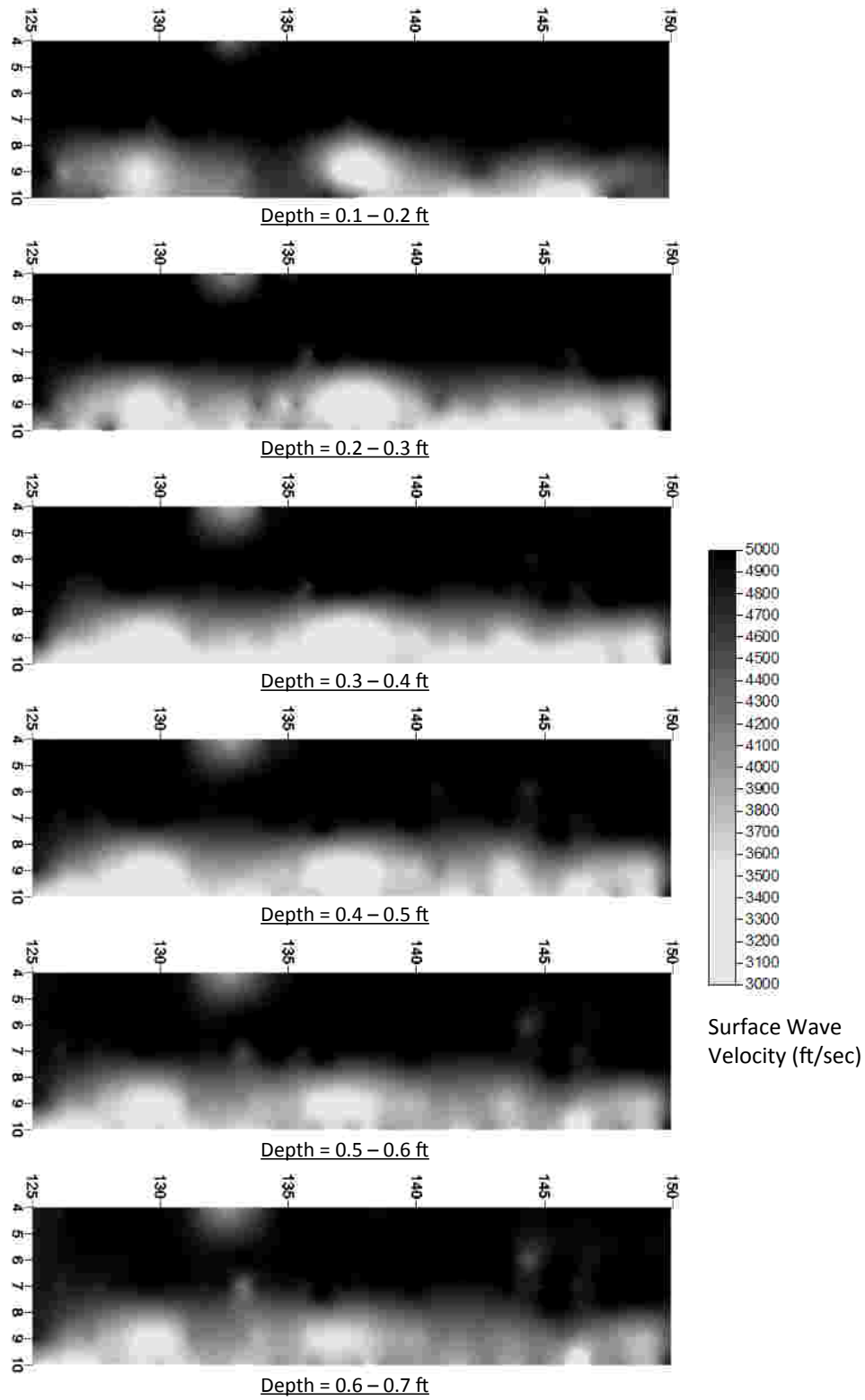
Note: Section 6 = 125 to 150 ft.

Figure 2.22. Profile plots of surface wave velocity.

Depth = 0.1 – 0.2 ft

Depth = 0.2 – 0.3 ft

Depth = 0.3 – 0.4 ft

Depth = 0.4 – 0.5 ft

Depth = 0.5 – 0.6 ft

Depth = 0.6 – 0.7 ft

Surface Wave Velocity (ft/sec)
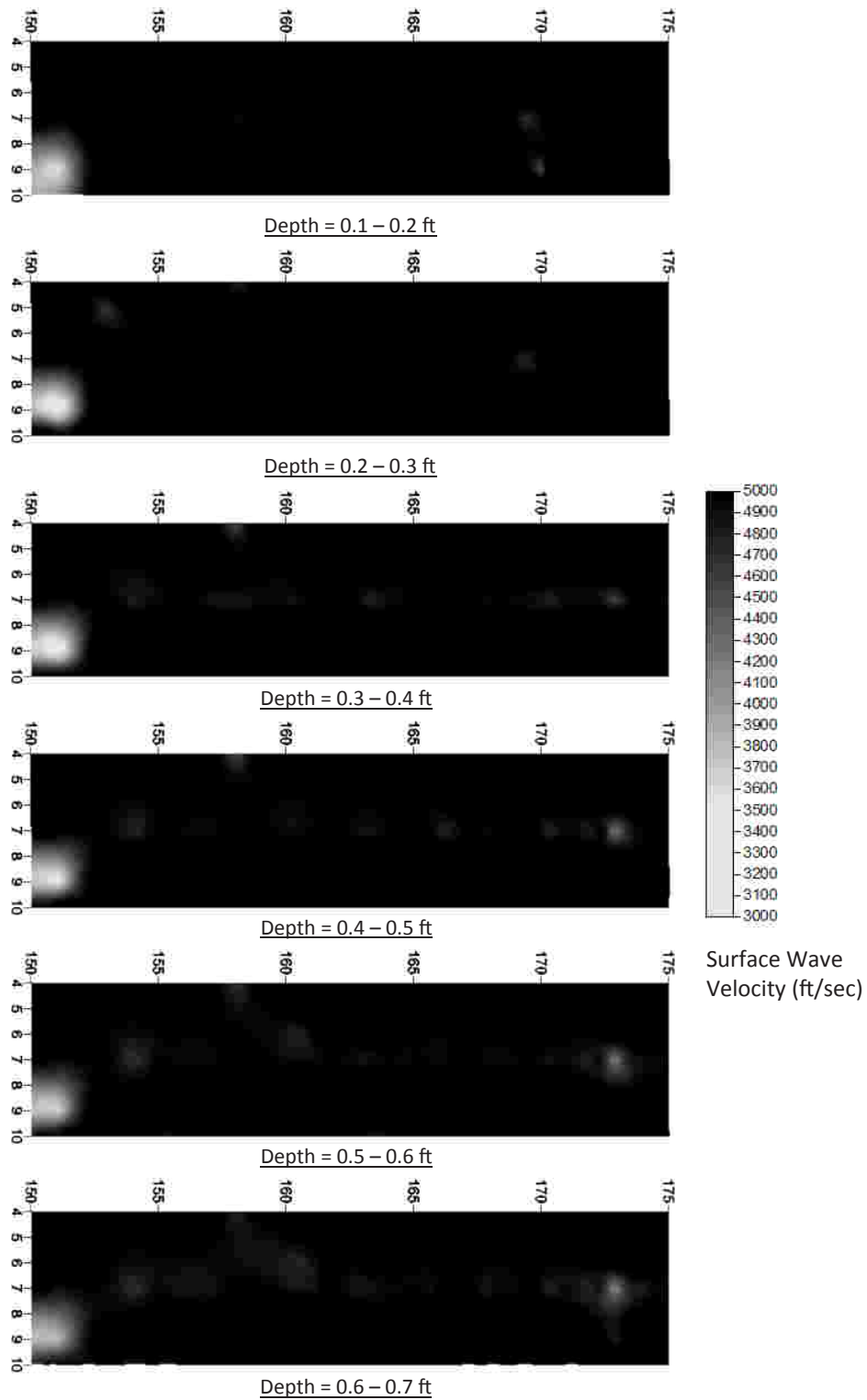
Note: Section 7 = 150 to 175 ft.

Figure 2.23. Profile plots of surface wave velocity.

Depth = 0.1 – 0.2 ft

Depth = 0.2 – 0.3 ft

Depth = 0.3 – 0.4 ft

Depth = 0.4 – 0.5 ft

Surface Wave
Velocity (ft/sec)

Depth = 0.5 – 0.6 ft

Depth = 0.6 – 0.7 ft
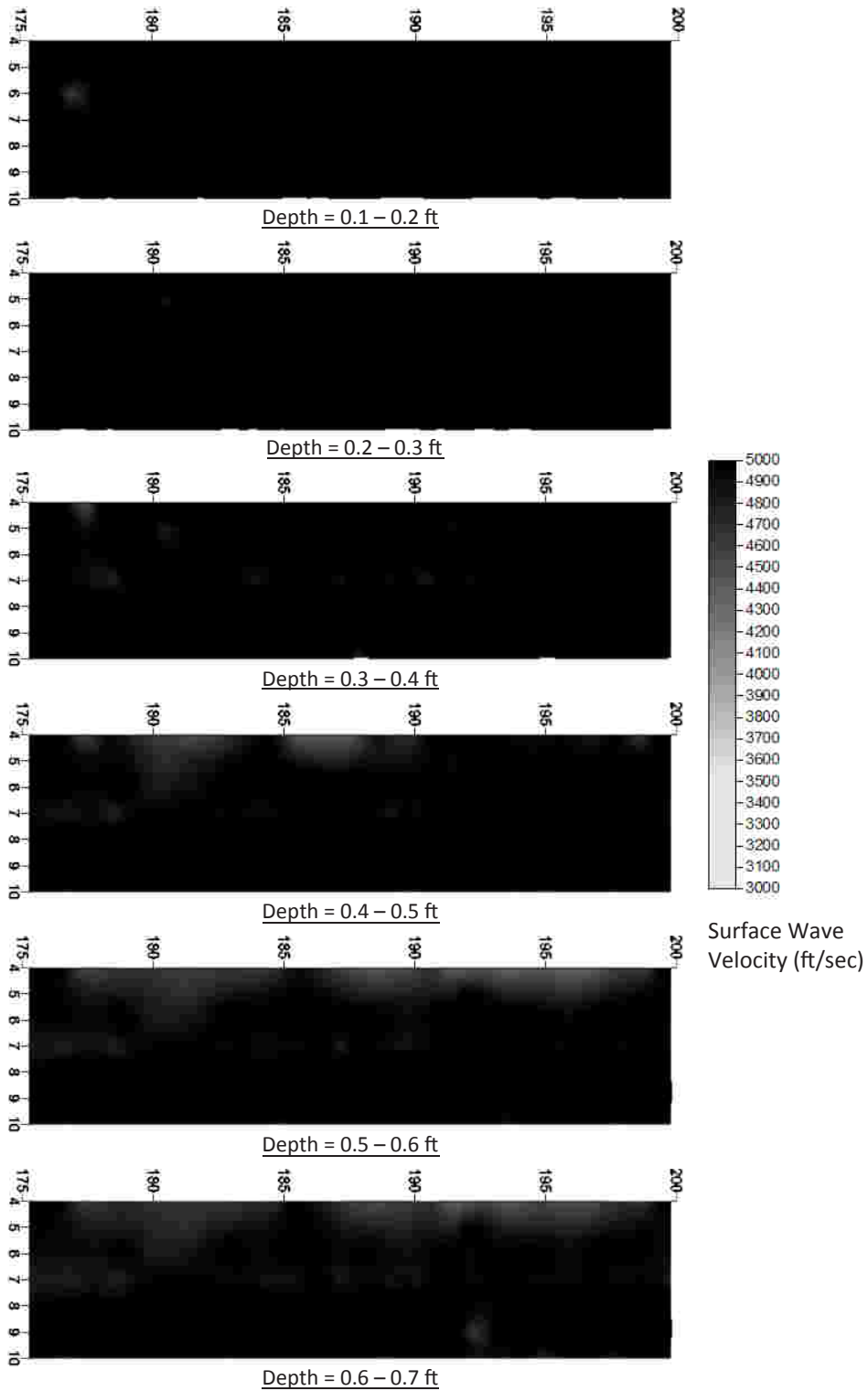
Note: Section 8 = 175 to 200 ft.

Figure 2.24. Profile plots of surface wave velocity.

Depth = 0.1 – 0.2 ft

Depth = 0.2 – 0.3 ft

Depth = 0.3 – 0.4 ft

Depth = 0.4 – 0.5 ft

Surface Wave
Velocity (ft/sec)

Depth = 0.5 – 0.6 ft

Depth = 0.6 – 0.7 ft
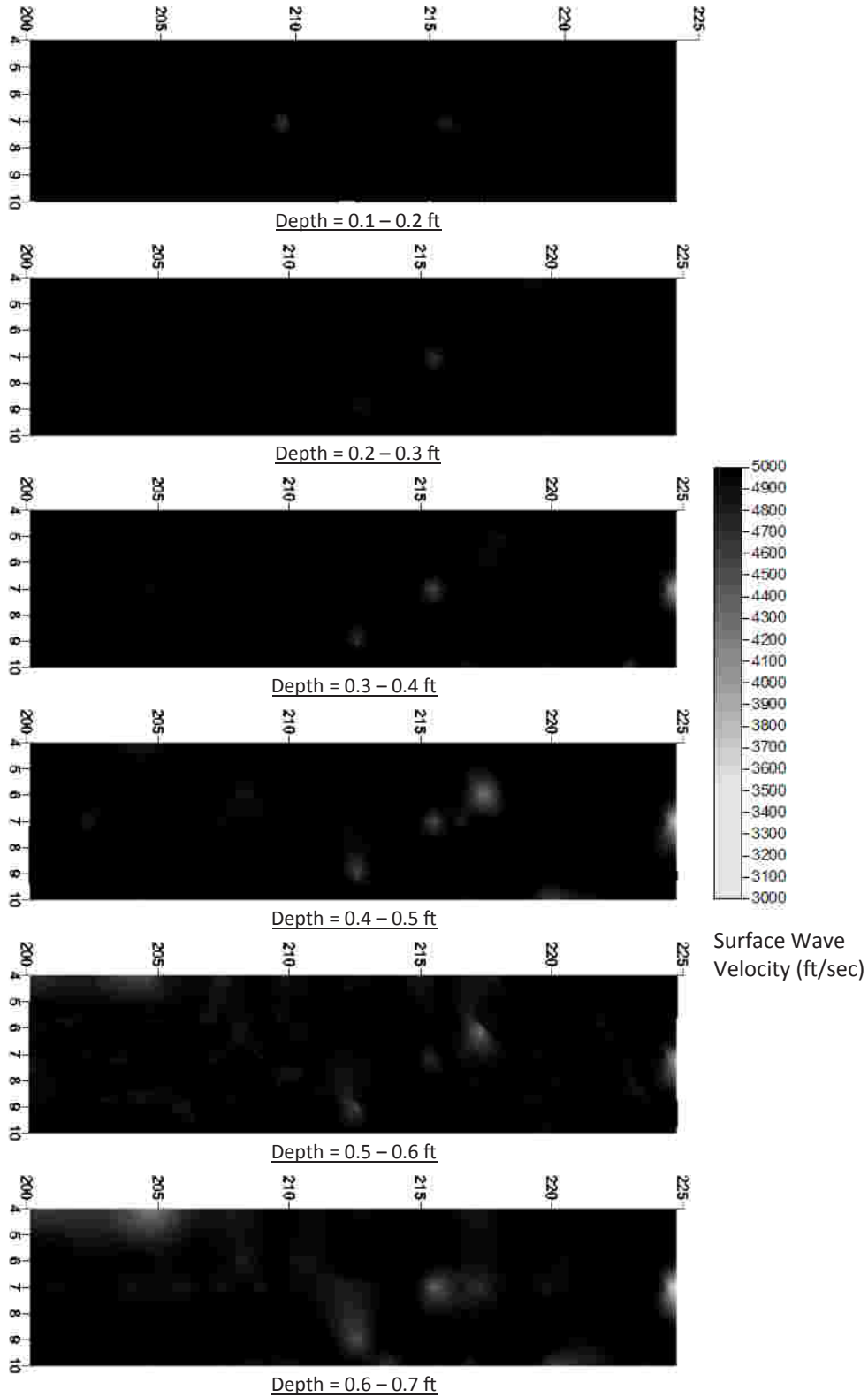
Note: Section 9 = 200 to 225 ft.

Figure 2.25. Profile plots of surface wave velocity.

Depth = 0.1 – 0.2 ft

Depth = 0.2 – 0.3 ft

Depth = 0.3 – 0.4 ft

Depth = 0.4 – 0.5 ft

Depth = 0.5 – 0.6 ft

Depth = 0.6 – 0.7 ft

Surface Wave
Velocity (ft/sec)
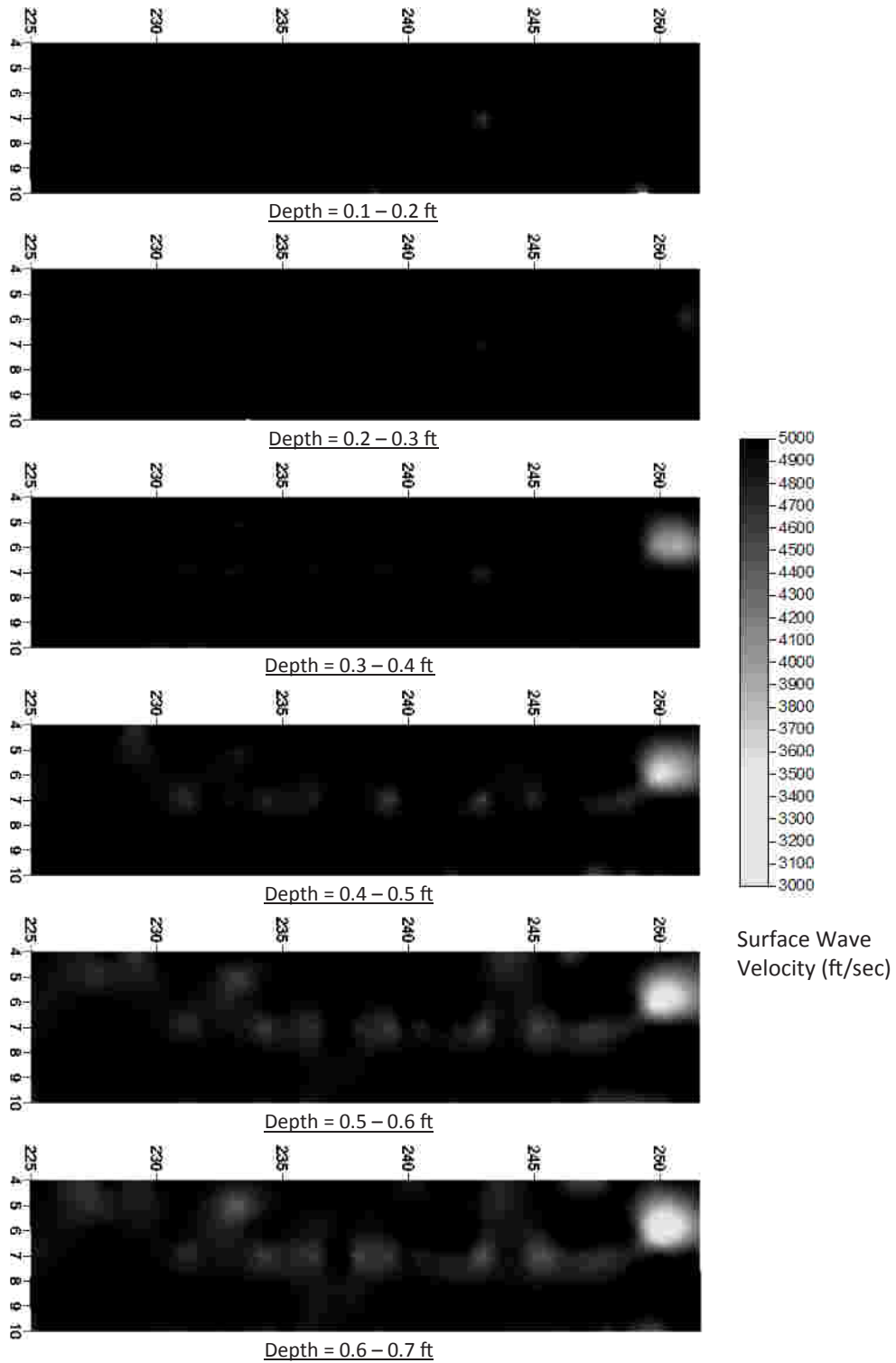
Note: Section 10 = 225 to 250 ft.

Figure 2.26. Profile plots of surface wave velocity.

(continued from page 15)

Reviews of Figure 2.26 (Section 10) show delamination below Grid Lines 6 and 7. The SASW scanning was performed past the end of the pavement section and the excess data are included in the plots.

Test Results from the IE Tests

Figure 2.27 shows the test results from the IE tests on the tested sections of the NCAT track. The plots are surface thickness tomograms separated into 50-ft sections and presented in a three-dimensional (3-D) thickness tomogram to graphically show the general condition of the tested pavement at the NCAT site. The color thickness/echo depth scales are in inches and are presented in Figure 2.27. Gray represents sound pavements where shallow echoes (indicative of delaminations) are not present. Red represents debonding at depths between 4 and 6 in. Yellow represents debonding at depths between 2 and 4 in.

Review of Figure 2.27 shows that the test results from the IE tests correctly identified debonding conditions at a depth

of 5 in. (Section 1 = 0 to 25 ft and Section 8 = 175 to 200 ft). Less than 25% of the test results from the IE tests correctly identified the debonding conditions at a depth of 5 in. in Sections 9 and 10 (200 to 250 ft). The IE test results were not able to identify the shallow debonding at 2 in. that was reported to be present in several sections as either a distinct echo peak corresponding to the depth of the debonding, or as a low-frequency flexural response indicative of delaminations. The asphalt surface temperature ranged from 61°F to 67°F during testing on February 27, 2011. This was warmer than during Phase 1 testing, when the asphalt surface temperature ranged from 54°F to 57°F during testing on March 19, 2010.

Florida Pavement Results

Test Setup

The Florida test site was on I-75 near Gainesville, Florida. The BDS system was connected to the hitch of a towing vehicle, as shown in Figure 2.28. The six transducer wheels were coupled
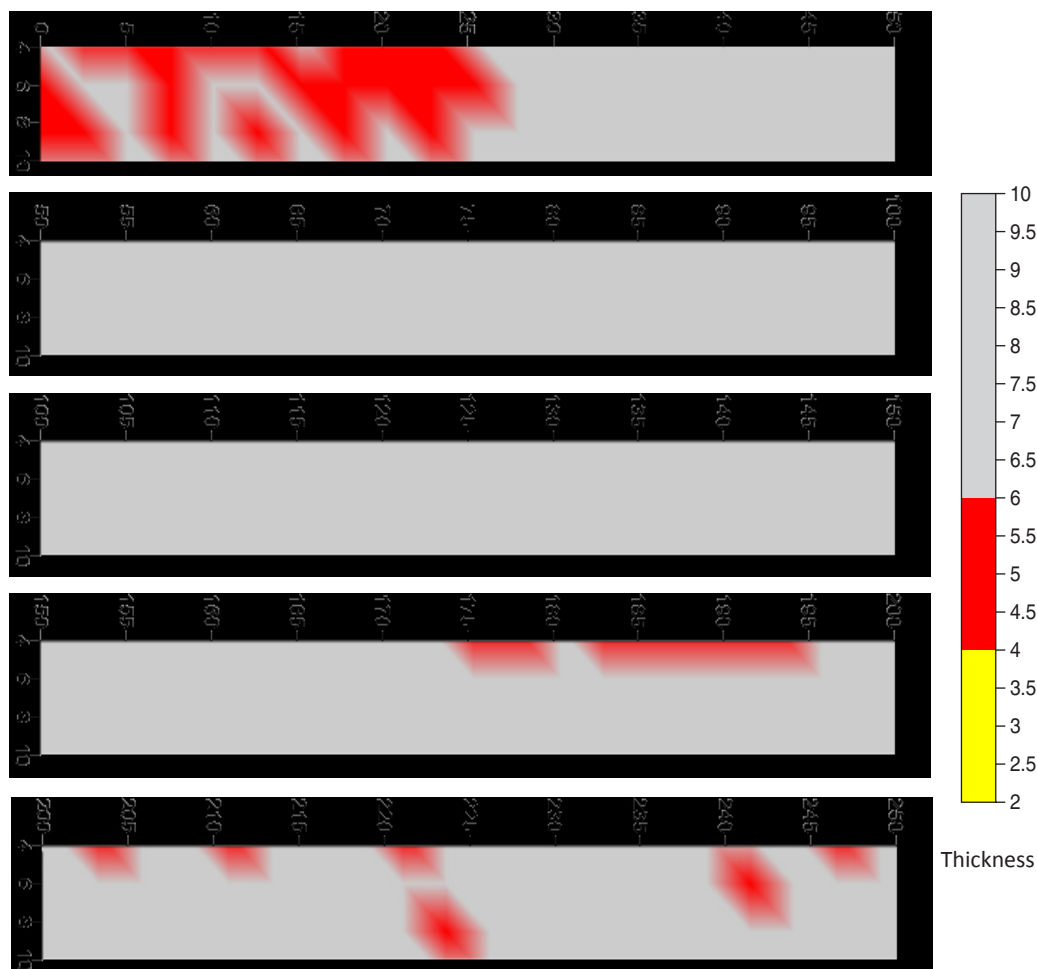
Note: Deeper delaminations are shown in red; shallow delaminations would be shown in yellow although none could be identified with the IE tests.

Figure 2.27. IE test results from the pavement at the NCAT site.

Note: The wheel pairs were spaced at 6 in.; separate wheel pairs were spaced at 2 ft on-center and two separate runs were performed to cover entire lane width.

Figure 2.28. Test setup for Florida test site with six transducer wheels.

into three pairs of two wheels. Each pair of wheels was set 6 in. apart. Separate pairs of wheels were spaced at 2 to 3 ft on-center from one another. The IE and SASW scanning was performed in two runs. For the first run, the centerlines of the right, middle, and left transducer wheel pairs were located at 3, 1, and −1 ft (0 is the centerline of the tested lane), respectively. For the second run, the test centerline locations were located at −0.5, 3, and 5 ft, respectively.

Test Results from SASW Scanning

Figures 3.1 through 3.44 in Chapter 3 of this volume graphically present the SASW results from the Florida pavement in 50-foot sections to allow detailed assessment. The discussion of the results that follows applies to overall trends within the data. The test results are presented in surface wave velocity

plots at different depths from 0.1 ft to 0.7 ft from the surface. Surface wave velocities are presented with a color scale ranging from 3,500 to 1,000 ft/s. This color scale is lower than that used at the NCAT test site, which had smooth asphalt and was adjusted based on the specific site results. In general, the higher the surface wave velocity, the better condition of the asphalt pavement. Anomalies can be observed as light spots (or zones) where the surface wave velocity is notably lower.

Overall, there were three categories of test results observed from the Florida test site. These categories include

1. A relatively constant and high value (≥3,500 ft/s) of surface wave velocity from depths of 0.1 to 0.7 ft, as shown in Figure 2.29. This condition indicates sound pavement. Note that fewer than 2% of the tested locations were assessed with this condition.
2. A sharp drop (≥500 ft/s drop) of surface wave velocity between 0.2 and 0.4 ft. The location of the drop was most likely the depth of debonding or a thin layer of low velocity (low strength) material. Figure 2.30 presents a dispersion curve from a location where debonding (or a layer of low-strength material) was most likely present at around 0.24 ft. Note that the majority of test results presented this type of condition.
3. A slow drop of surface wave velocity in the dispersion curve, as shown in Figure 2.31. This category indicates the condition of degradation of pavement at greater depths. Note that approximately 5% of the tested locations were identified with this type of condition.

Although a significant amount of surface distress was observed on the surface of the test pavement, the majority of the data from the Florida test site had relatively high surface wave velocities (>3,500 ft/s) near the pavement surface (depths between 0.1 and 0.2 ft). This indicates that the visually observed distress only occurs on the shallow surface of the pavement.
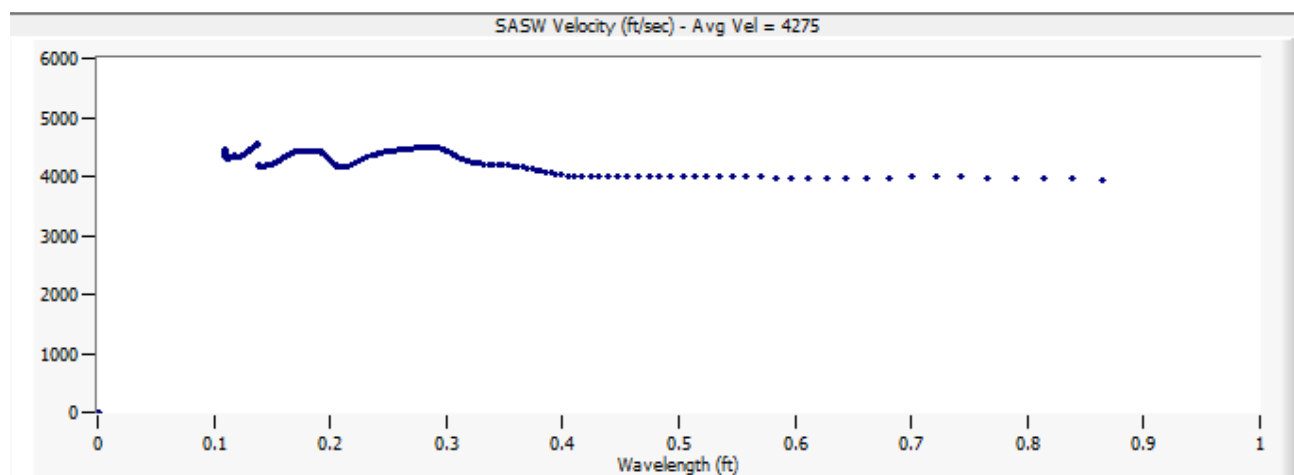
Figure 2.29. Example of dispersion curve indicative of sound pavement.
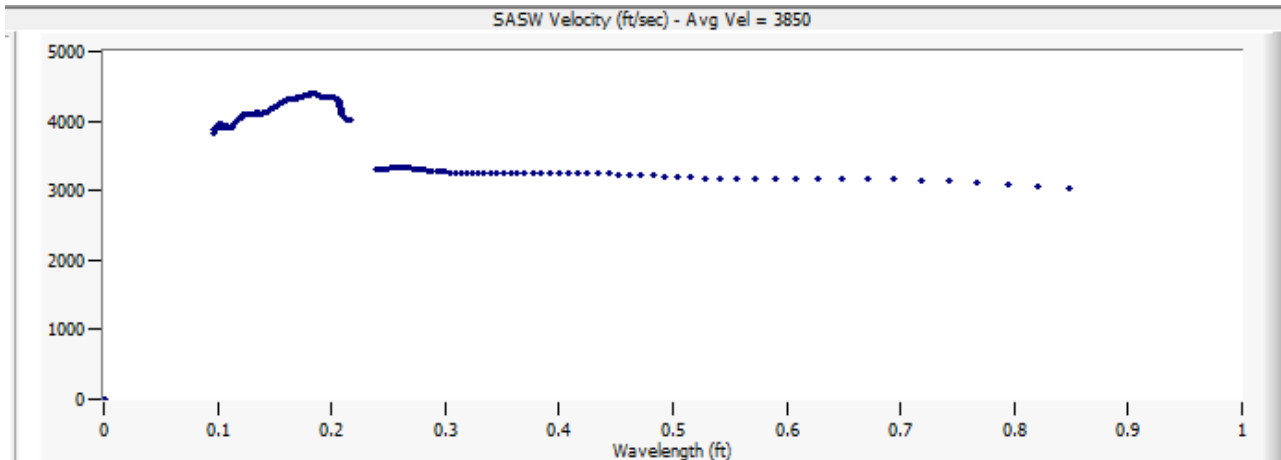
Figure 2.30. Example of dispersion curve indicative of debonding condition.

In general, the conditions of all test locations on the 2,000-ft section of the tested Florida pavement are similar. The majority of test locations showed a sharp drop of surface velocity at depths between 0.2 and 0.4 ft. This drop is indicative of either possible debonding at these depths or the existence of a thin layer of low-strength material at those depths. In addition, the condition of the pavement at the centerline of the lane seemed to be in better condition than that of the wheelpaths. Last, the pavement on the right wheelpath (0 to −5 ft) appeared to be in worse condition than that of the left wheelpath (0 to 5 ft). It should be noted that the Florida pavement was rough with exposed aggregate as compared to the smoother Kansas pavement and the smooth NCAT test track.

Kansas Pavement Results

Test Setup

The Kansas test site was on US-400 near Pittsburg, Kansas. The BDS system was connected to the hitch of a towing vehicle, as

shown in Figure 2.32. The six transducer wheels were coupled into three pairs of two. Each pair of wheels was set at a spacing of 6 in. Separate pairs of wheels were spaced at 2 ft on-center from one another. The IE and SASW scanning tests were performed in two runs. For the first run, the centerlines of the right, middle, and left transducer wheel pairs were located at 10.7, 8.7, and 6.7 ft from the centerline of the roadway, respectively. For the second run, the test centerline locations were at 5.7, 3.7, and 1.7 ft from the roadway centerline, respectively.

Test Results from the SASW Scanning

Figures 4.1 through 4.72 in Chapter 4 graphically present the SASW results in 50-foot sections to allow detailed assessment. This discussion of the results applies to overall trends within the data. The test results are presented in surface wave velocity plots at different depths from 0.1 ft to 0.7 ft from the surface. Surface wave velocities are presented with a color scale ranging from 3,000 to 1,000 ft/s. This color scale is lower
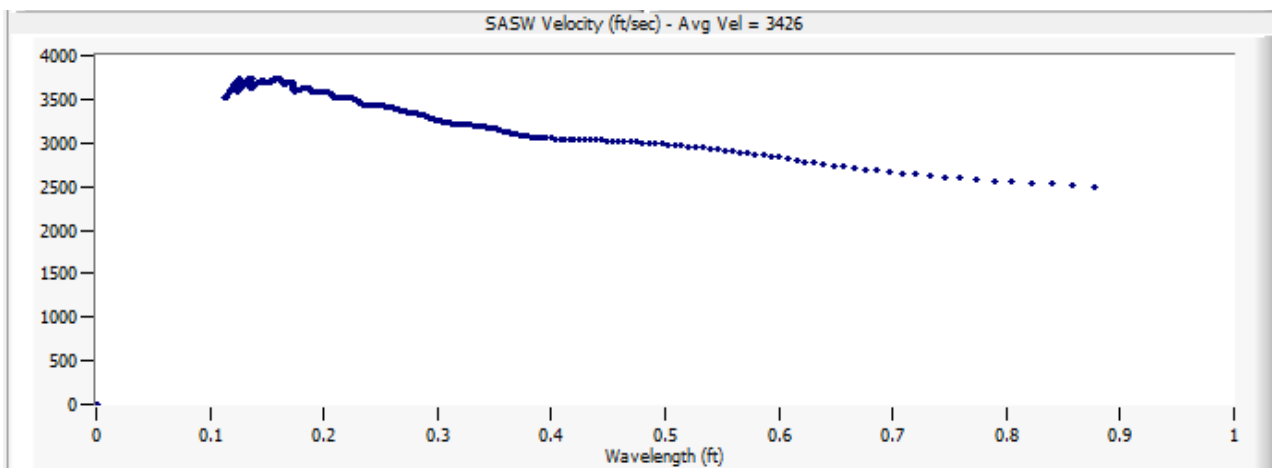
Figure 2.31. Example of dispersion curve indicative of degradation of pavement at greater depths.

Note: The wheel pairs were spaced at 6 in.; separate wheel pairs were spaced at 2 feet on-center, and two separate runs were performed to cover the entire lane width.

Figure 2.32. Test setup for Kansas test site with six transducer wheels.

than that used at the NCAT test site and was adjusted on the basis of specific site results. In general, the higher the surface wave velocity, the better the condition of the asphalt pavement. Anomalies can be observed as light spots (or zones) where the surface wave velocity is notably lower.

Overall, the majority of the data from the Kansas test site had relatively high surface wave velocities (>3,000 ft/s) near the pavement surface (<0.3 ft deep) and decreasing velocities with depth, thus indicating weaker underlying materials. Overall interpretation of the data is that the road has a relatively new asphalt overlay of good condition with an older underlying pavement composed of weaker material with widely variable condition. In some areas, the velocity decrease with depth was gradual and was interpreted as an expected result of newer materials overlaying older material. However, in other areas the velocity decrease was sharp and severe, indicating that the underlying materials were of poor condition. Sharp drops in the dispersion curve (such as those observed at the NCAT test track) were not typically observed in the data. Instead, the drop

in the surface wave velocity was typically steady and indicated a more gradual change in material strength with depth. However, the degree of change appears severe. In many areas, dispersion curves at depths of 0.4 to 0.7 ft were less than half of those at the pavement surface.

- 0 to 160 ft. In this section the roadway is actually a concrete bridge deck that had velocity far above the color scale maximum of 3,000 ft/s.
- 160 to 210 ft. The section immediately after the concrete bridge had relatively high velocities throughout the pavement section and exhibited less of a velocity decrease with depth. This may indicate stiffer subbase preparation for the bridge approach slab.
- 210 to 350 ft. In relation to much of the Kansas test segment, this section appeared to be in reasonably good condition with slightly lower velocities and velocity values decreasing with depth.
- 350 to 1,000 ft. This section showed significant degradation with depth from 0 to 5 ft from the centerline of the roadway. As noted above, the surface layer still had reasonably sound velocities, but the lower layers had significantly lower velocities.
- 1,000 to 2,200 ft. The degradation in this section was similar to that in the previous section but extended across the full lane width. Again, the surface layer had reasonable surface wave velocities, which then drastically decreased with depth.
- 2,200 to 2,500 ft. This section had relatively high velocities throughout the cross section and was considered one of the best areas of the test segment.
- 2,500 to 3,100 ft. This section showed typical degradation, increases with depth, and full lane width.
- 3,100 to 3,285 ft. This section has relatively high velocities throughout the cross section and was considered one of the best areas of the test segment.
- 3,285 to 3,495 ft. This section showed typical degradation, increases with depth, and full lane width.
- 3,495 to 3,600 ft. This section had relatively high velocities throughout the cross section and was considered one of the best areas of the test segment.

CHAPTER 3

Olson Engineering, Inc., SASW Test Results from Florida Test Section

This chapter describes the results of Phase 2 subcontract research conducted by Olson Engineering, Inc., at the National Center for Asphalt Technology (NCAT), Auburn University, in Alabama, and at test sites in Gainesville, Florida. The research examined nondestructive testing (NDT) and evaluation of the pavement at these sites with stress wave methods for debonded hot-mix asphalt (HMA) layers. The field portion of this investigation was performed in accordance with generally accepted testing procedures. Research team members were Patrick K. Miller, Yajai Tinkey, and Larry D. Olson.

Field testing of the Olson scanning IE/SASW system was carried out in Florida on a selected 0.4-mi section of I-75. The distance log was recorded as 0 to 2,167 ft. This chapter provides a graphical summary of the SASW results for each 50-ft length. The results are presented for incremental depths from 0.1 to 0.7 ft from the surface. The surface wave velocities are shown by using a color scale, and higher velocities represent better pavement condition. Analysis of these data are reported in Volume 1. Figures 3.1 to 3.44 present various SASW test results.

Note: Length = 0 to 50 ft.
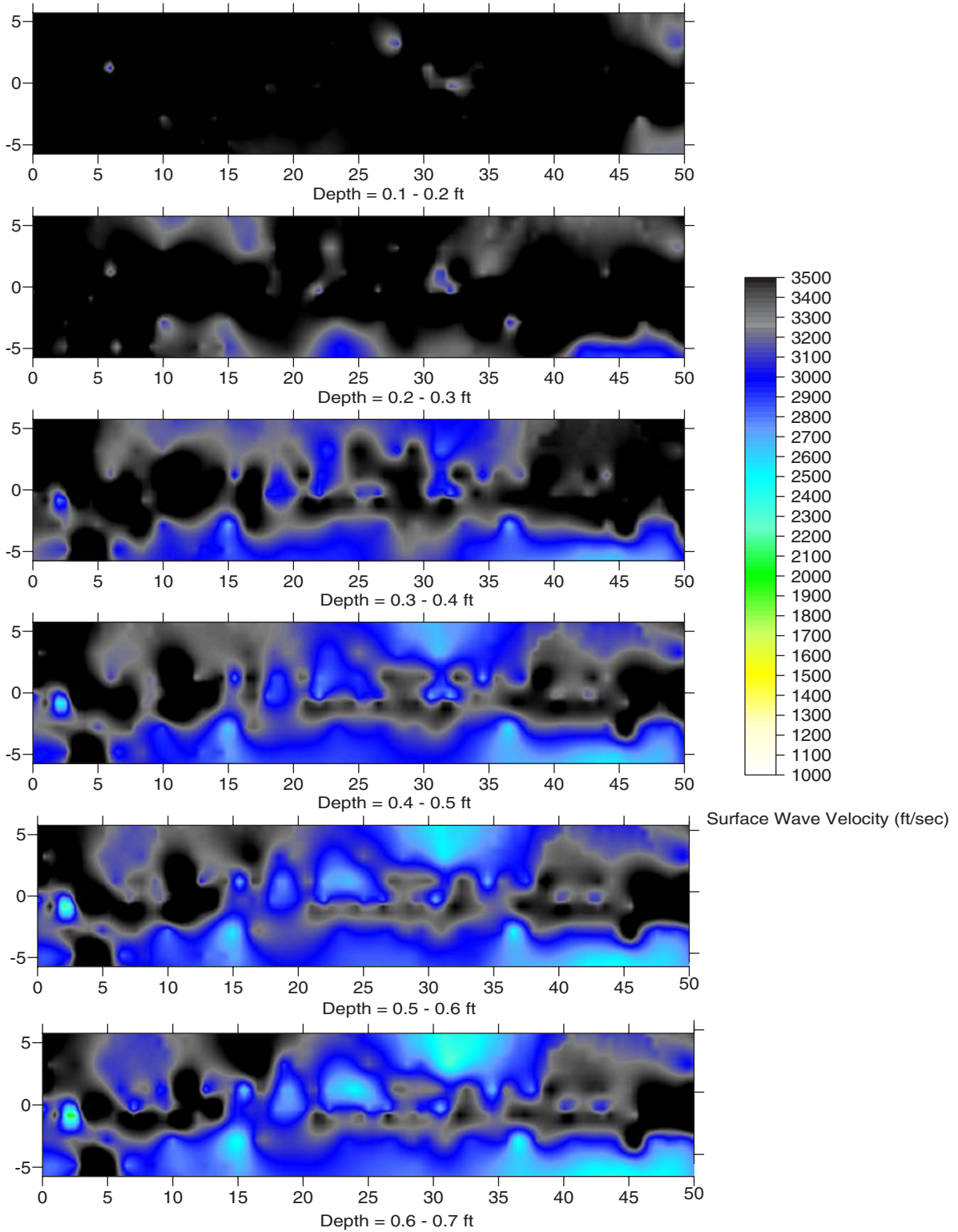
Figure 3.1. SASW test results from the Florida section.

Figure 3.2. SASW test results from the Florida section.
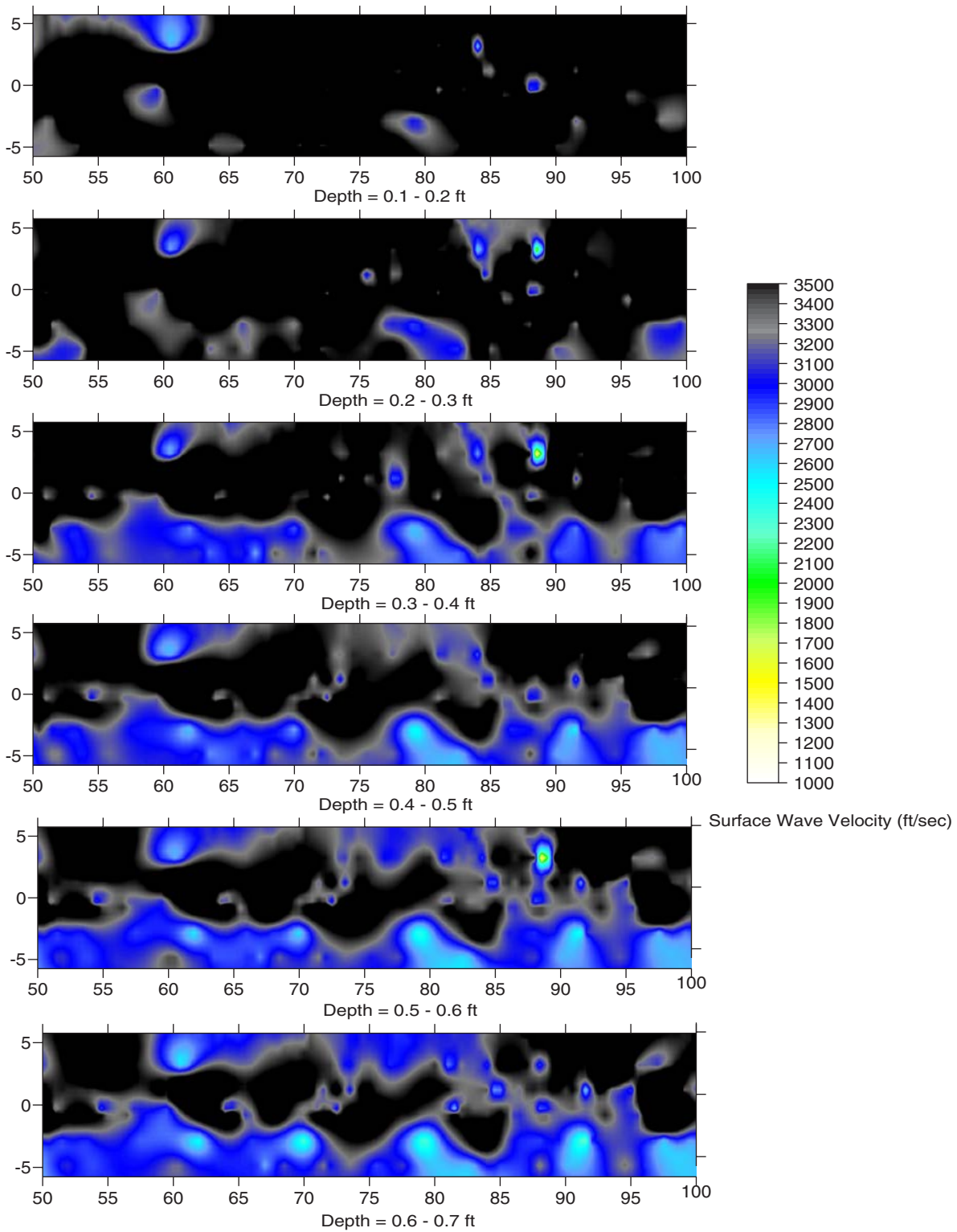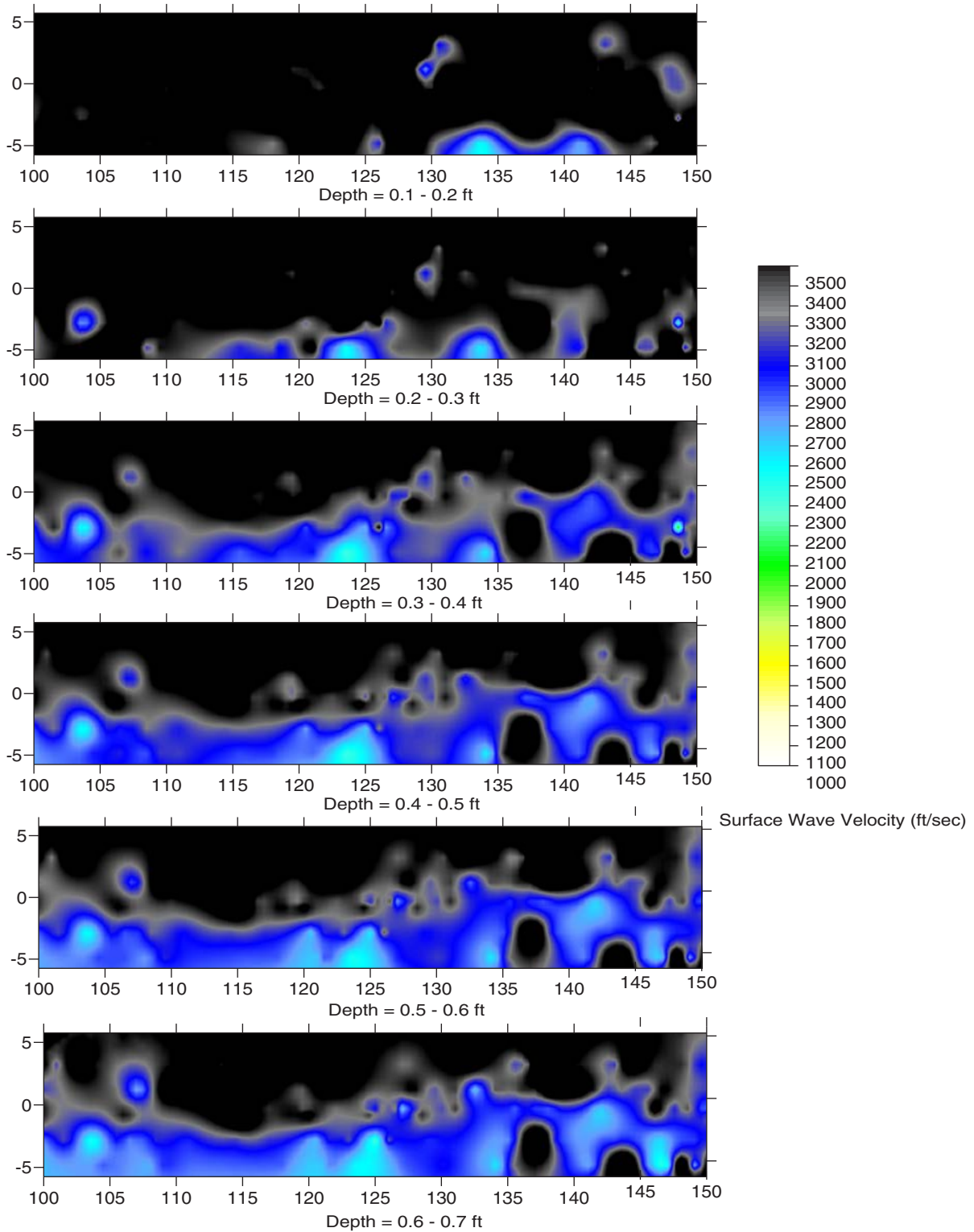
Note: Length = 50 to 100 ft.

Figure 3.3. SASW test results from the Florida section.

Note: Length = 100 to 150 ft.
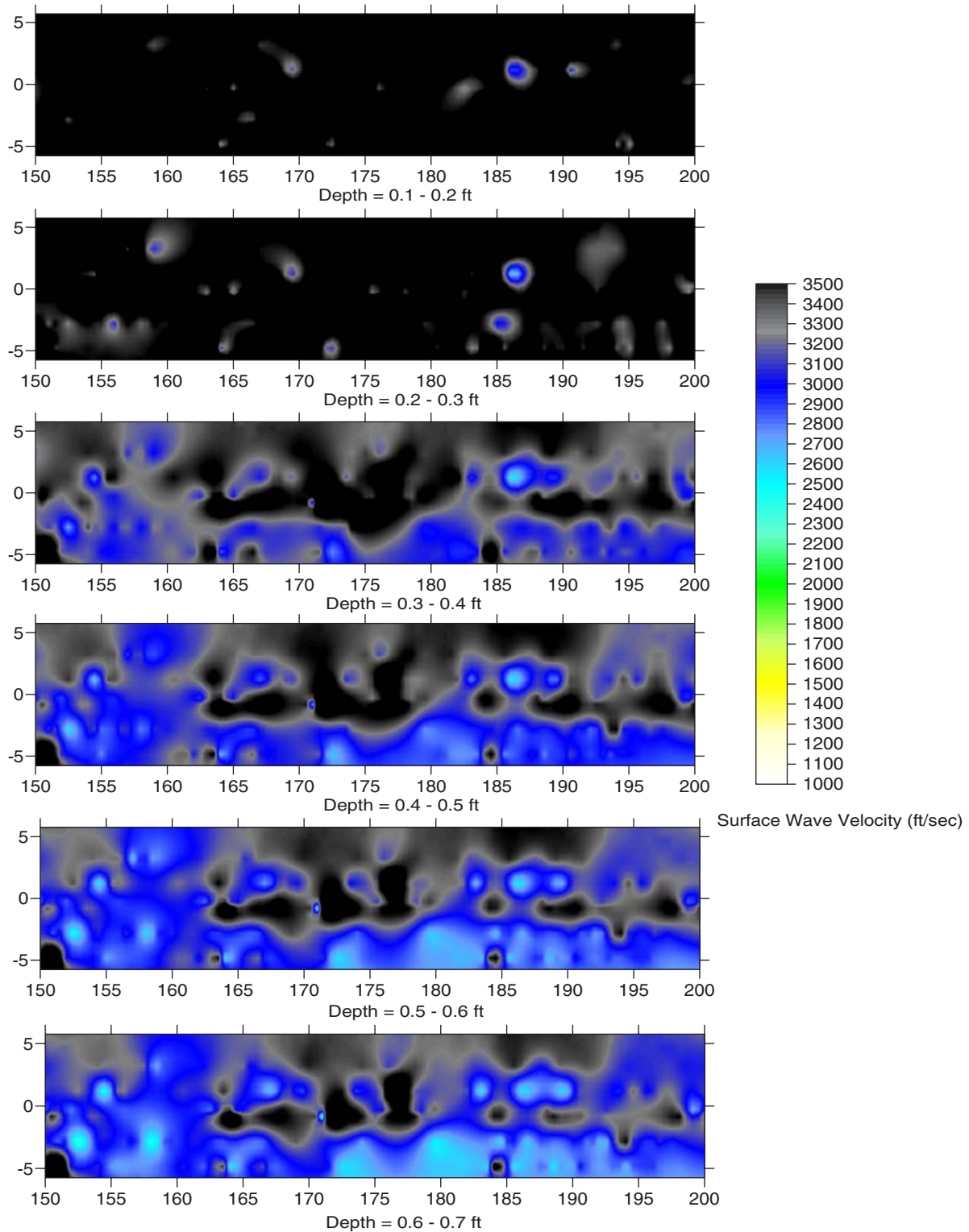
Note: Length = 150 to 200 ft.

Figure 3.4. SASW test results from the Florida section.
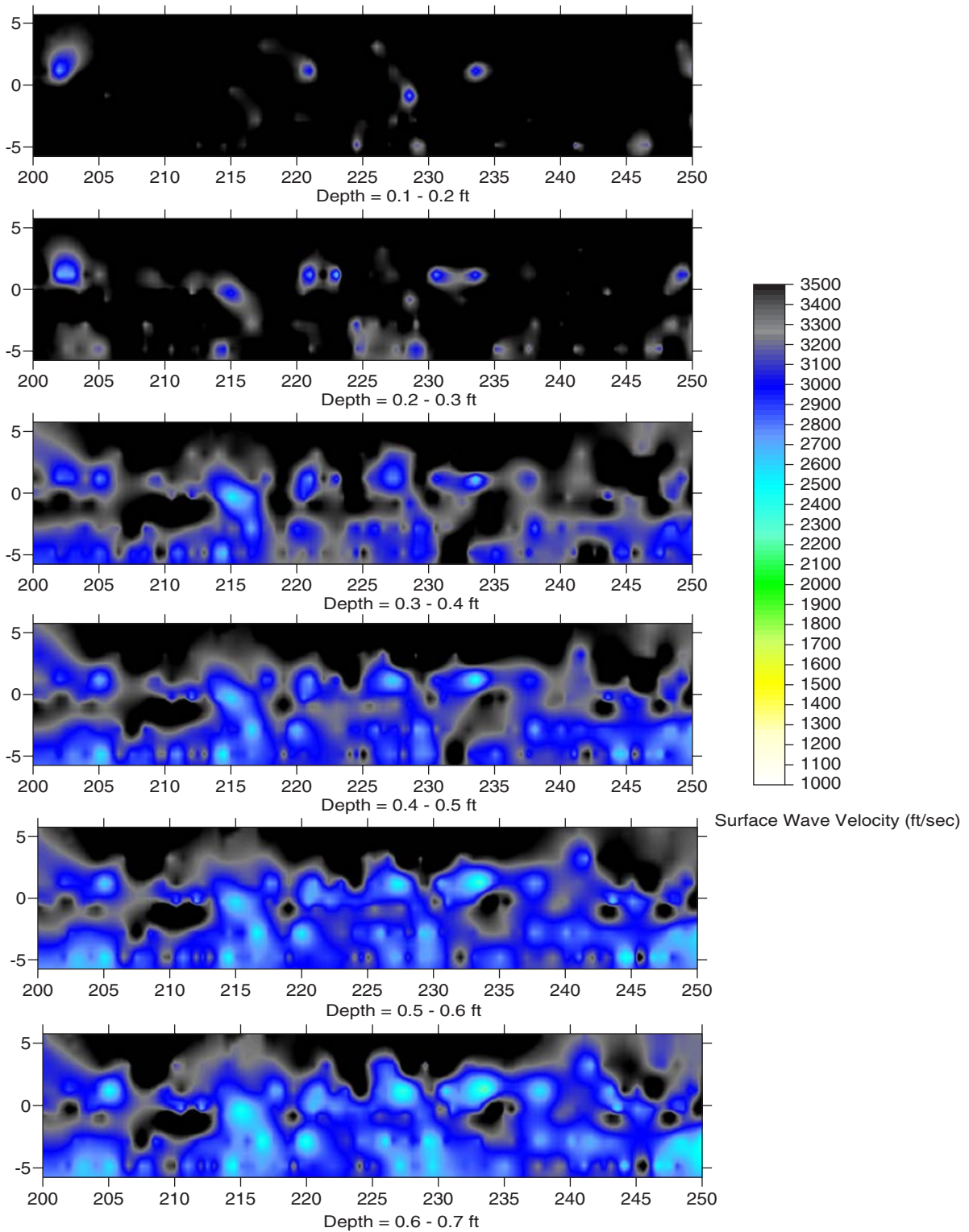
Note: Length = 200 to 250 ft.

Figure 3.5. SASW test results from the Florida section.
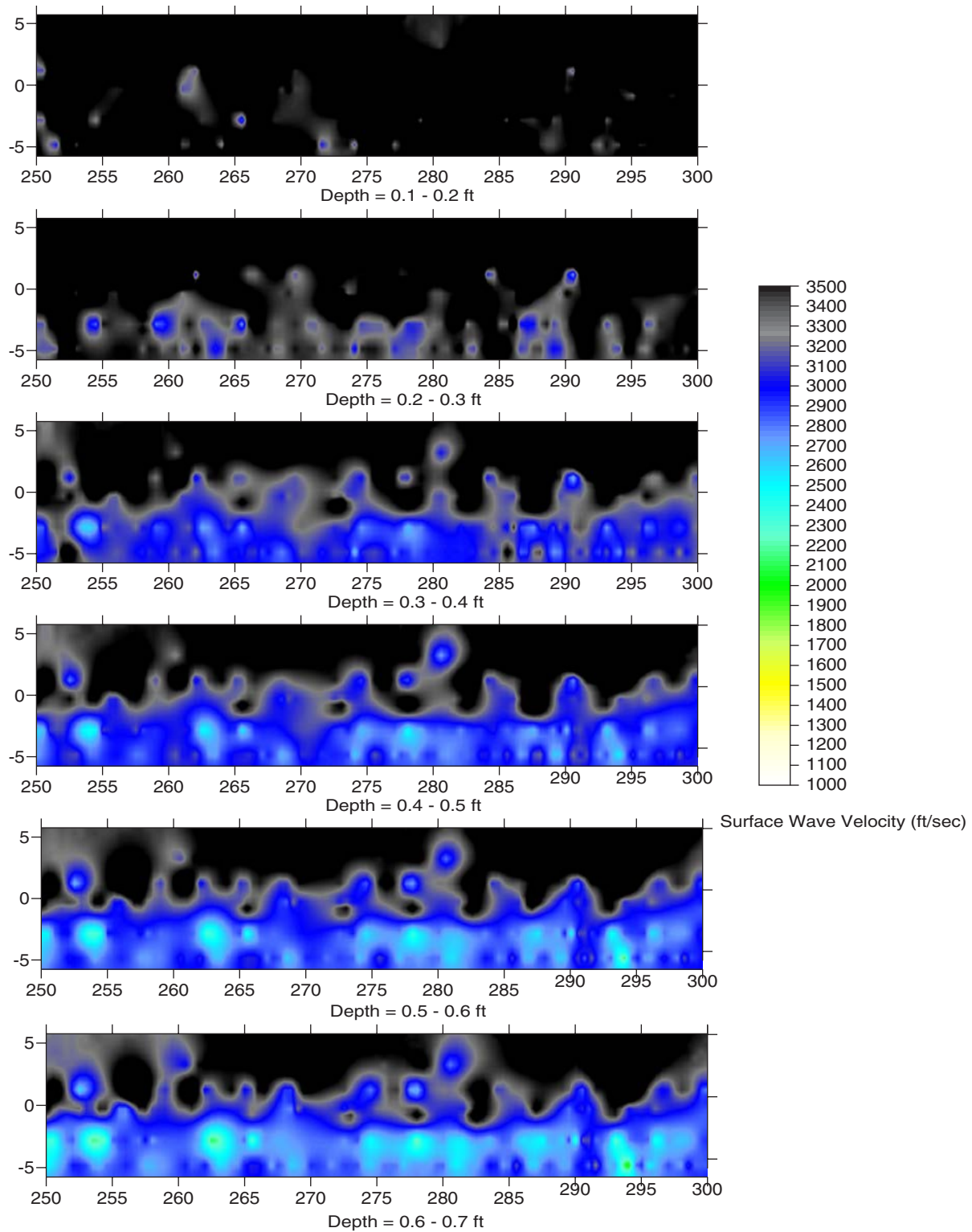
Note: Length = 250 to 300 ft.

Figure 3.6. SASW test results from the Florida section.
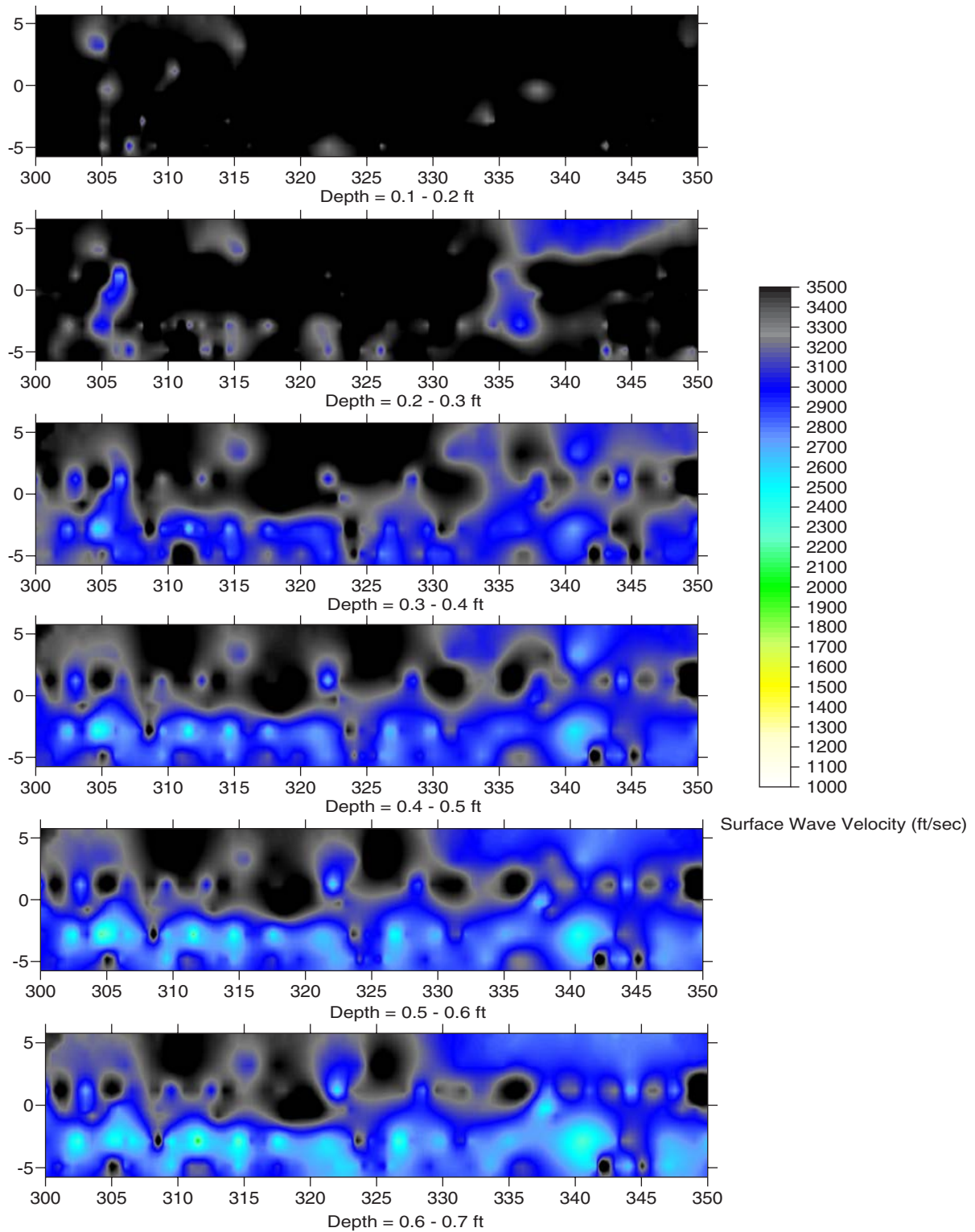
Note: Length = 300 to 350 ft.

Figure 3.7. SASW test results from the Florida section.
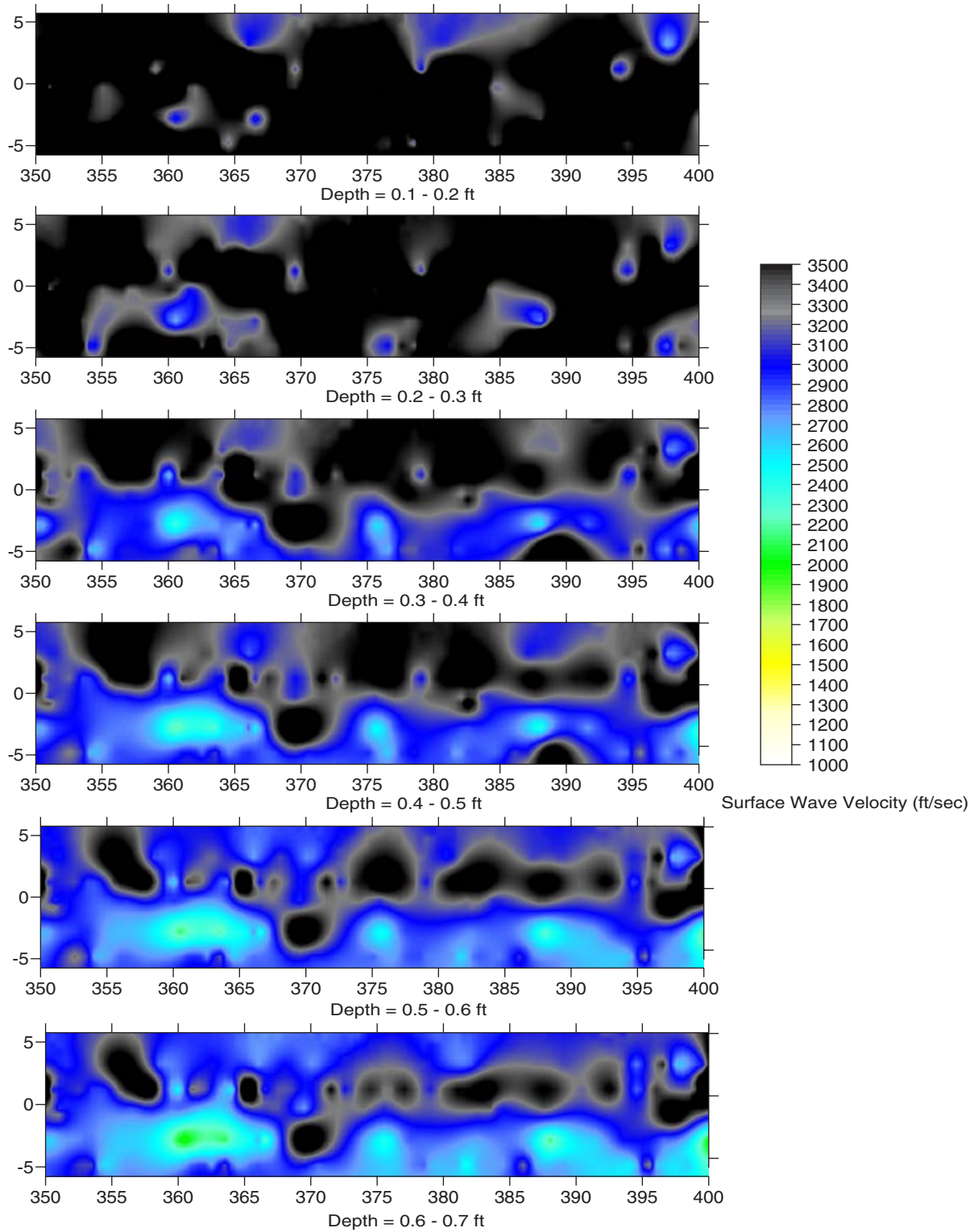
Note: Length = 350 to 400 ft.

Figure 3.8. SASW test results from the Florida section.
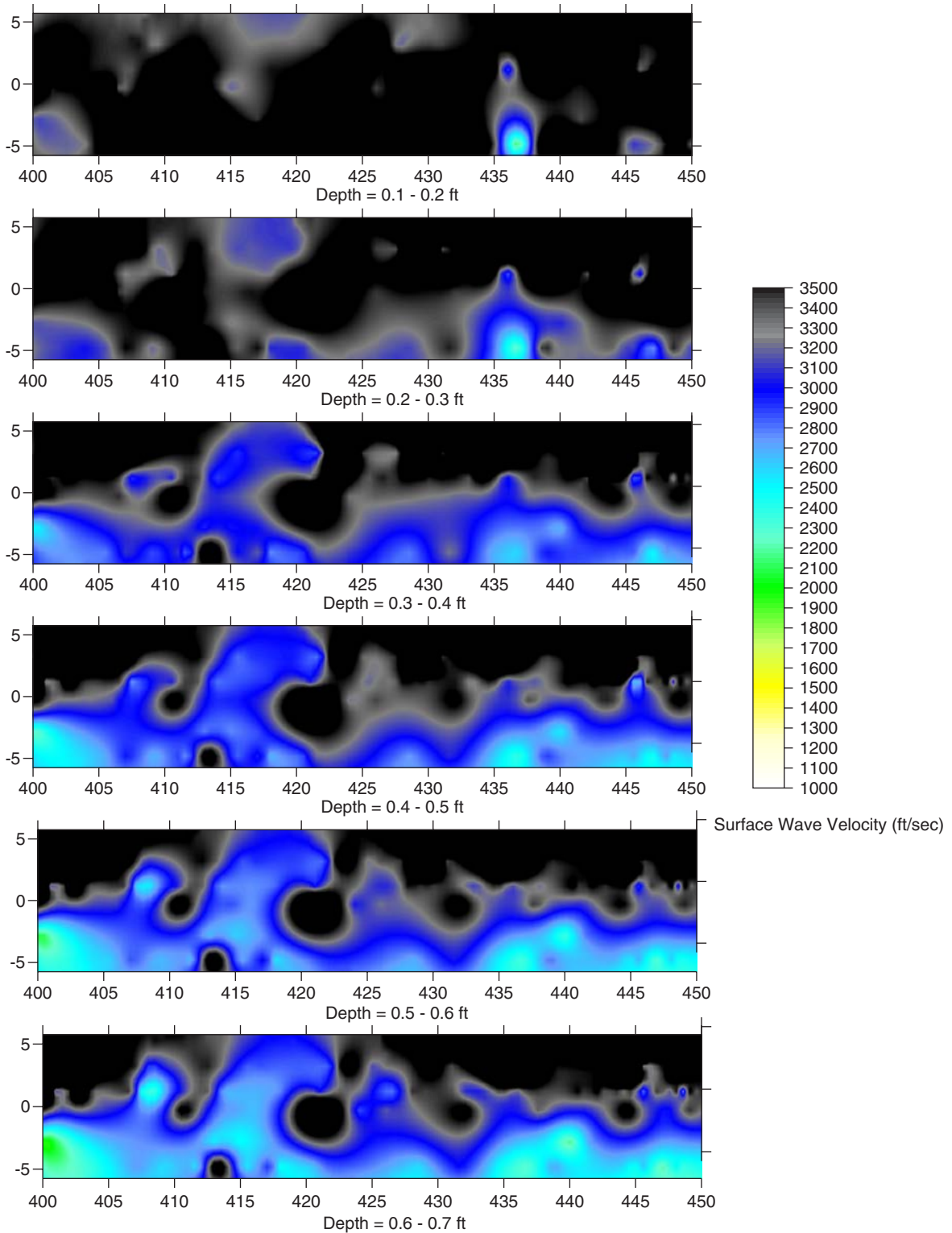
Note: Length = 400 to 450 ft.

Figure 3.9. SASW test results from the Florida section.
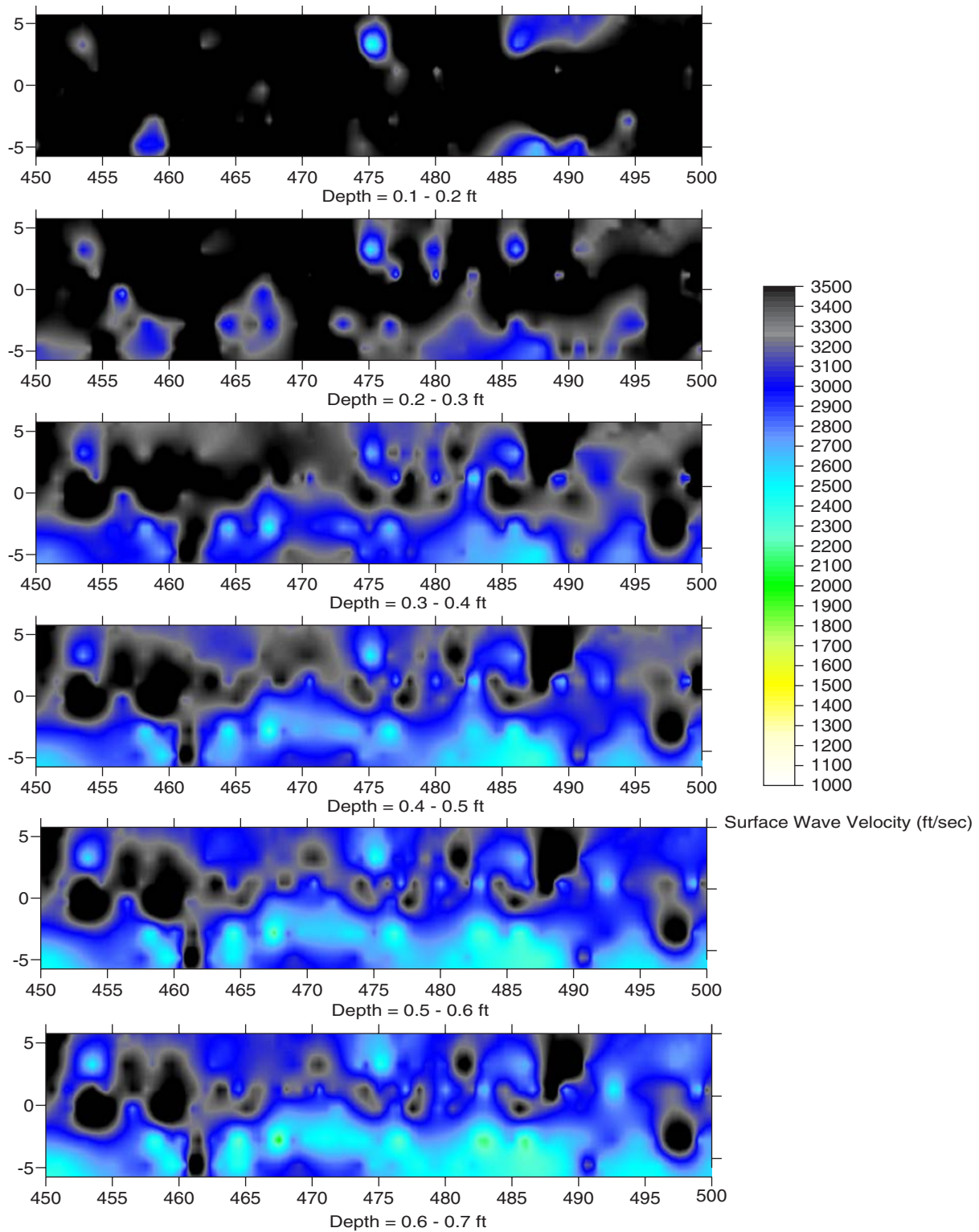
Note: Length = 450 to 500 ft.

Figure 3.10. SASW test results from the Florida section.
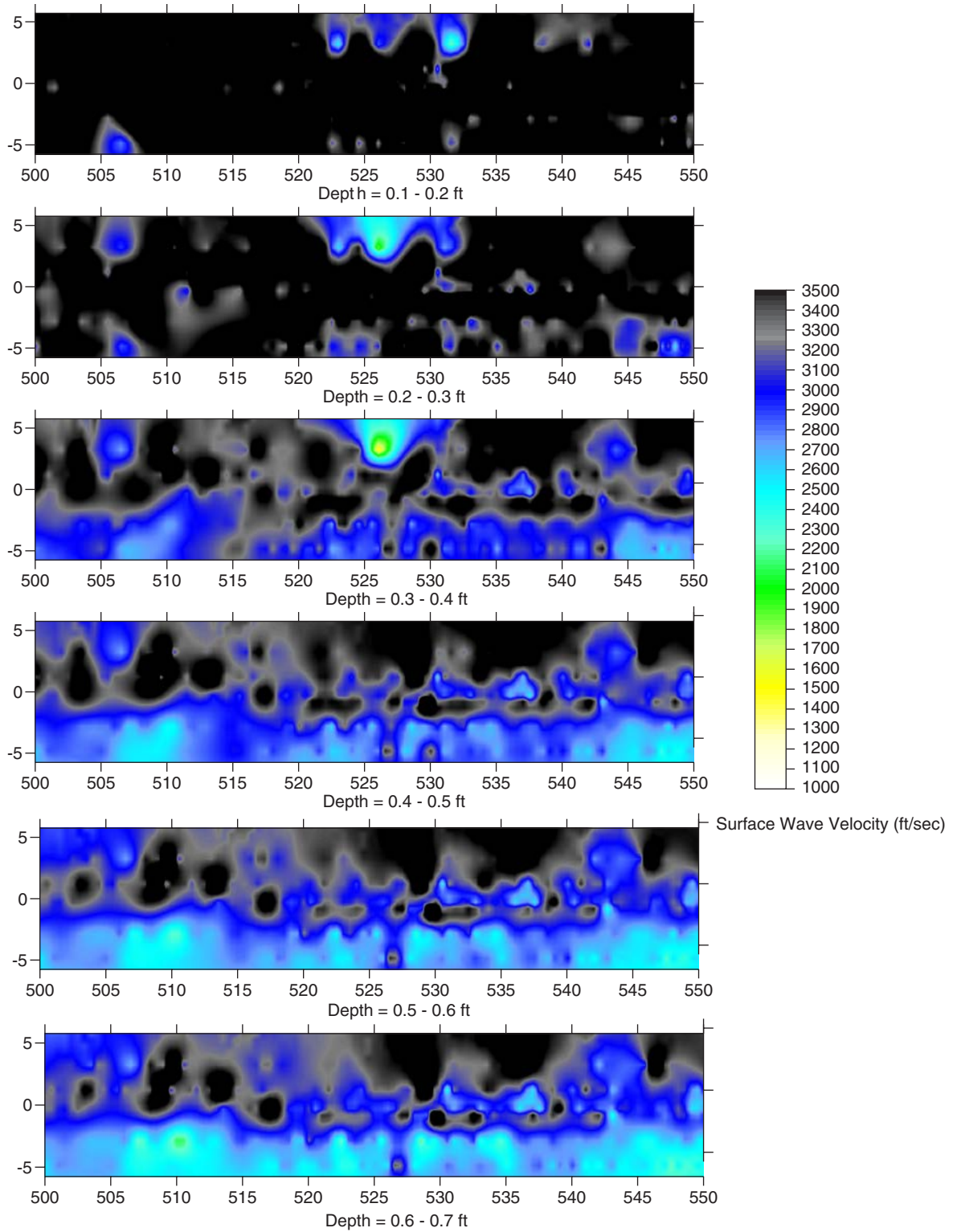
Note: Length = 500 to 550 ft.

Figure 3.11. SASW test results from the Florida section.
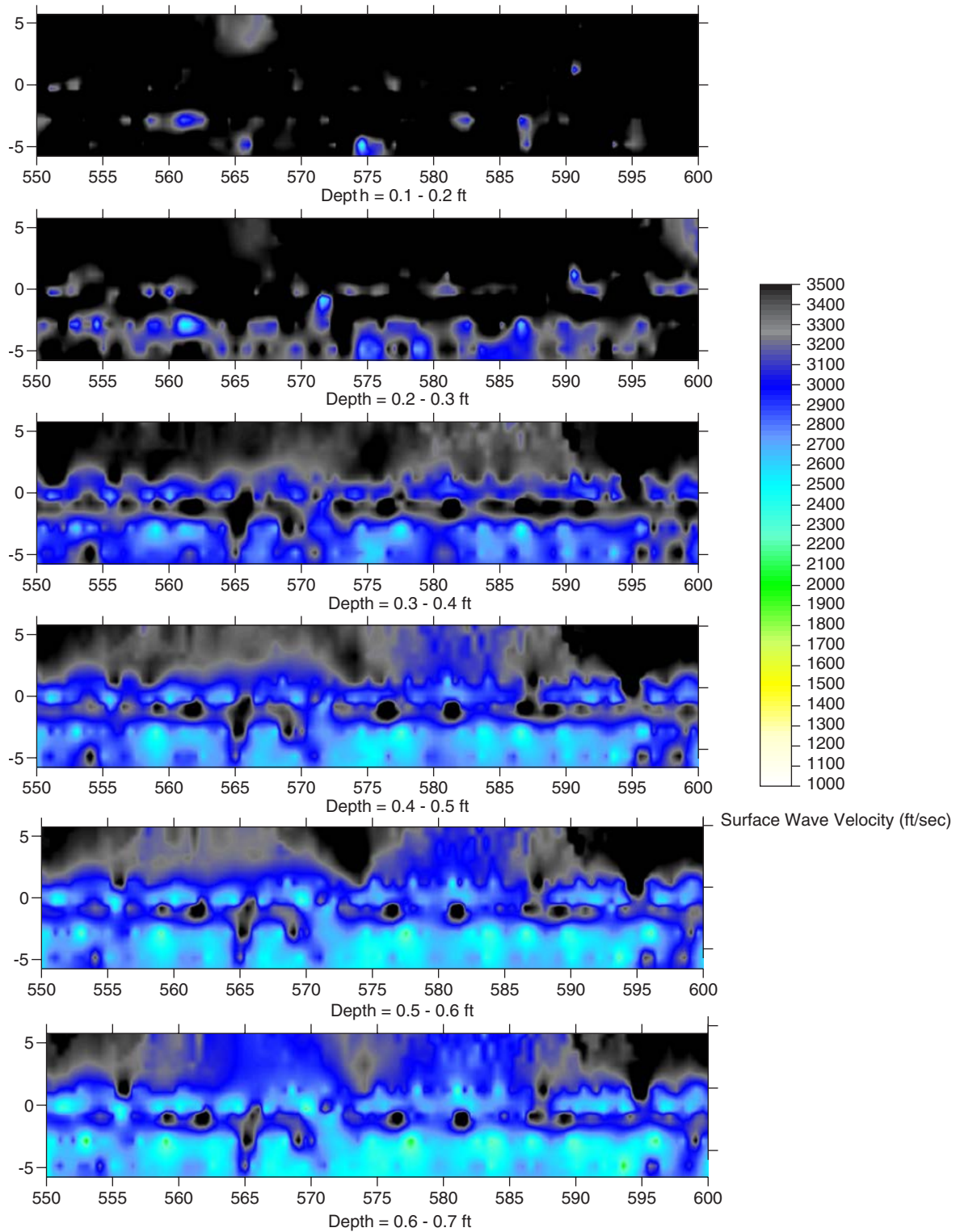
Note: Length = 550 to 600 ft.

Figure 3.12. SASW test results from the Florida section.
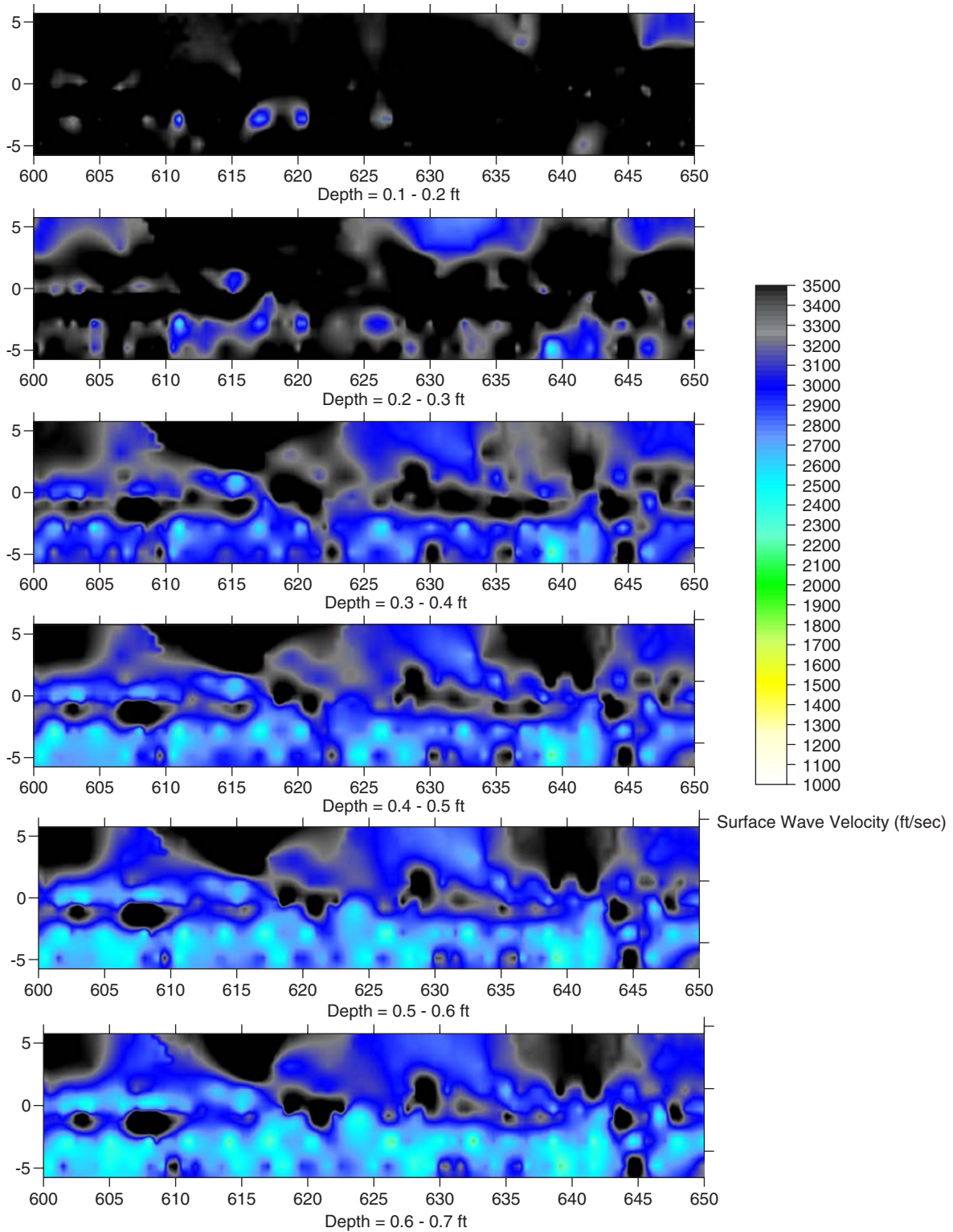
Note: Length = 600 to 650 ft.

Figure 3.13. SASW test results from the Florida section.
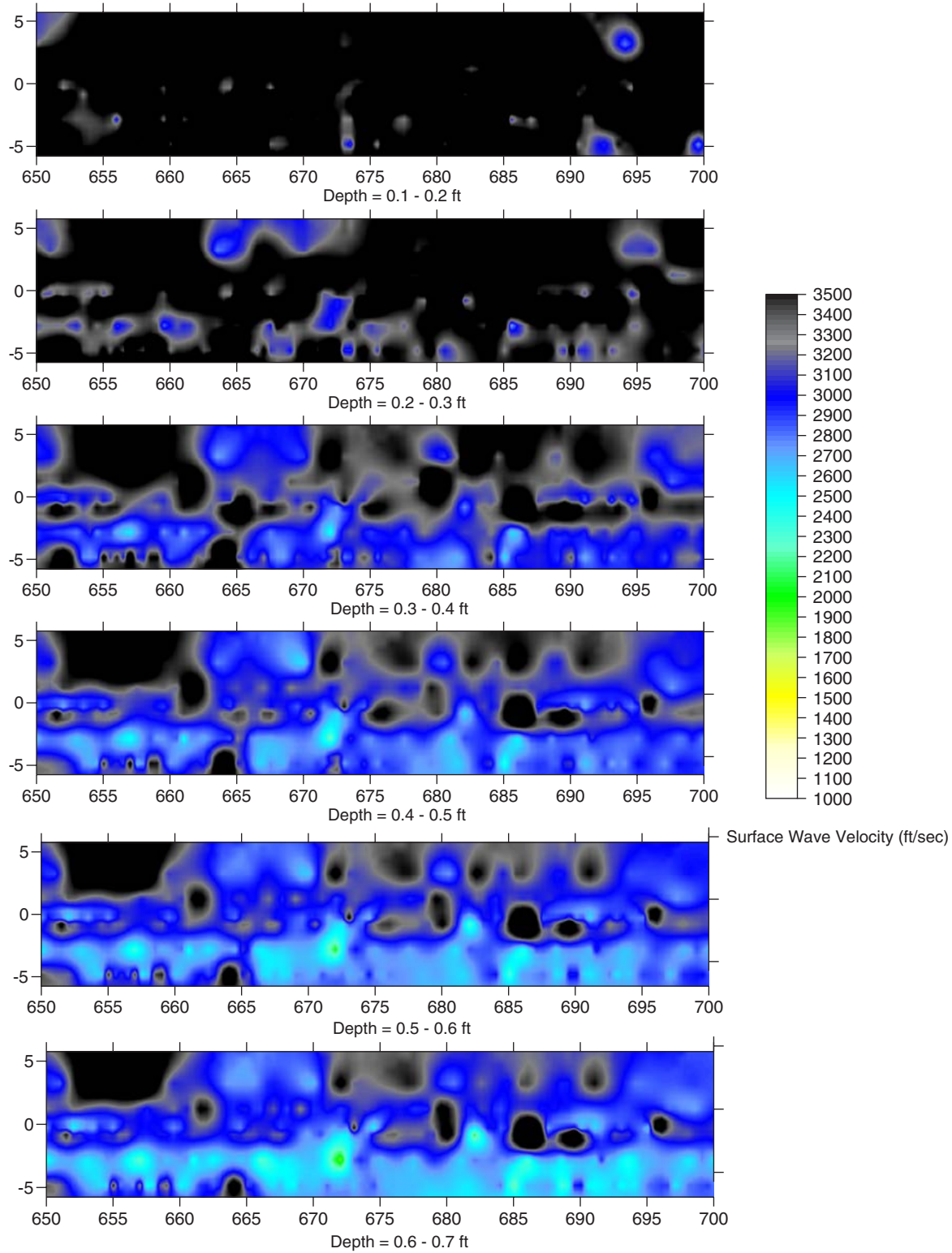
Note: Length = 650 to 700 ft.

Figure 3.14. SASW test results from the Florida section.
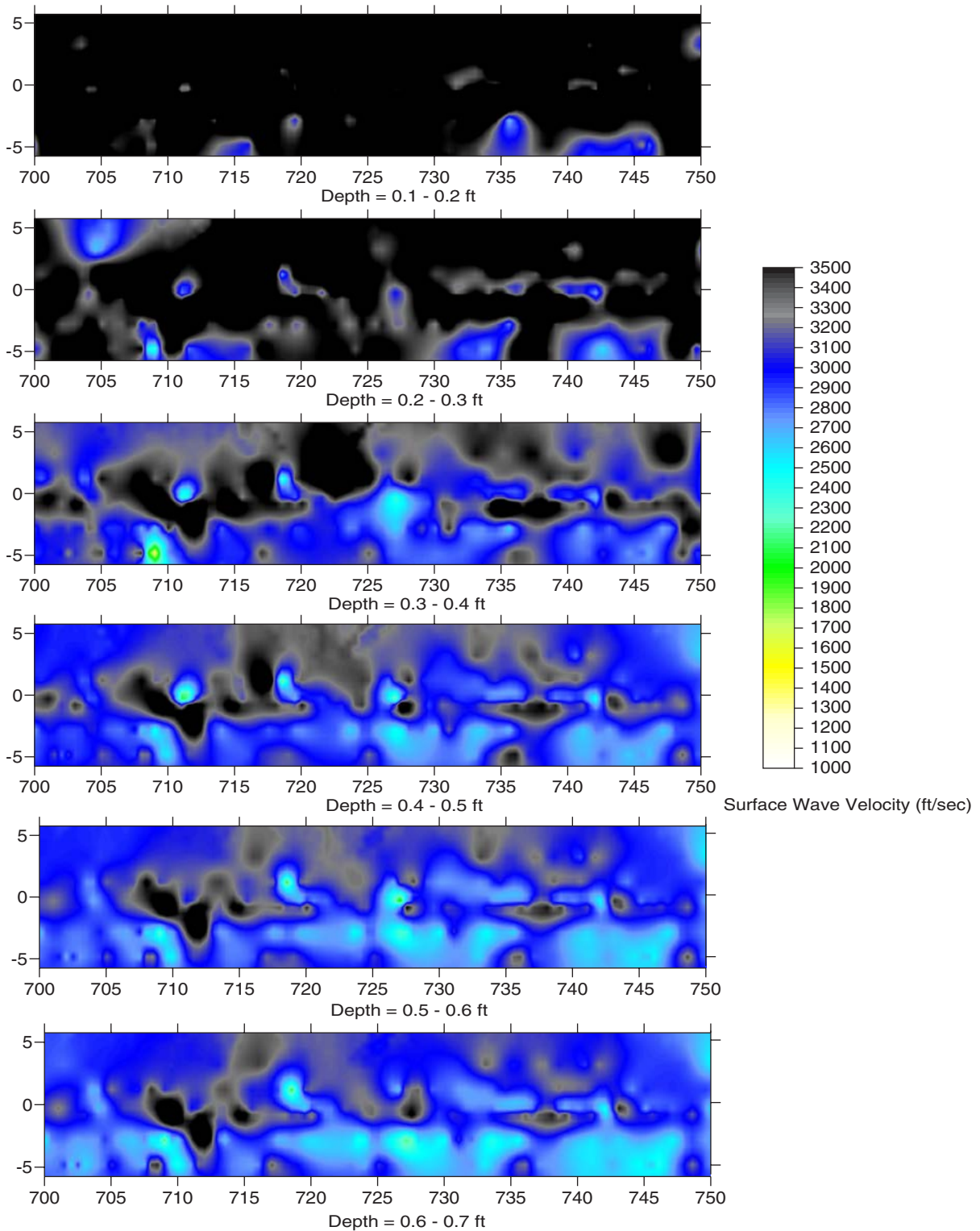
Note: Length = 700 to 750 ft.

Figure 3.15. SASW test results from the Florida section.
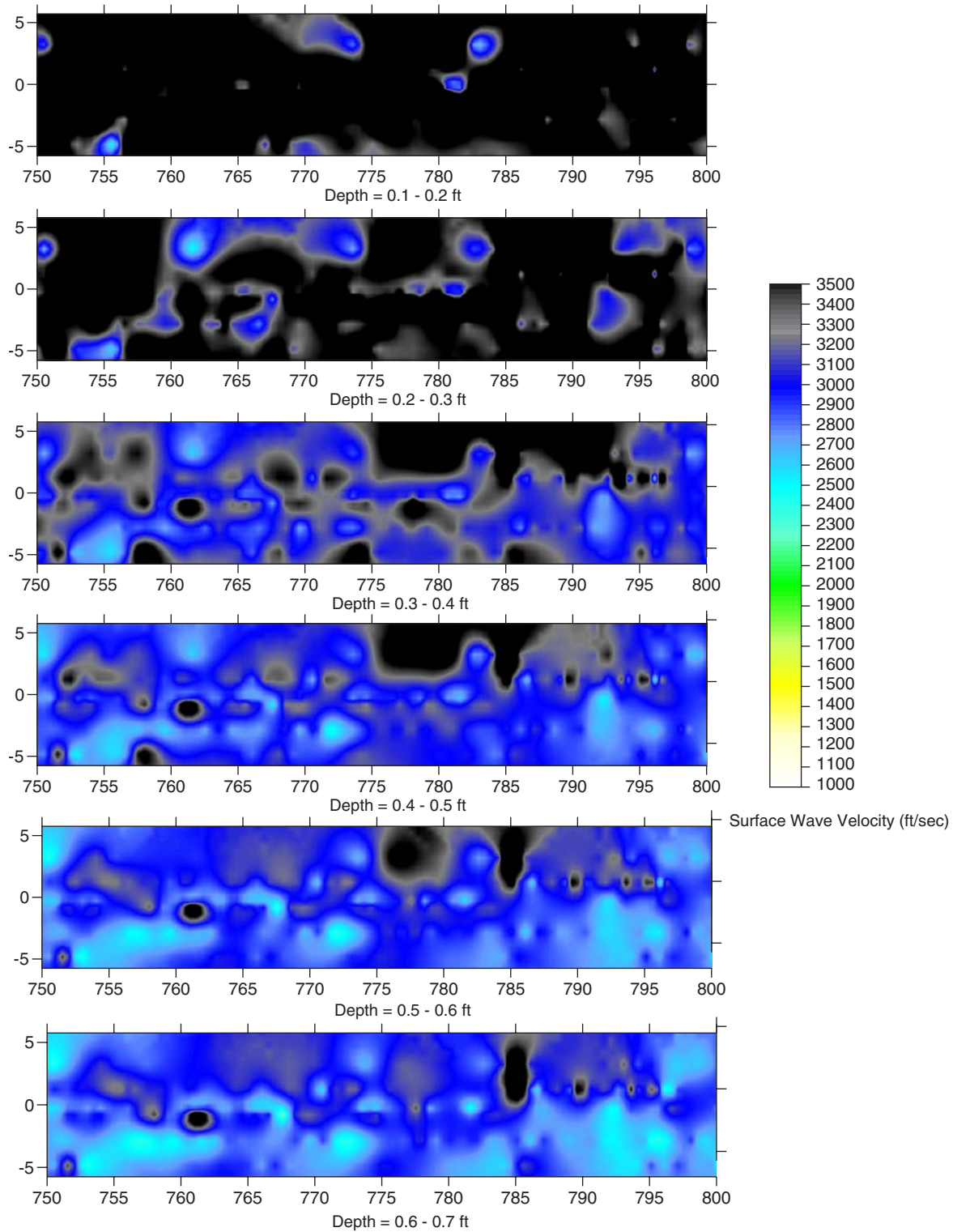
Note: Length = 750 to 800 ft.

Figure 3.16. SASW test results from the Florida section.
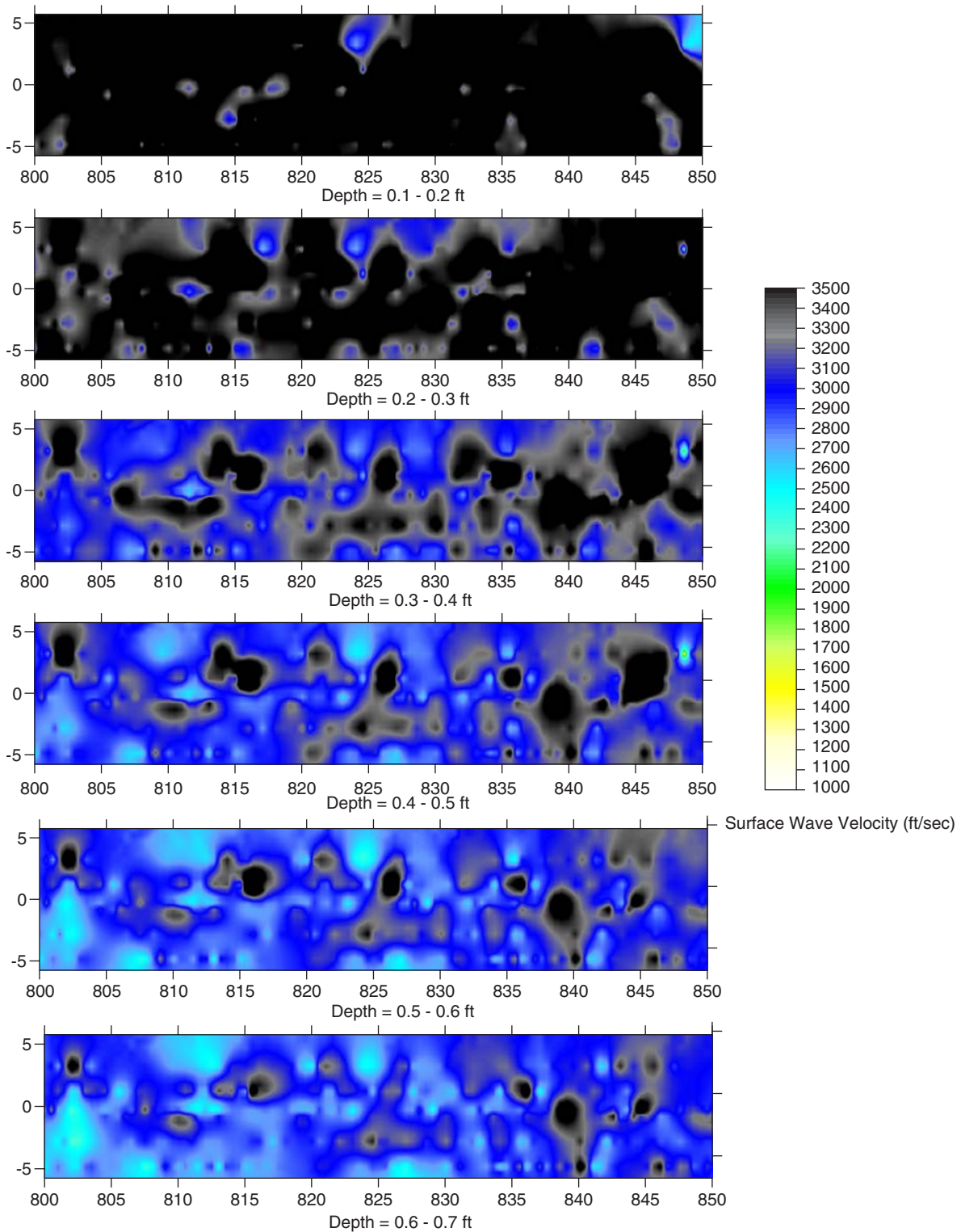
Note: Length = 800 to 850 ft.

Figure 3.17. SASW test results from the Florida section.
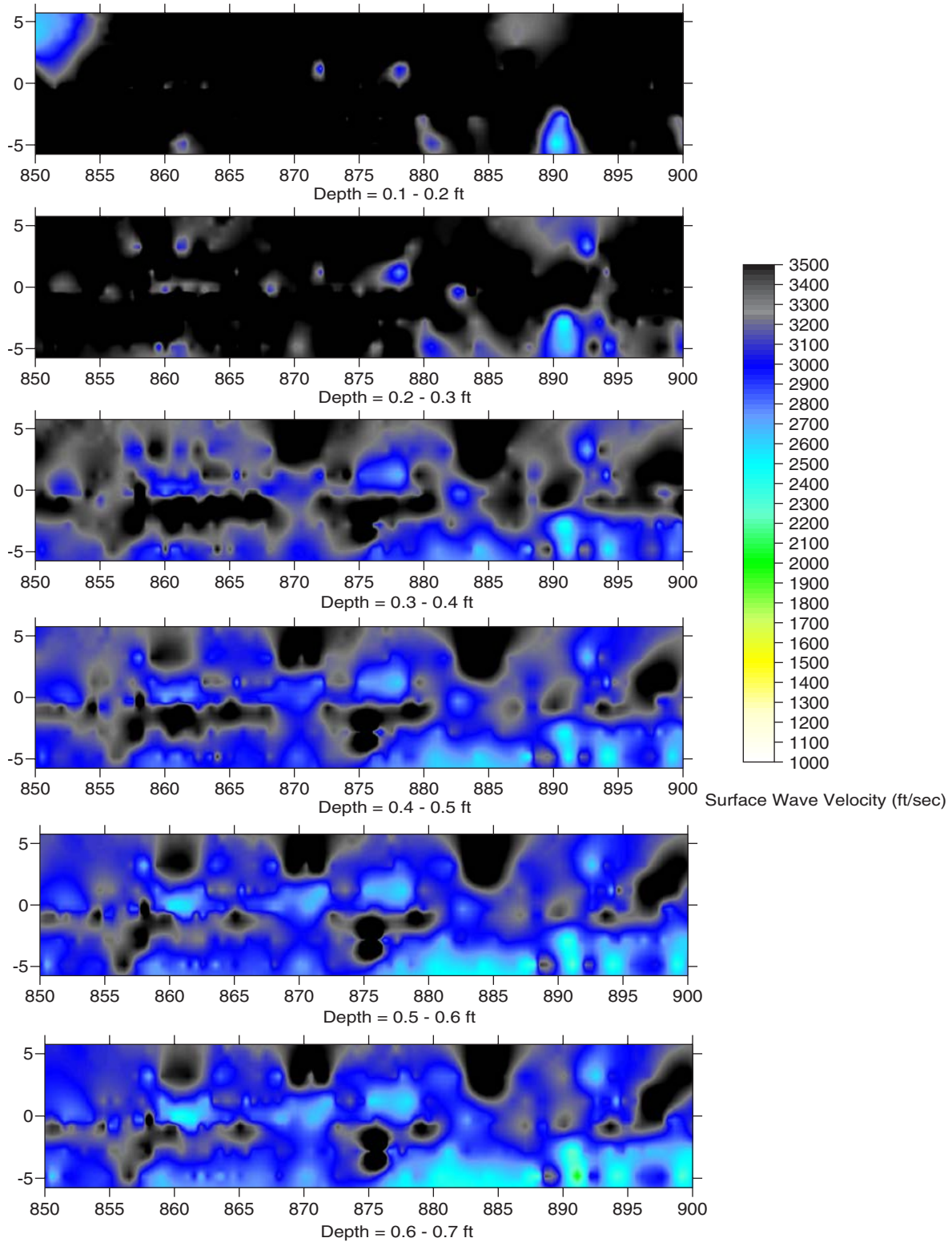
Note: Length = 850 to 900 ft.

Figure 3.18. SASW test results from the Florida section.

Note: Length = 900 to 950 ft.
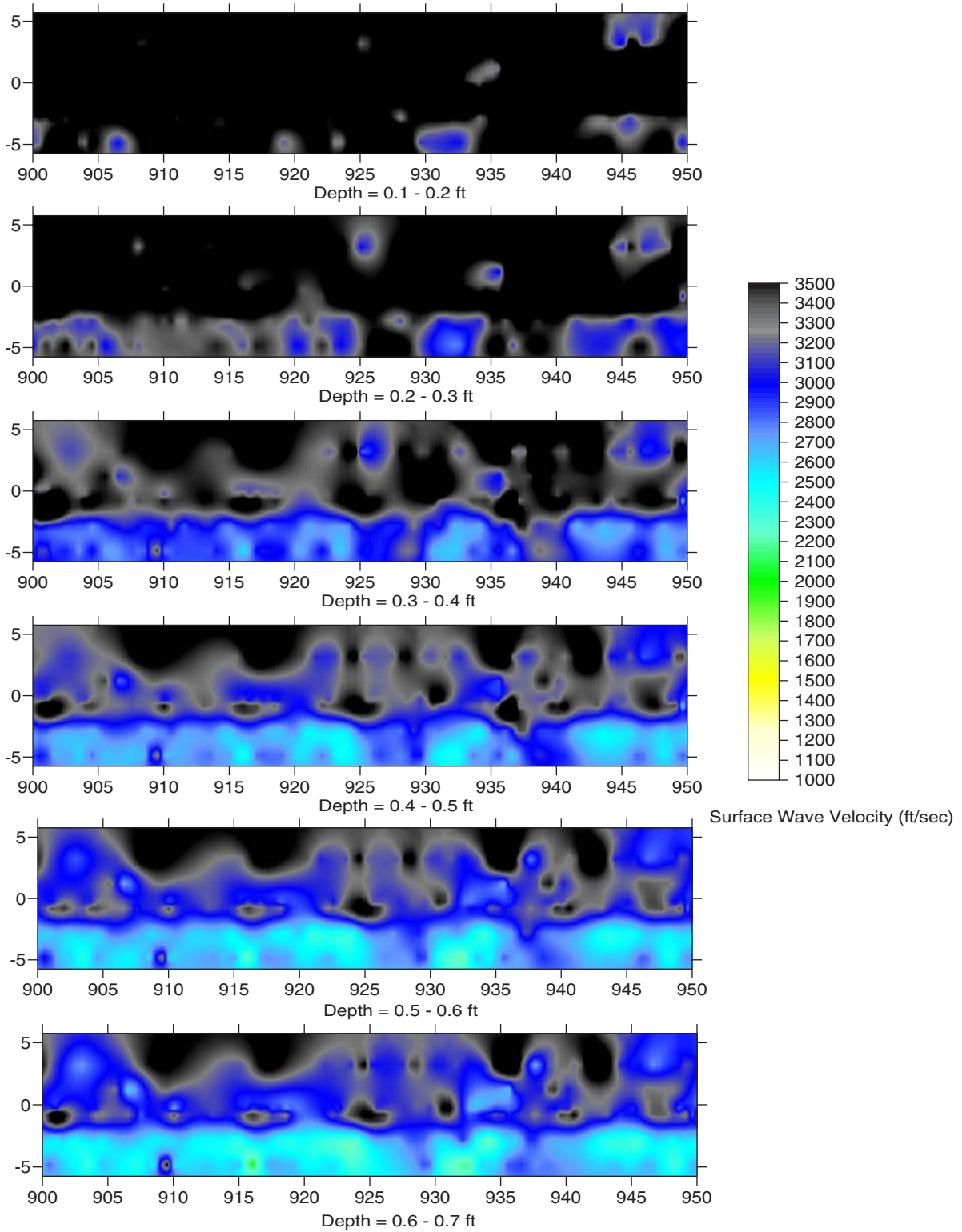
Figure 3.19. SASW test results from the Florida section.

Note: Length = 950 to 1,000 ft.
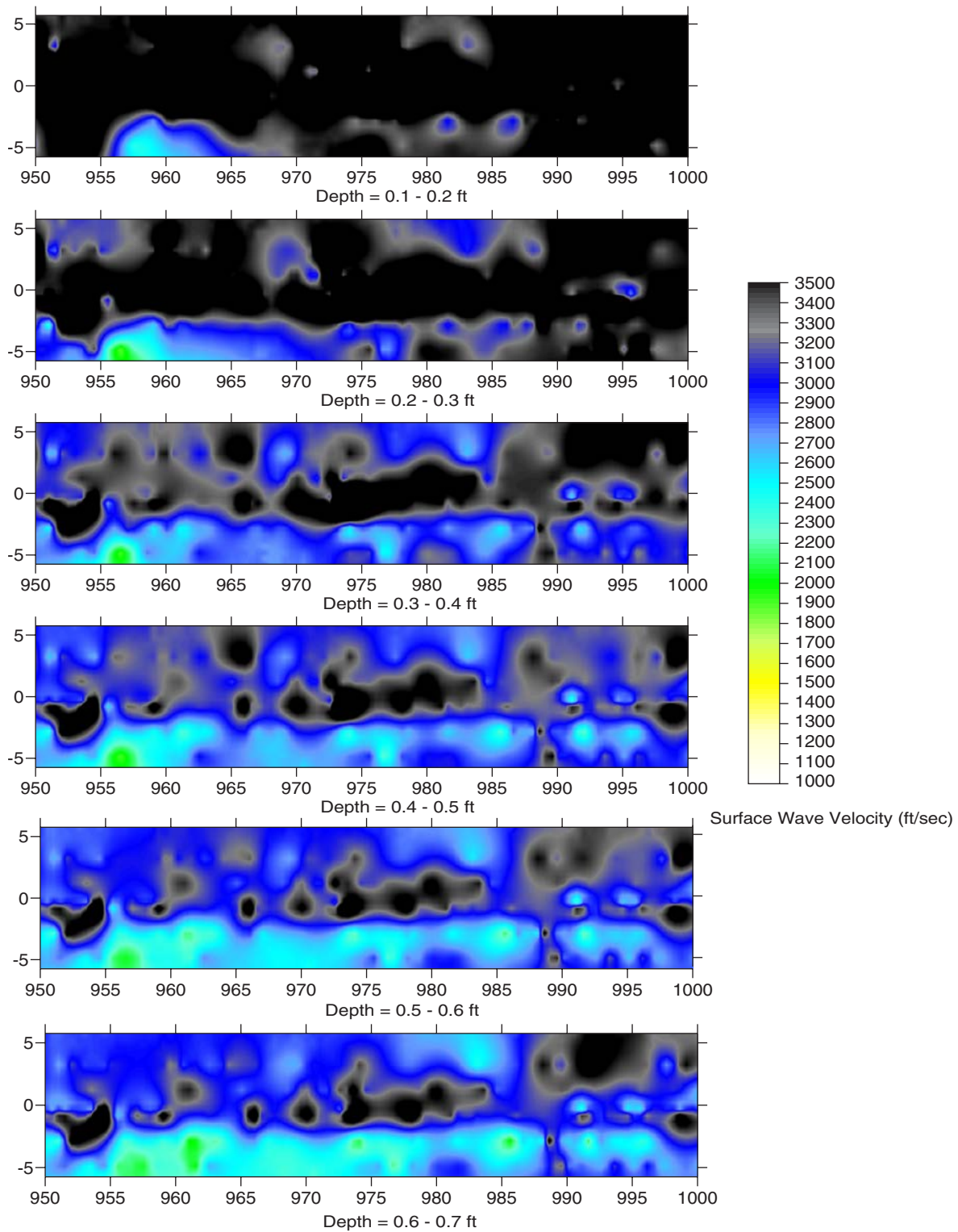
Figure 3.20. SASW test results from the Florida section.
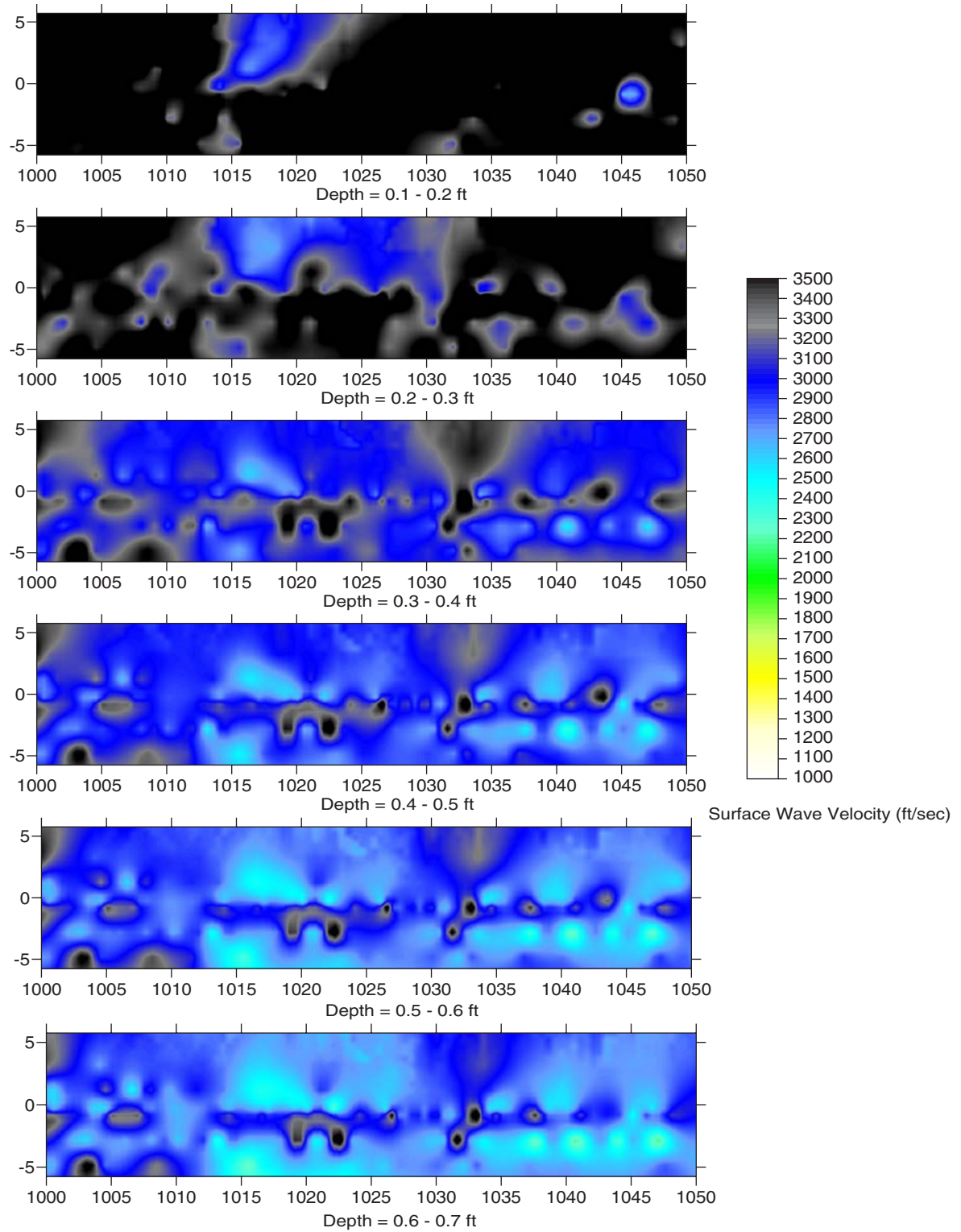
Note: Length = 1,000 to 1,050 ft.

Figure 3.21. SASW test results from the Florida section.

Figure 3.22. SASW test results from the Florida section.
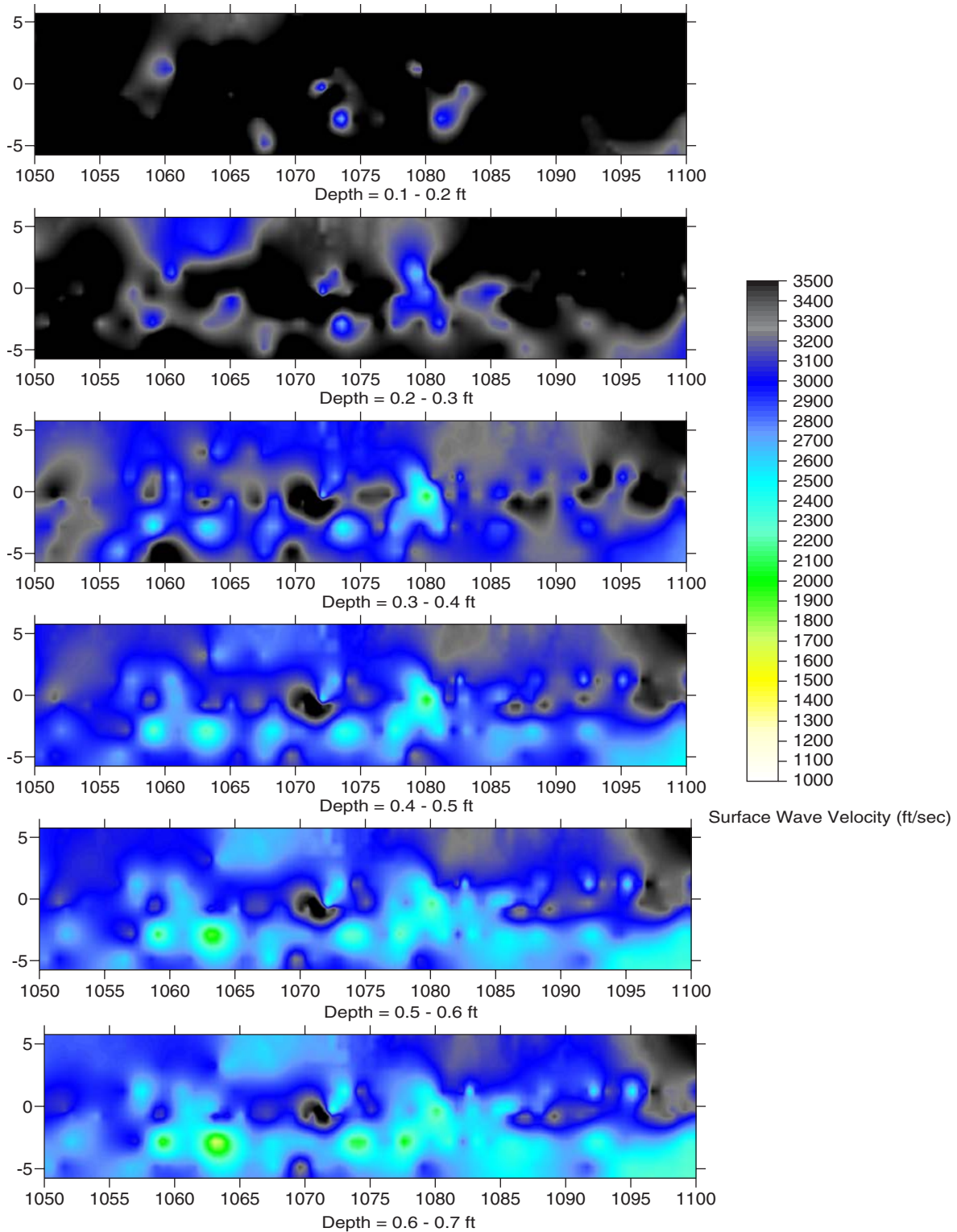
Note: Length = 1,050 to 1,100 ft.
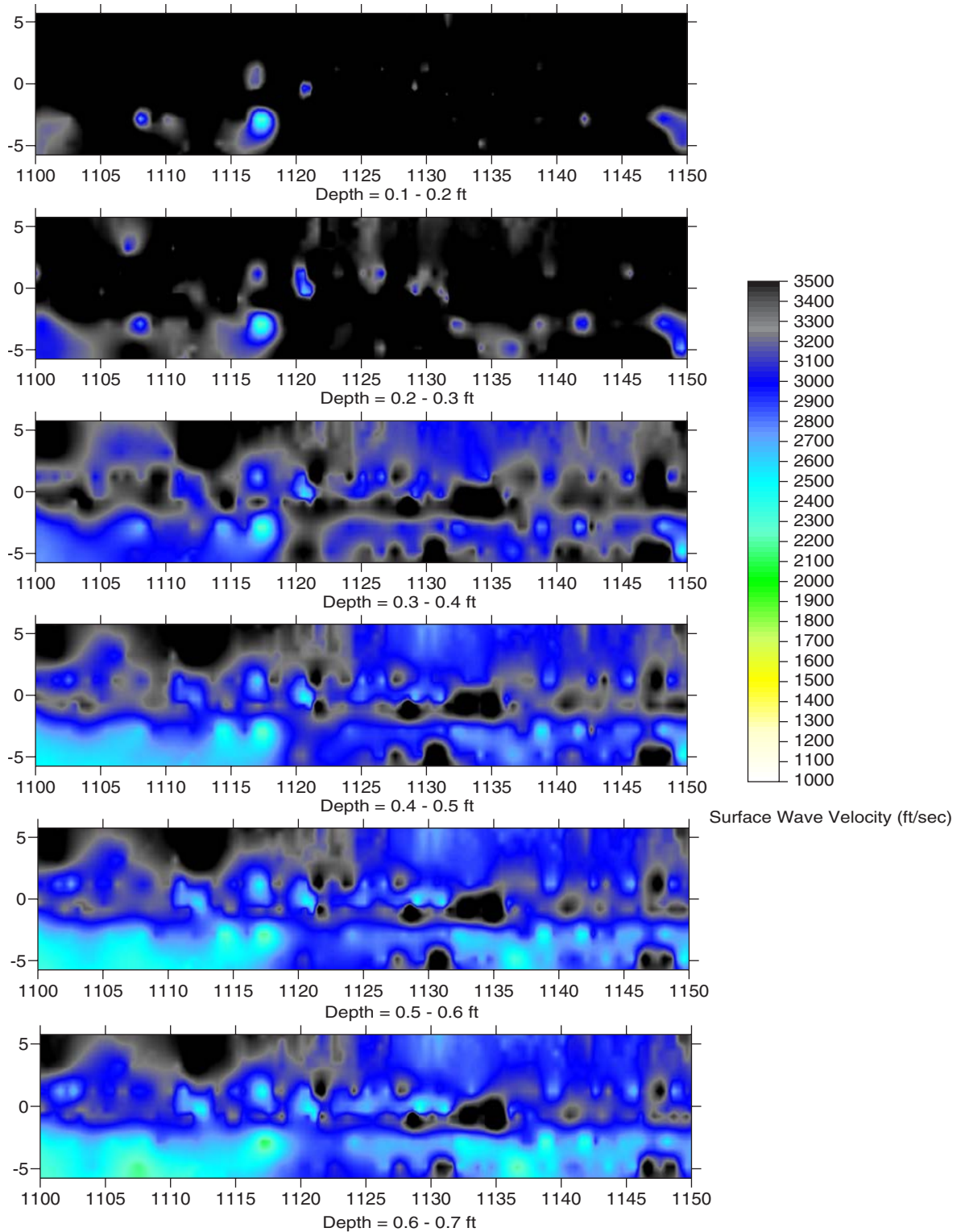
Note: Length = 1,100 to 1,150 ft.

Figure 3.23. SASW test results from the Florida section.
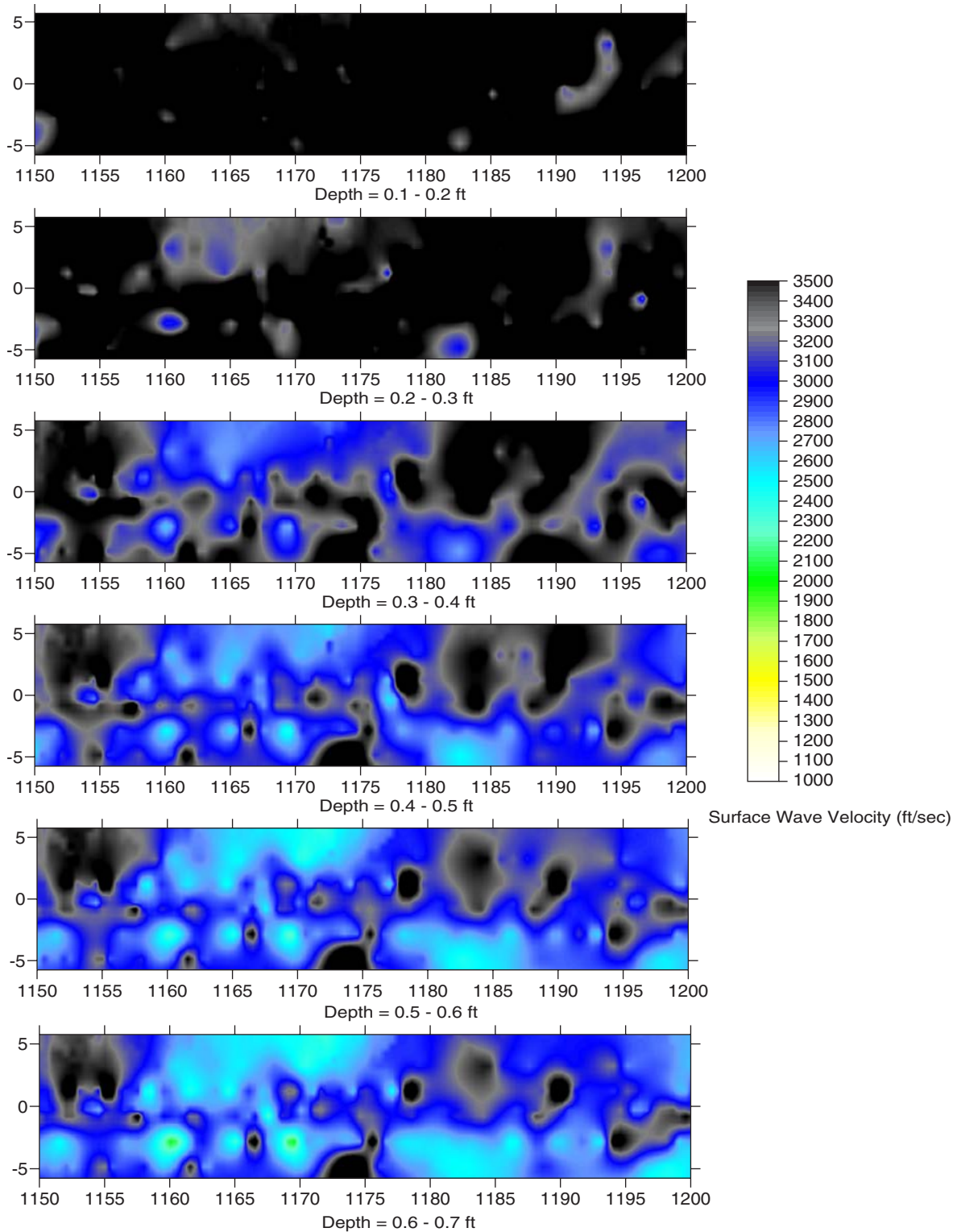
Note: Length = 1,150 to 1,200 ft.

Figure 3.24. SASW test results from the Florida section.
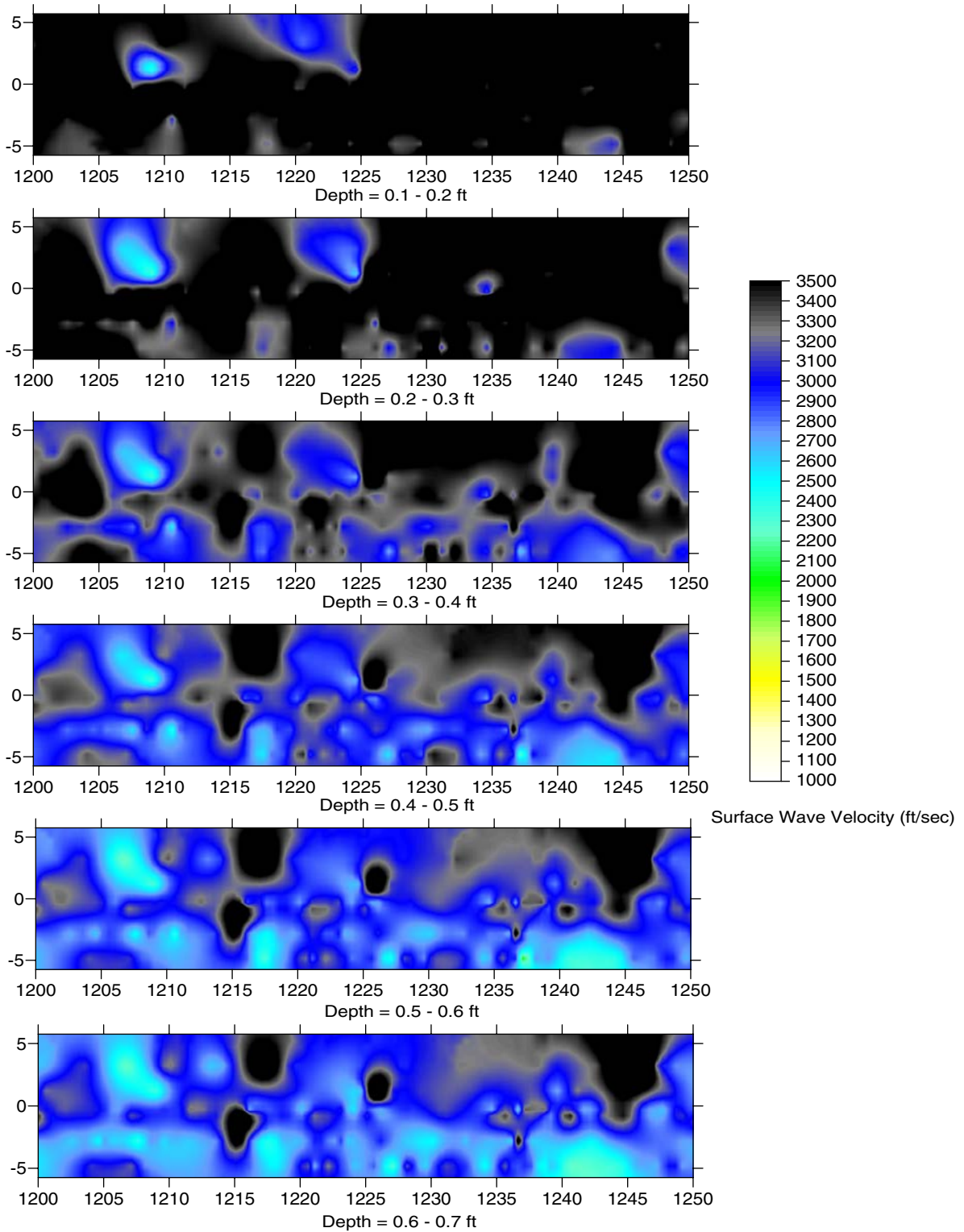
Note: Length = 1,200 to 1,250 ft.

Figure 3.25. SASW test results from the Florida section.
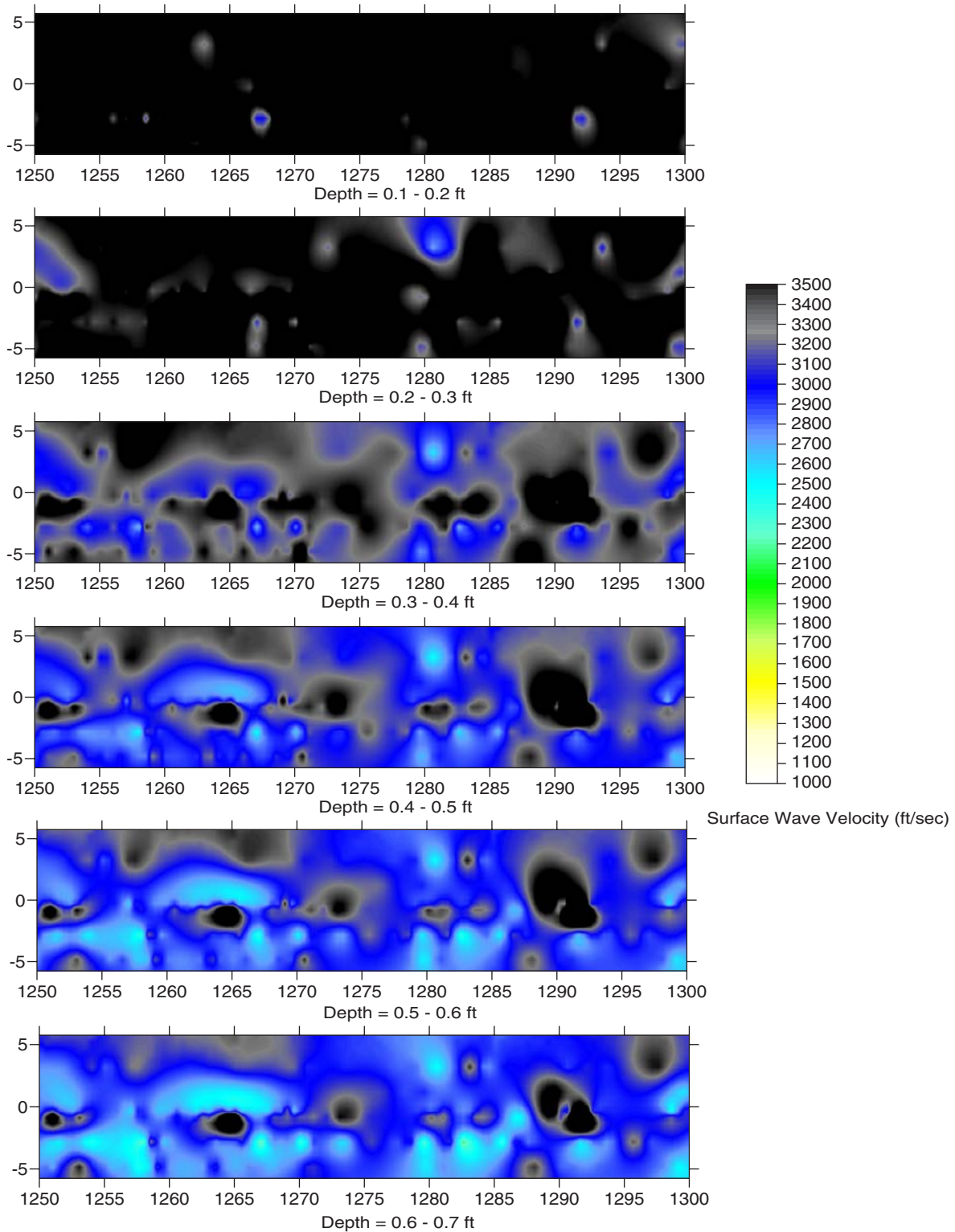
Note: Length = 1,250 to 1,300 ft.

Figure 3.26. SASW test results from the Florida section.
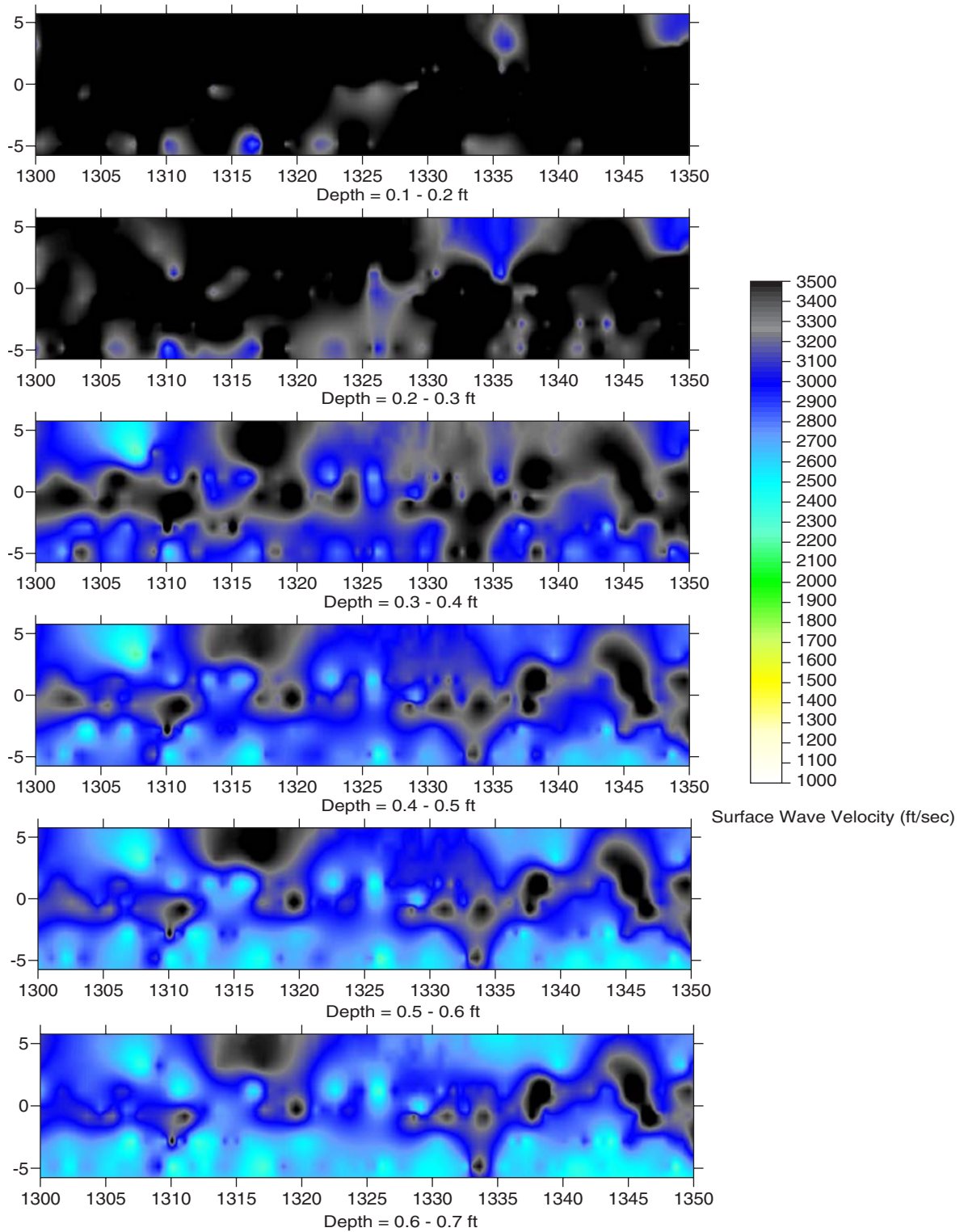
Note: Length = 1,300 to 1,350 ft.

Figure 3.27. SASW test results from the Florida section.

Figure 3.28. SASW test results from the Florida section.
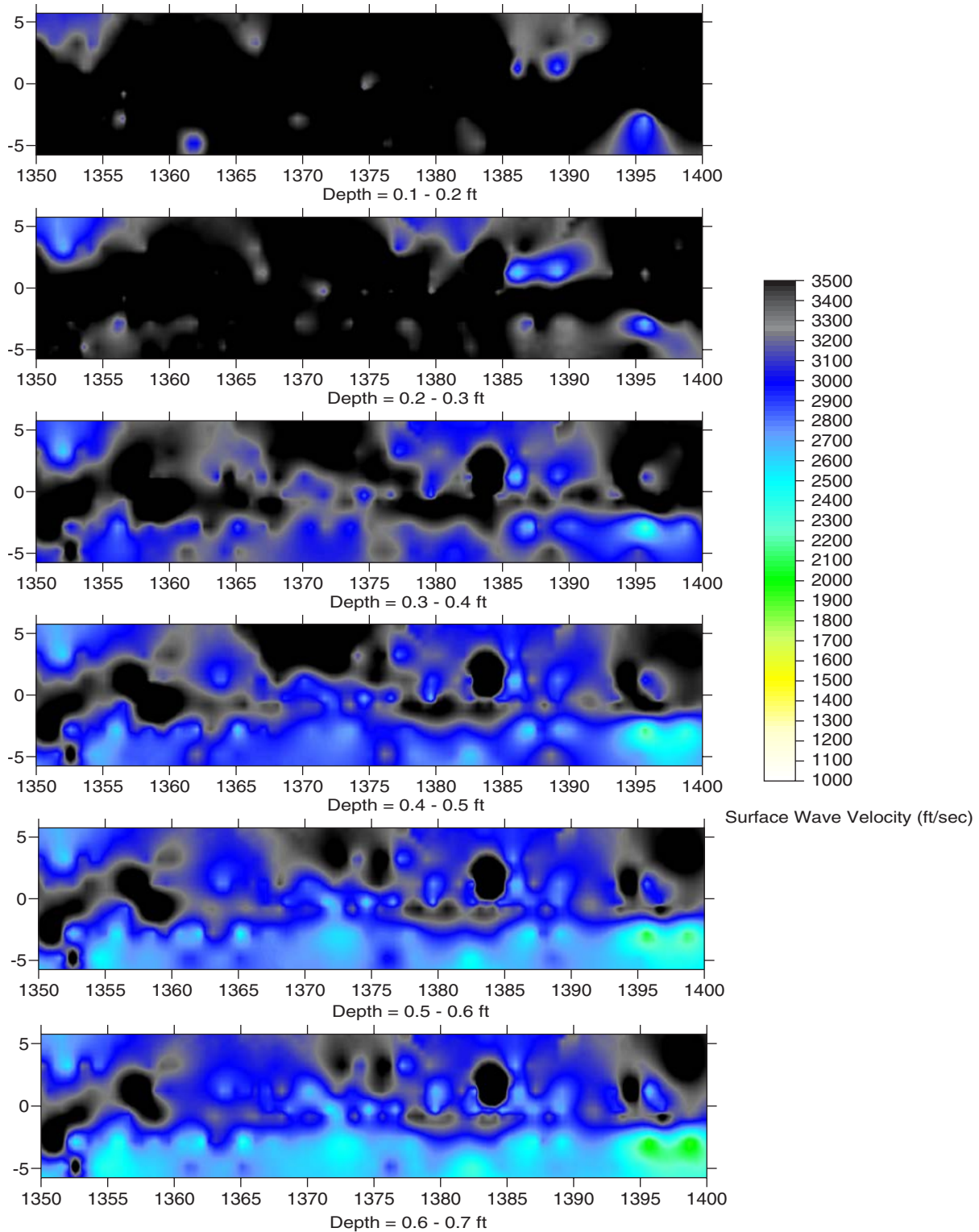
Note: Length = 1,350 to 1,400 ft.
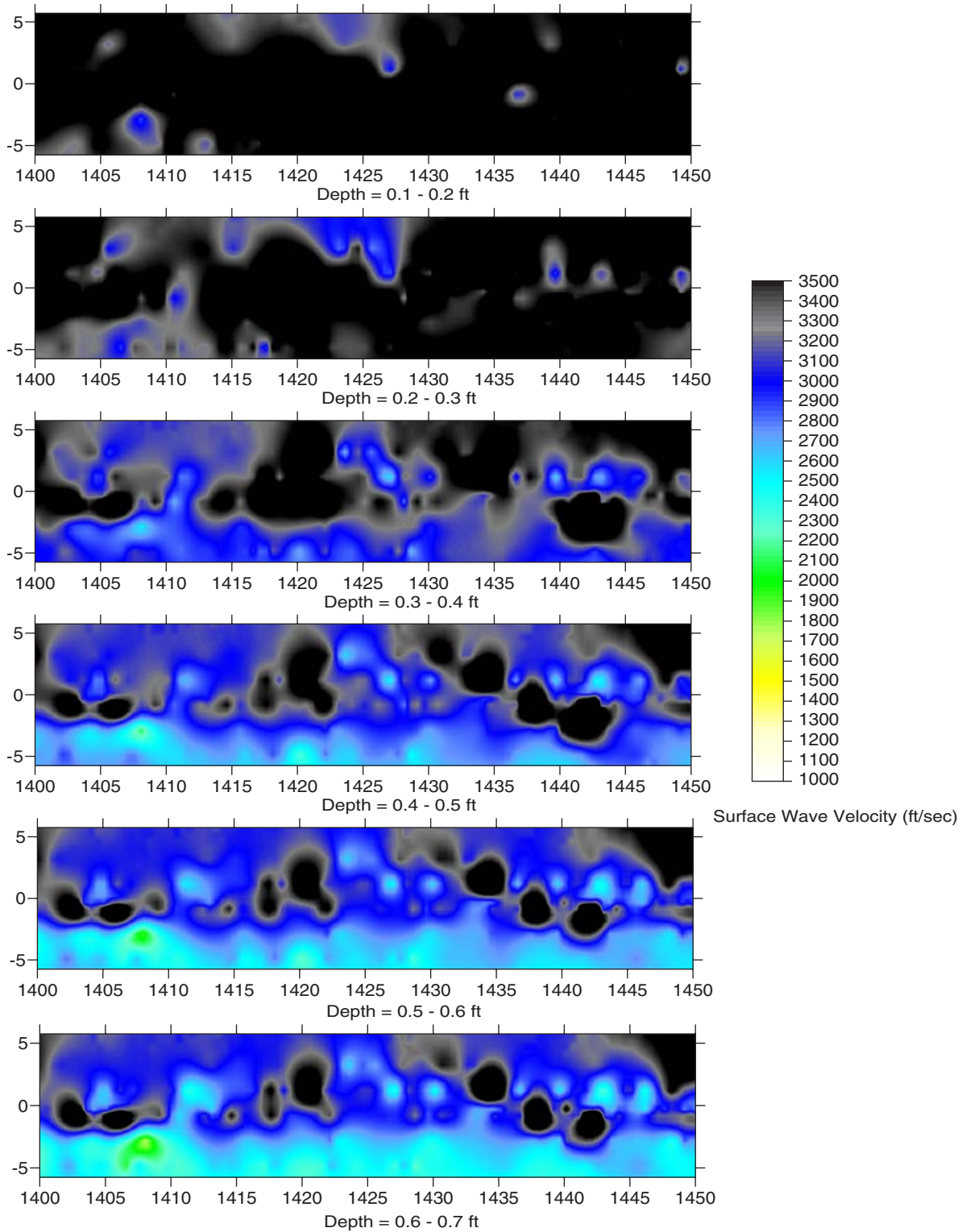
Note: Length = 1,400 to 1,450 ft.

Figure 3.29. SASW test results from the Florida section.
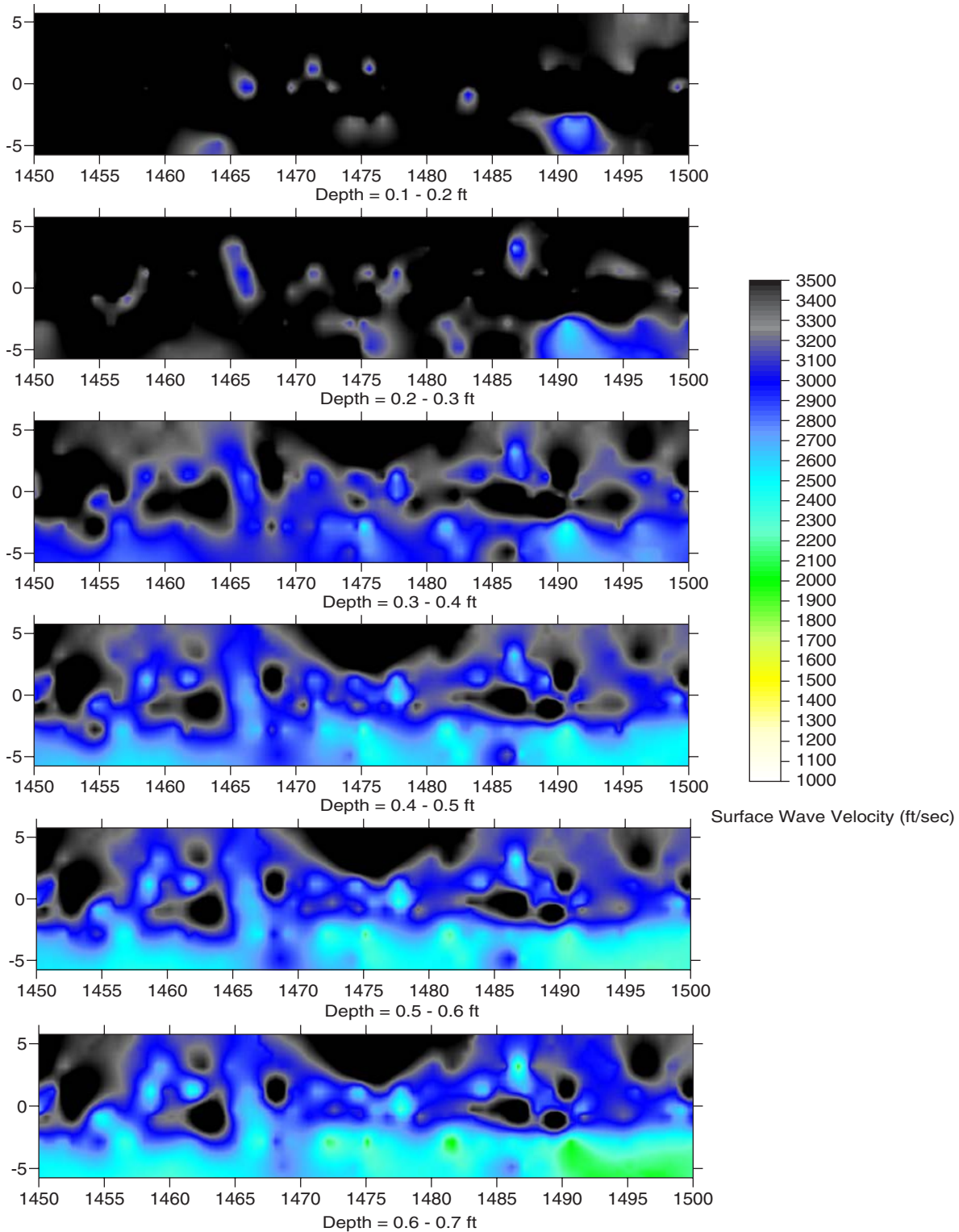
Note: Length = 1,450 to 1,500 ft.

Figure 3.30. SASW test results from the Florida section.
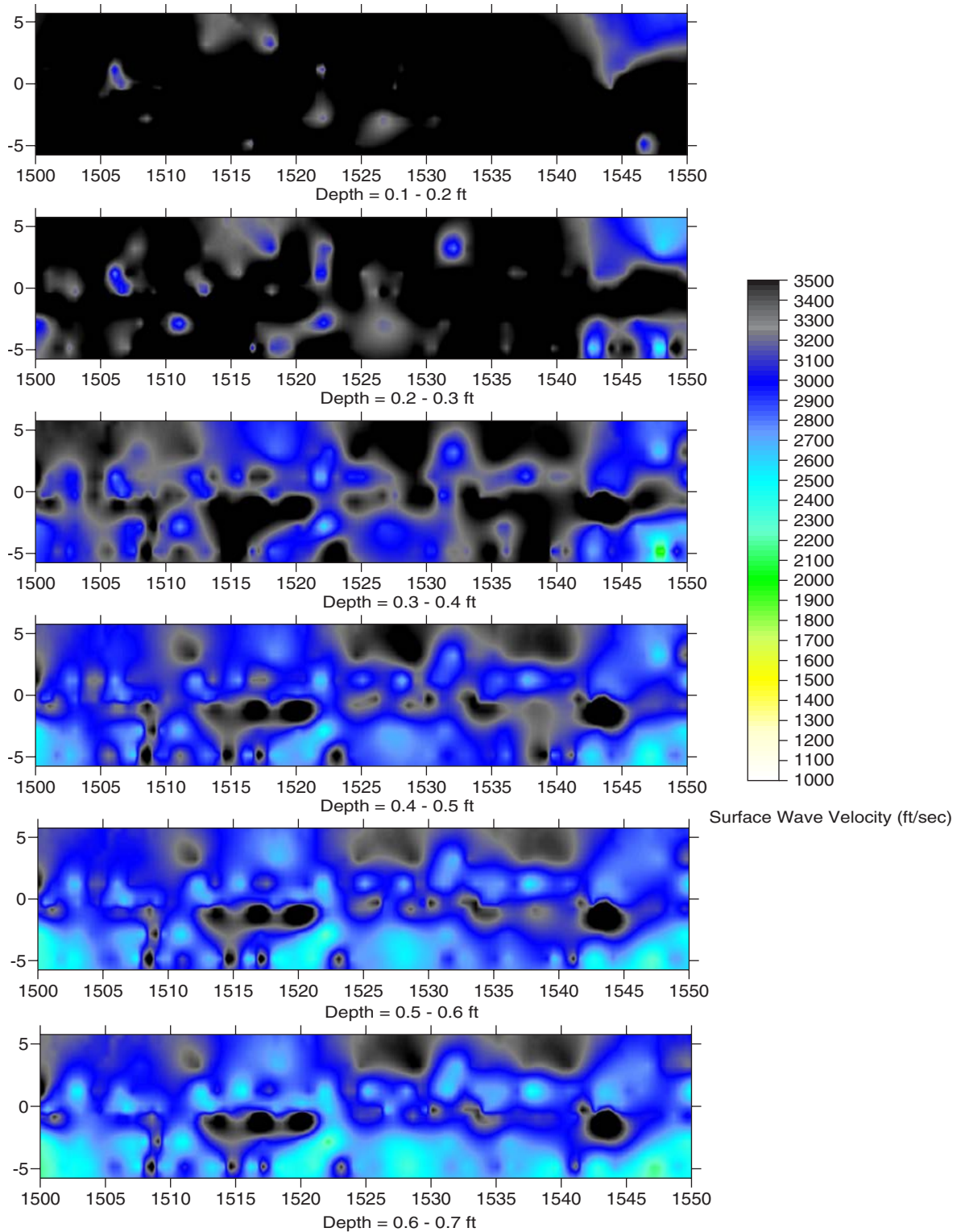
Note: Length = 1,500 to 1,550 ft.

Figure 3.31. SASW test results from the Florida section.
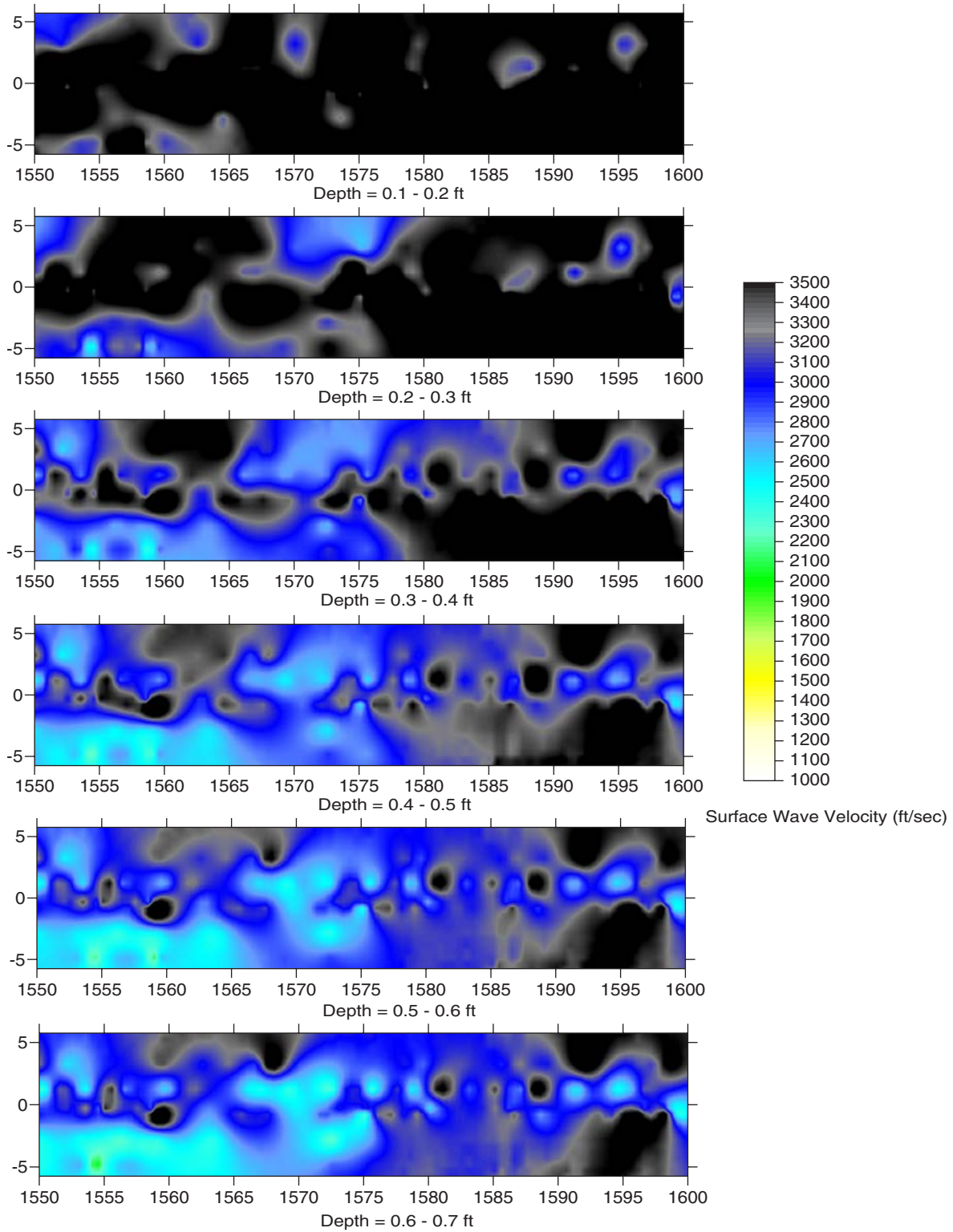
Note: Length = 1,550 to 1,600 ft.

Figure 3.32. SASW test results from the Florida section.

Note: Length = 1,600 to 1,650 ft.
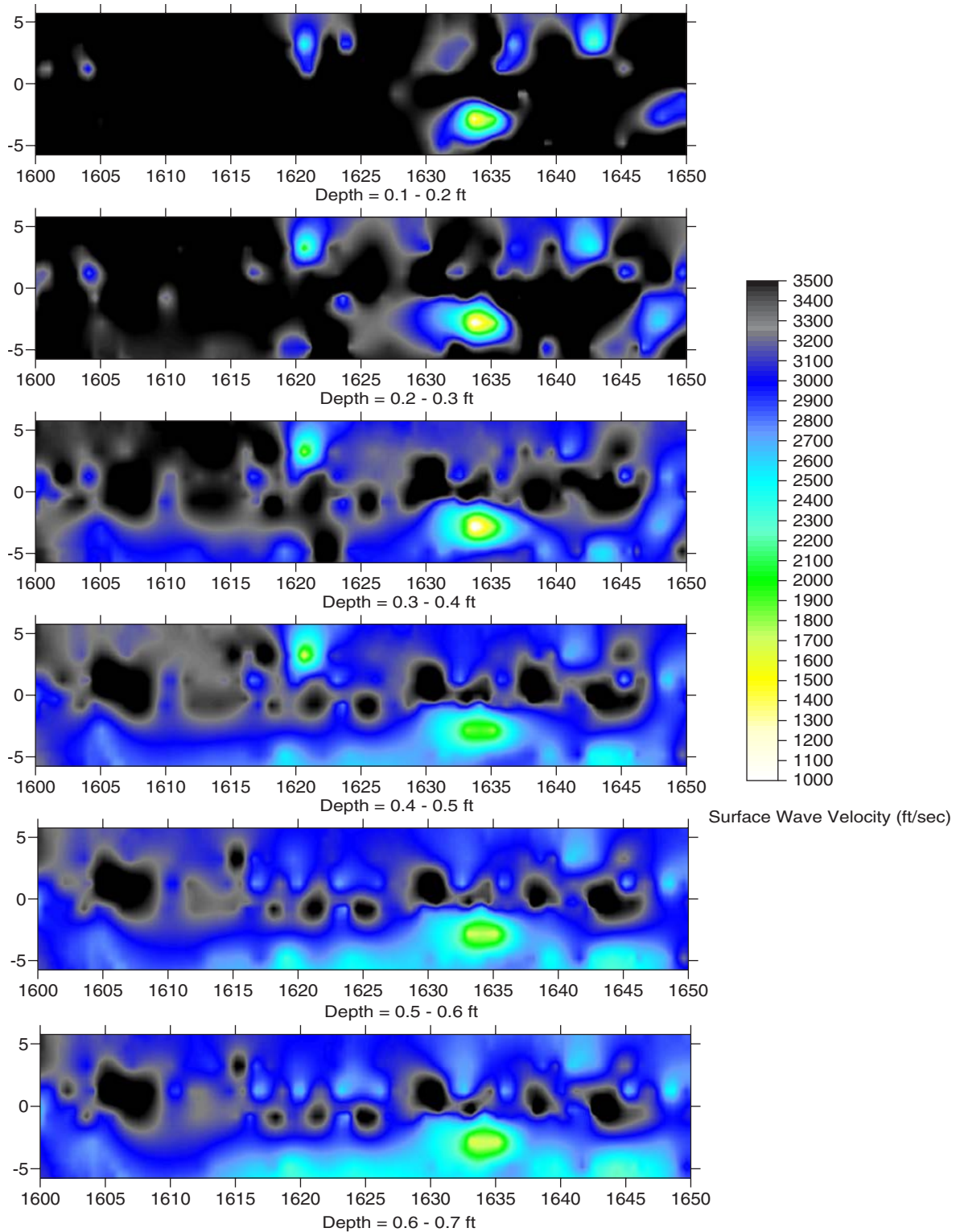
Figure 3.33. SASW test results from the Florida section.
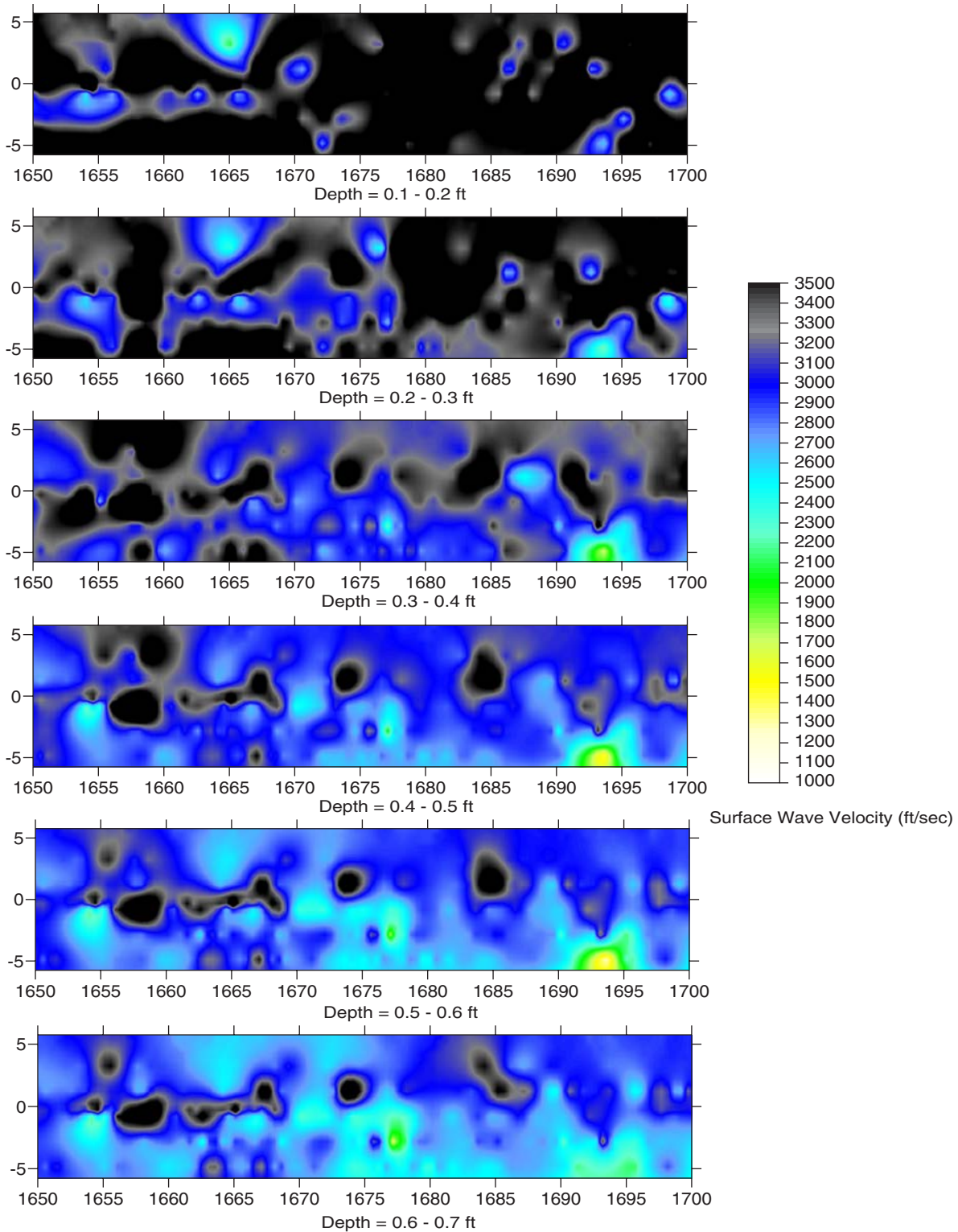
Note: Length = 1,650 to 1,700 ft.

Figure 3.34. SASW test results from the Florida section.

Note: Length = 1,700 to 1,750 ft.
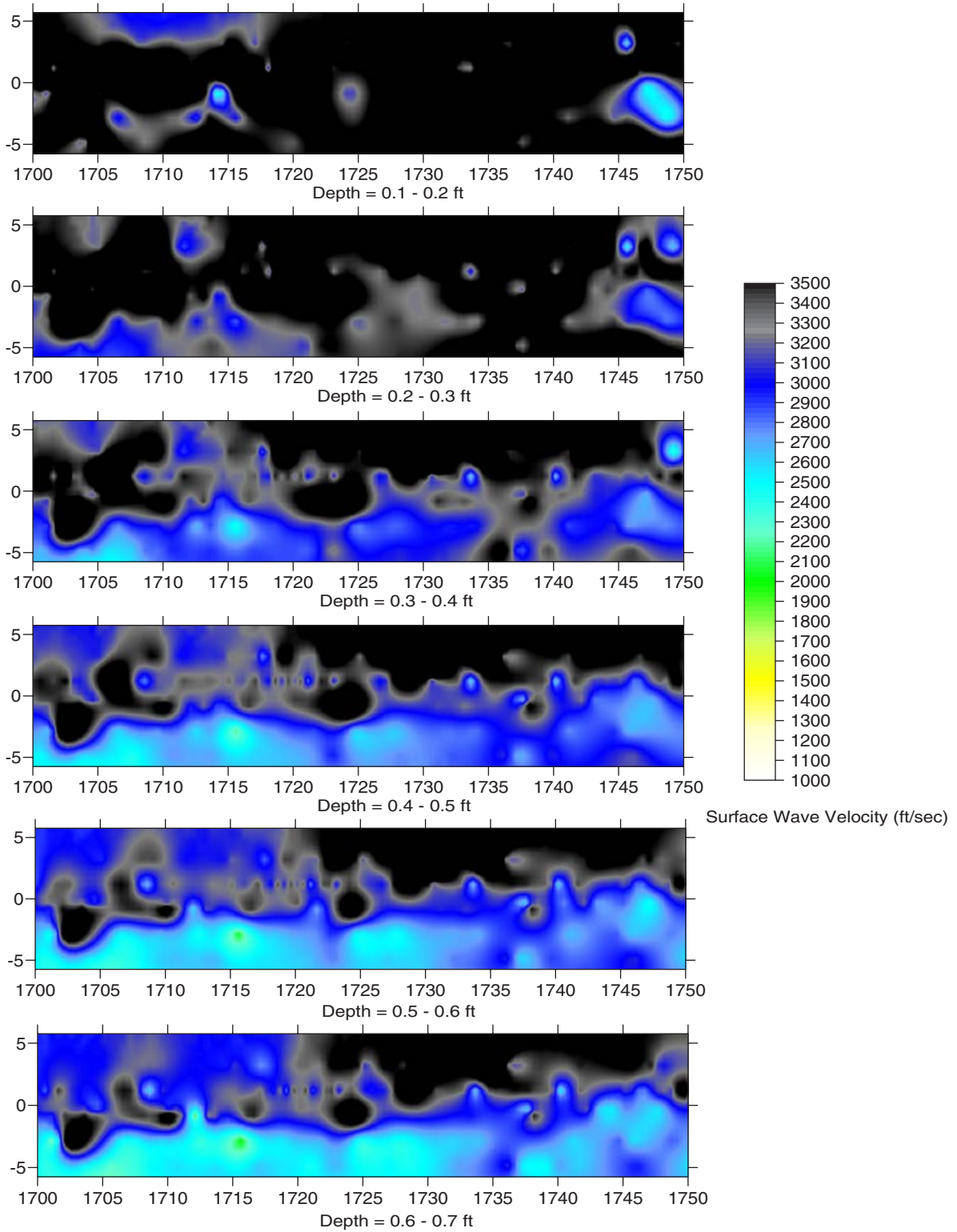
Figure 3.35. SASW test results from the Florida section.
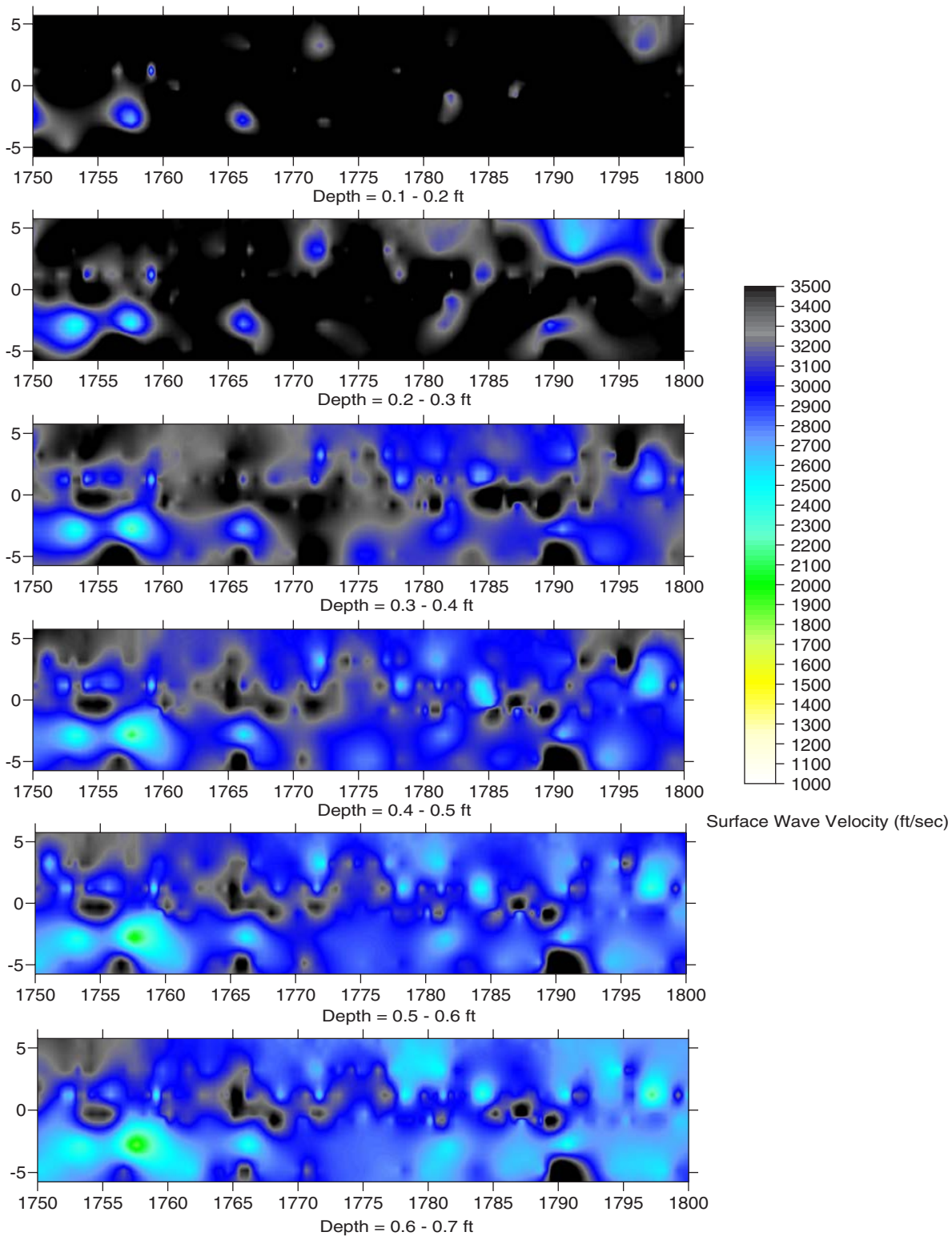
Note: Length = 1,750 to 1,800 ft.

Figure 3.36. SASW test results from the Florida section.

Note: Length = 1,800 to 1,850 ft.
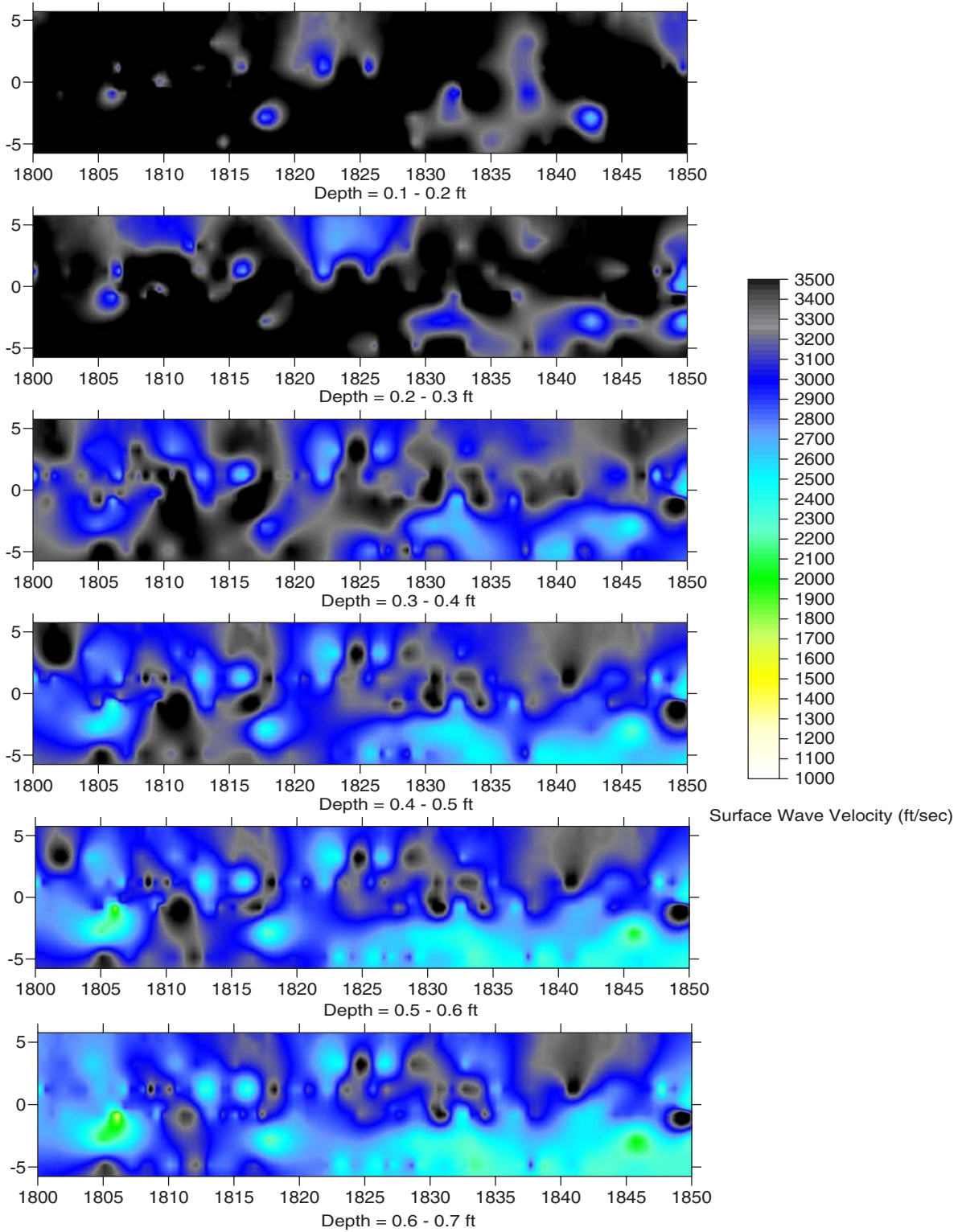
Figure 3.37. SASW test results from the Florida section.

Note: Length = 1,850 to 1,900 ft.
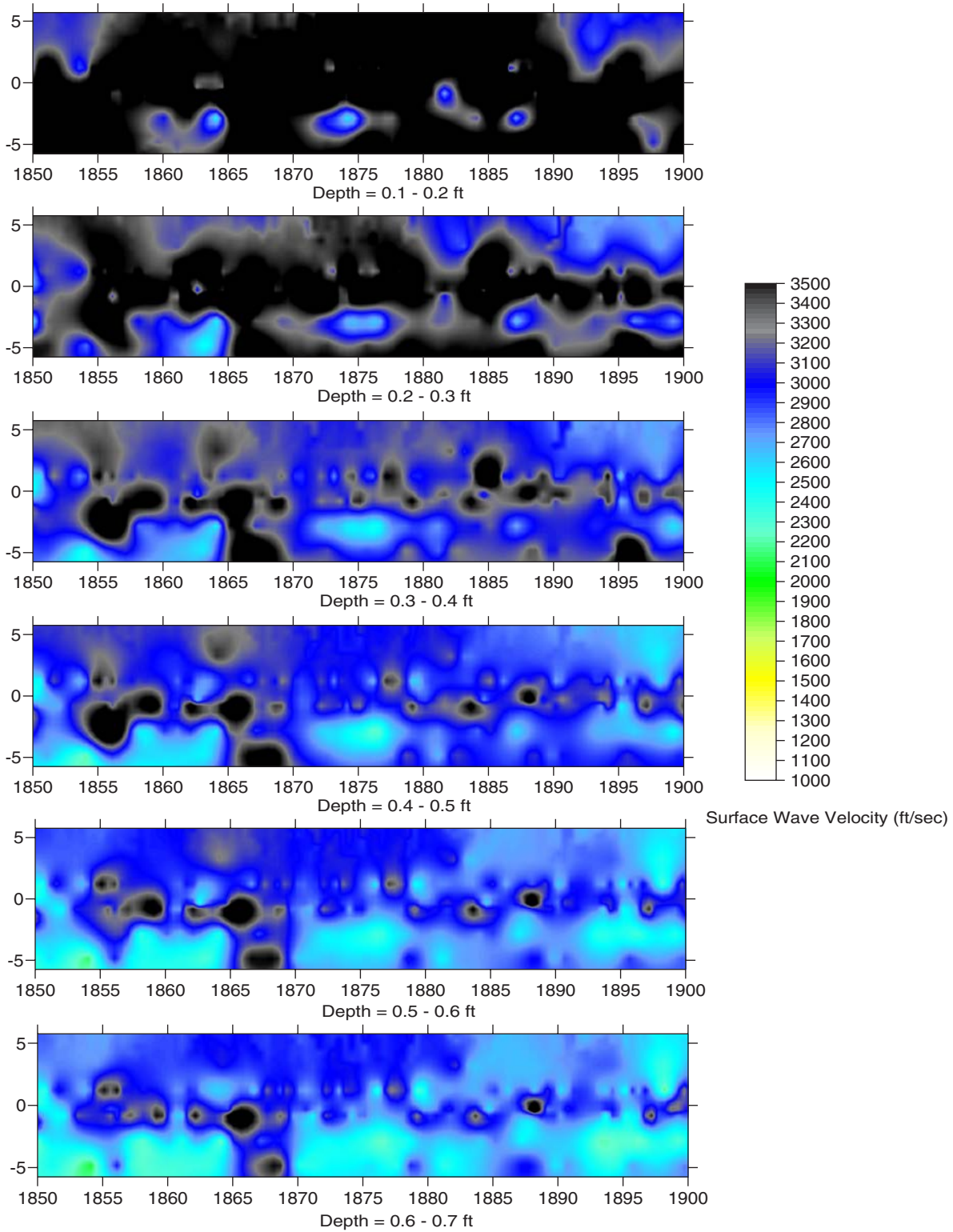
Figure 3.38. SASW test results from the Florida section.

Note: Length = 1,900 to 1,950 ft.
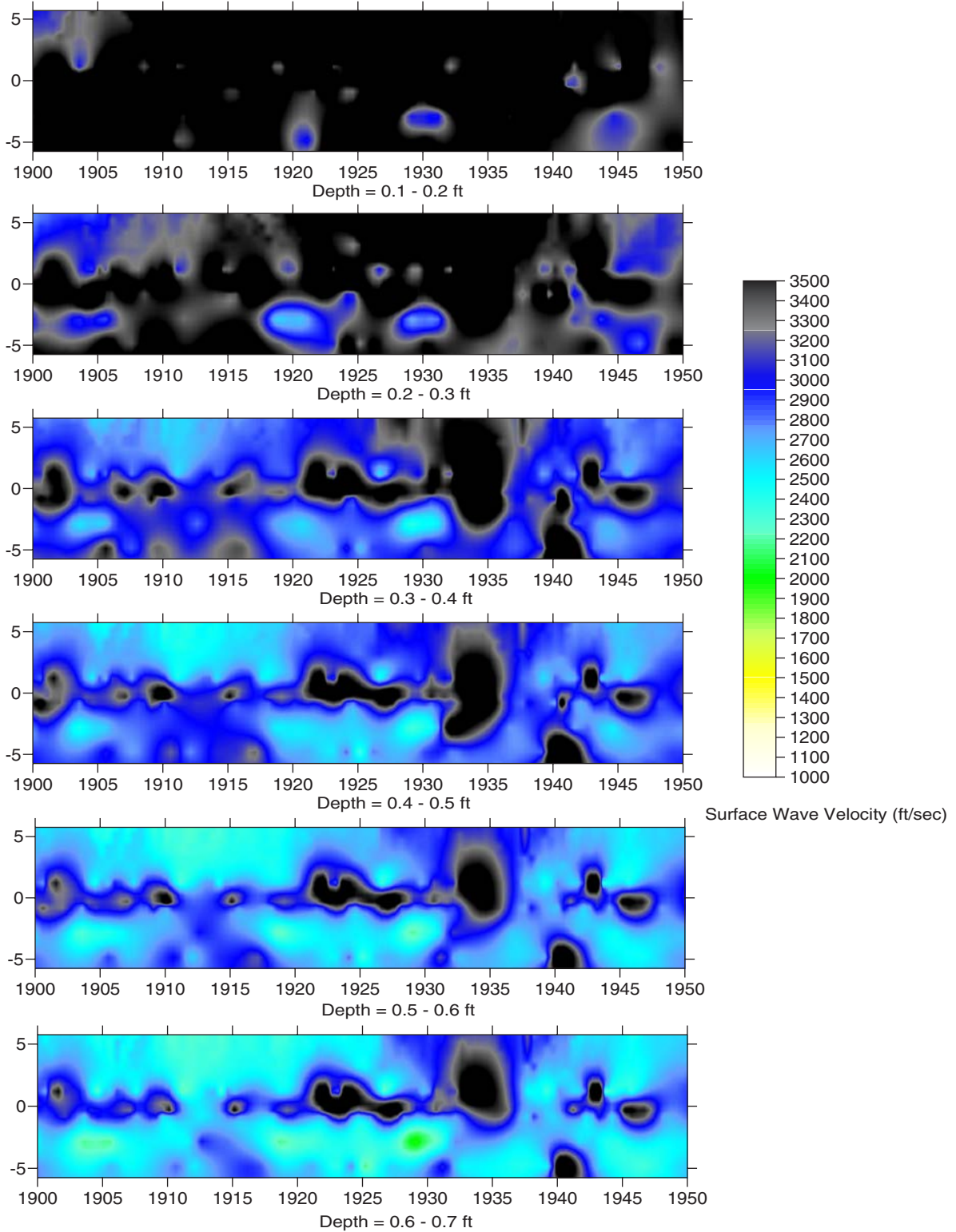
Figure 3.39. SASW test results from the Florida section.
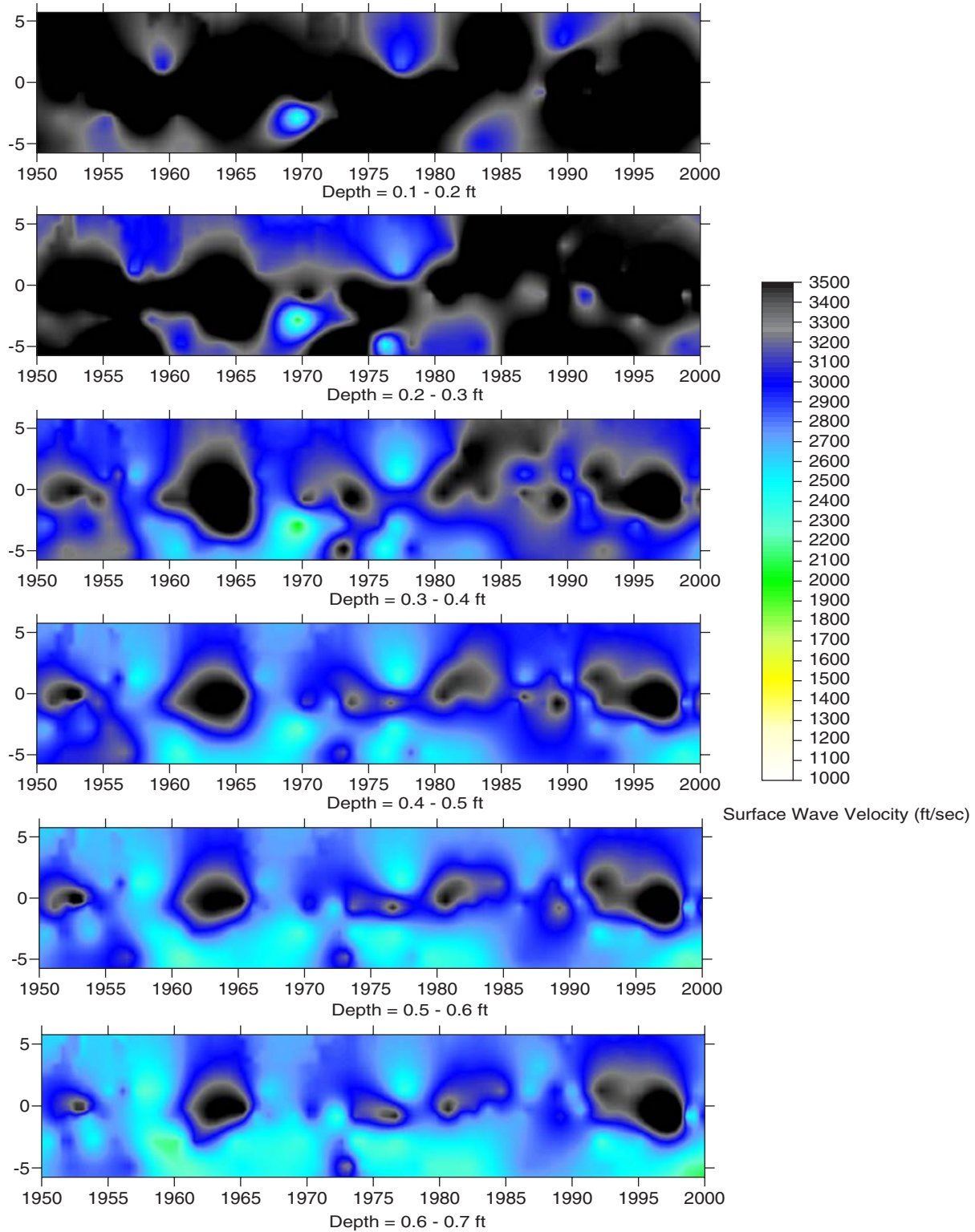
Note: Length = 1,950 to 2,000 ft.

Figure 3.40. SASW test results from the Florida section.

Note: Length = 2,000 to 2,050 ft.
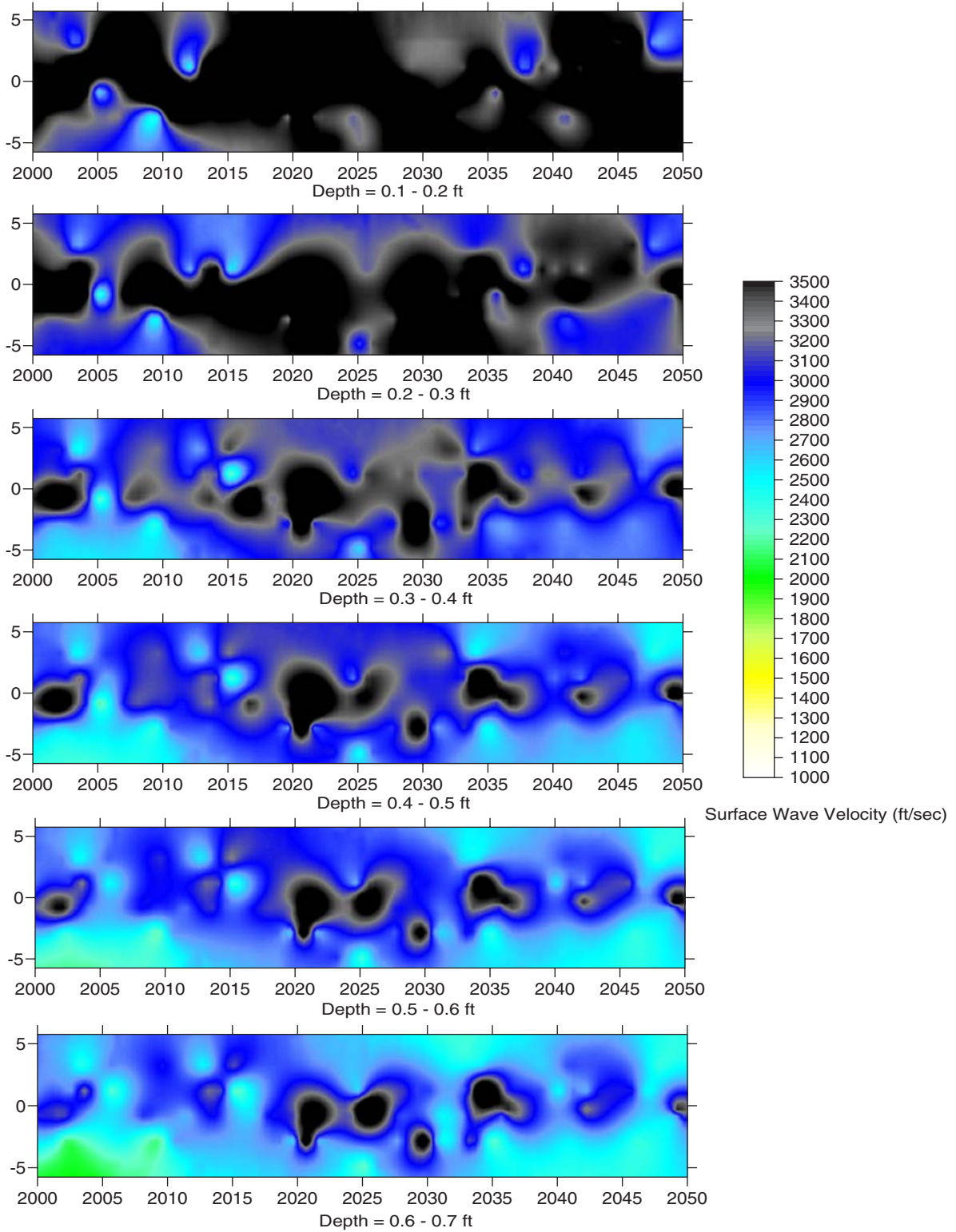
Figure 3.41. SASW test results from the Florida section.
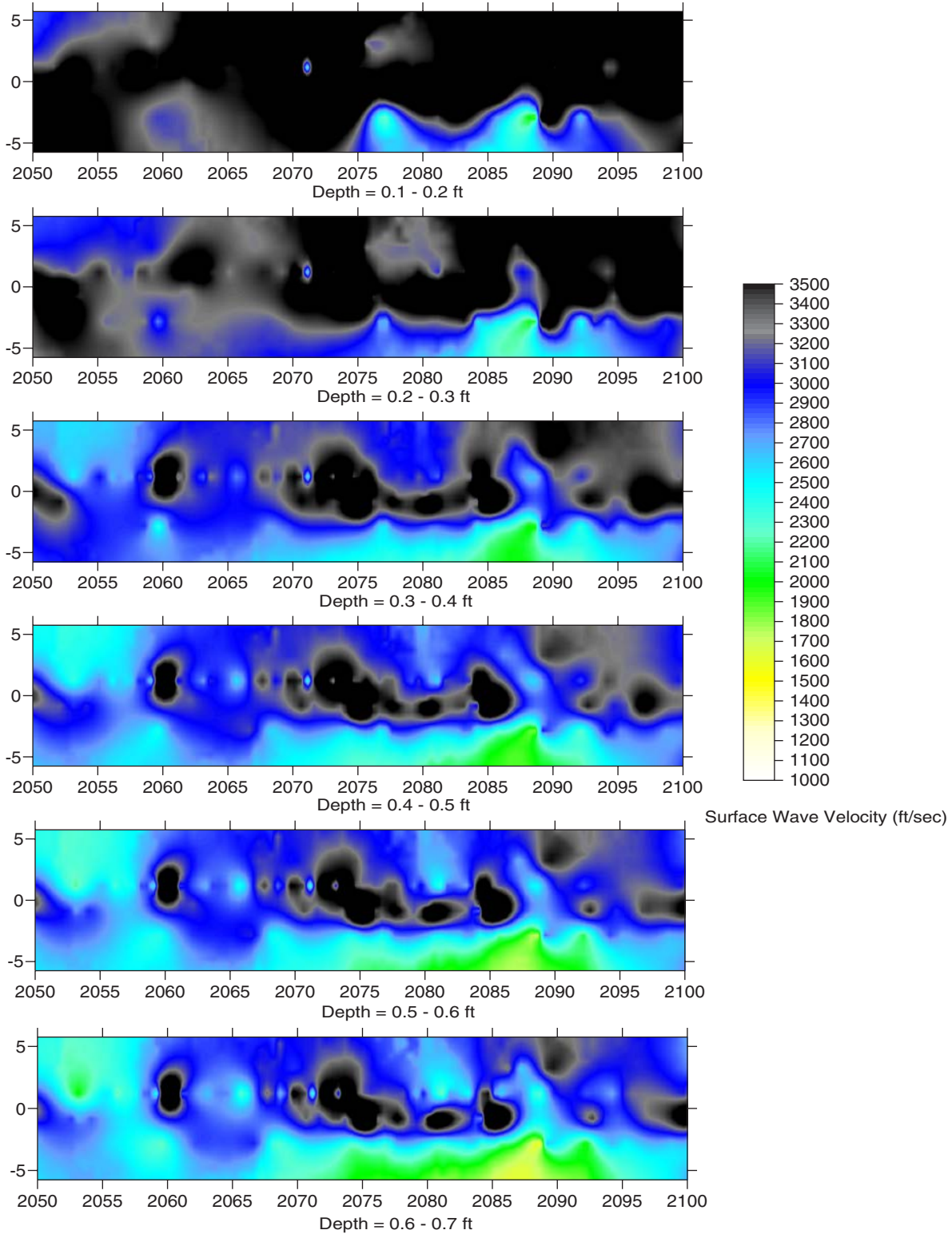
Note: Length = 2,050 to 2,100 ft.

Figure 3.42. SASW test results from the Florida section.
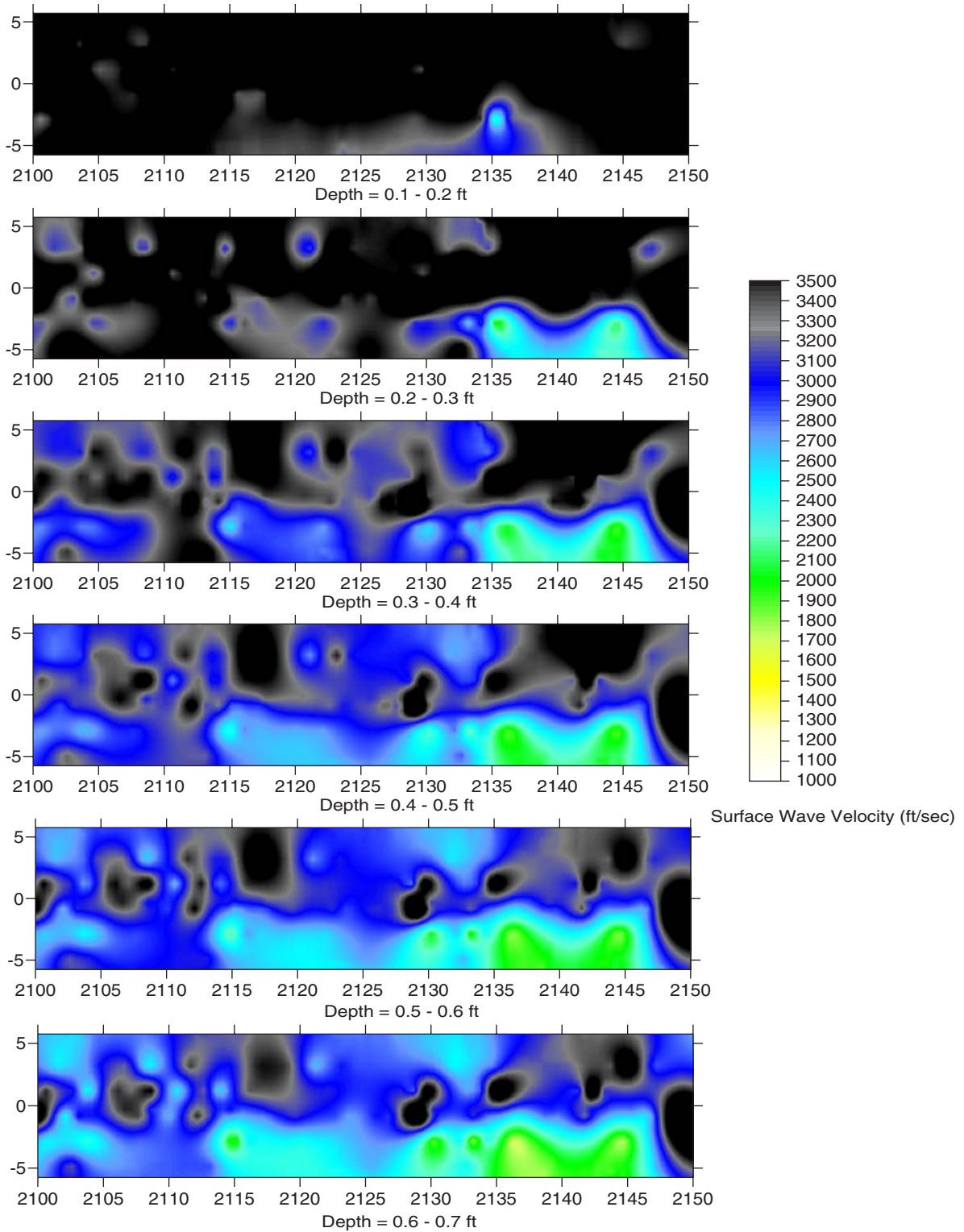
Note: Length = 2,100 to 2,150 ft.

Figure 3.43. SASW test results from the Florida section.

Note: Length = 2,150 to 2,200 ft.
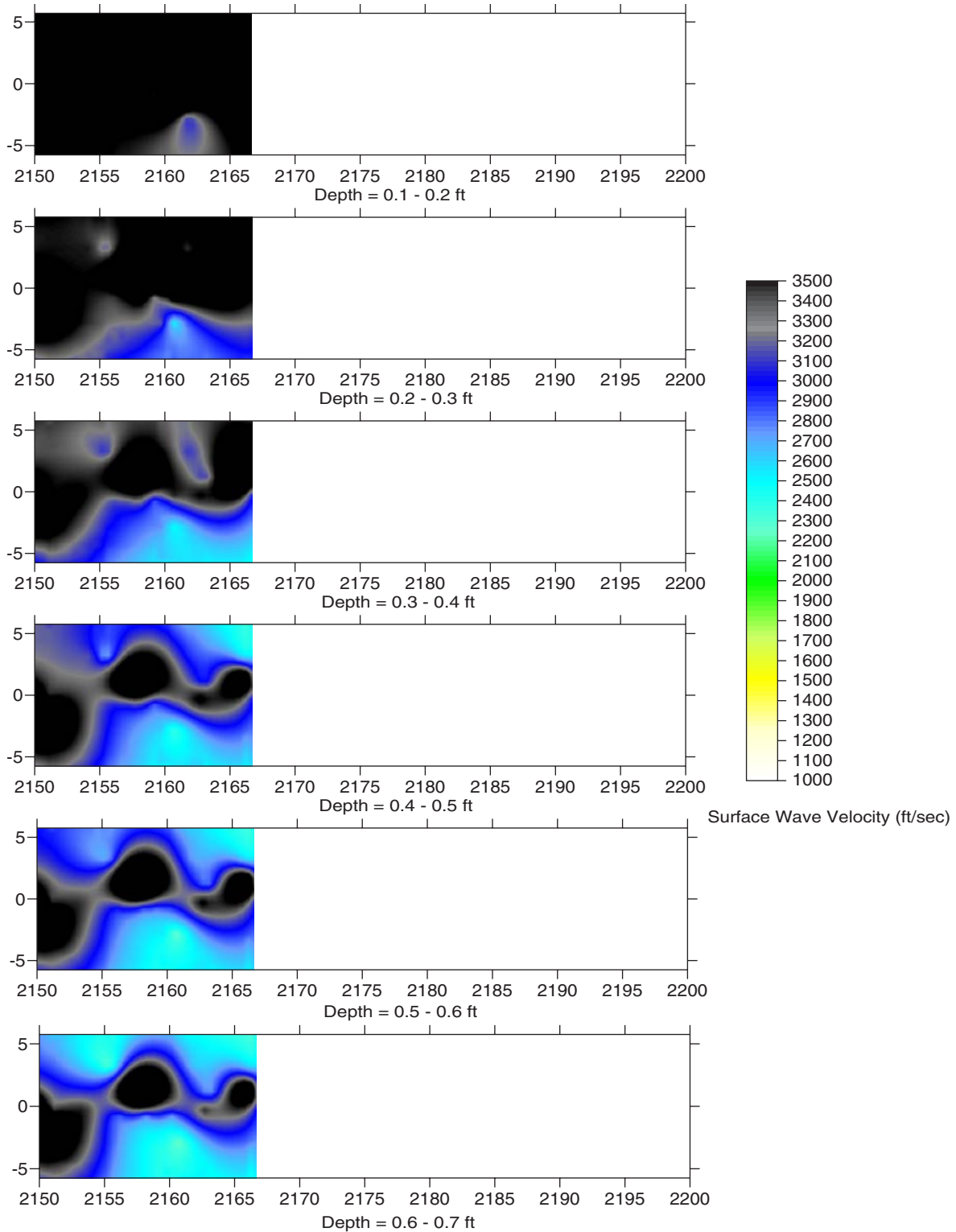
Figure 3.44. SASW test results from the Florida section.

Olson Engineering, Inc., SASW Test Results from Kansas Test Section

This chapter describes the results of Phase 2 subcontract research conducted by Olson Engineering, Inc., at the National Center for Asphalt Technology (NCAT), Auburn University, in Alabama, and at test sites in Pittsburg, Kansas. The research examined nondestructive testing (NDT) and evaluation of the pavement at these sites with stress wave methods for debonded hot-mix asphalt (HMA) layers. The field portion of this investigation was performed in accordance with generally accepted testing procedures. Research team members were Patrick K. Miller, Yajai Tinkey, and Larry D. Olson.

Field testing of the Olson Engineering, Inc., scanning IE/SASW system was carried out in Kansas on a selected 0.7-mi-long section of US-400. This report provides a graphical summary of the SASW results for each 50-foot length. The results are presented for incremental depths from 0.1 to 0.7 ft. from the surface. The surface wave velocities are shown with a color scale, and higher velocities represent better pavement conditions. Analysis of these data are reported in Volume 1. Figures 4.1 through 4.72 present SASW test results.
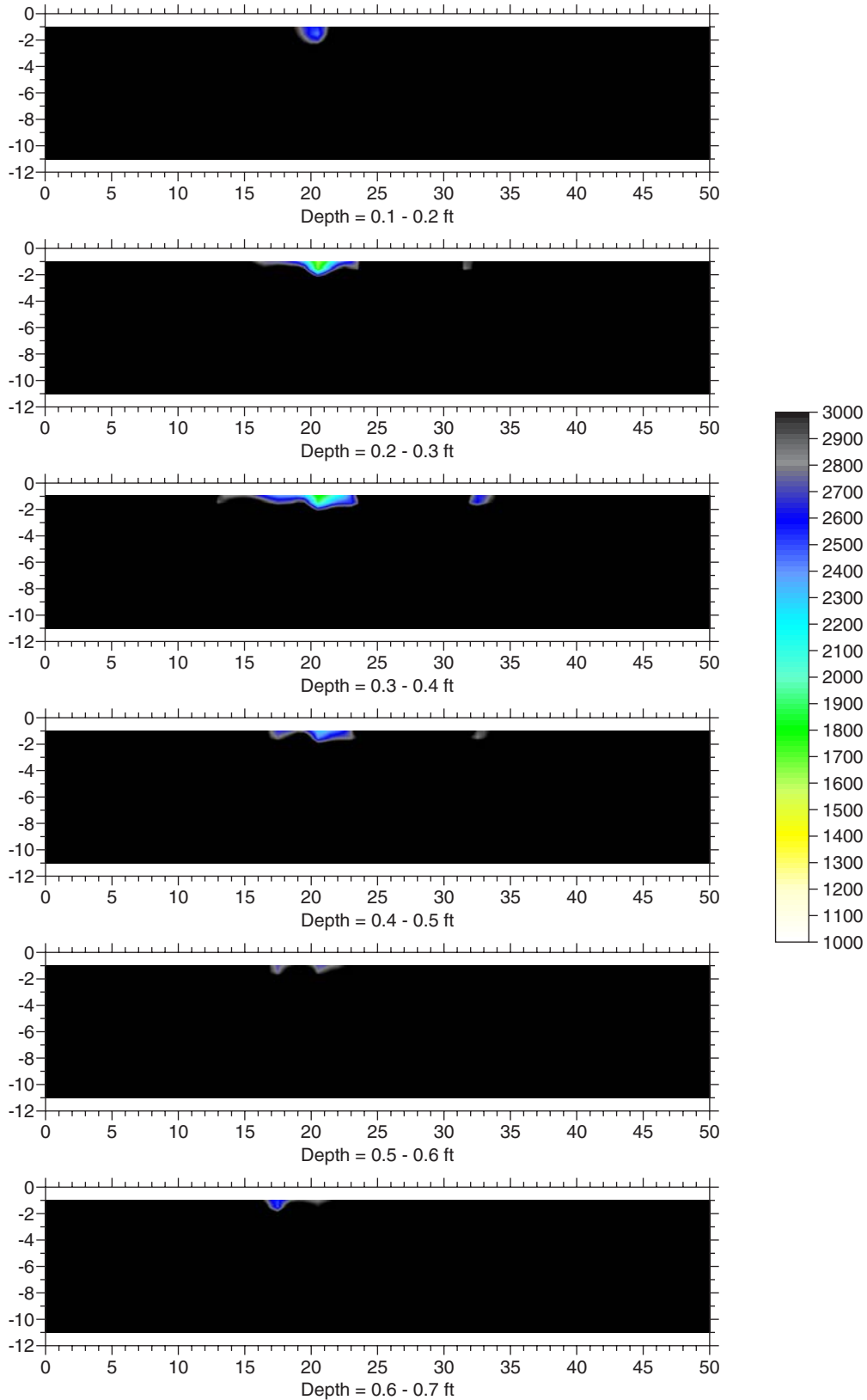
Figure 4.1. Kansas Test Section 0 to 50.
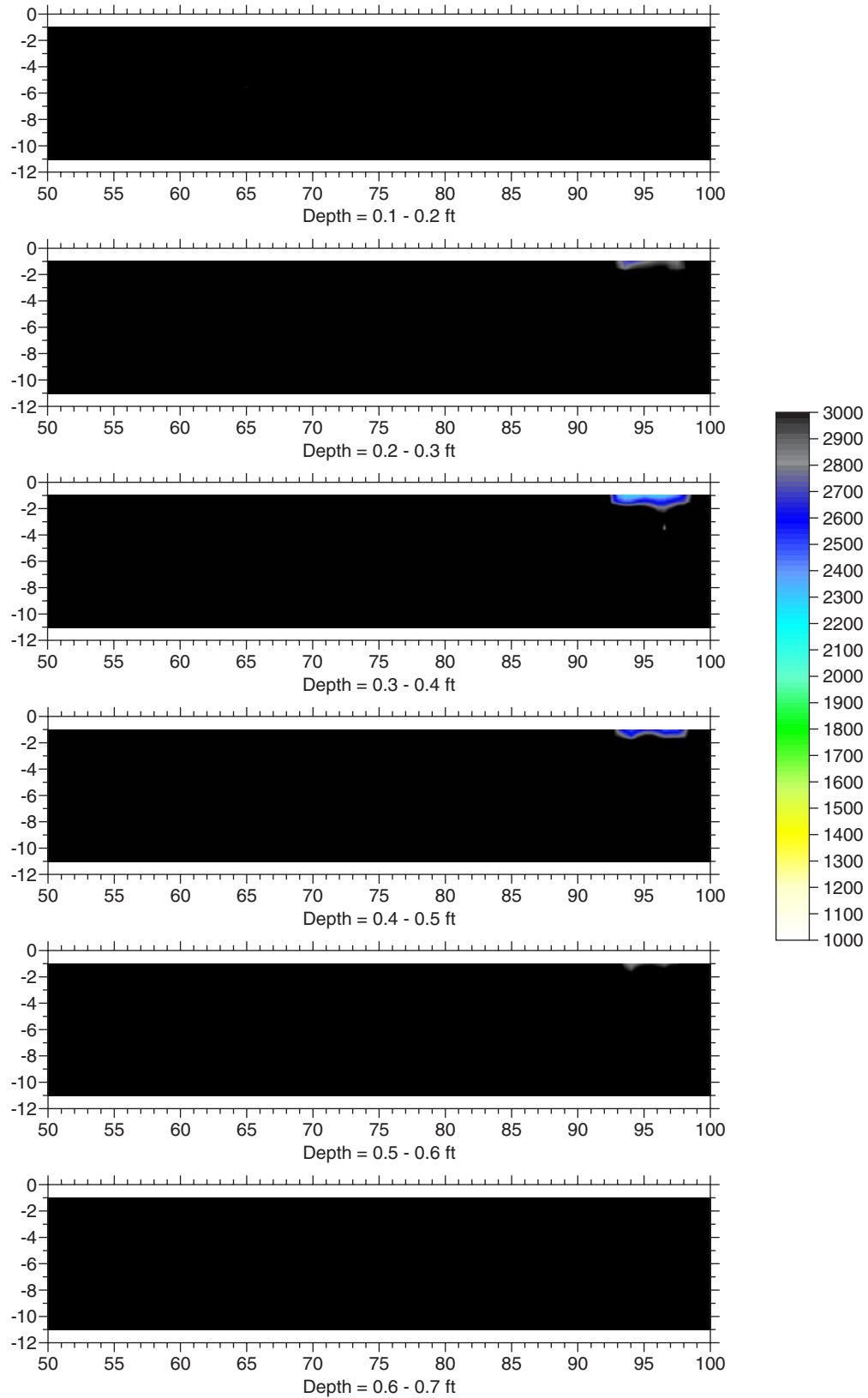
**Figure 4.2. Section 50 to 100.**
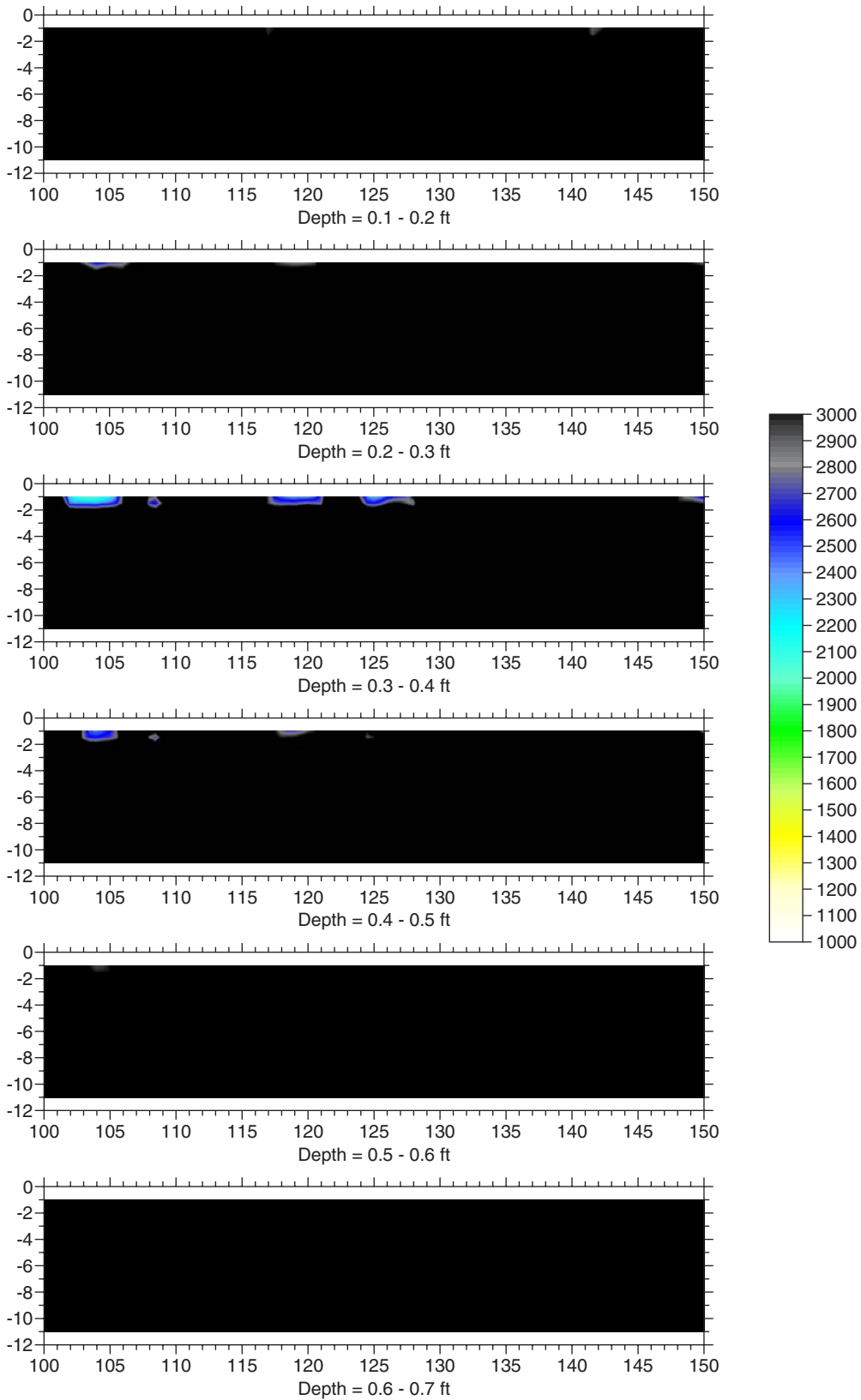
**Figure 4.3. Section 100 to 150.**
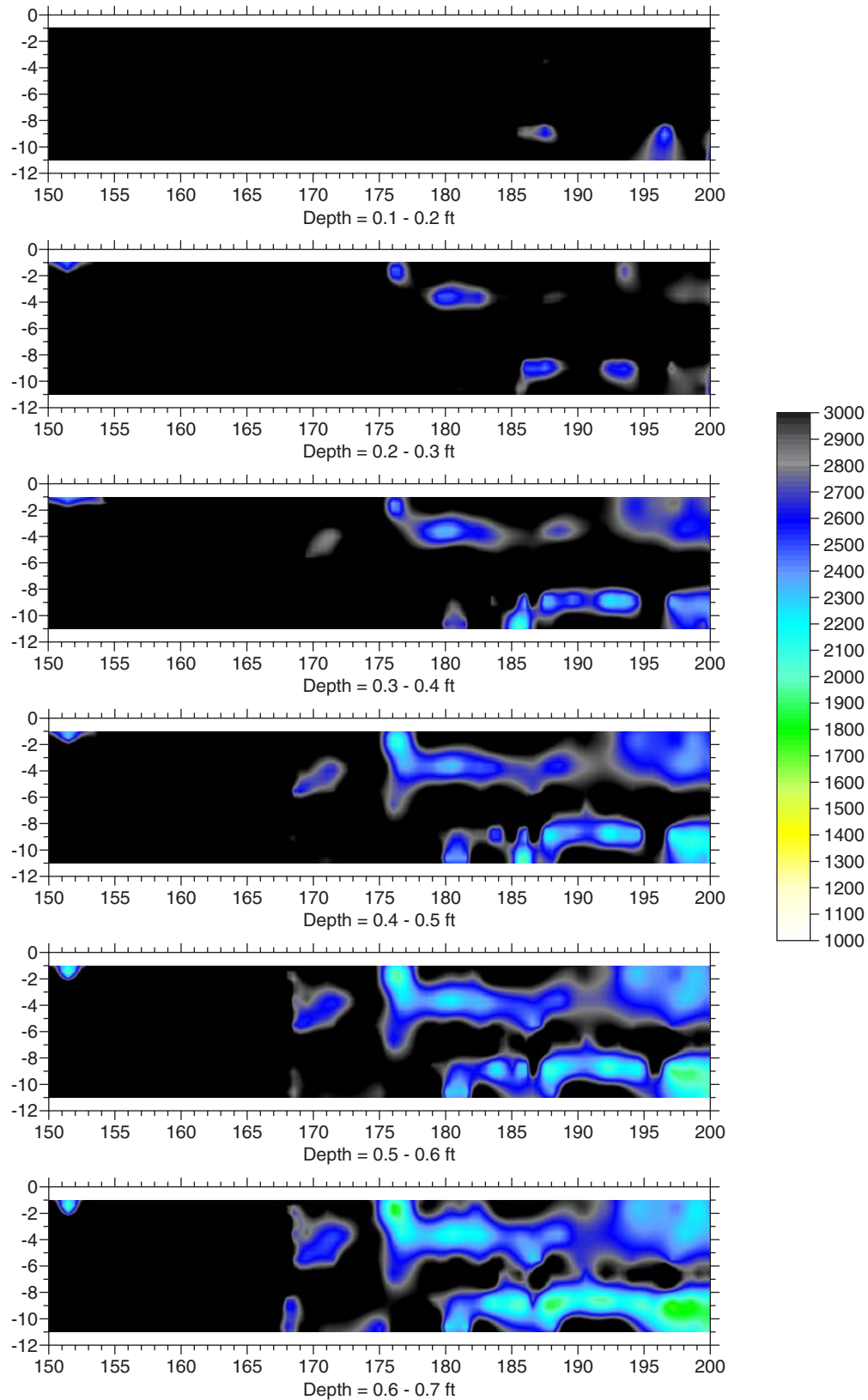
**Figure 4.4. Section 150 to 200.**
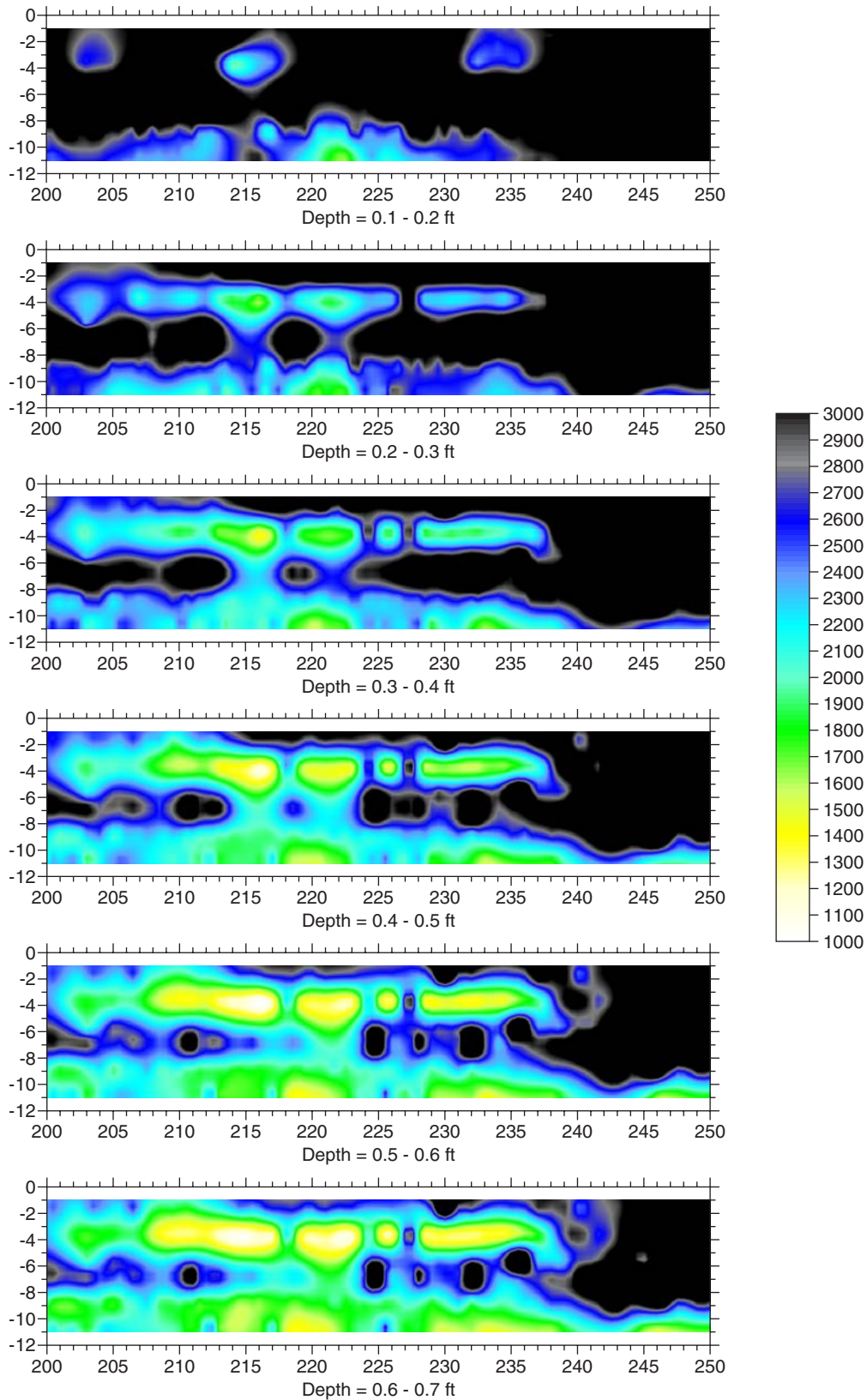
**Figure 4.5. Section 200 to 250.**
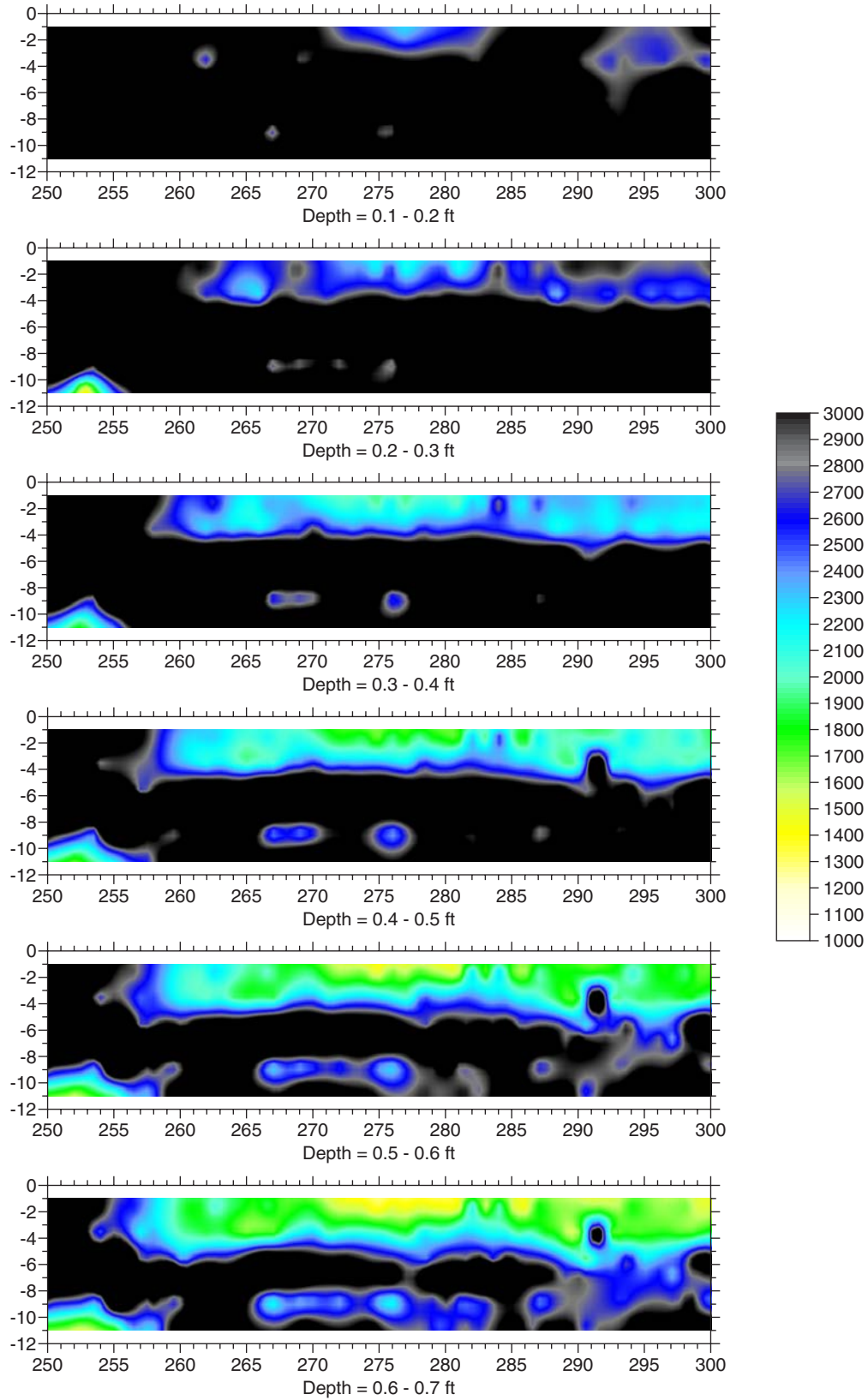
Figure 4.6. Section 250 to 300.
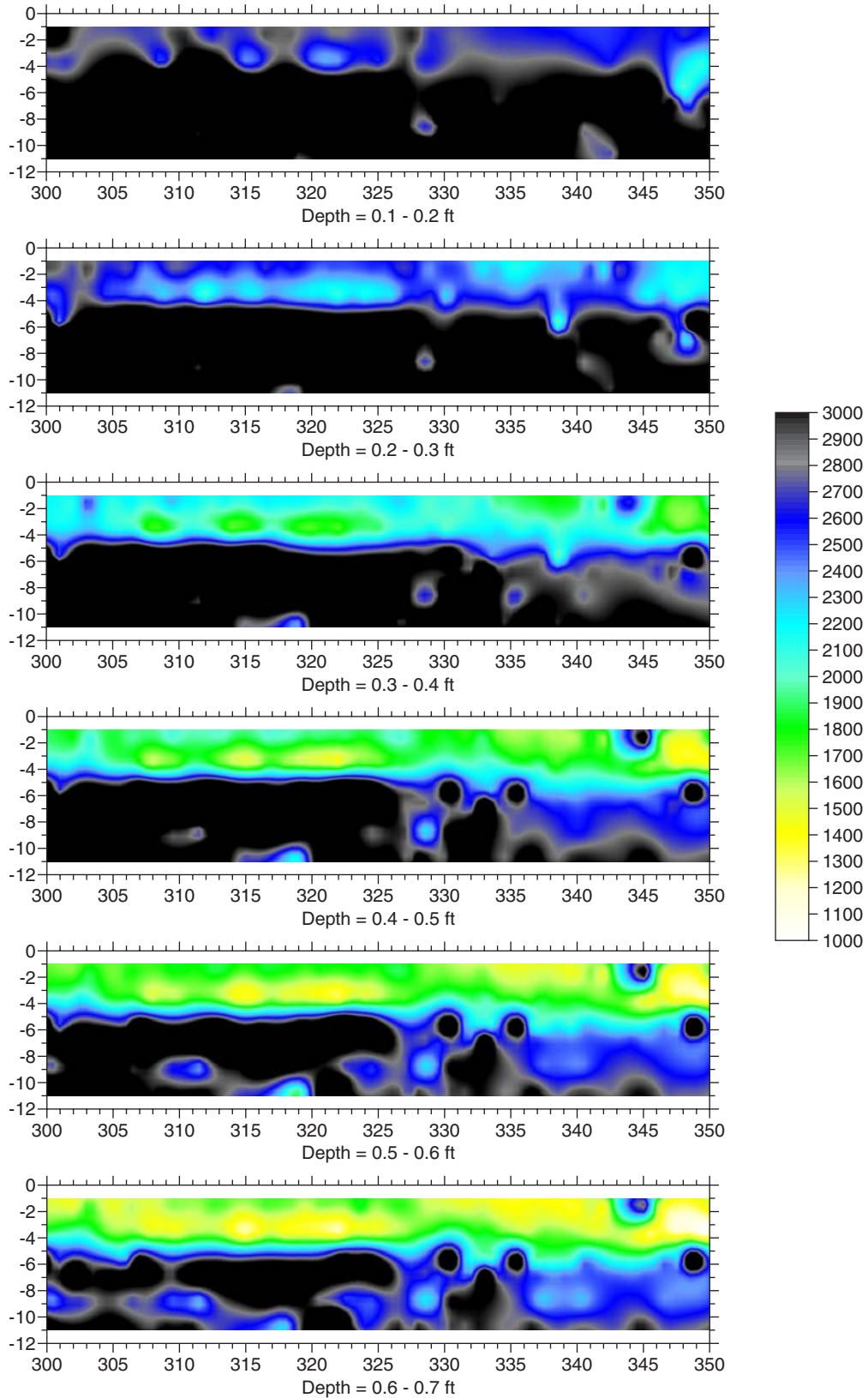
Figure 4.7. Section 300 to 350.
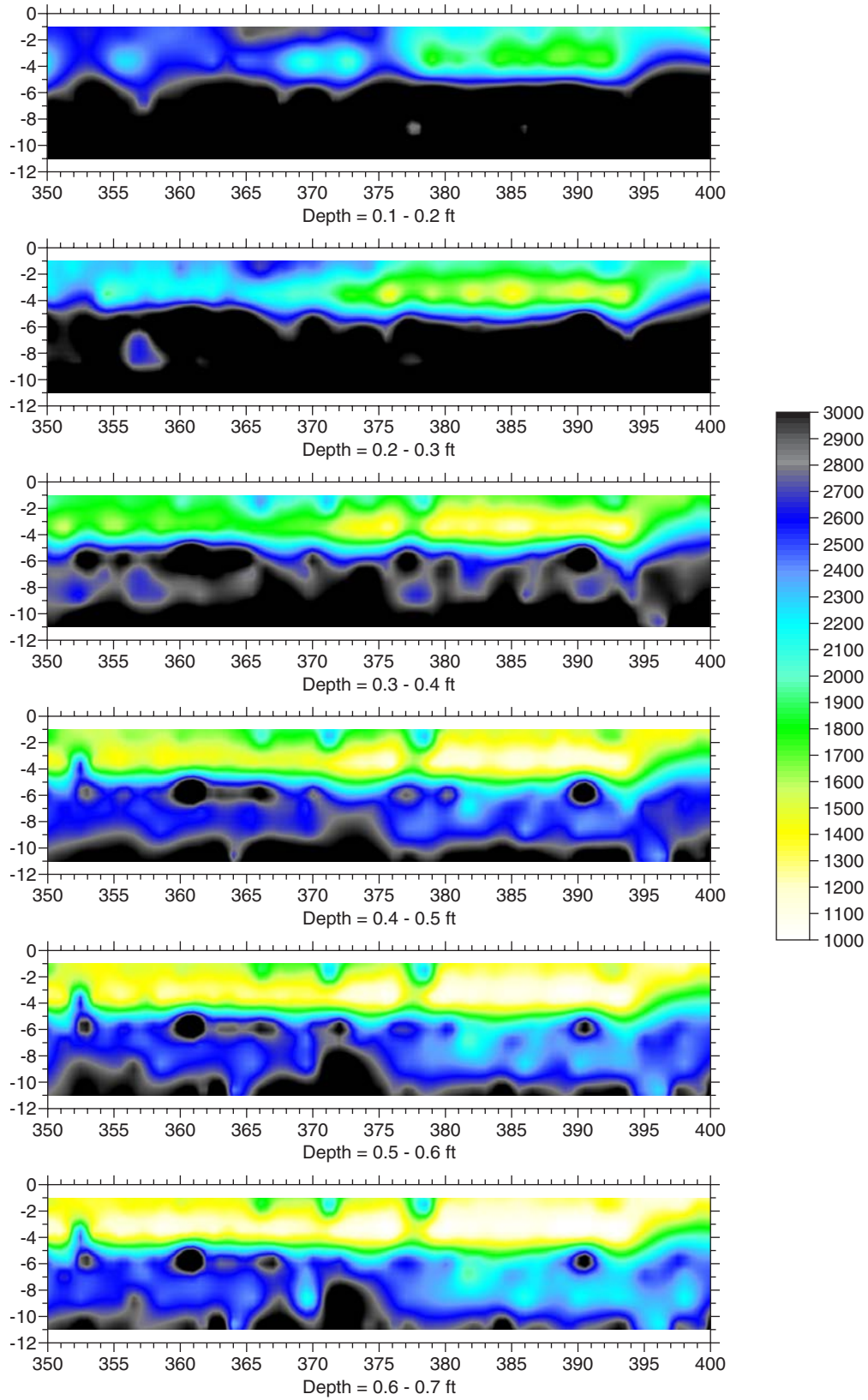
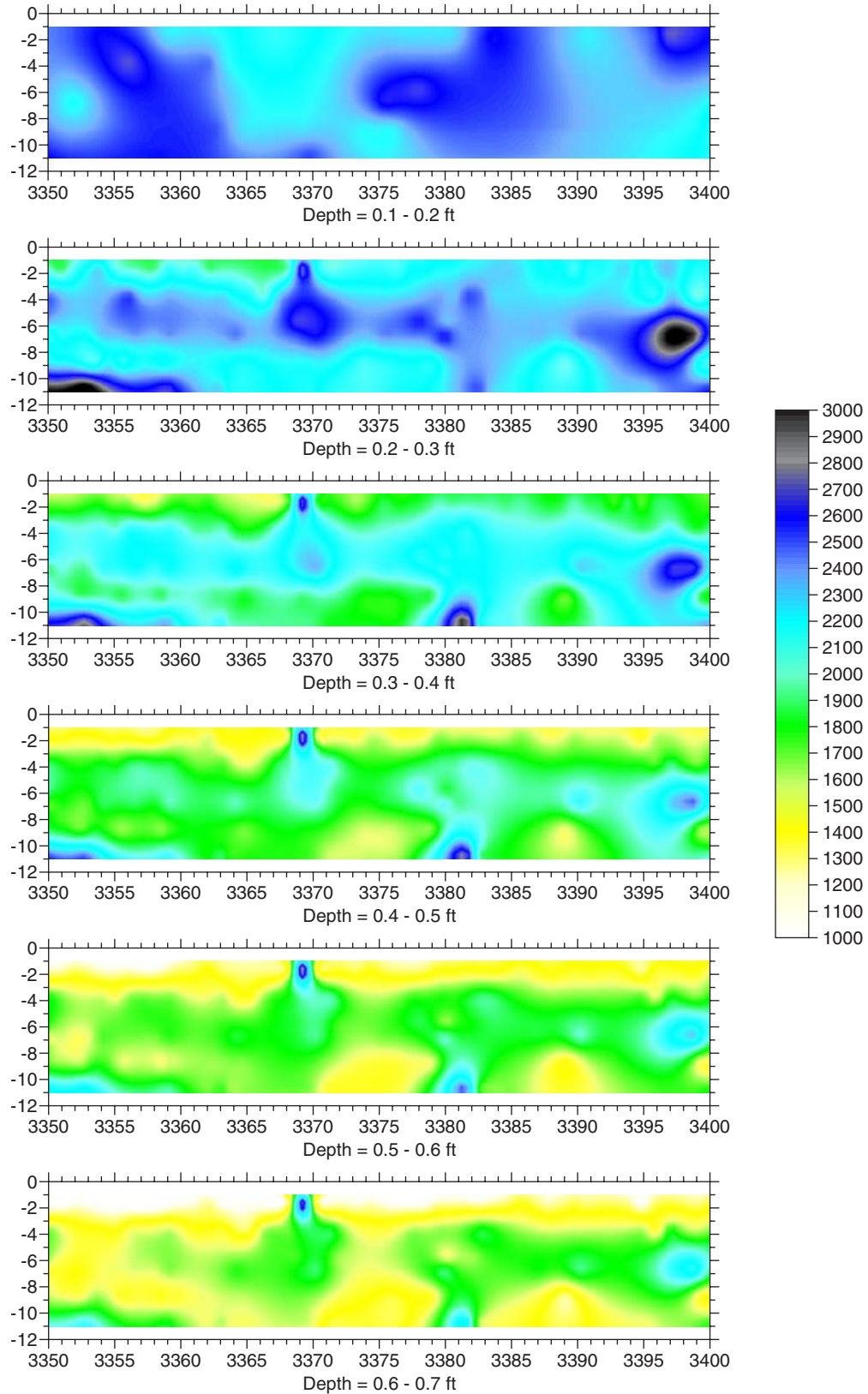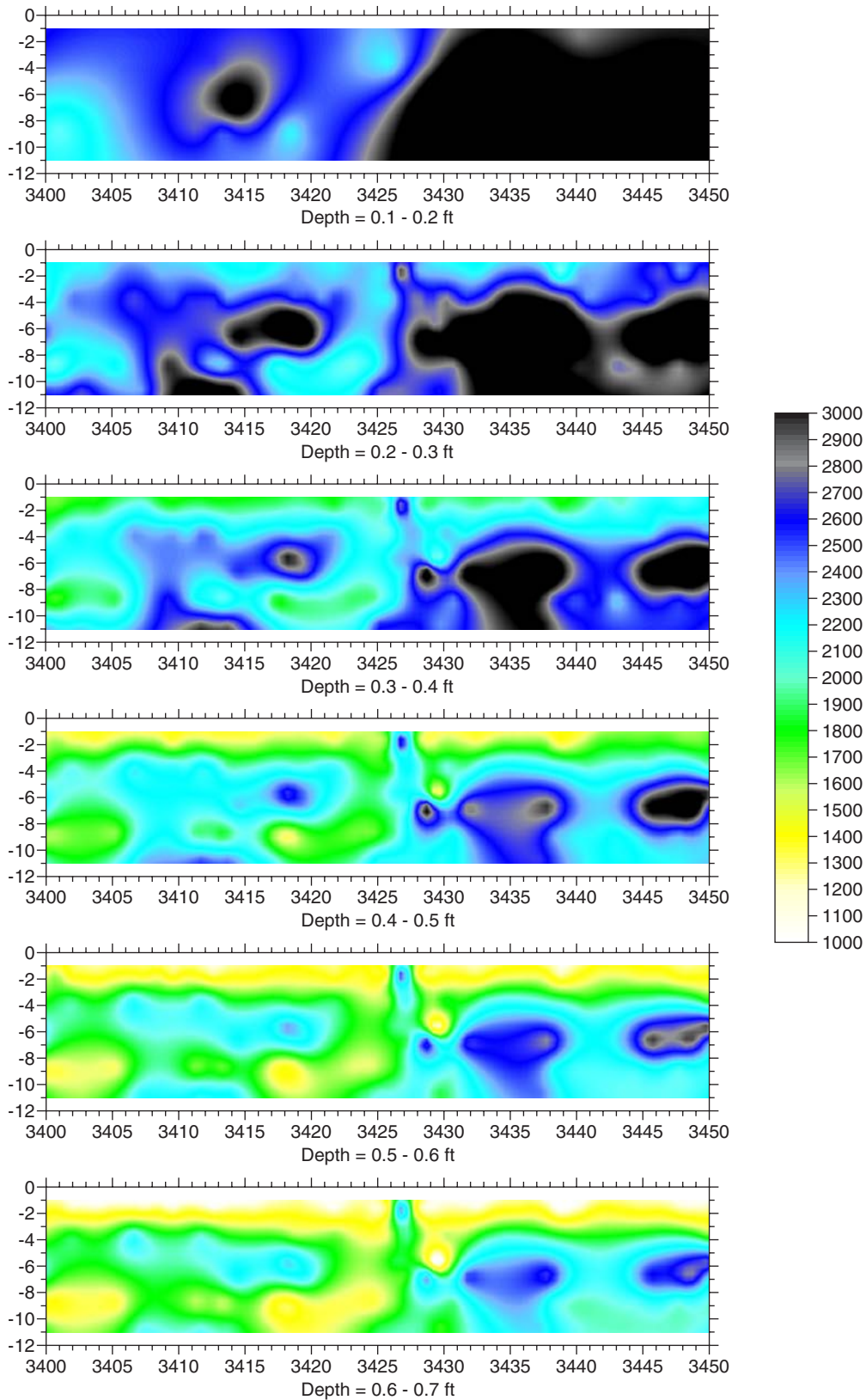**Figure 4.8. Section 350 to 400.**
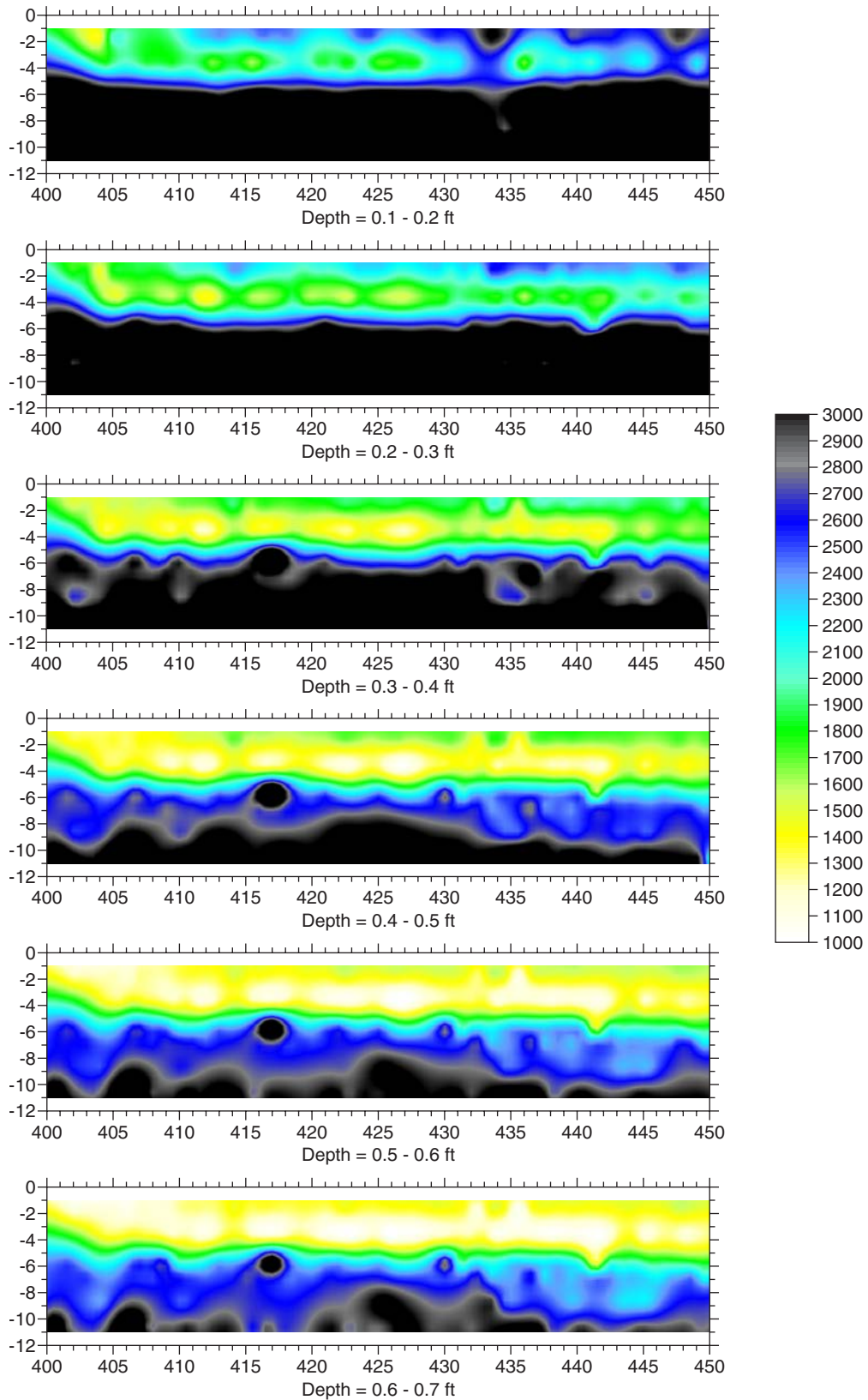
Figure 4.9. Section 400 to 450.
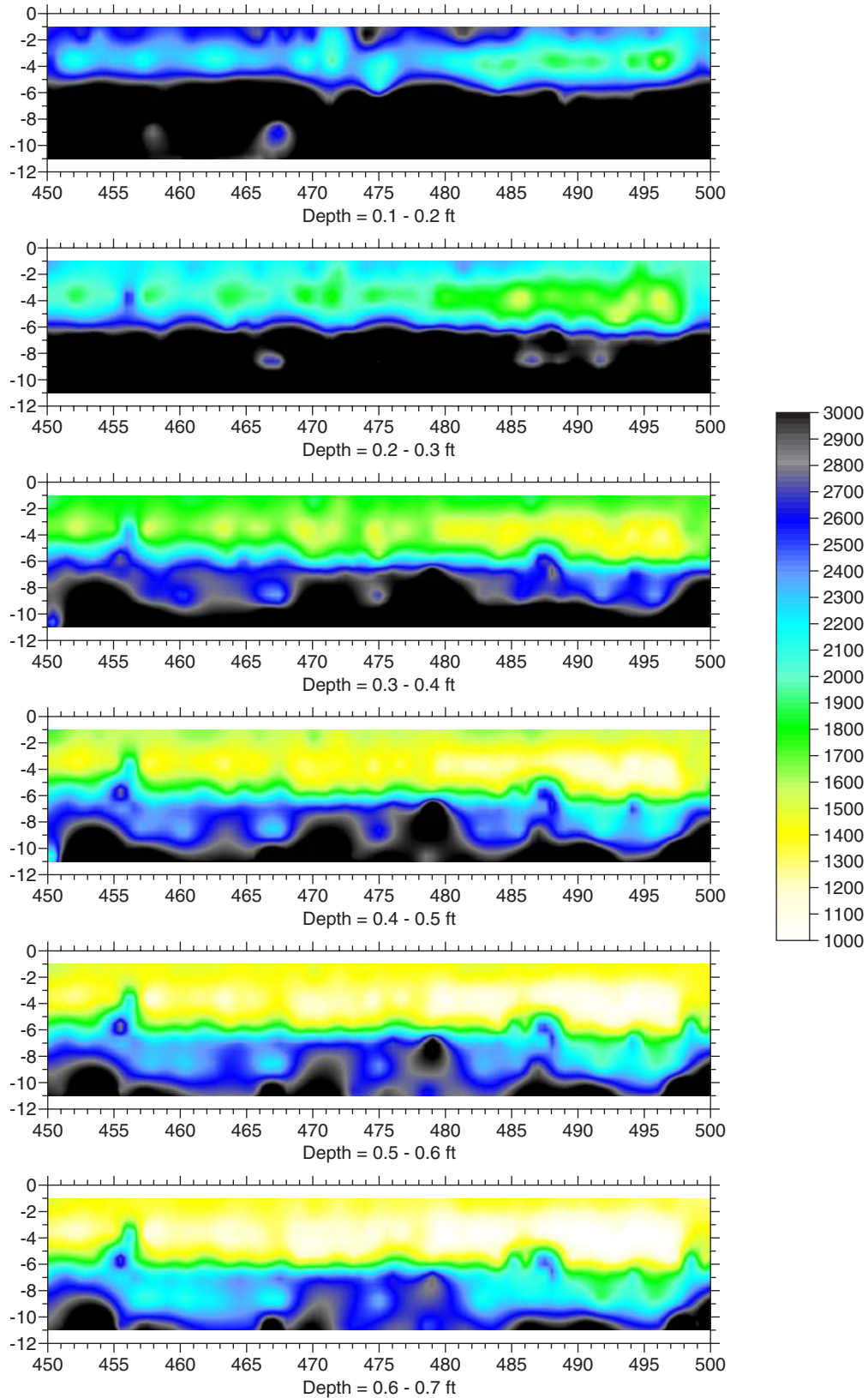
Figure 4.10. Section 450 to 500.
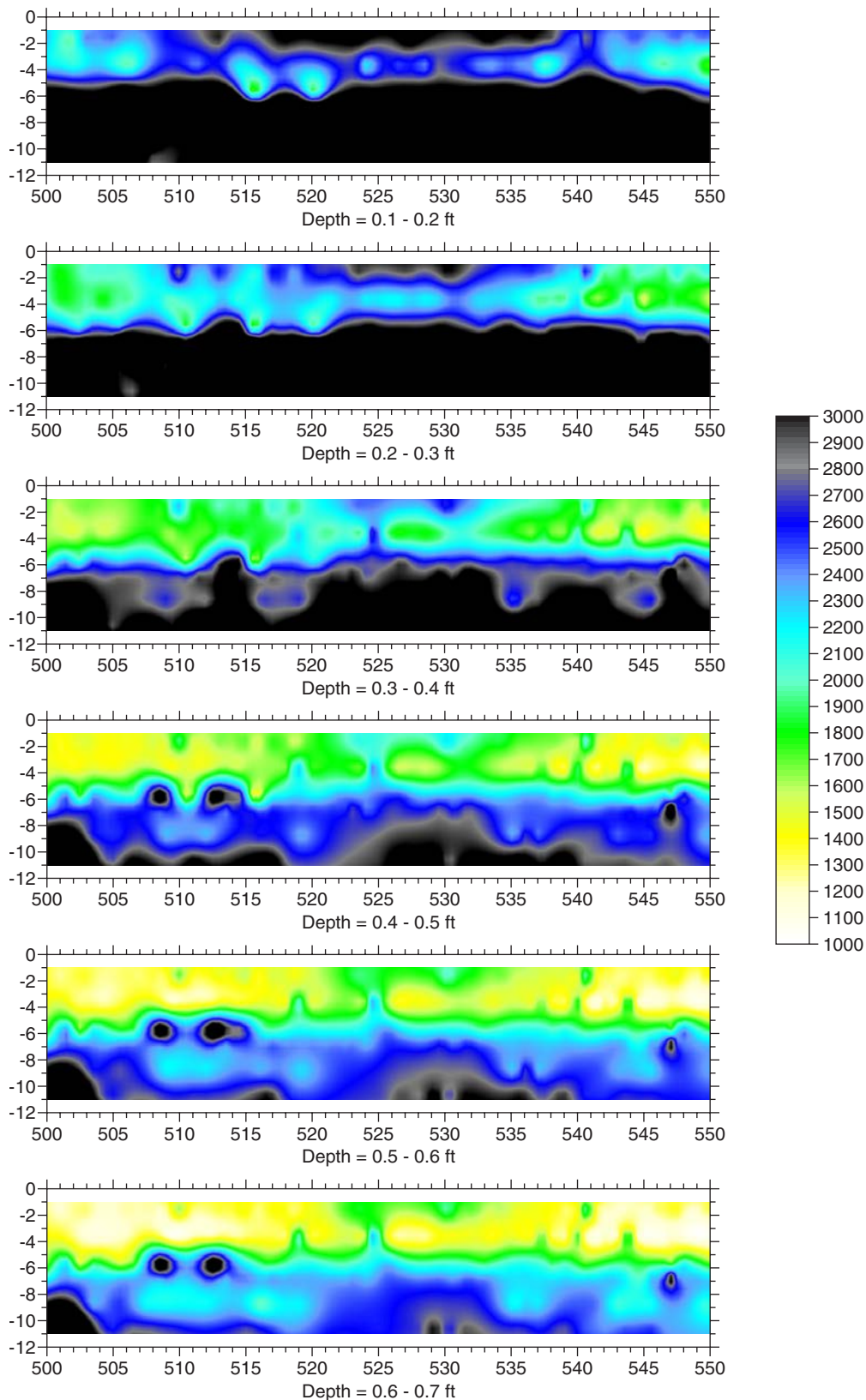
Figure 4.11. Section 500 to 550.
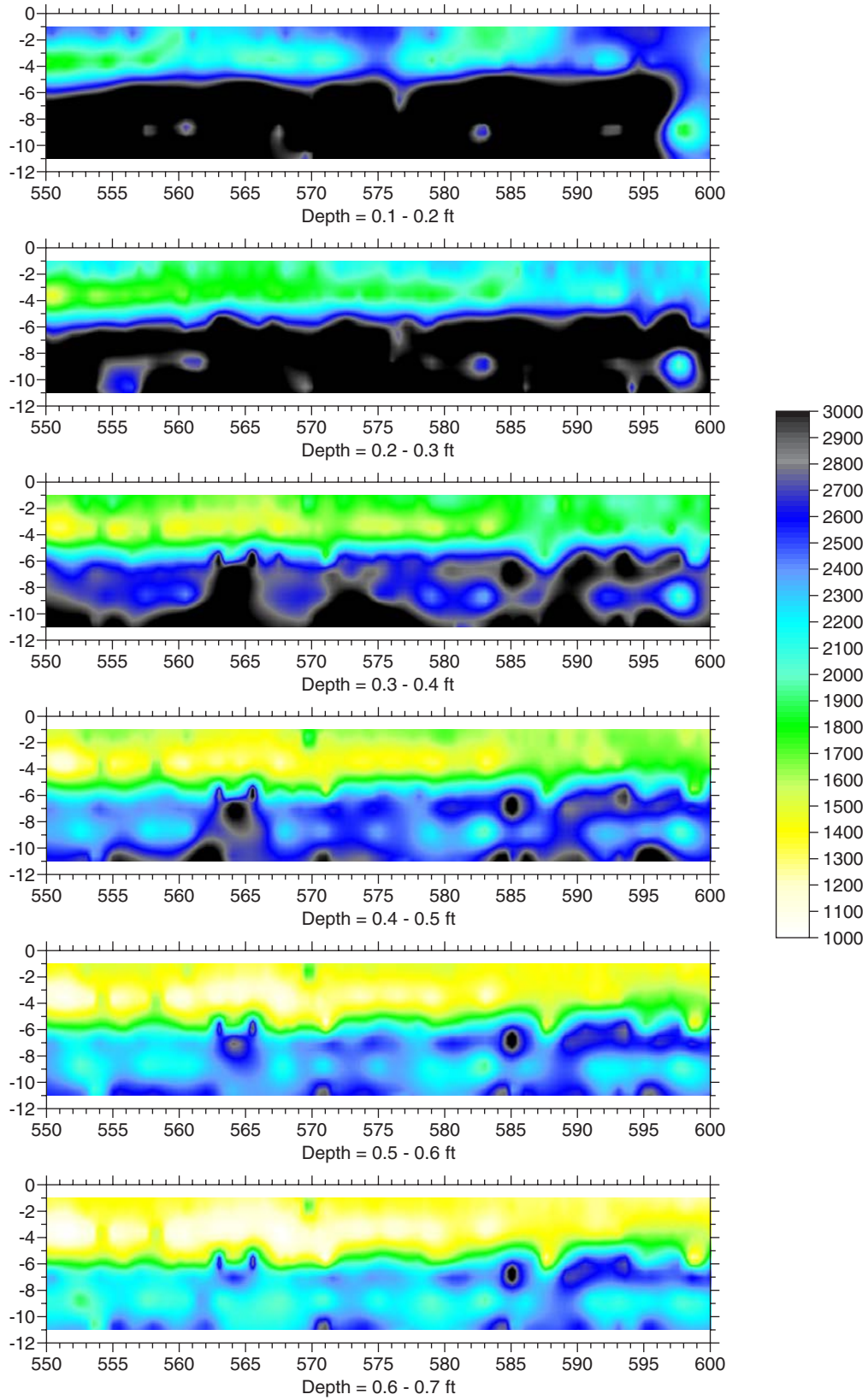
Figure 4.12. Section 550 to 600.
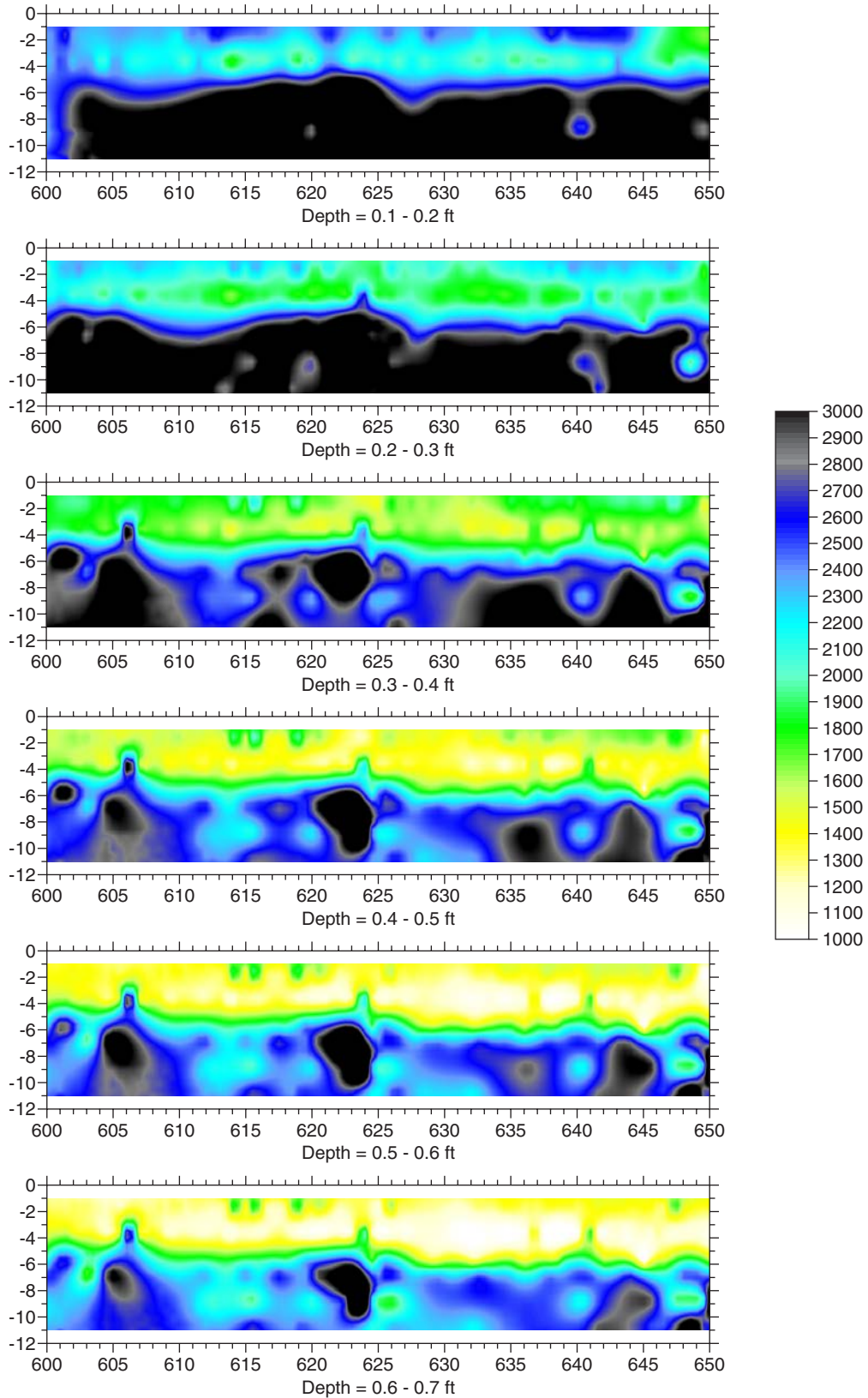
Figure 4.13. Section 600 to 650.
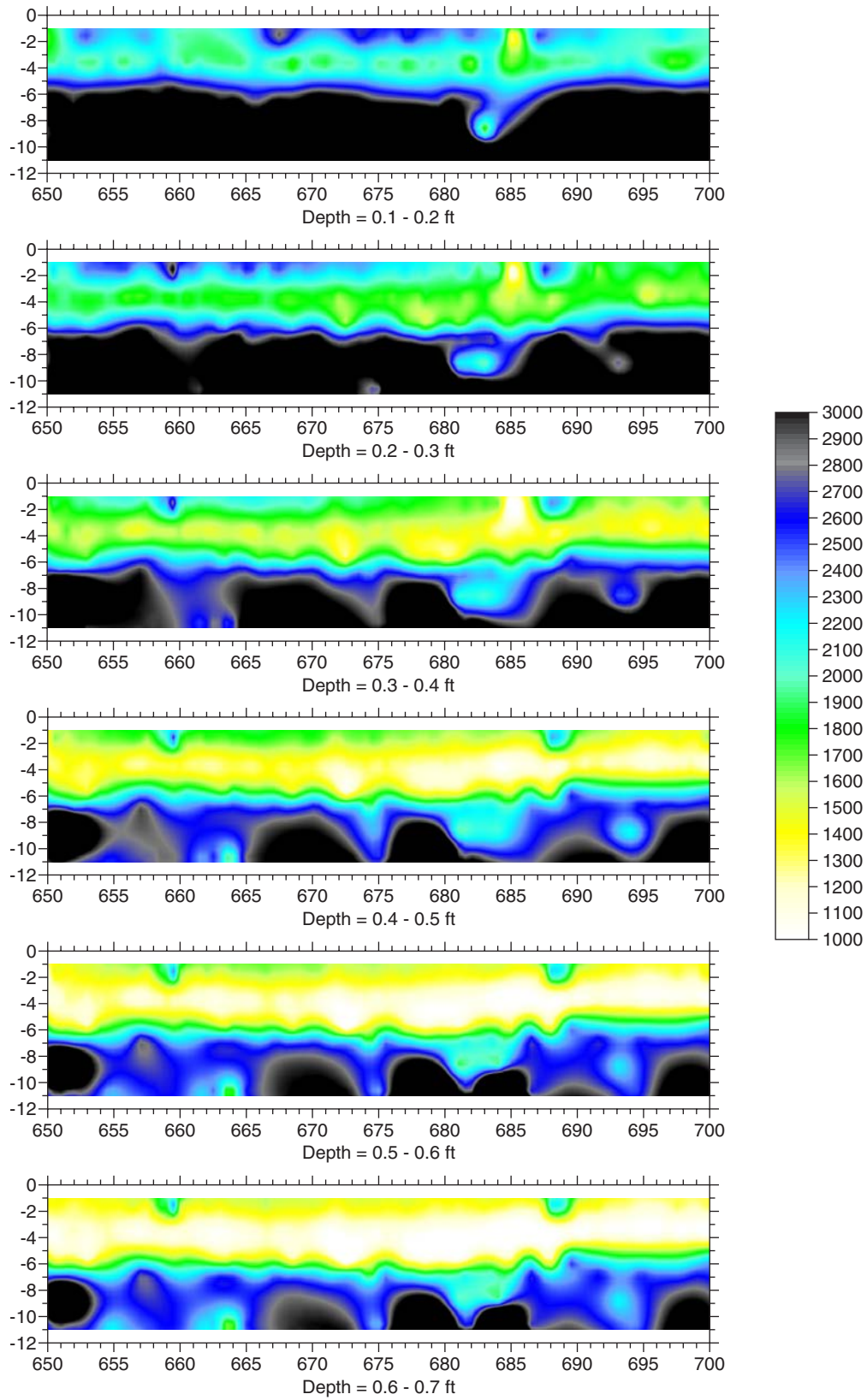
Figure 4.14. Section 650 to 700.
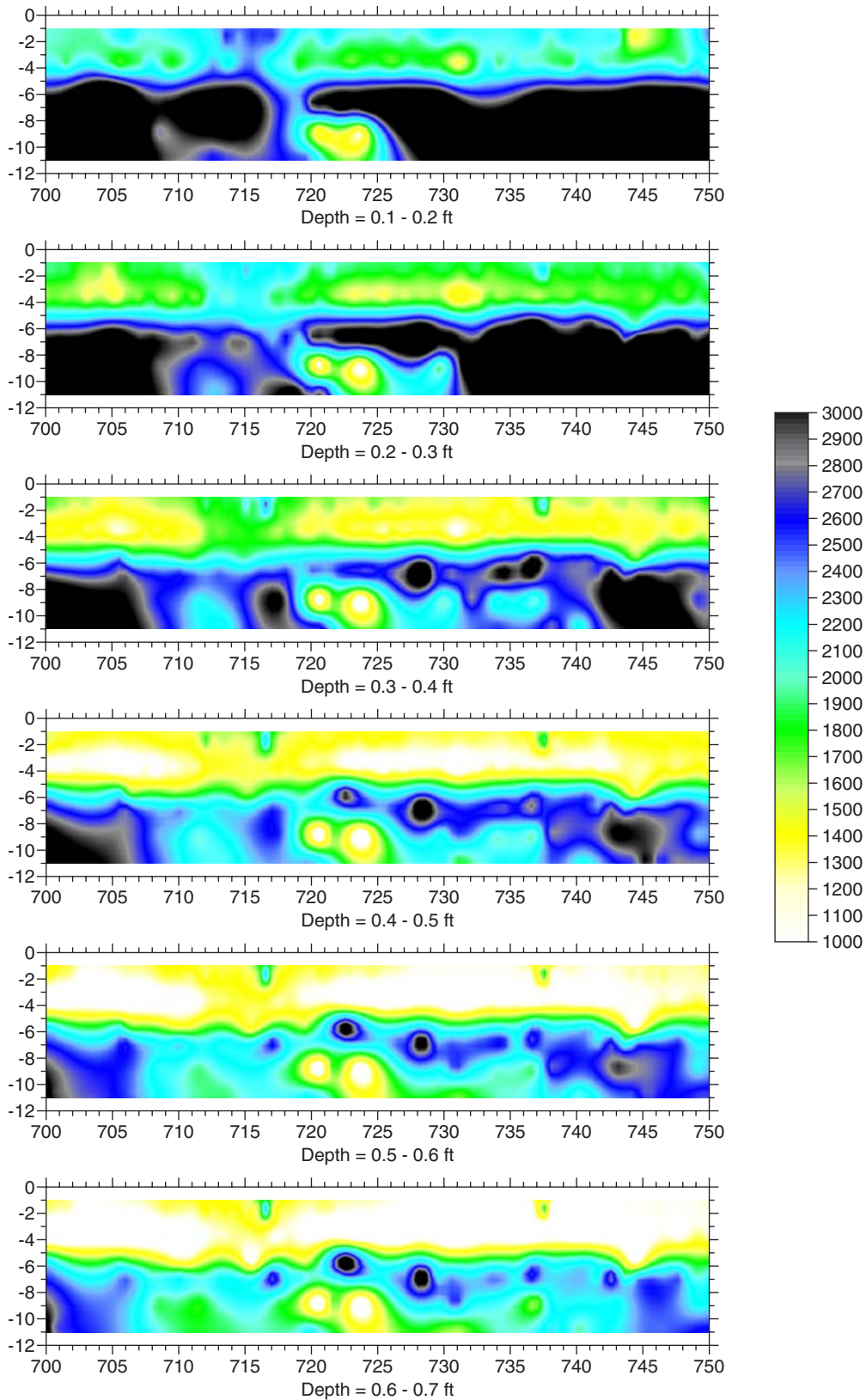
Figure 4.15. Section 700 to 750.
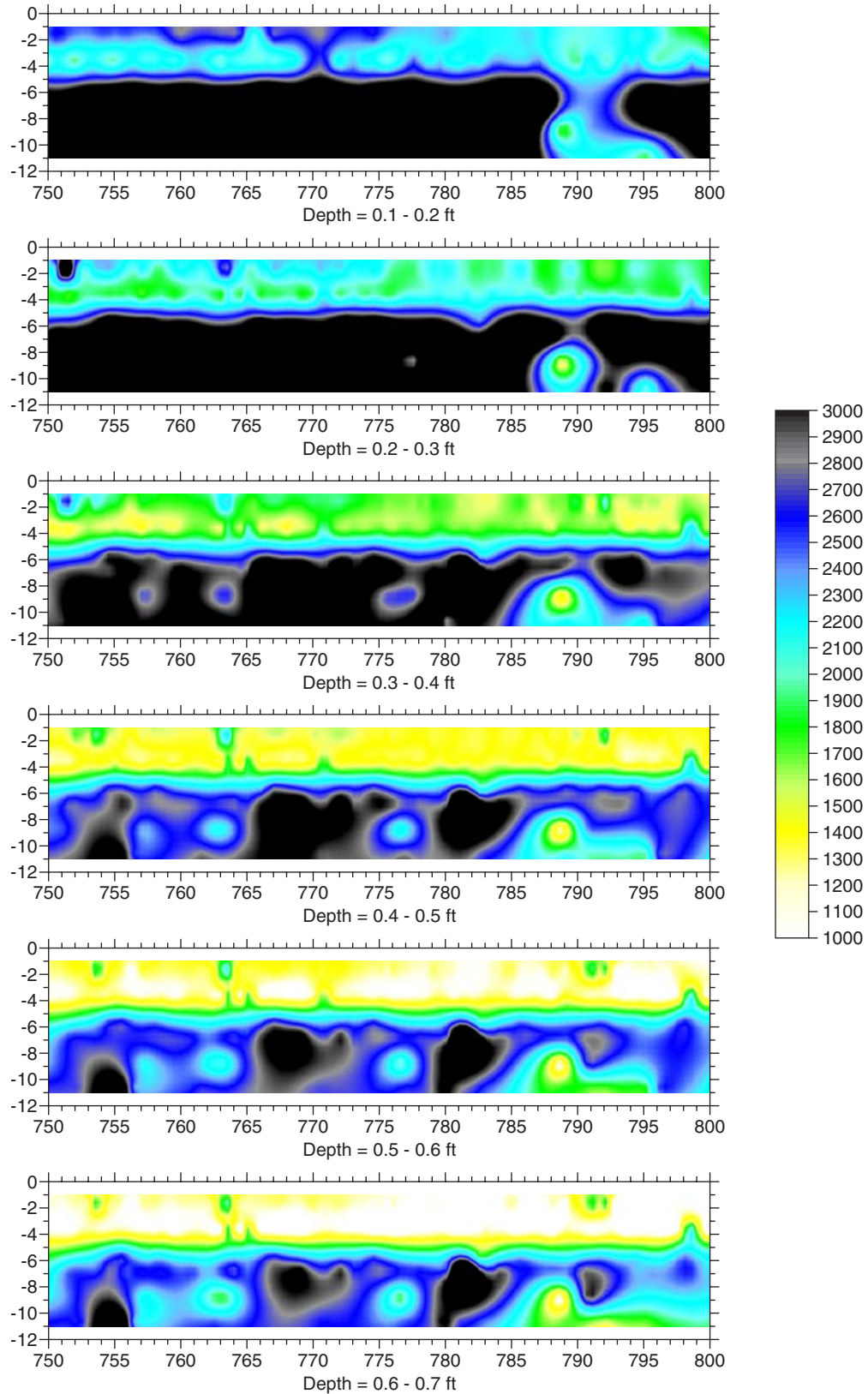
Figure 4.16. Section 750 to 800.
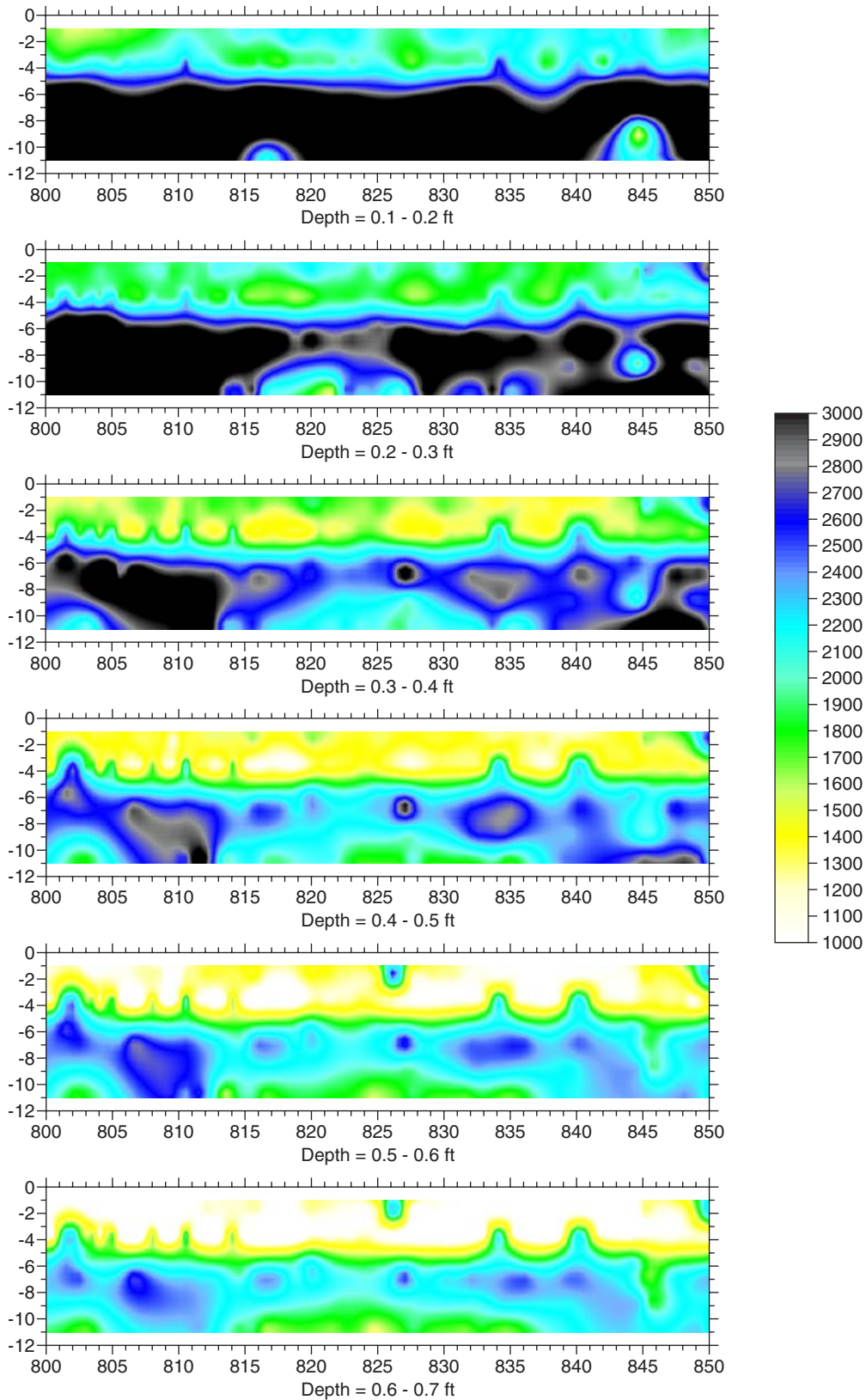
Figure 4.17. Section 800 to 850.
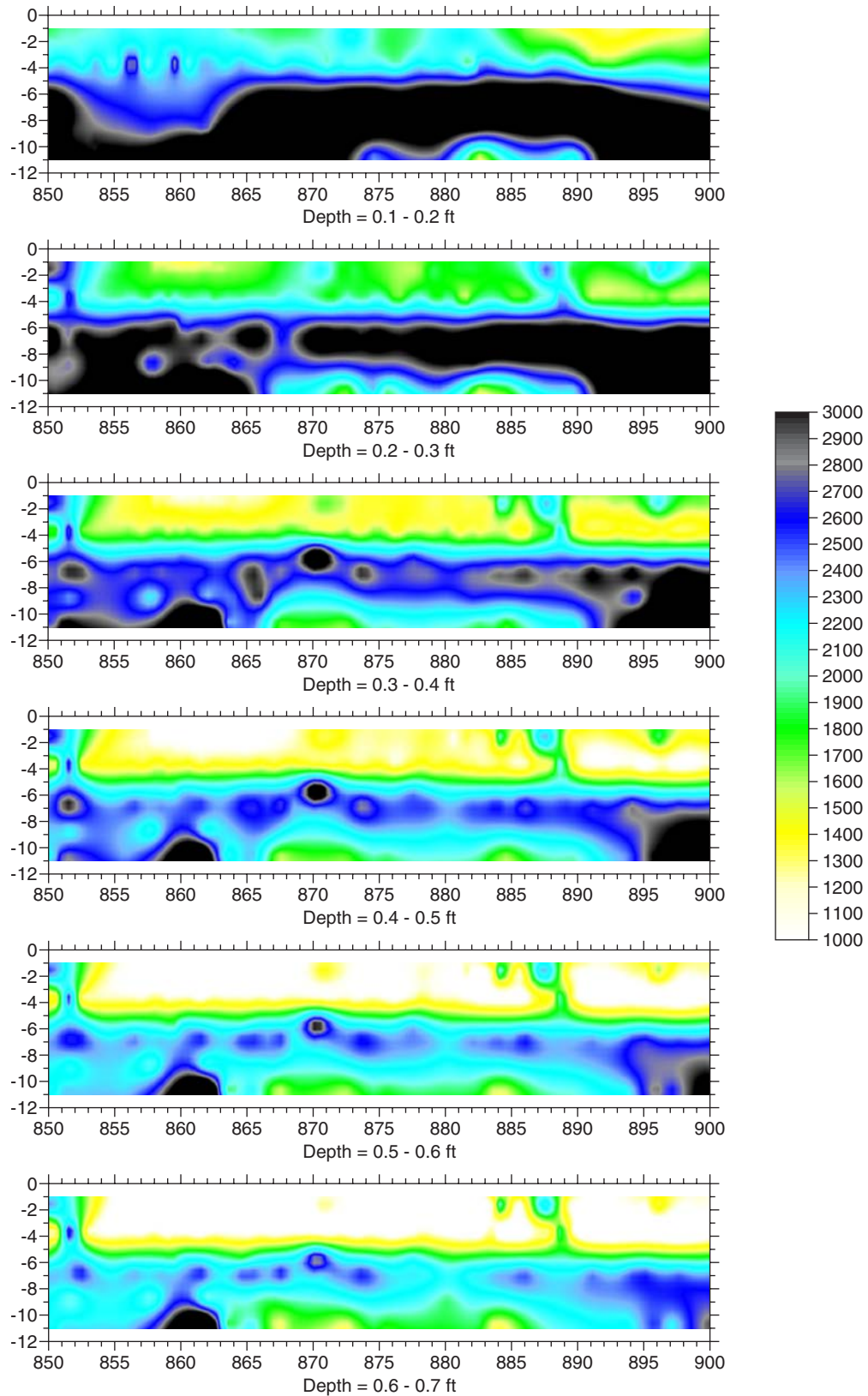
Figure 4.18. Section 850 to 900.
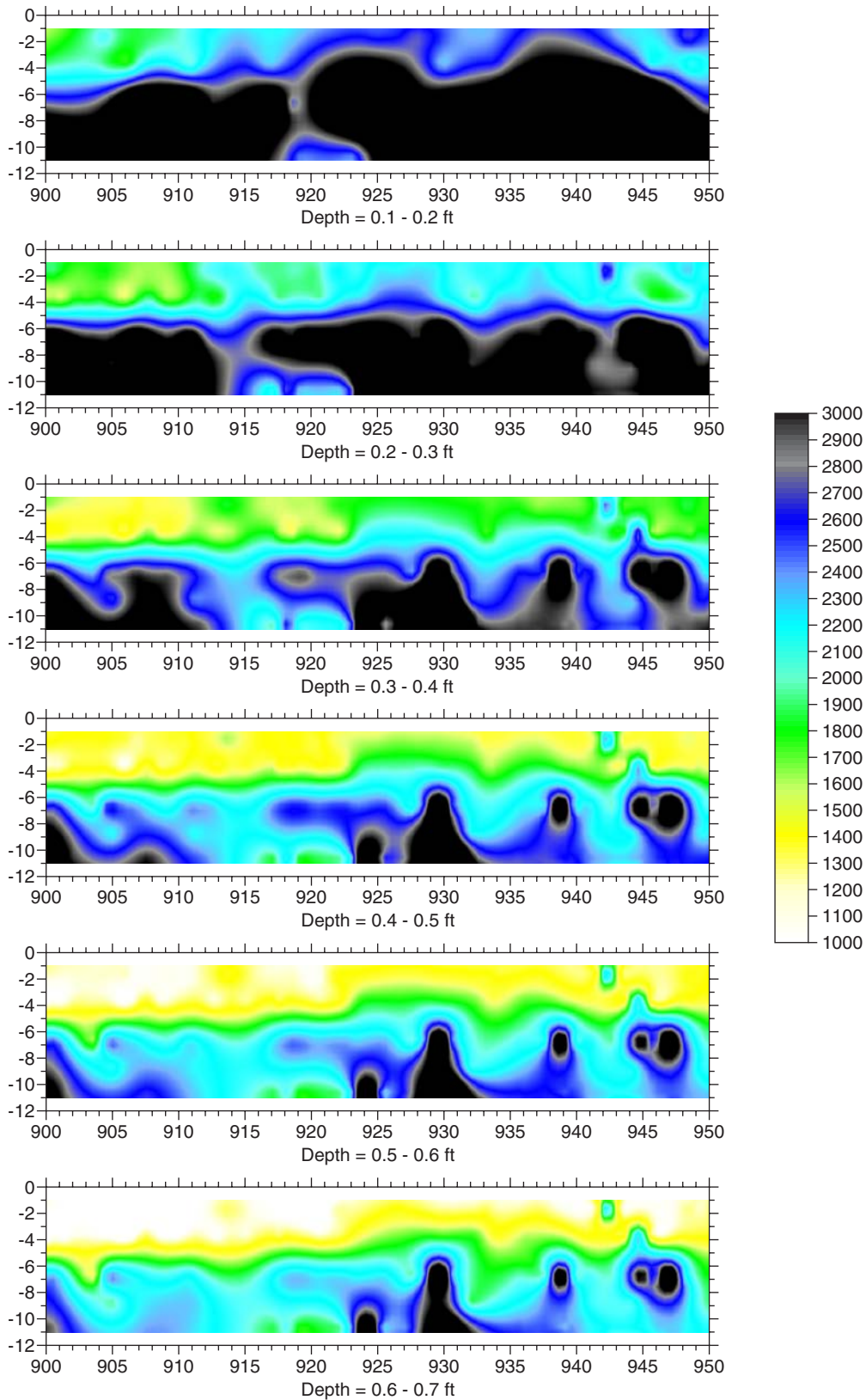
Figure 4.19. Section 900 to 950.
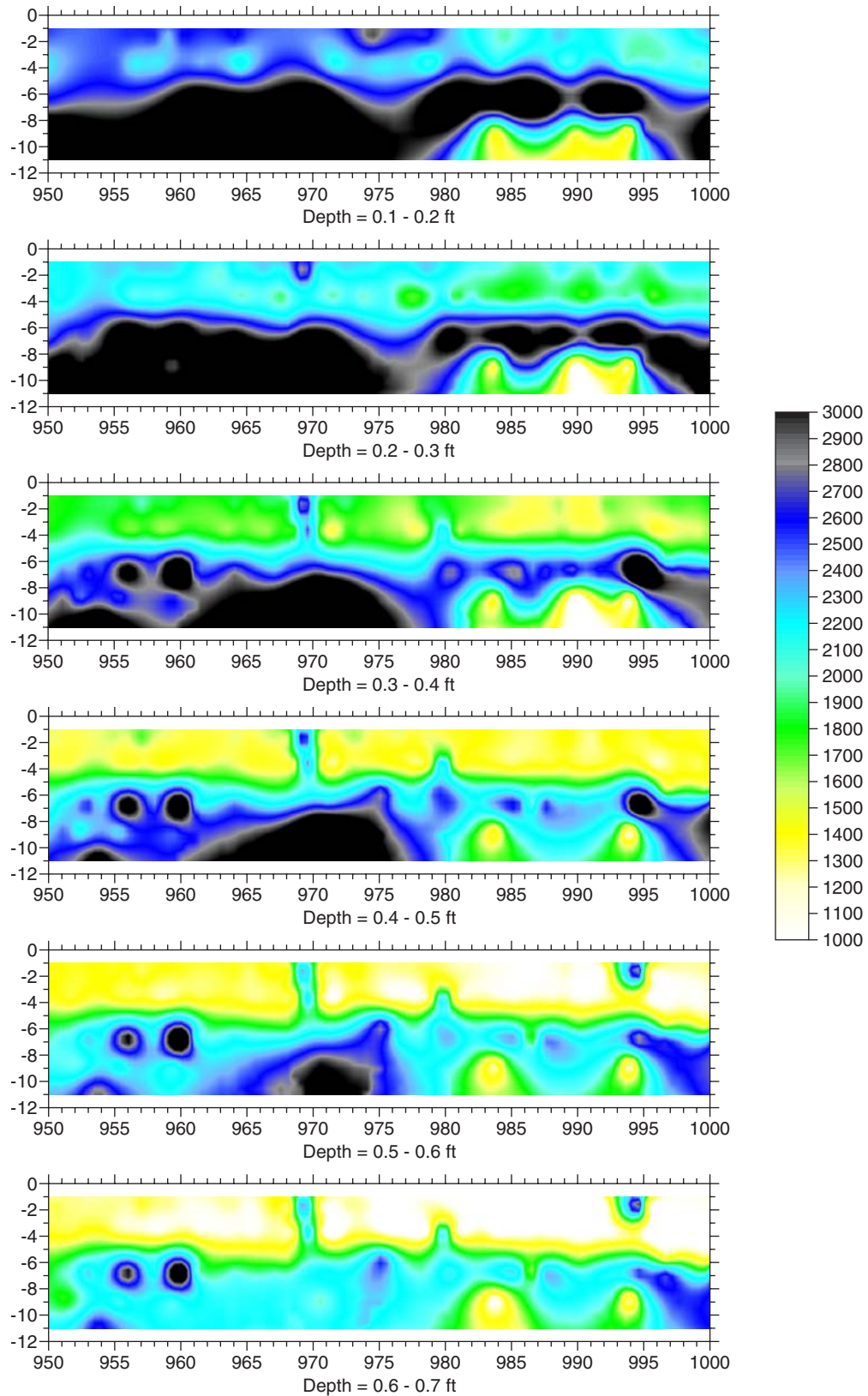
Figure 4.20. Section 950 to 1,000.
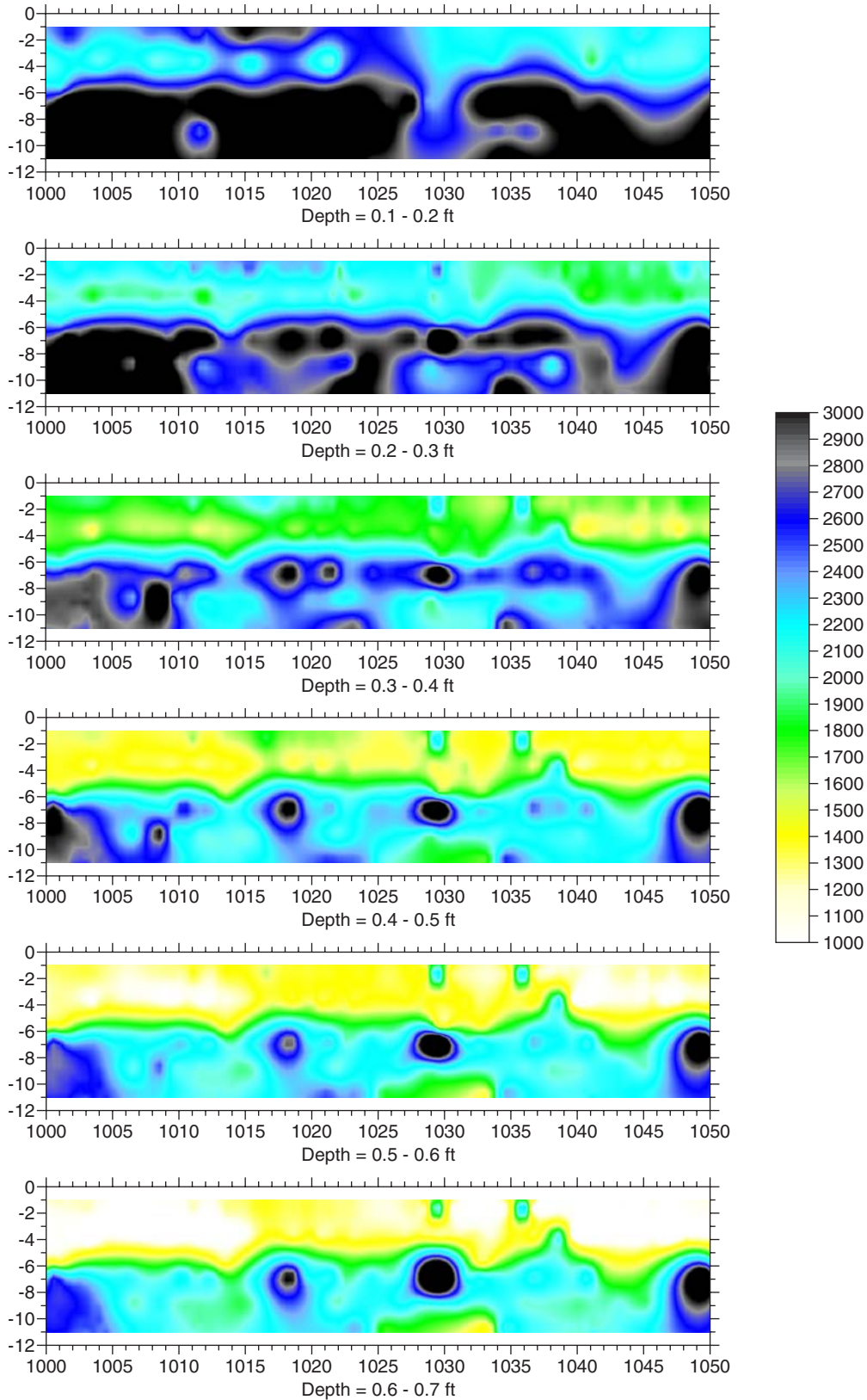
Figure 4.21. Section 1,000 to 1,050.
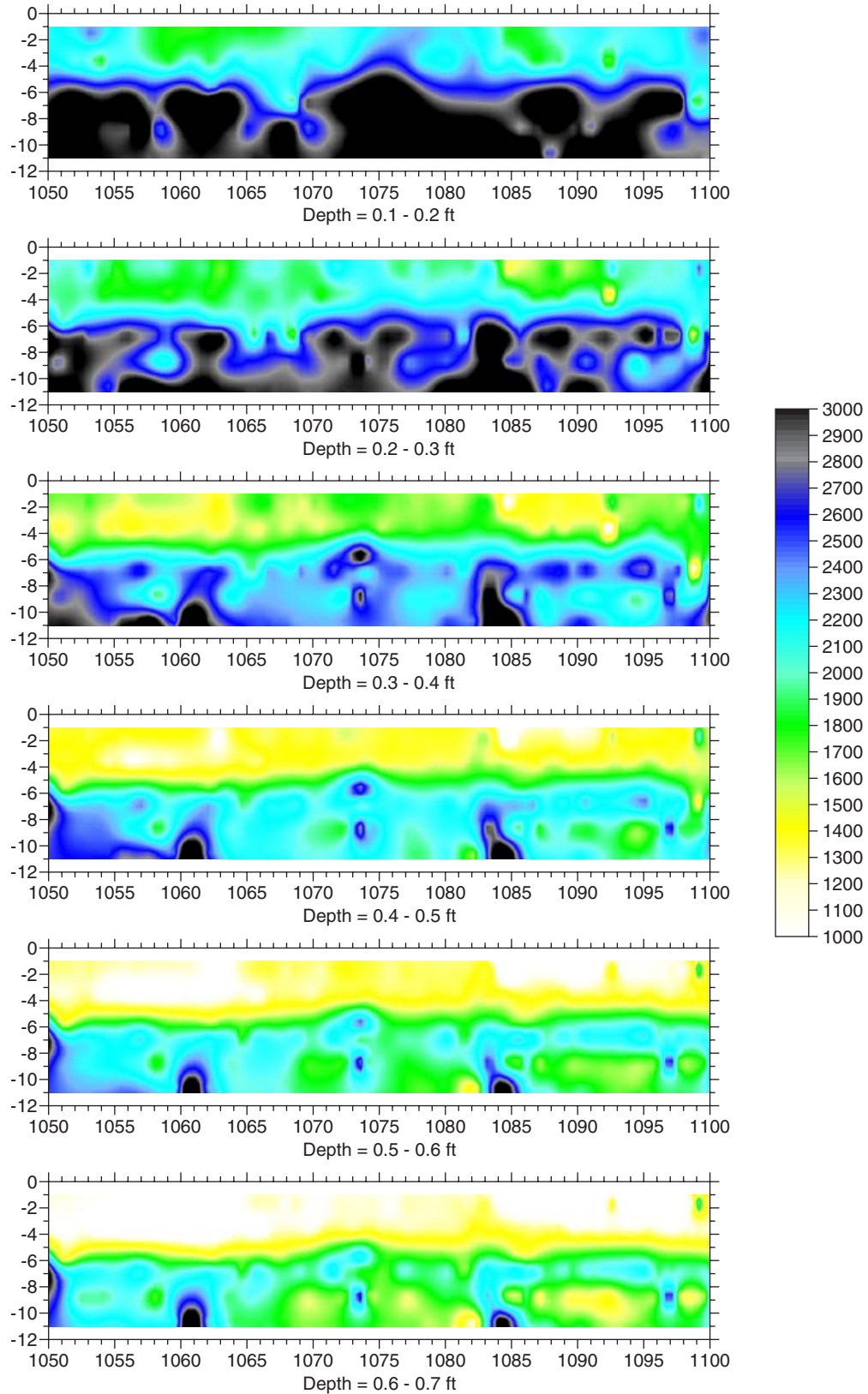
Figure 4.22. Section 1,050 to 1,100.
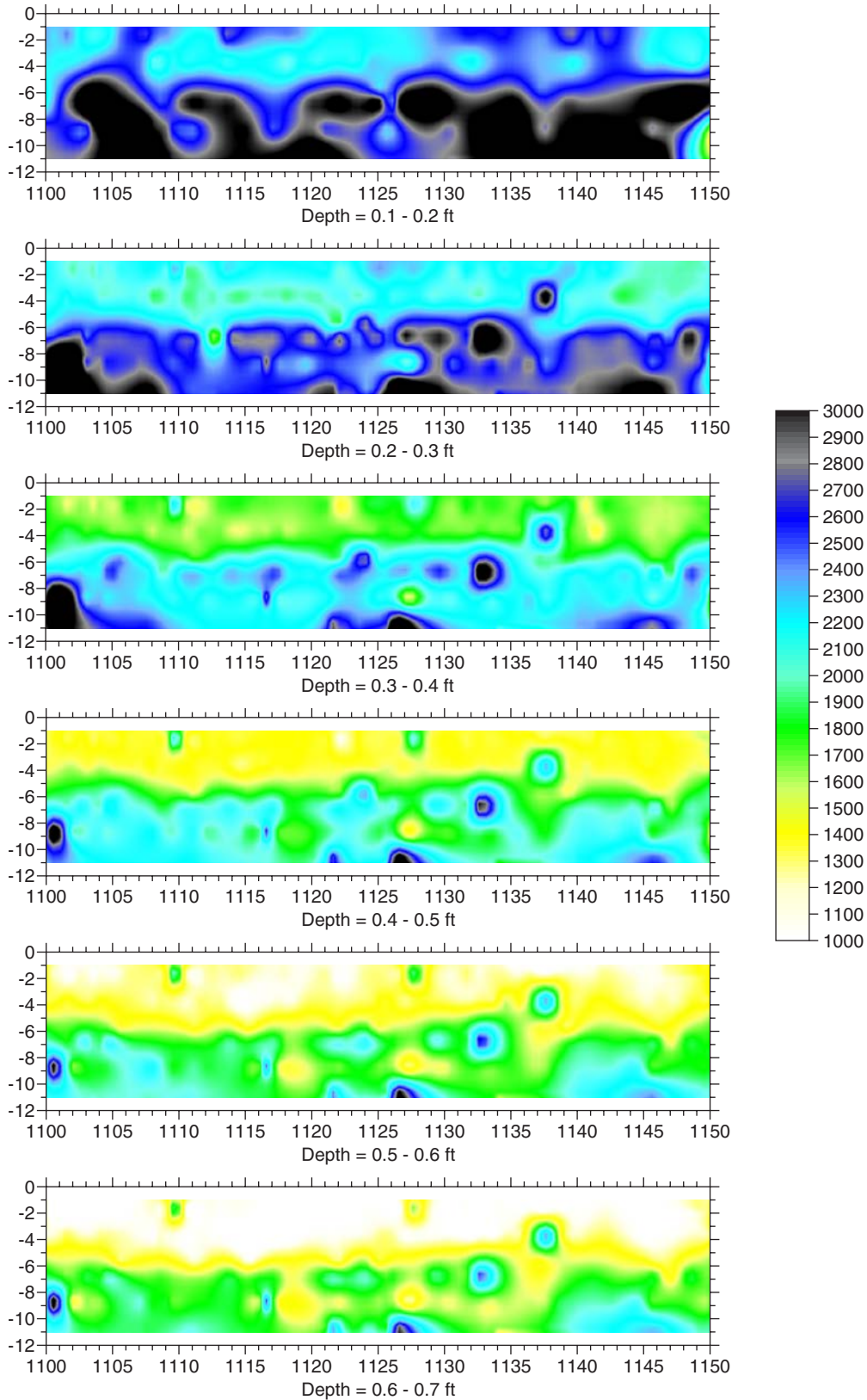
Figure 4.23. Section 1,100 to 1,150.
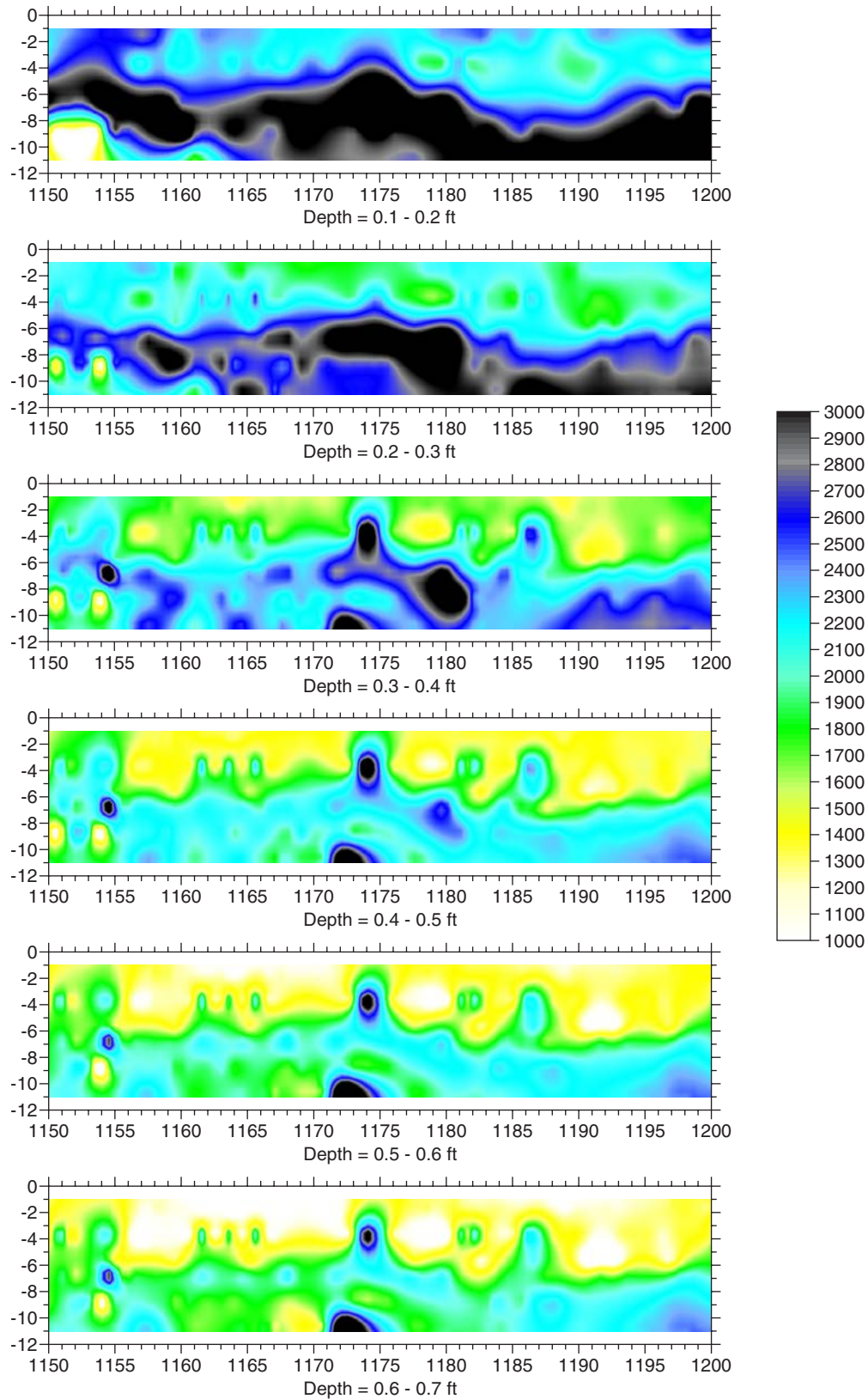
Figure 4.24. Section 1,150 to 1,200.
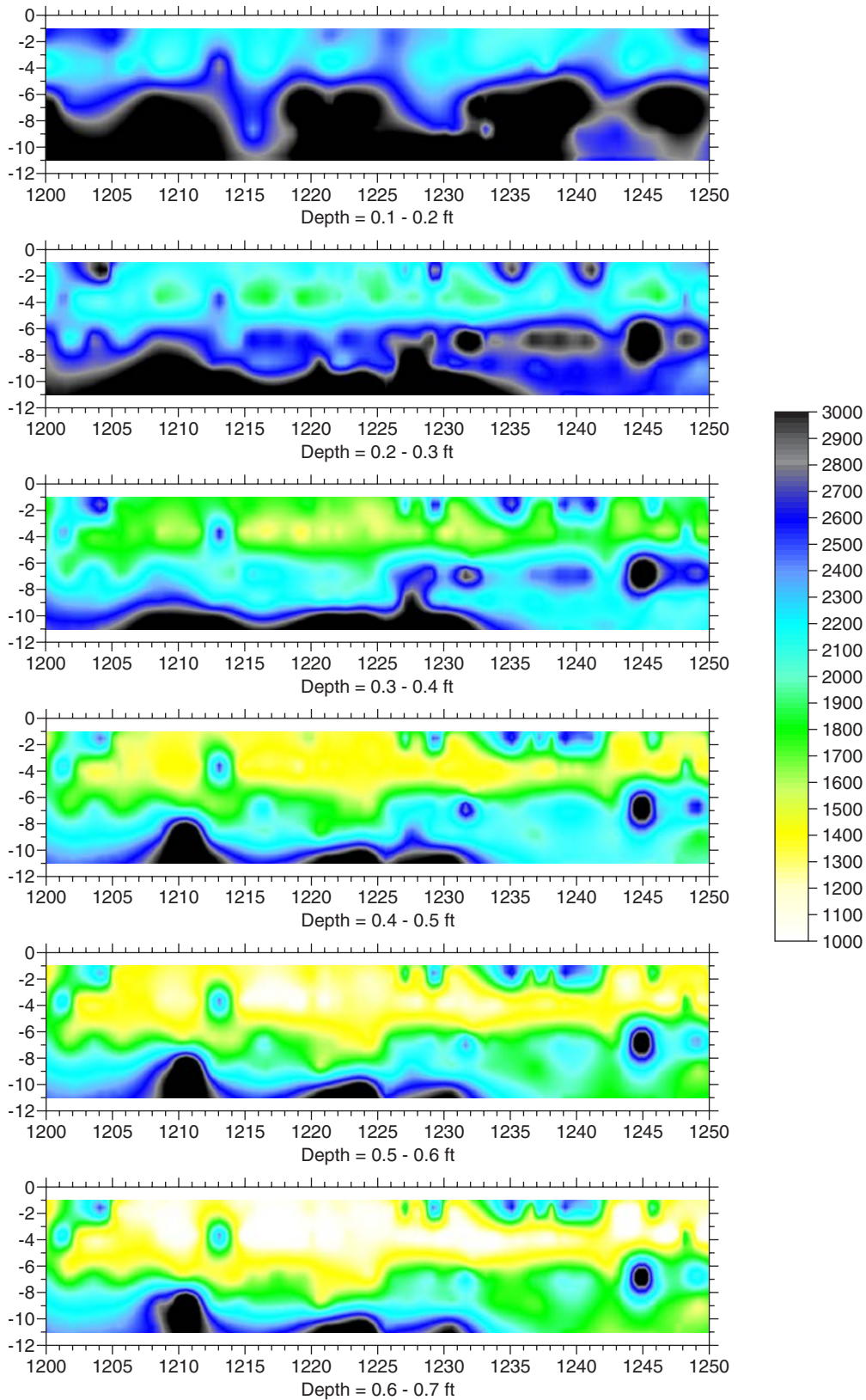
Figure 4.25. Section 1,200 to 1,250.
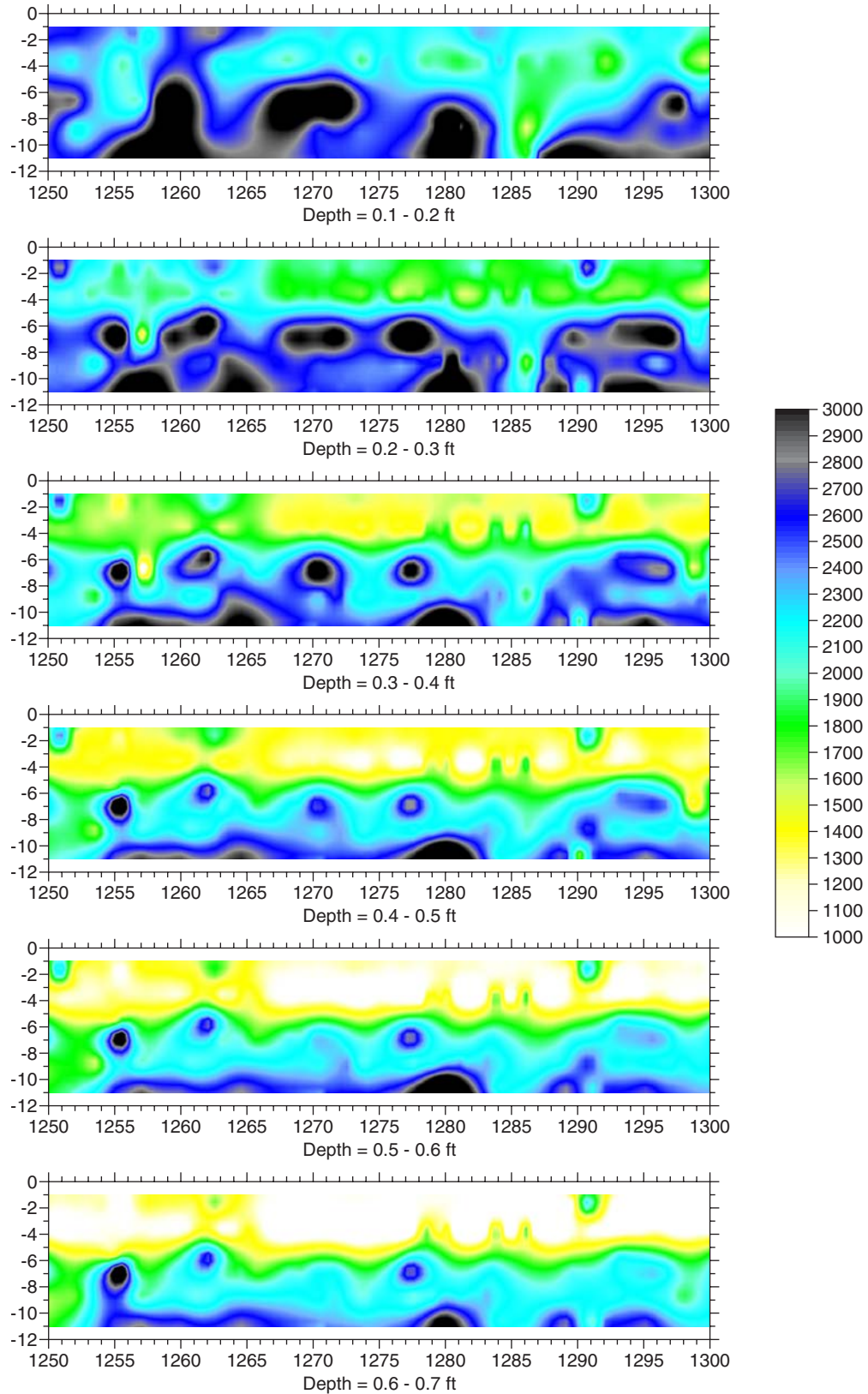
Figure 4.26. Section 1,250 to 1,300.
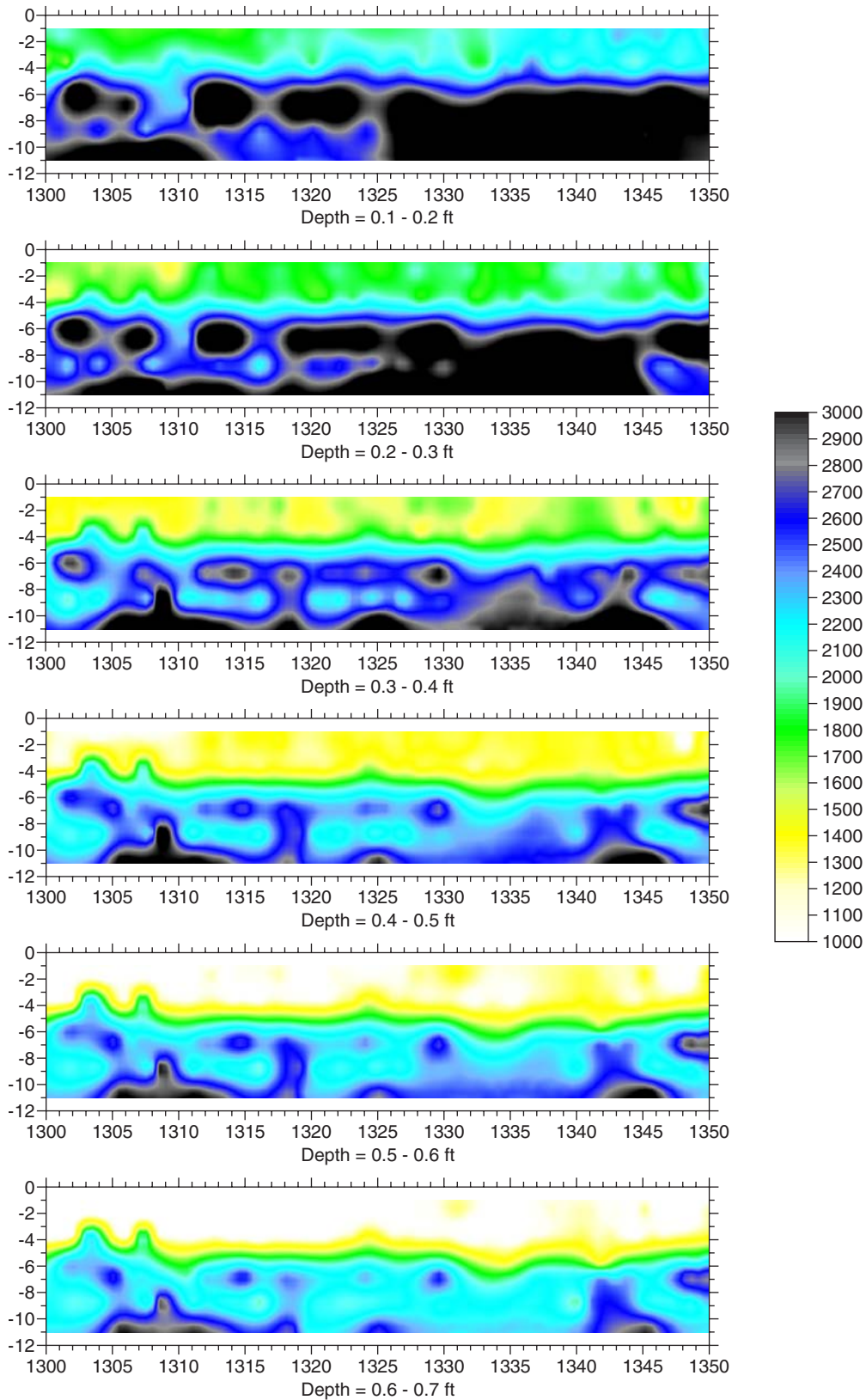
Figure 4.27. Section 1,300 to 1,350.
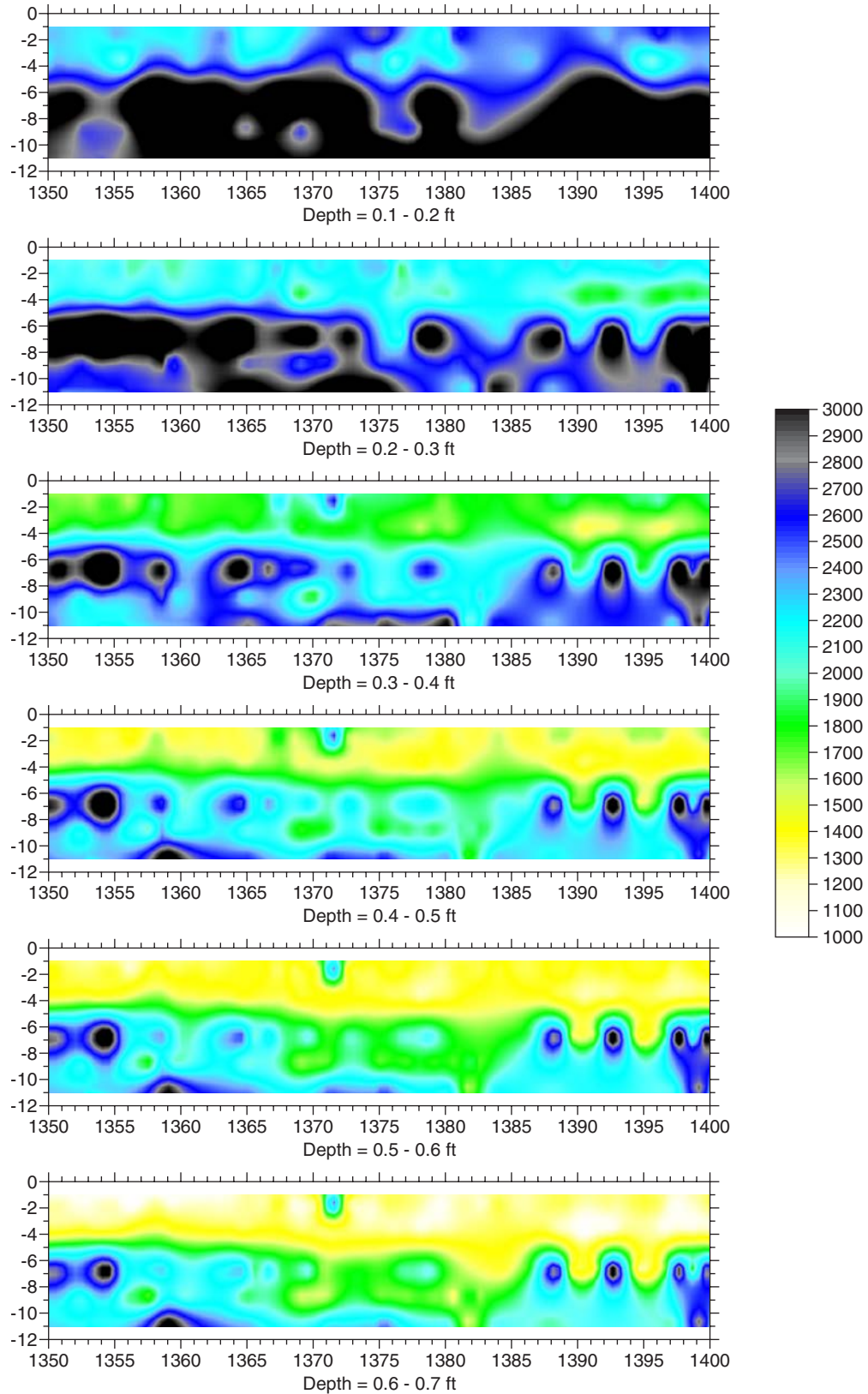
Figure 4.28. Section 1,350 to 1,400.
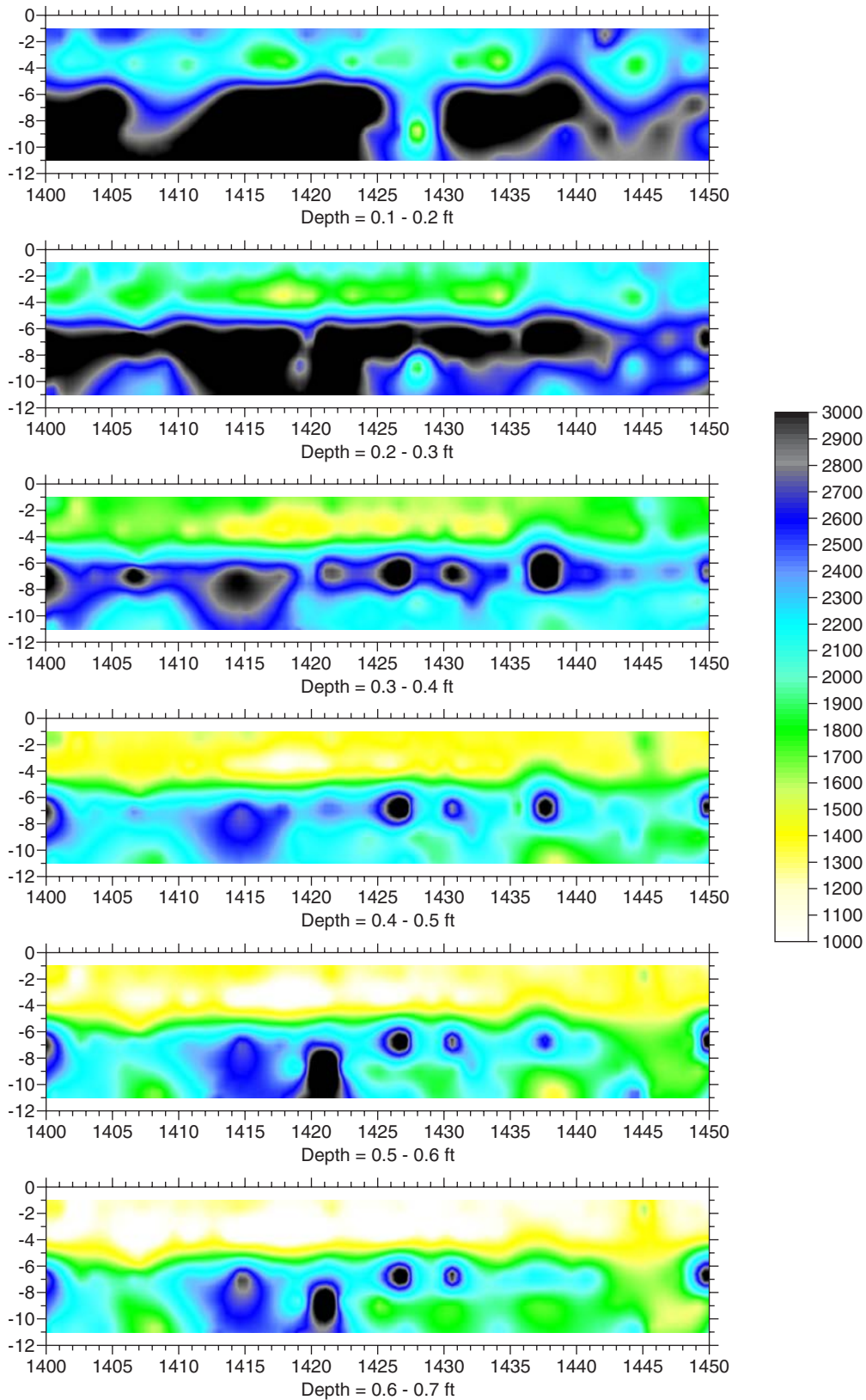
Figure 4.29. Section 1,400 to 1,450.
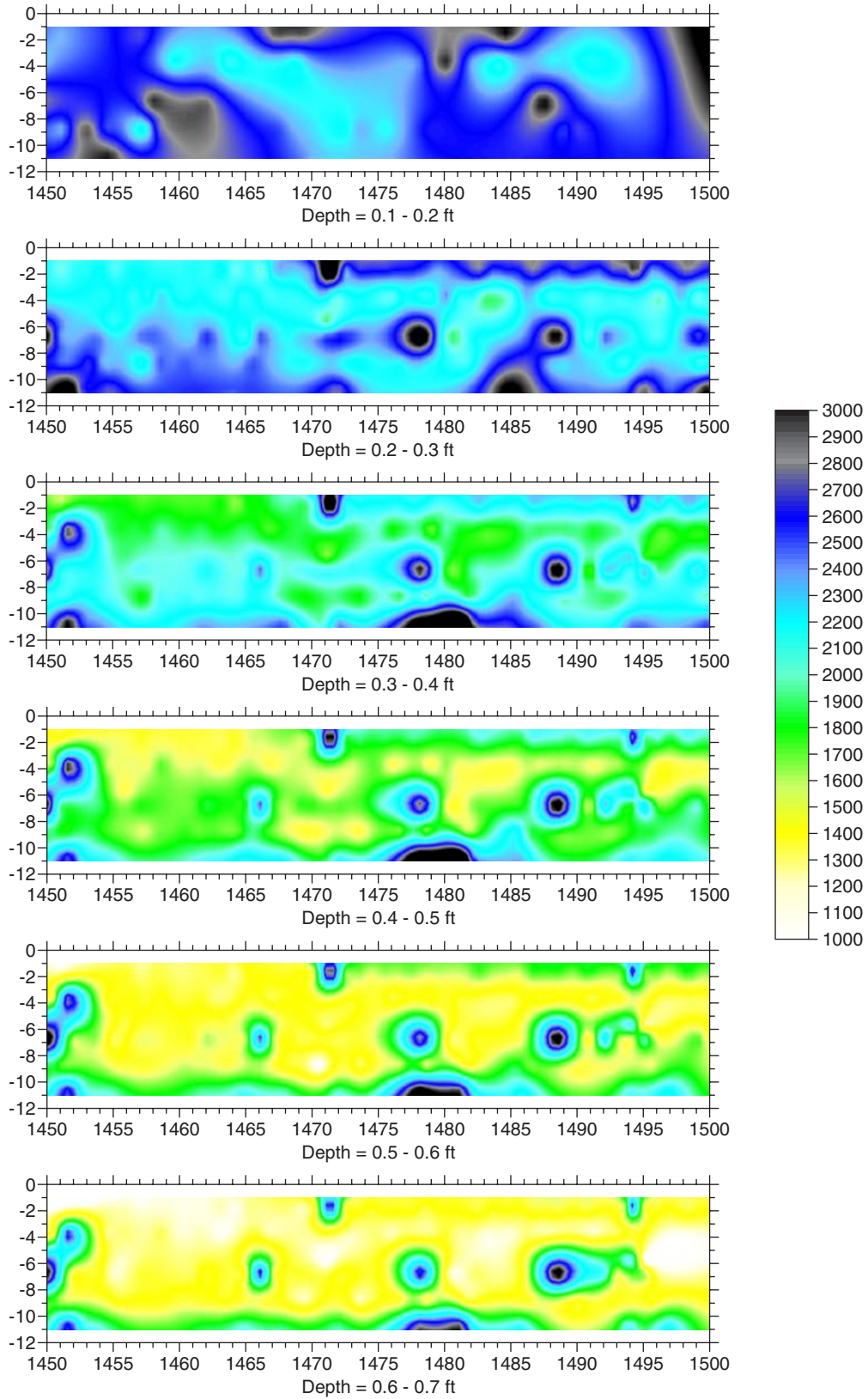
Figure 4.30. Section 1,450 to 1,500.
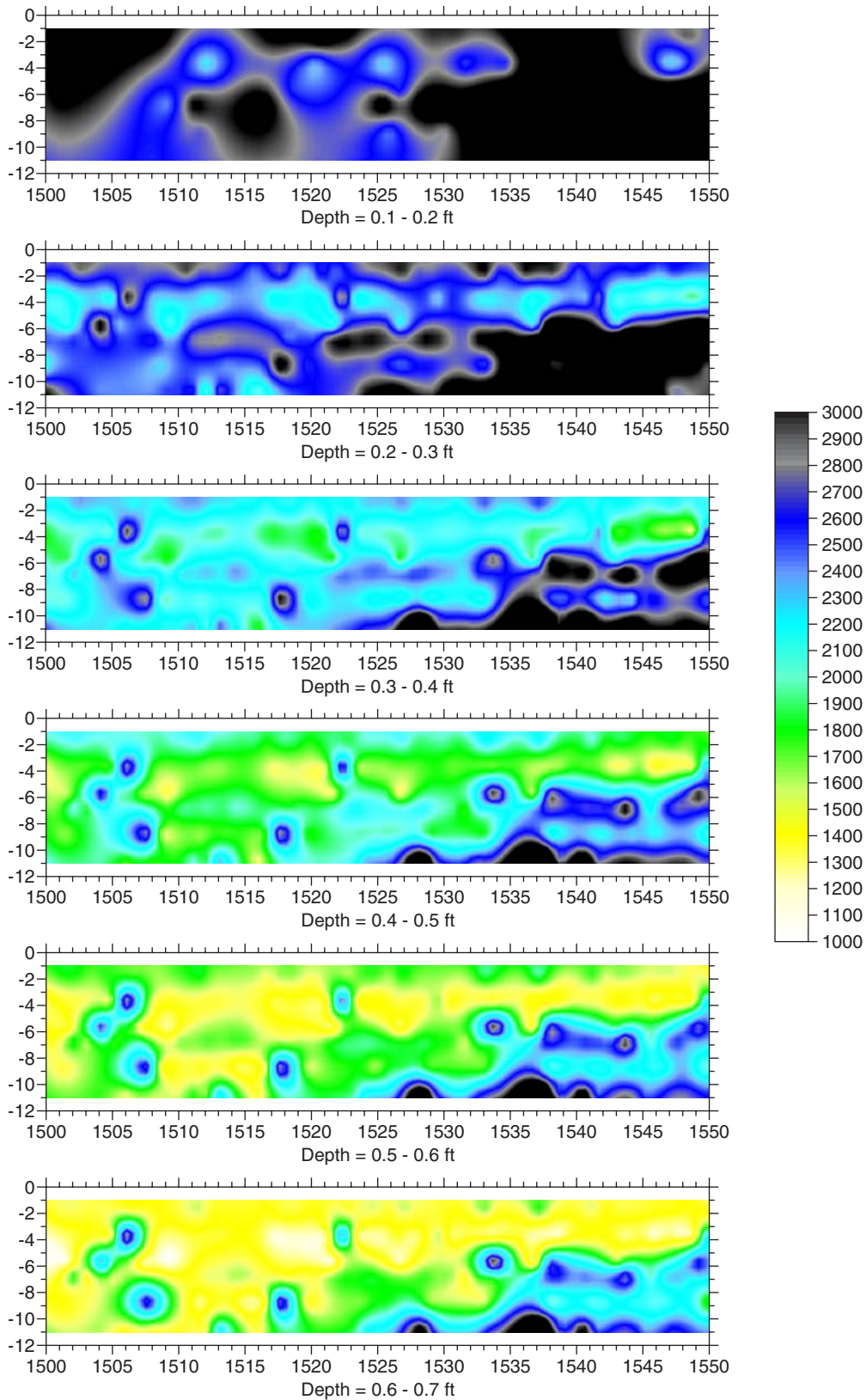
Figure 4.31. Section 1,500 to 1,550.
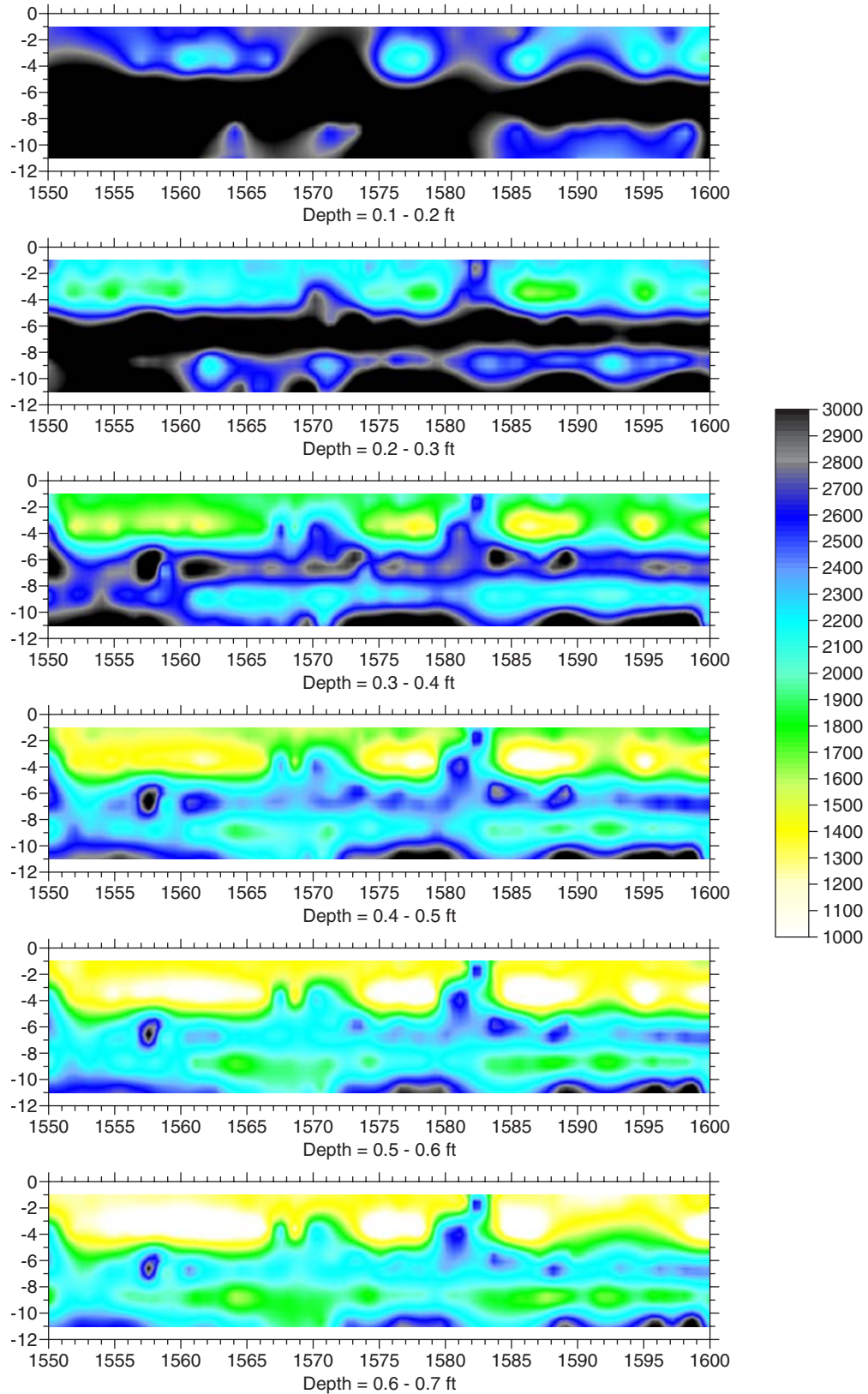
Figure 4.32. Section 1,550 to 1,600.
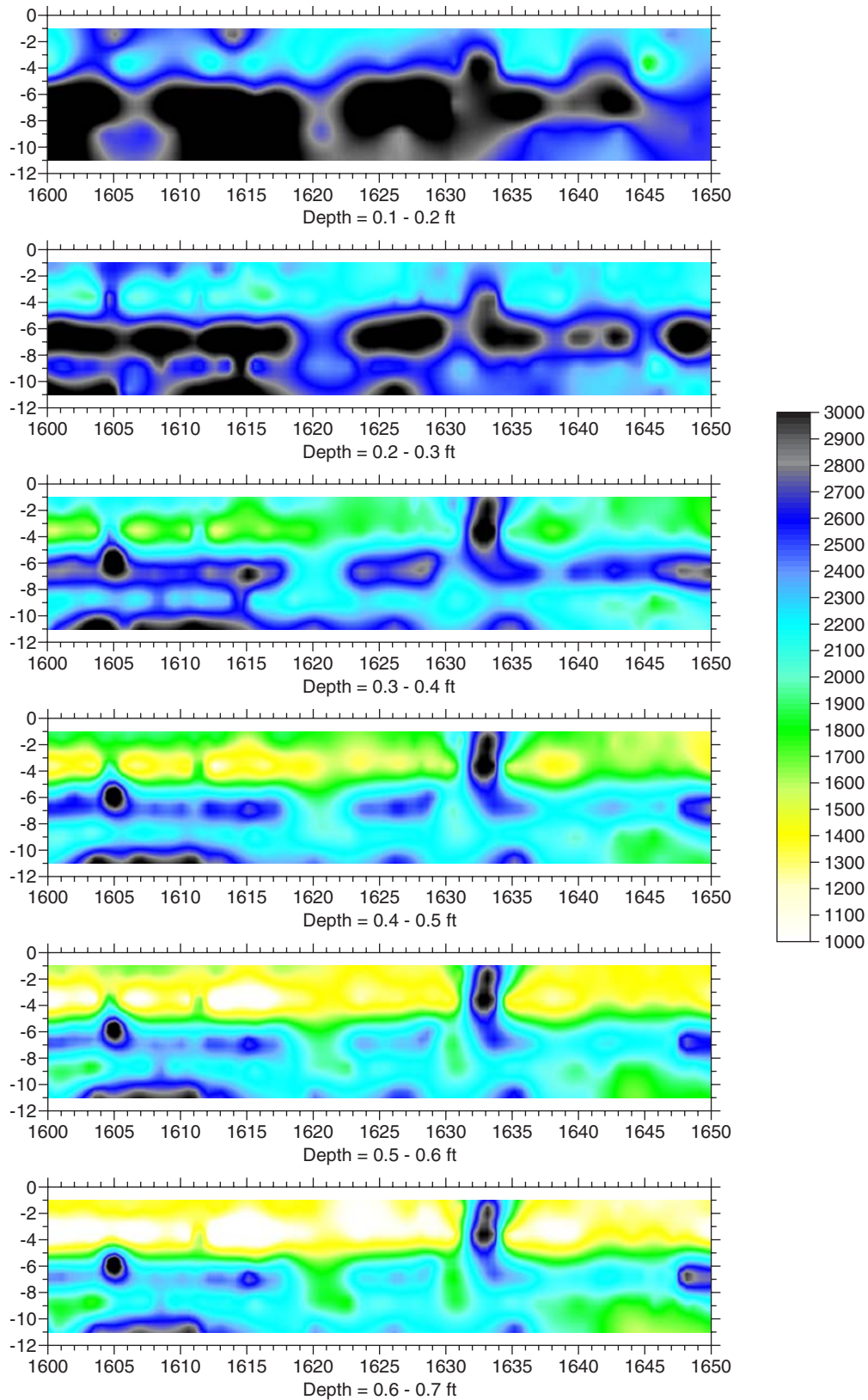
Figure 4.33. Section 1,600 to 1,650.
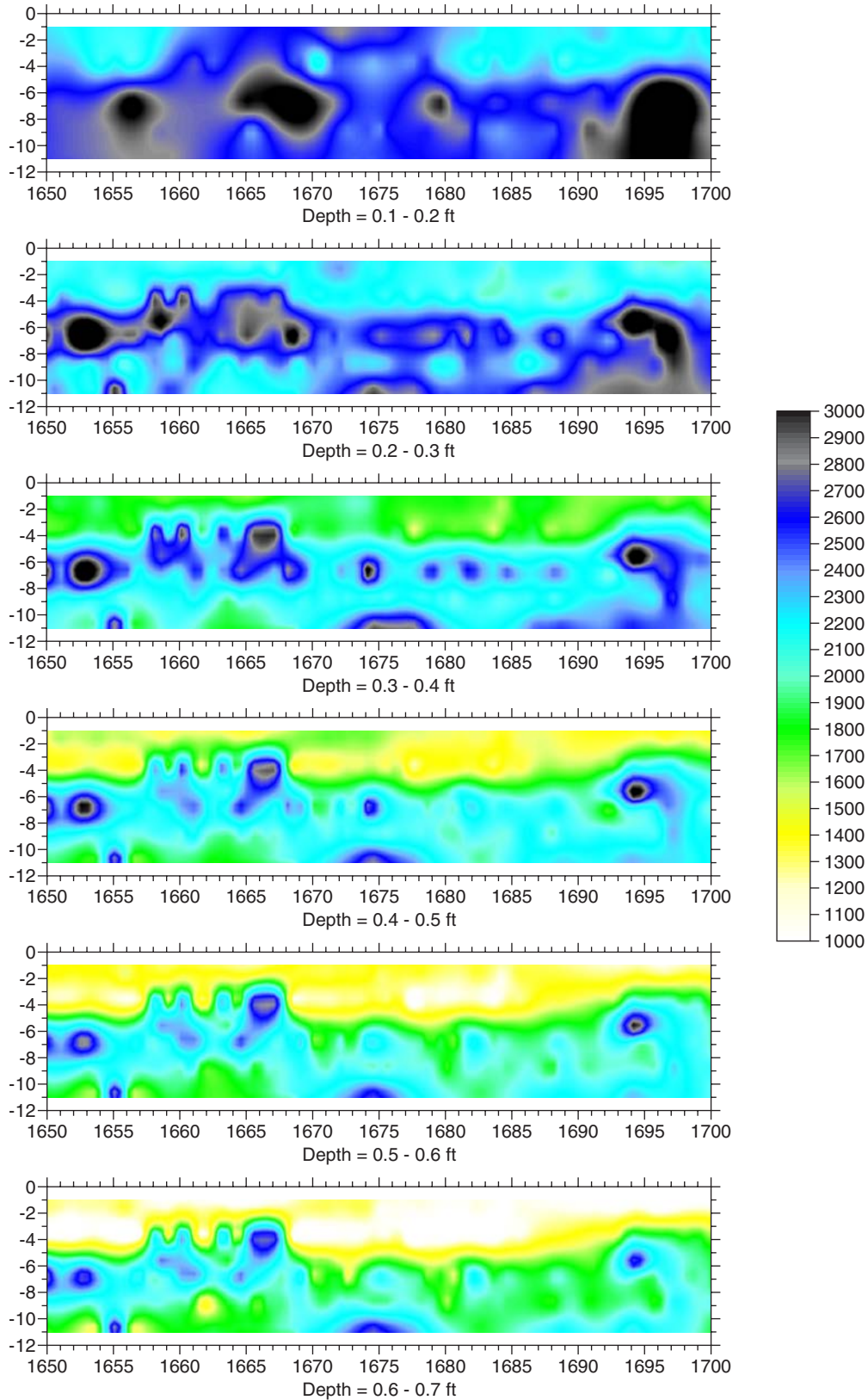
Figure 4.34. Section 1,650 to 1,700.
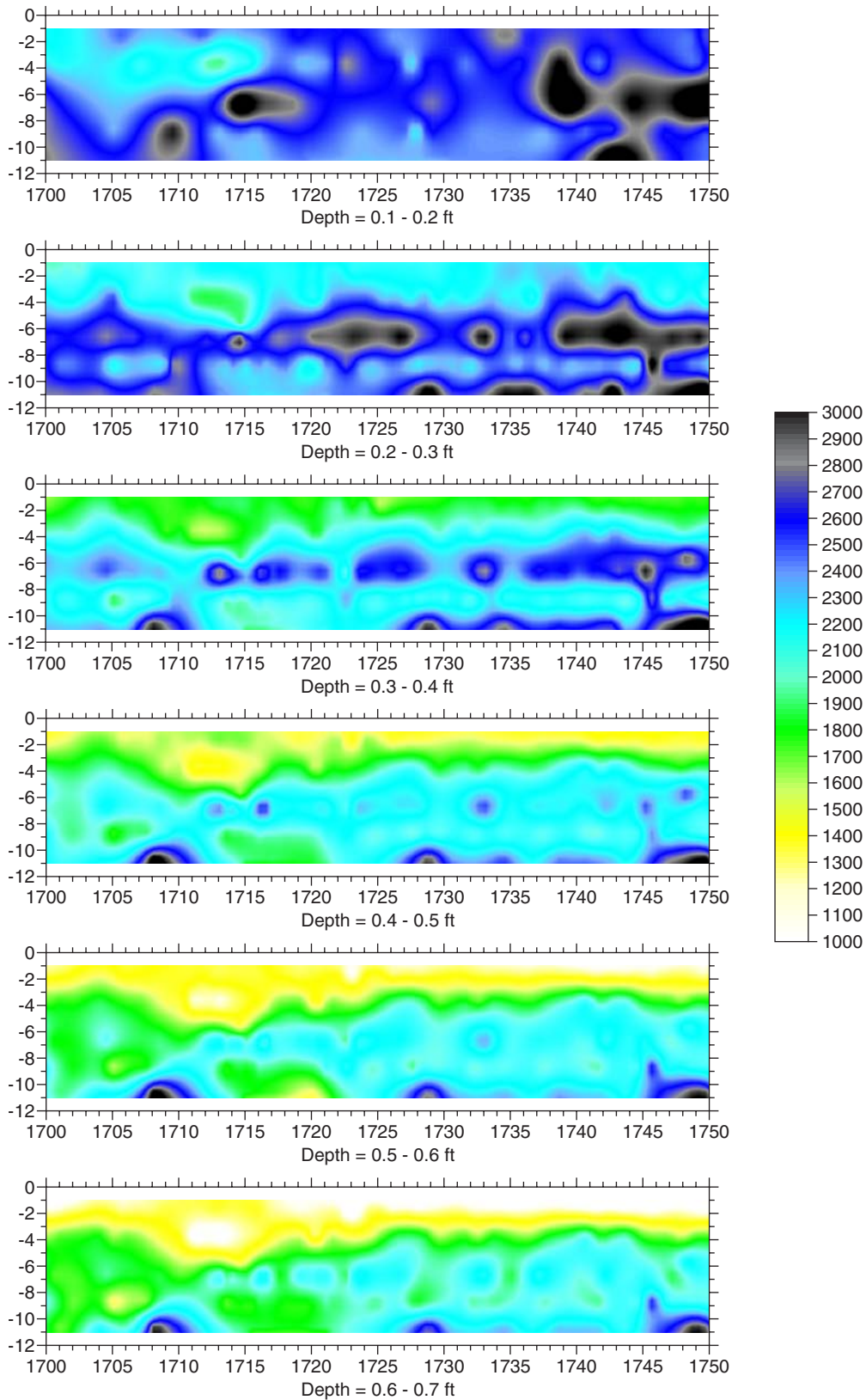
Figure 4.35. Section 1,700 to 1,750.
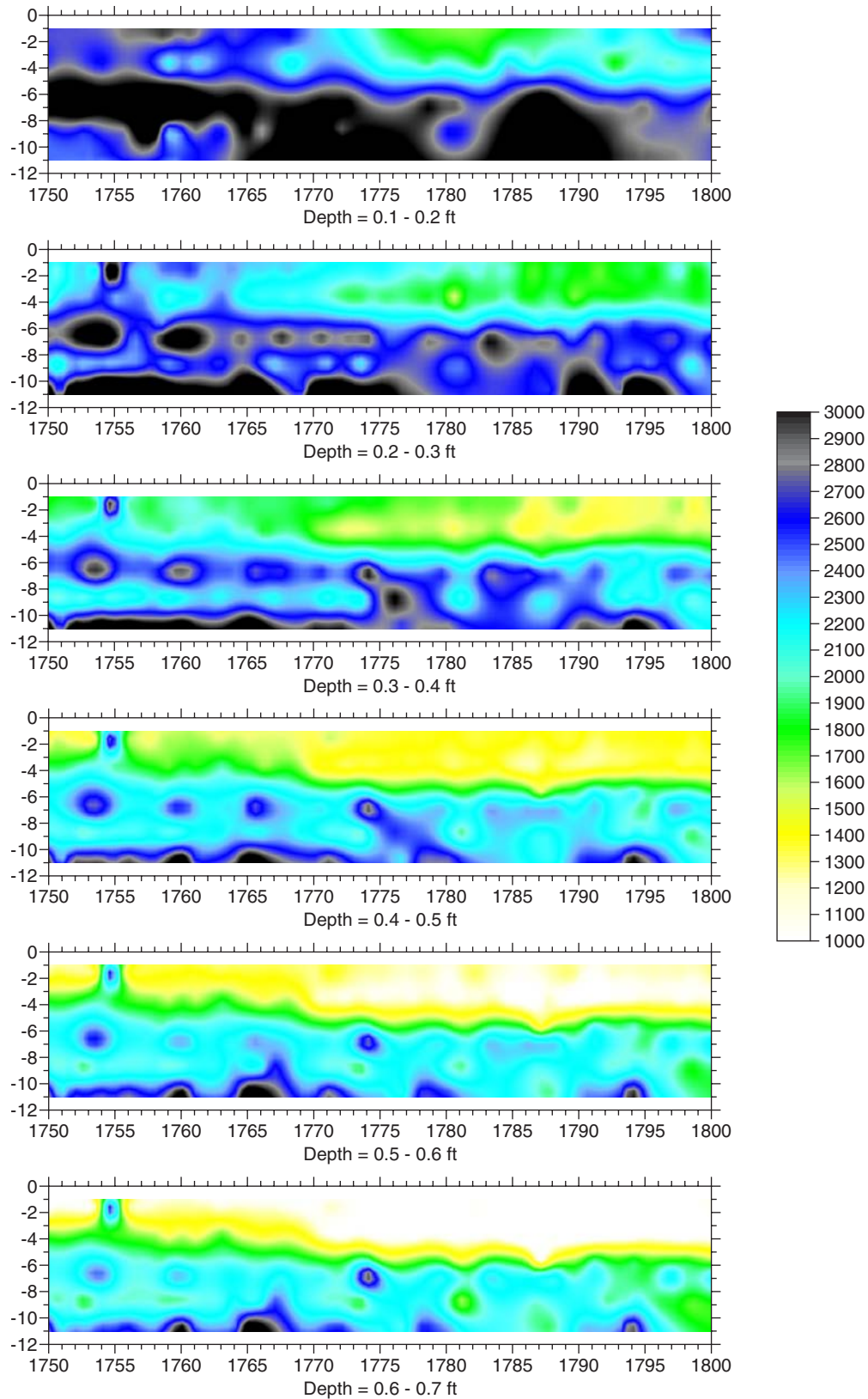
Figure 4.36. Section 1,750 to 1,800.
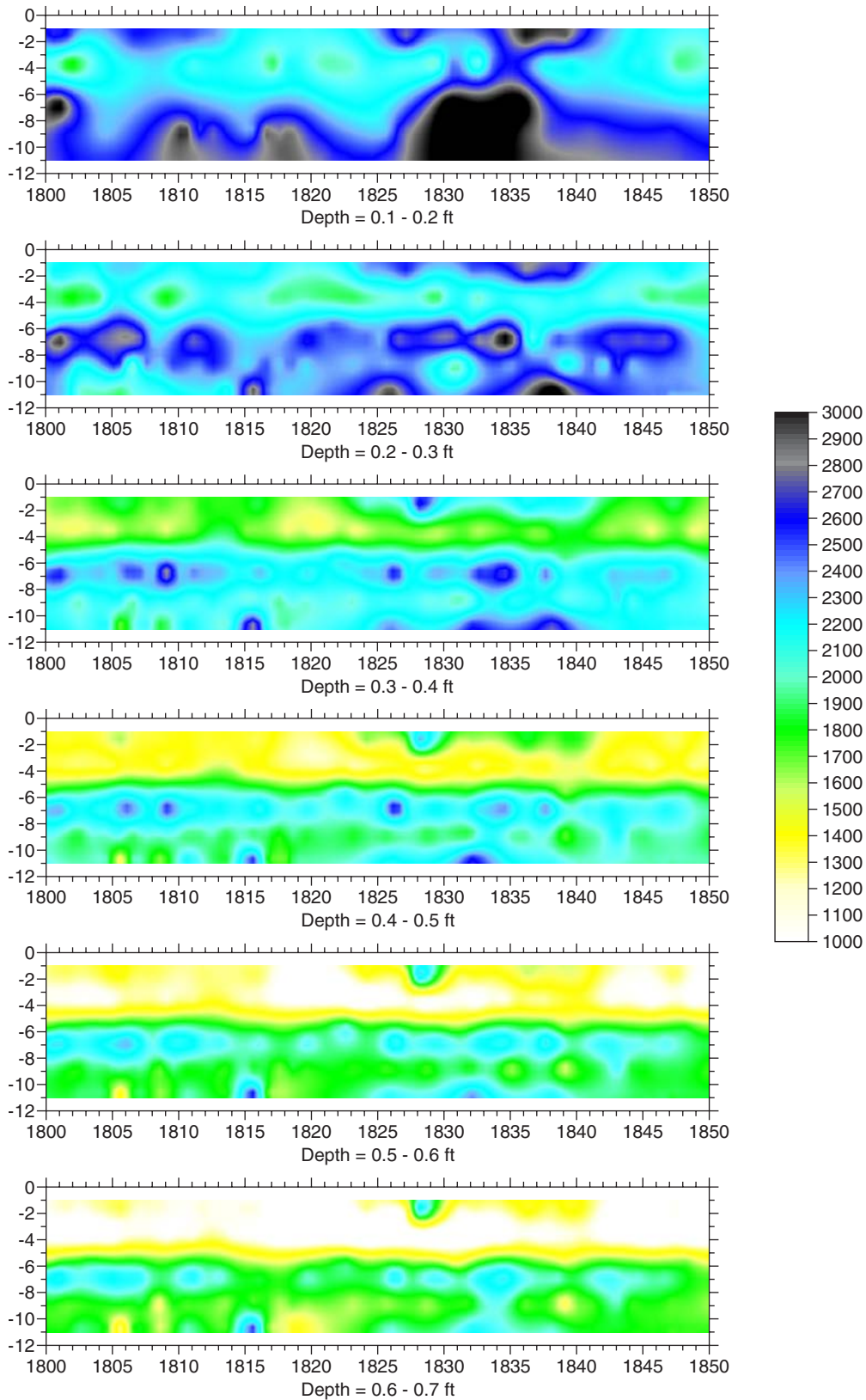
Figure 4.37. Section 1,800 to 1,850.
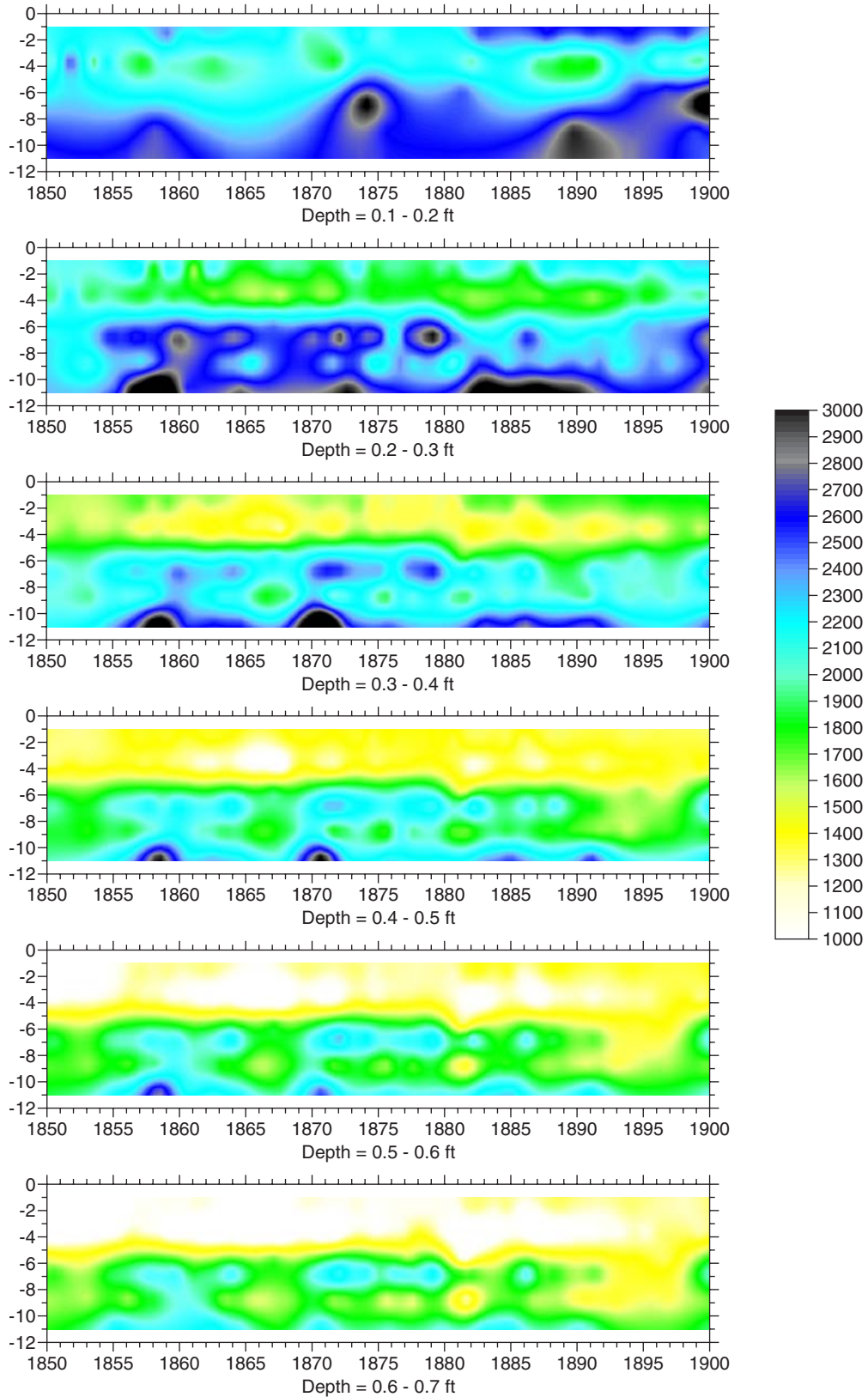
Figure 4.38. Section 1,850 to 1,900.
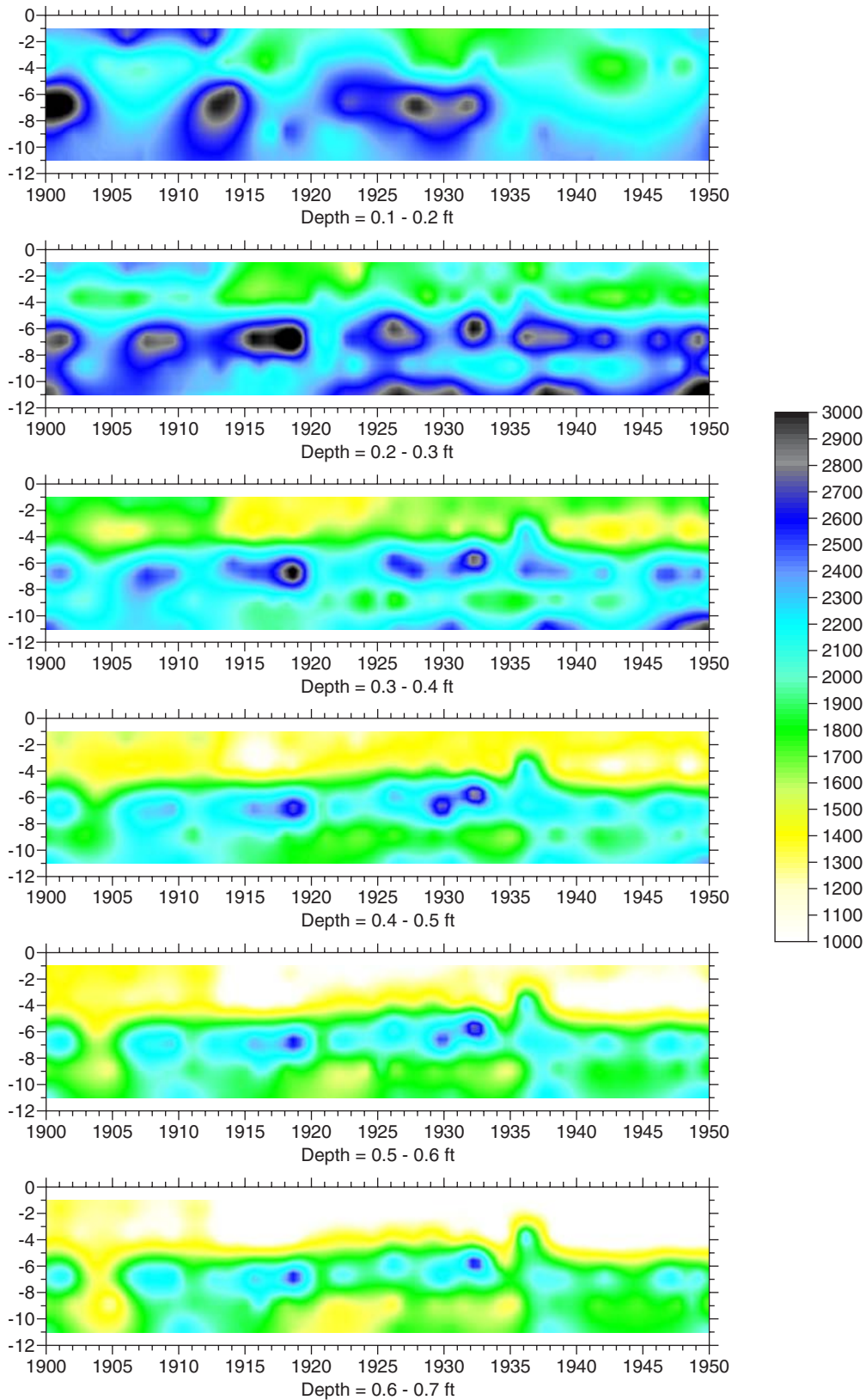
Figure 4.39. Section 1,900 to 1,950.
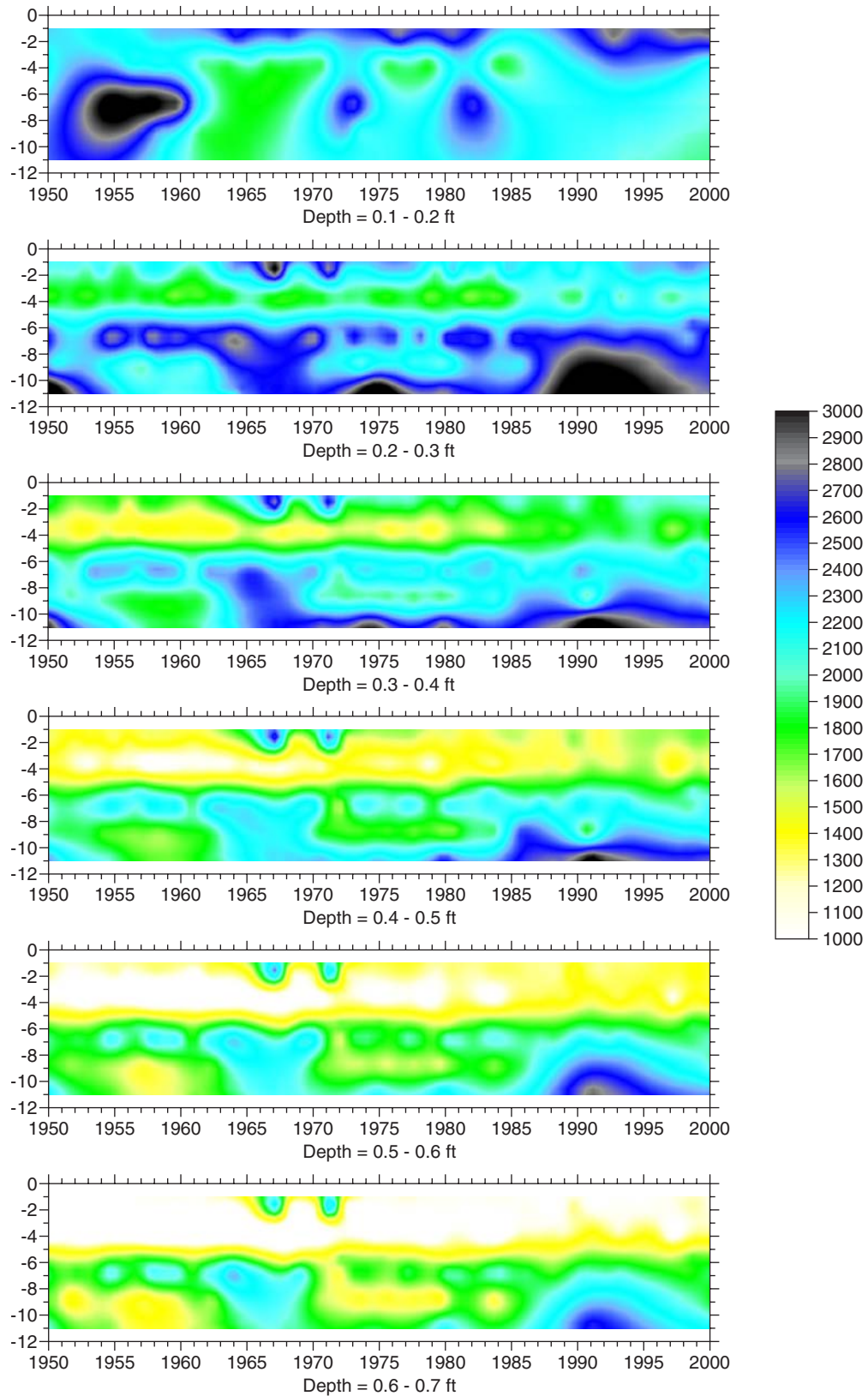
Figure 4.40. Section 1,950 to 2,000.
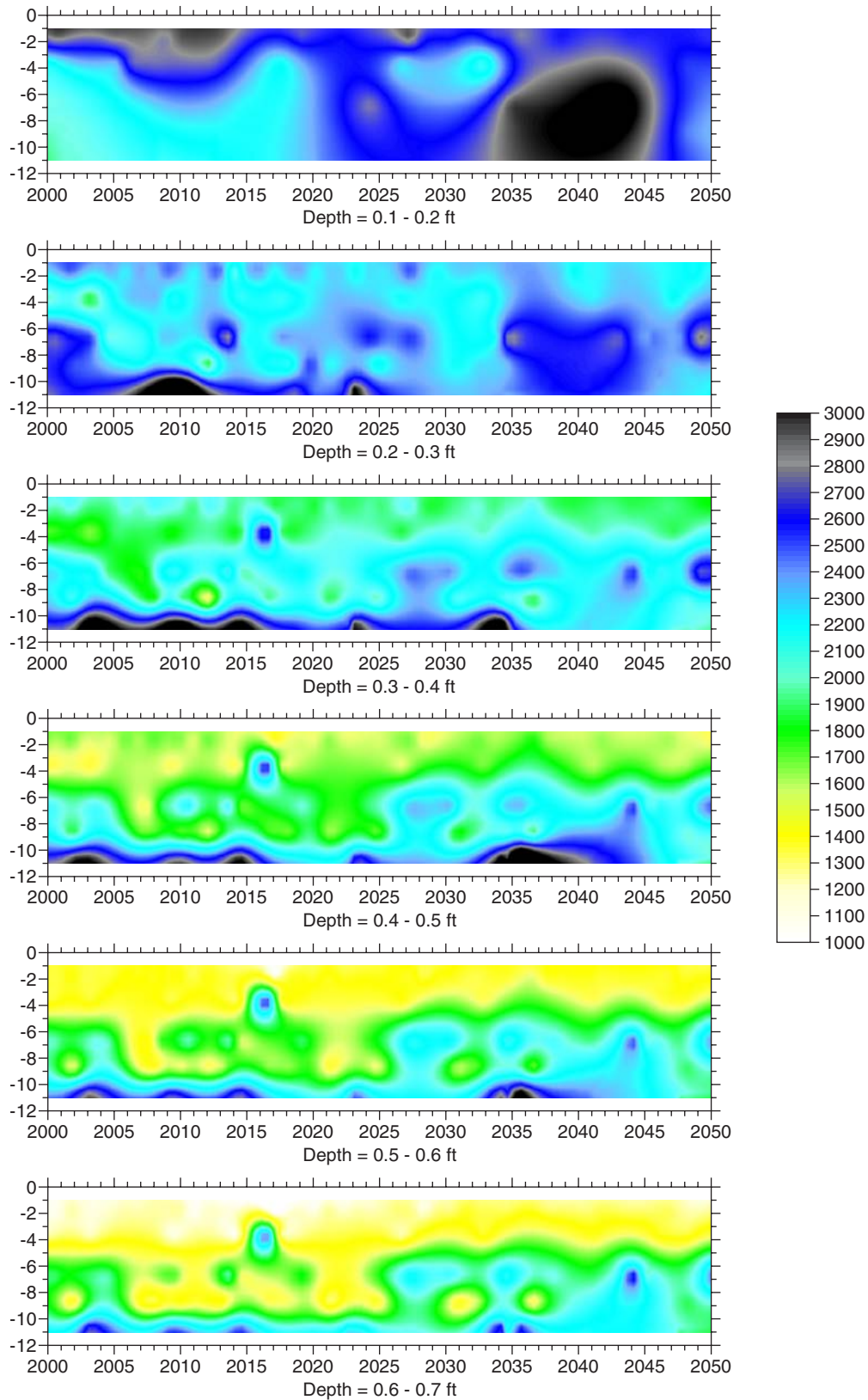
Figure 4.41. Section 2,000 to 2,050.
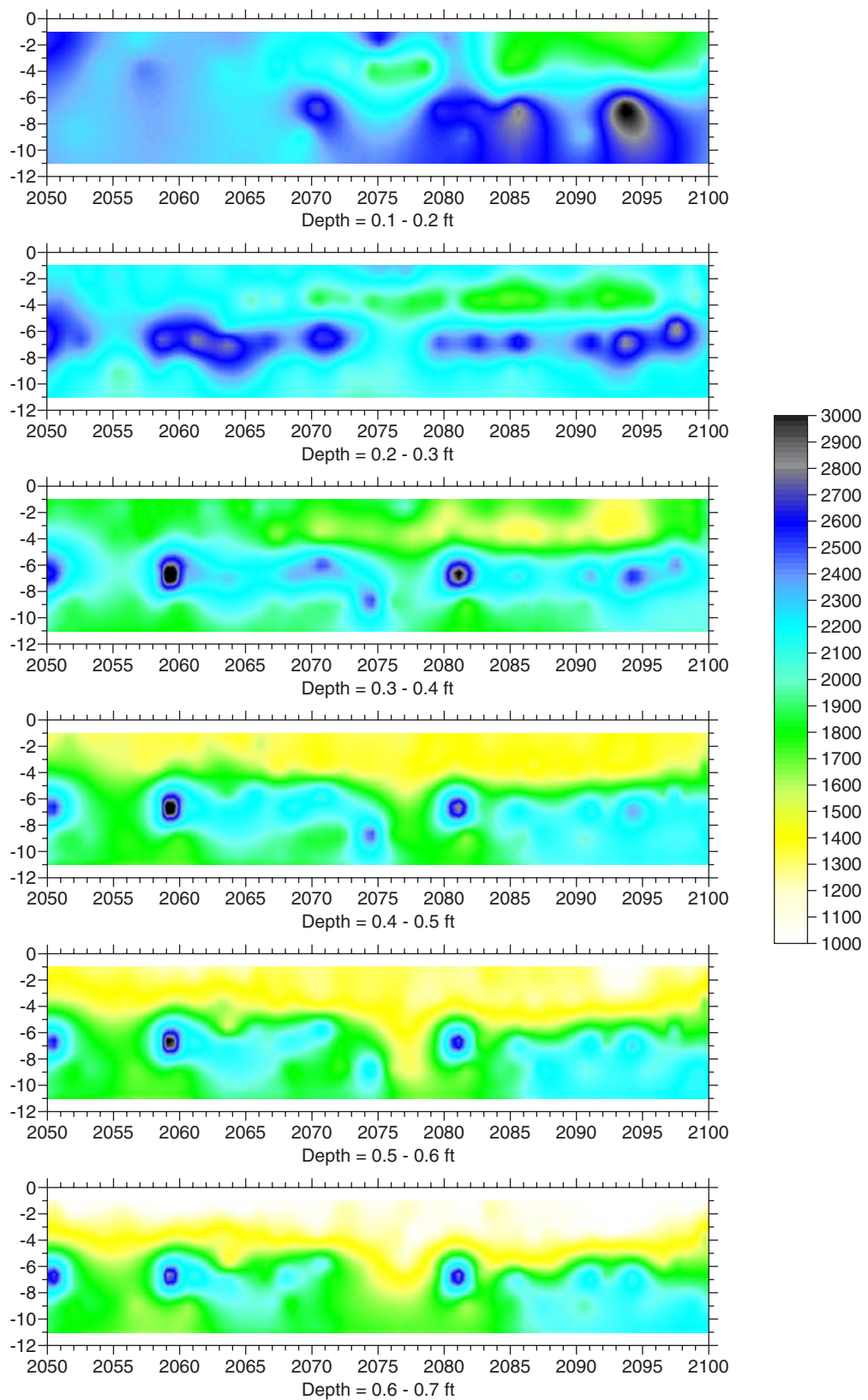
Figure 4.42. Section 2,050 to 2,100.
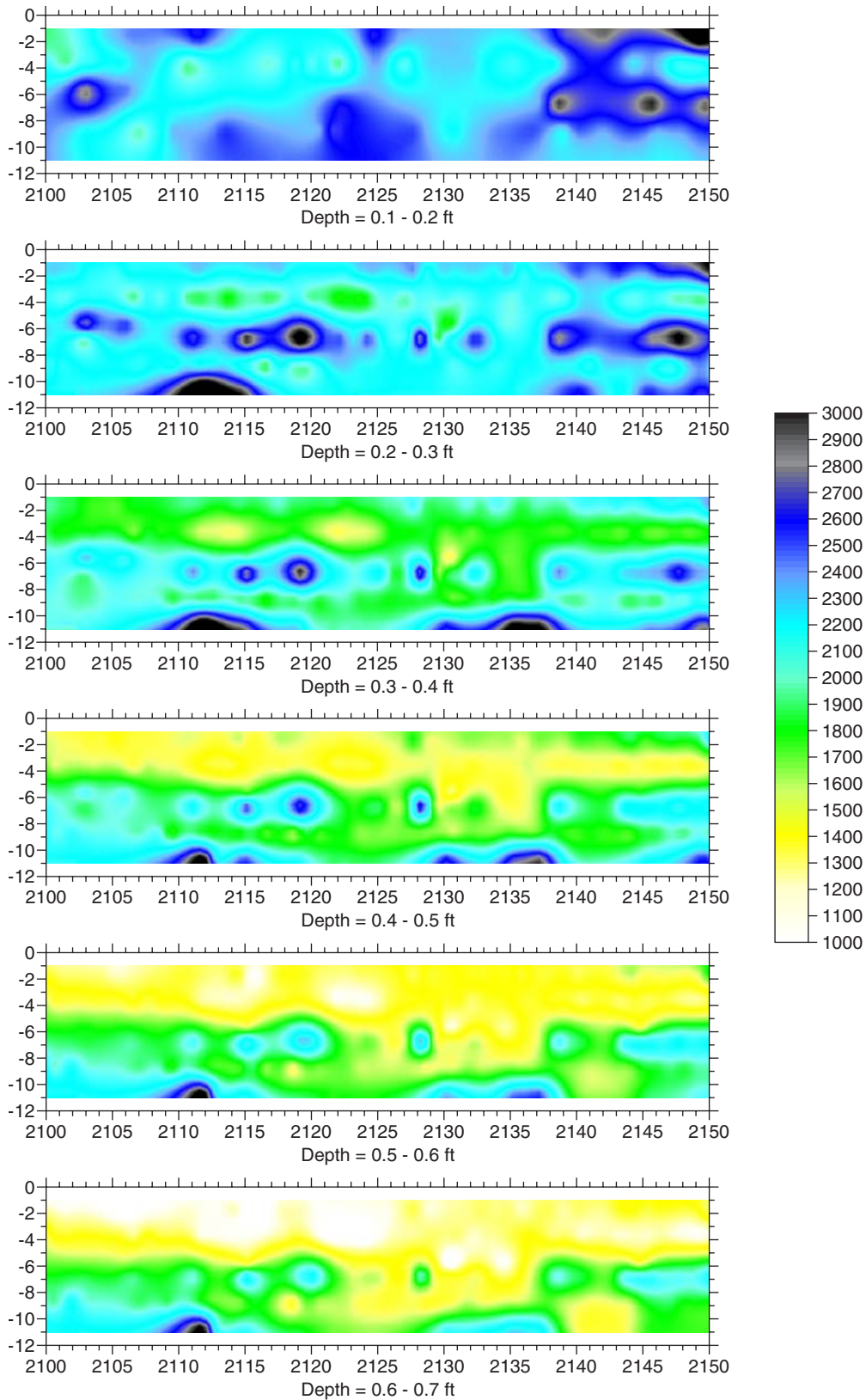
Figure 4.43. Section 2,100 to 2,150.
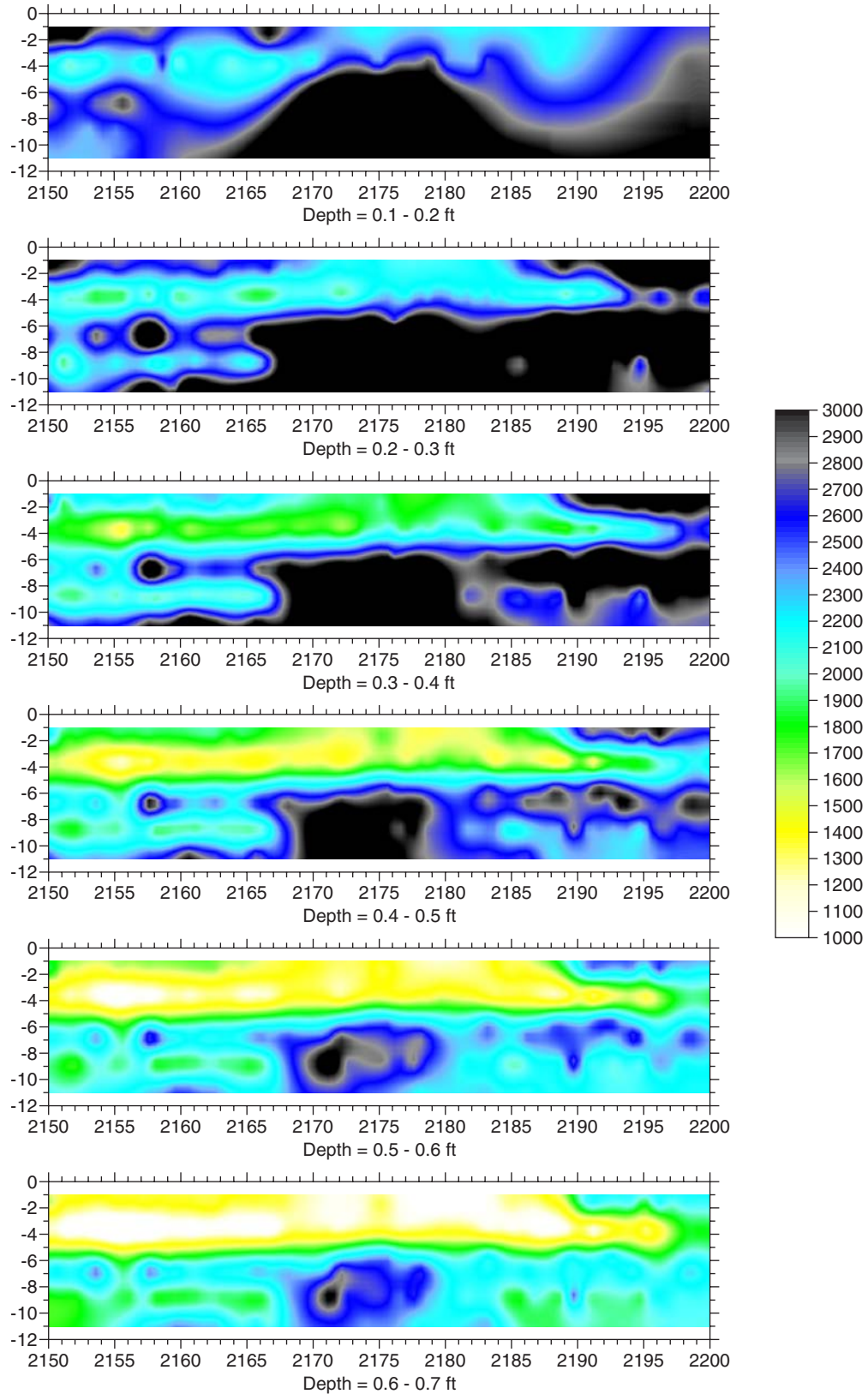
Figure 4.44. Section 2,150 to 2,200.
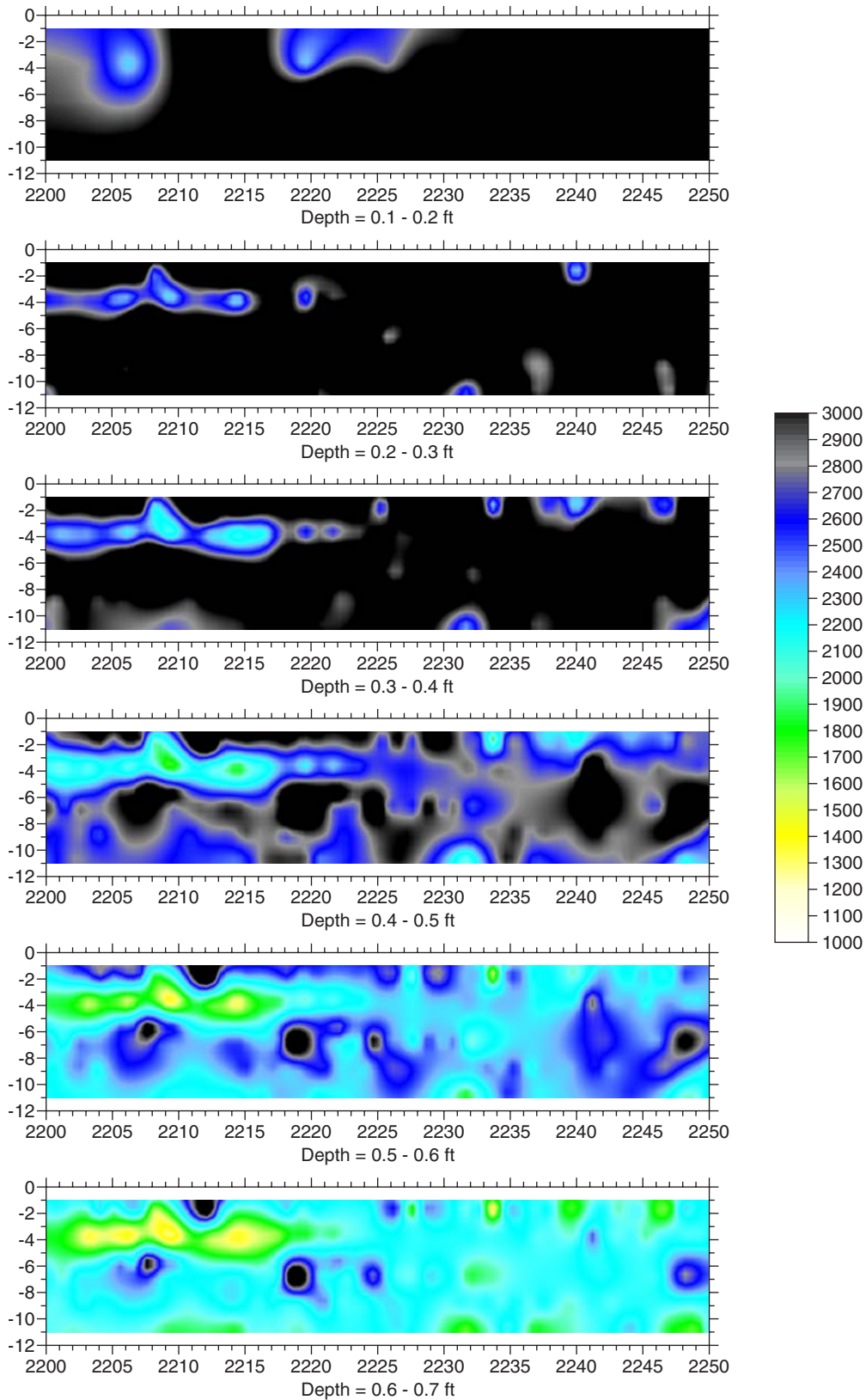
Figure 4.45. Section 2,200 to 2,250.
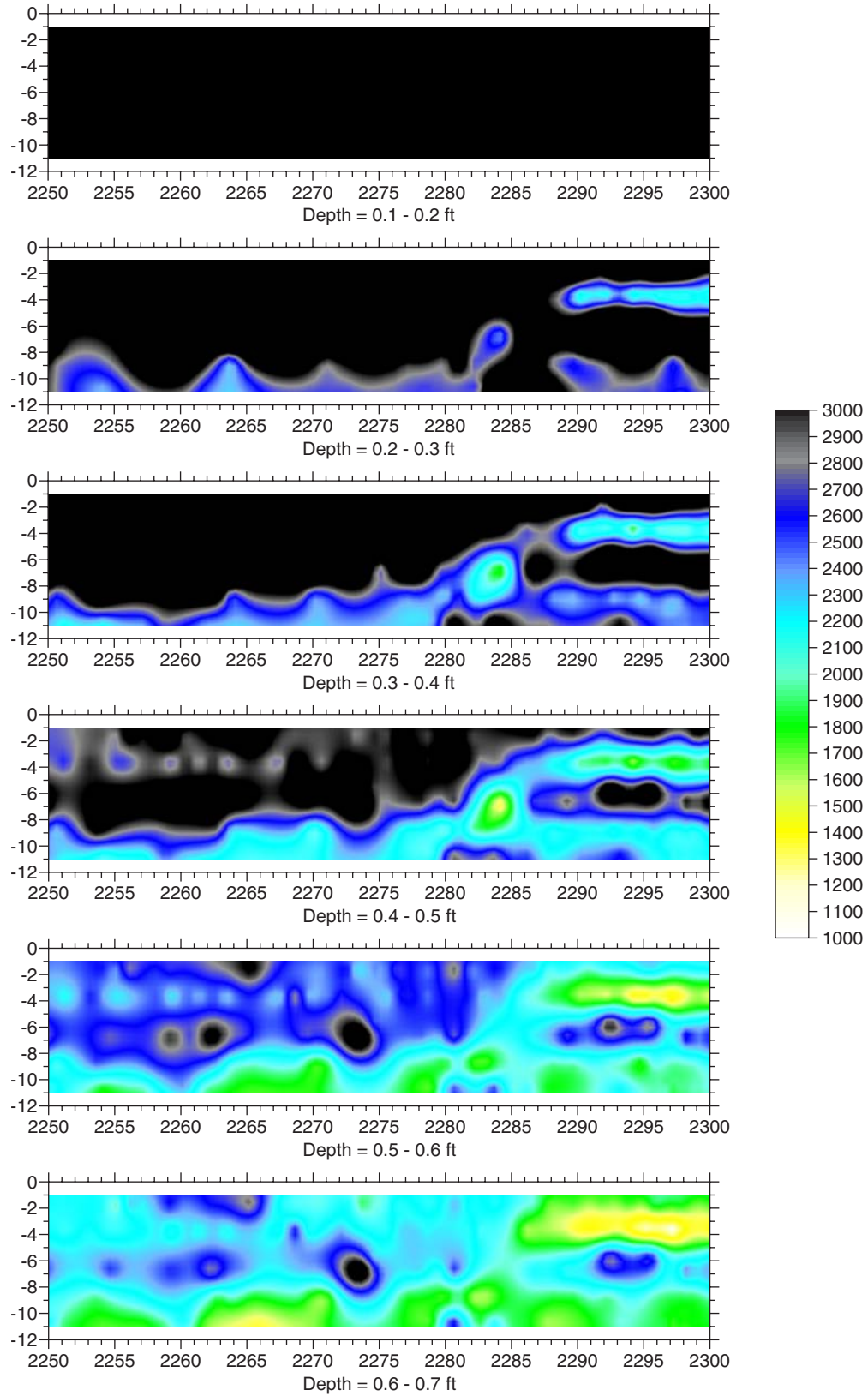
Figure 4.46. Section 2,250 to 2,300.
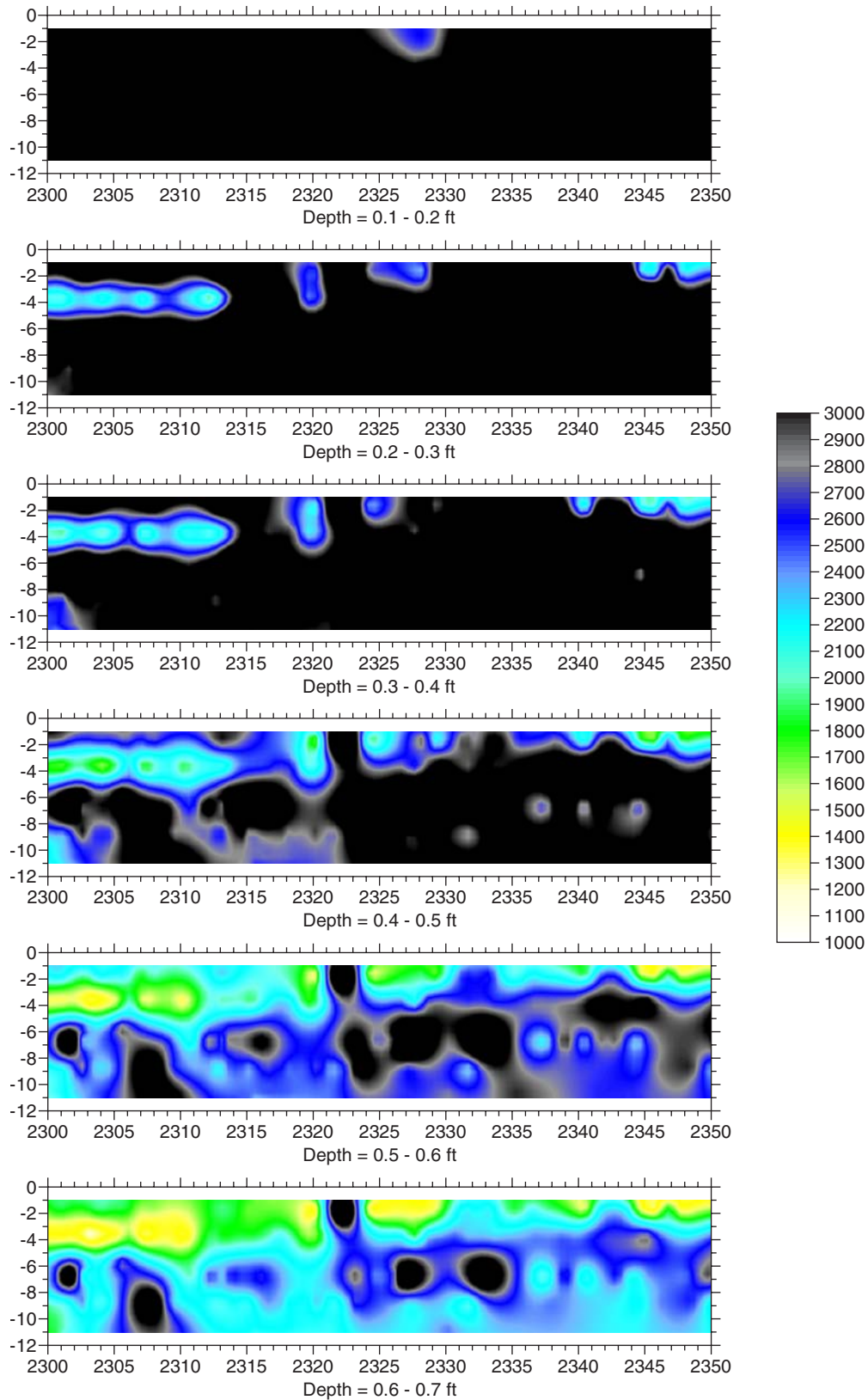
Figure 4.47. Section 2,300 to 2,350.
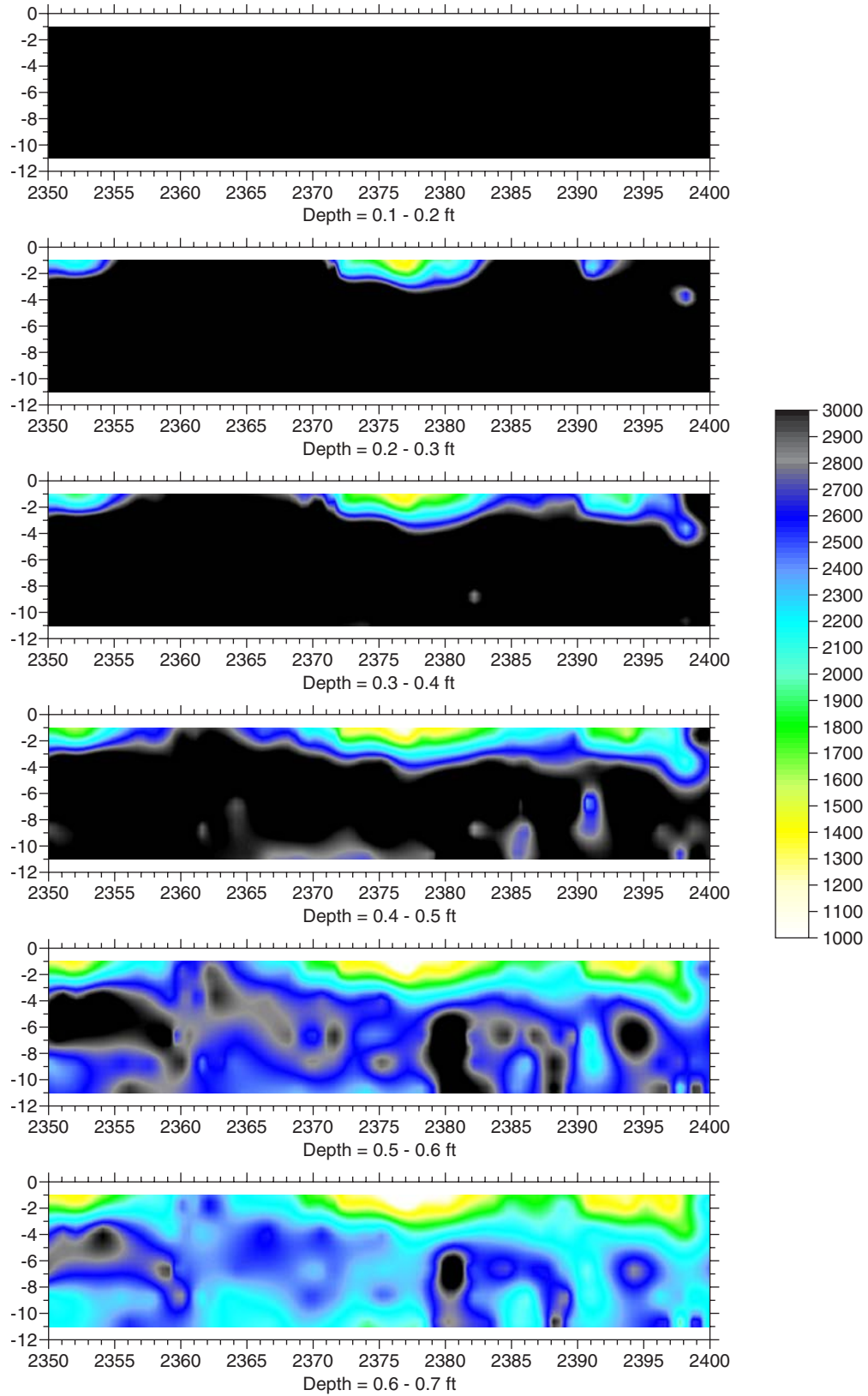
Figure 4.48. Section 2,350 to 2,400.
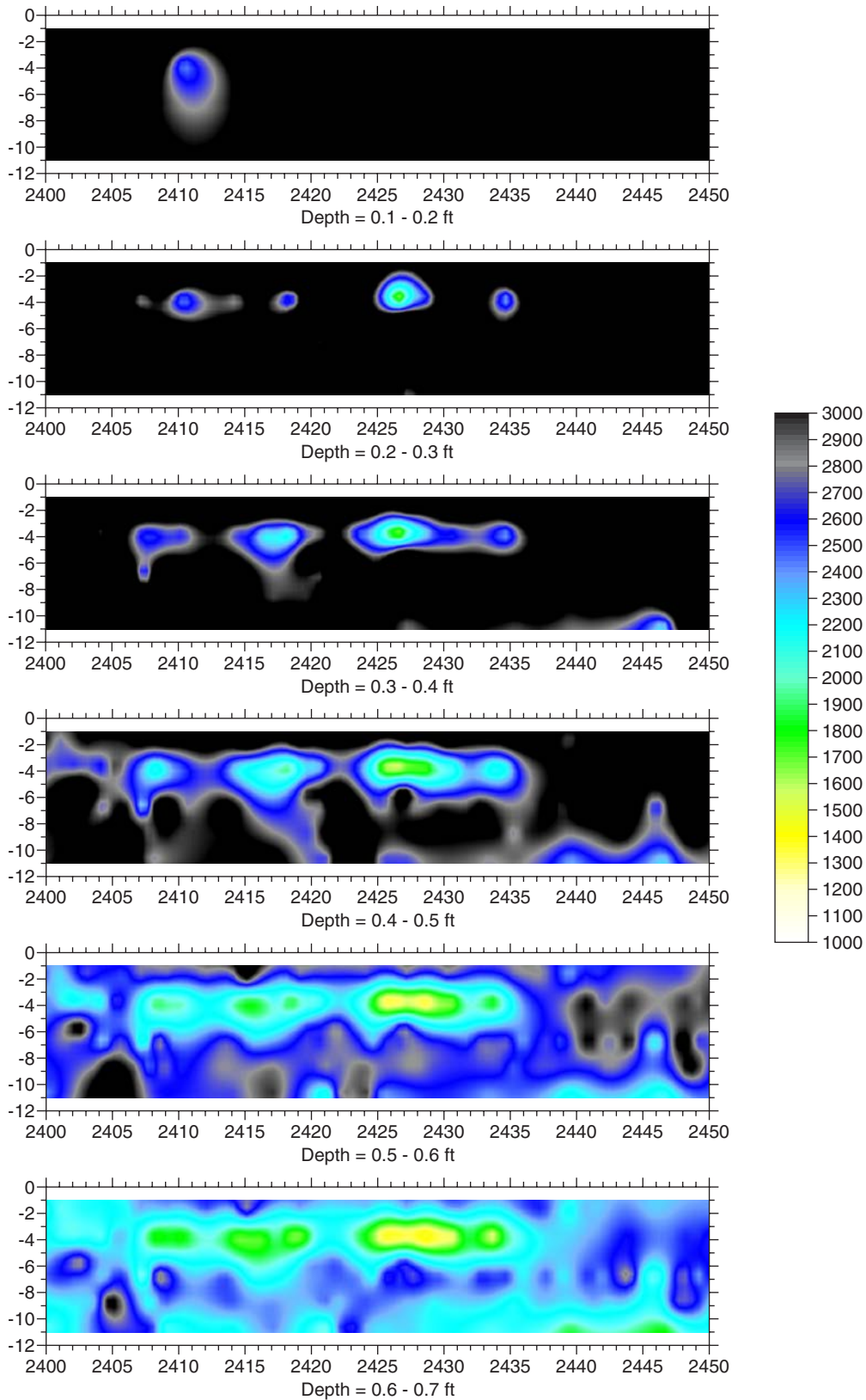
Figure 4.49. Section 2,400 to 2,450.
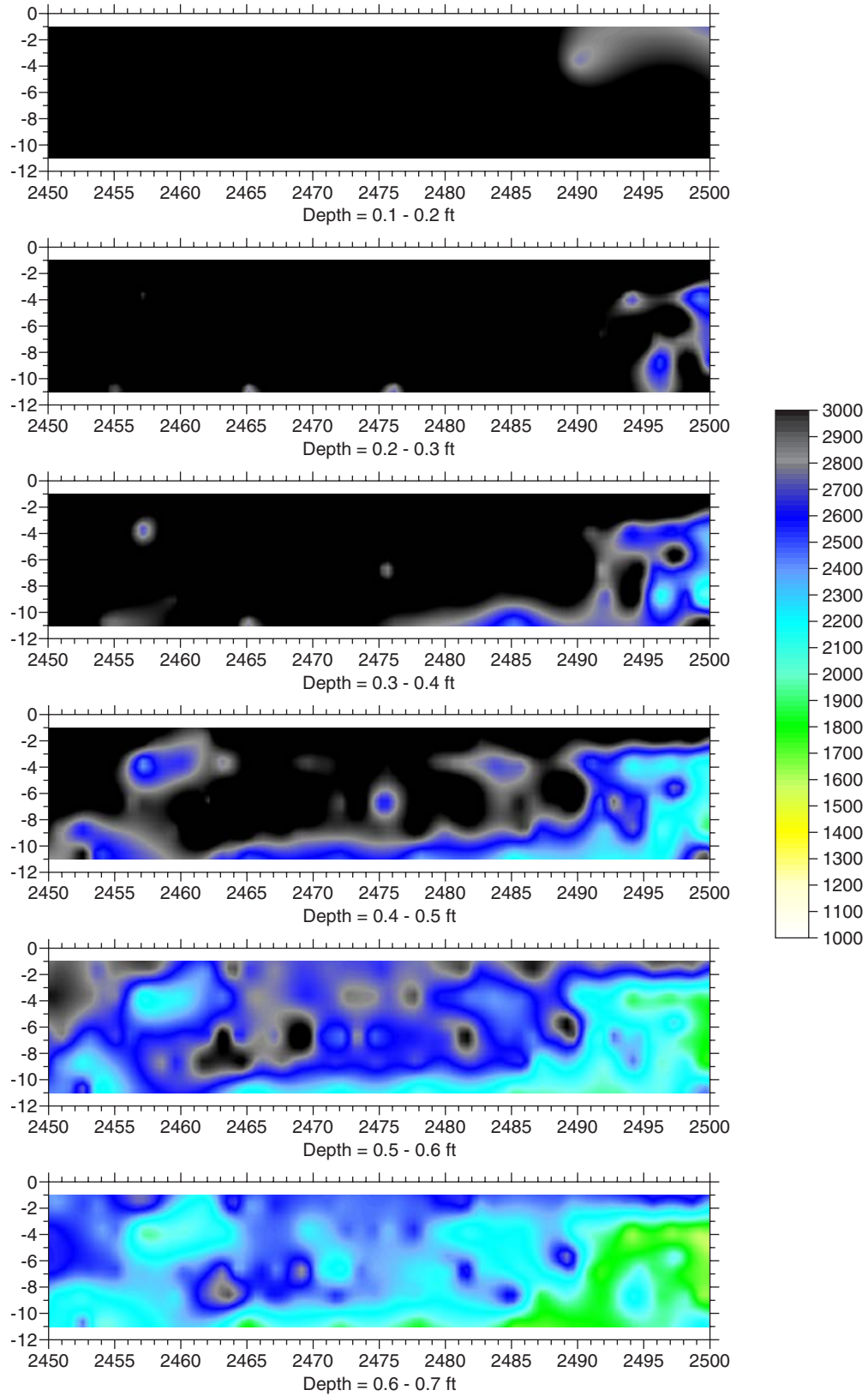
Figure 4.50. Section 2,450 to 2,500.
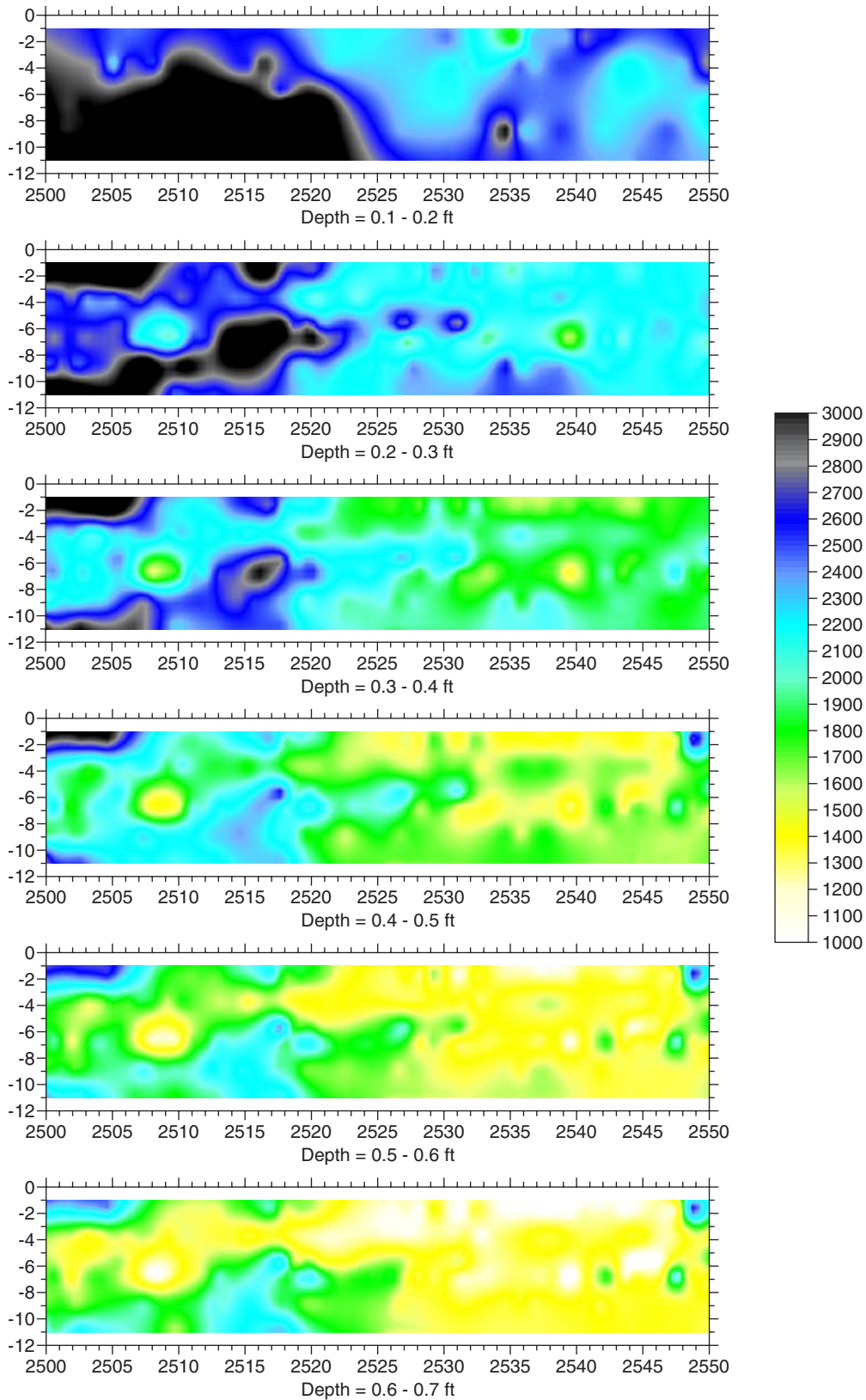
Figure 4.51. Section 2,500 to 2,550.
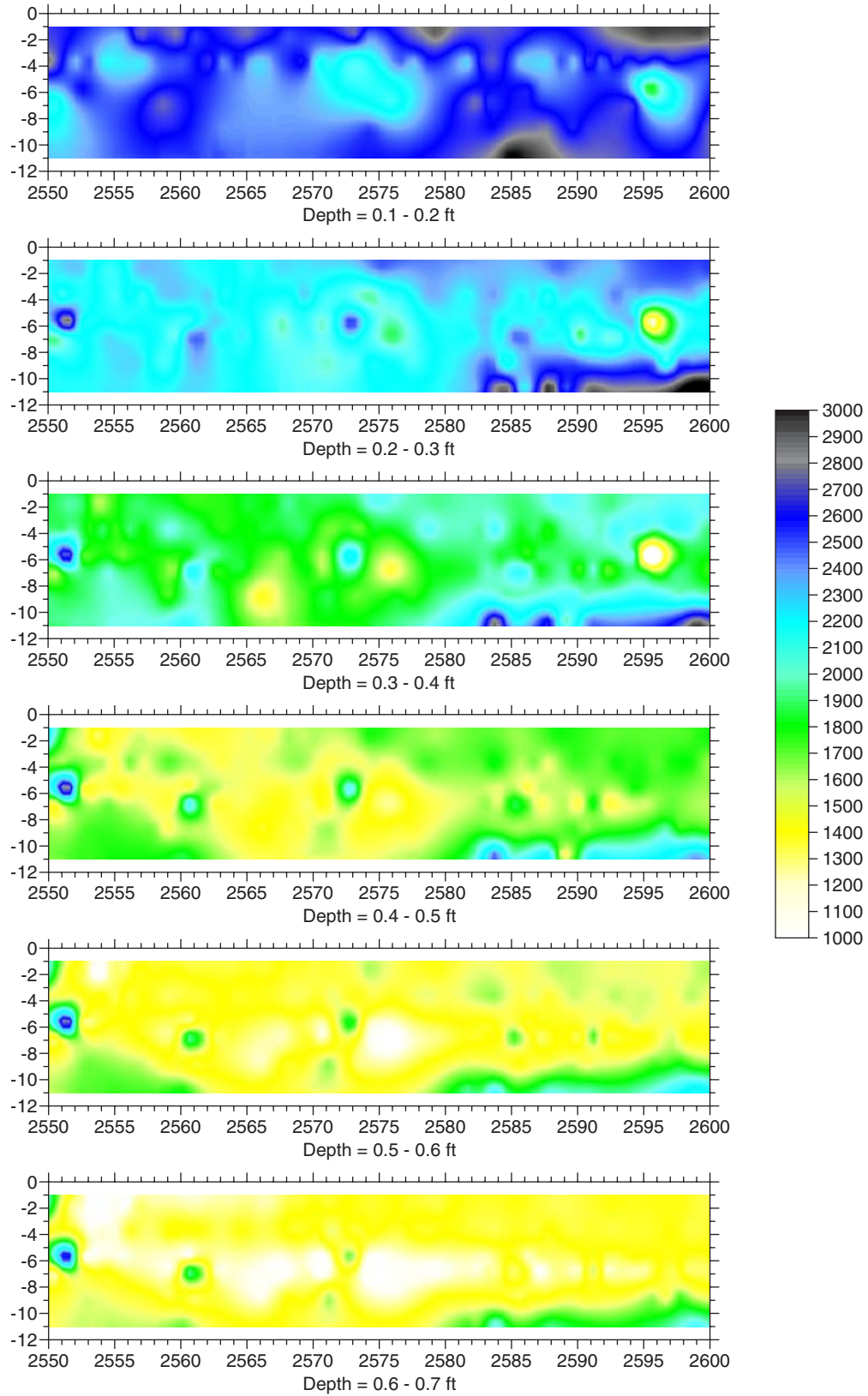
Figure 4.52. Section 2,550 to 2,600.
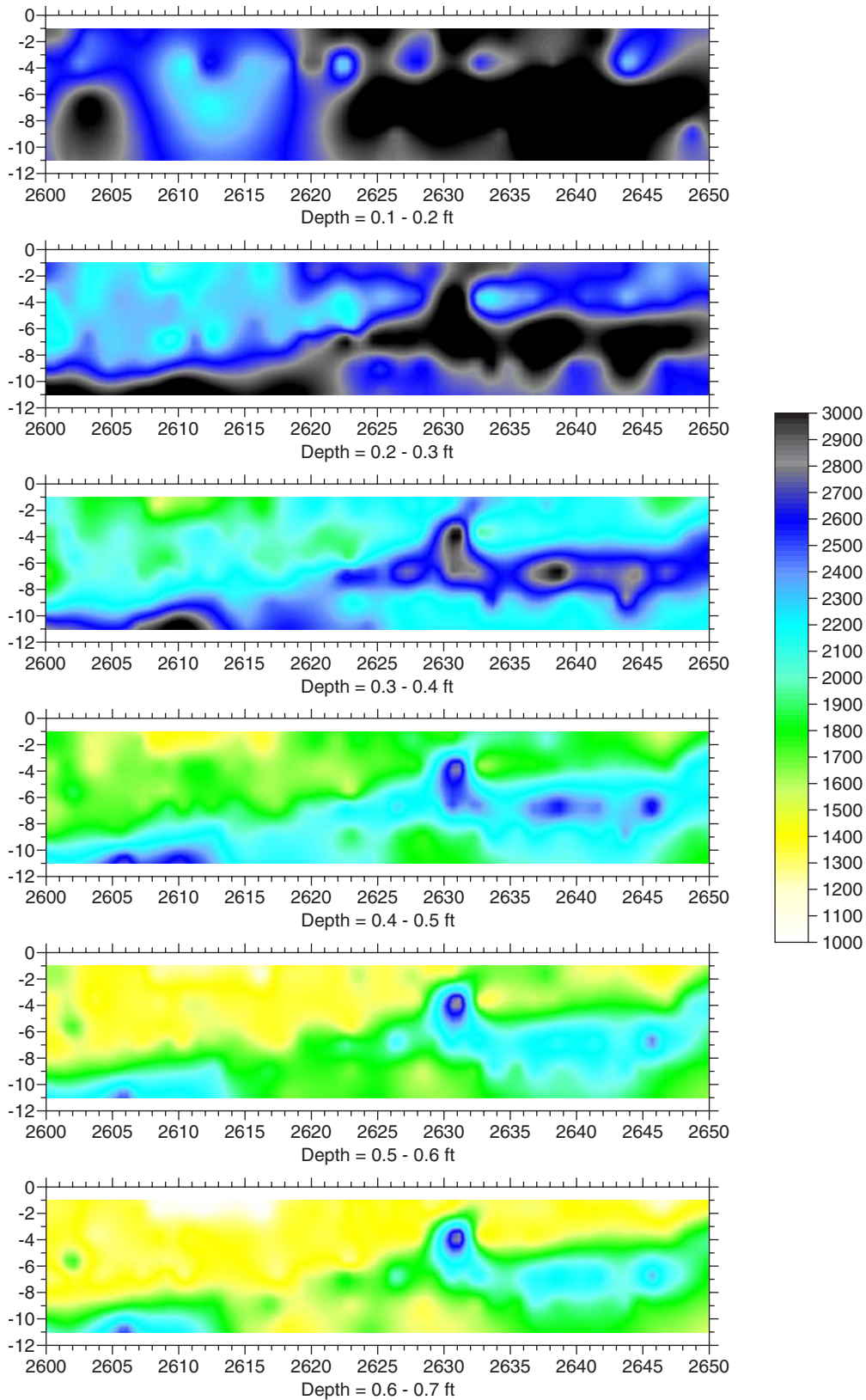
Figure 4.53. Section 2,600 to 2,650.
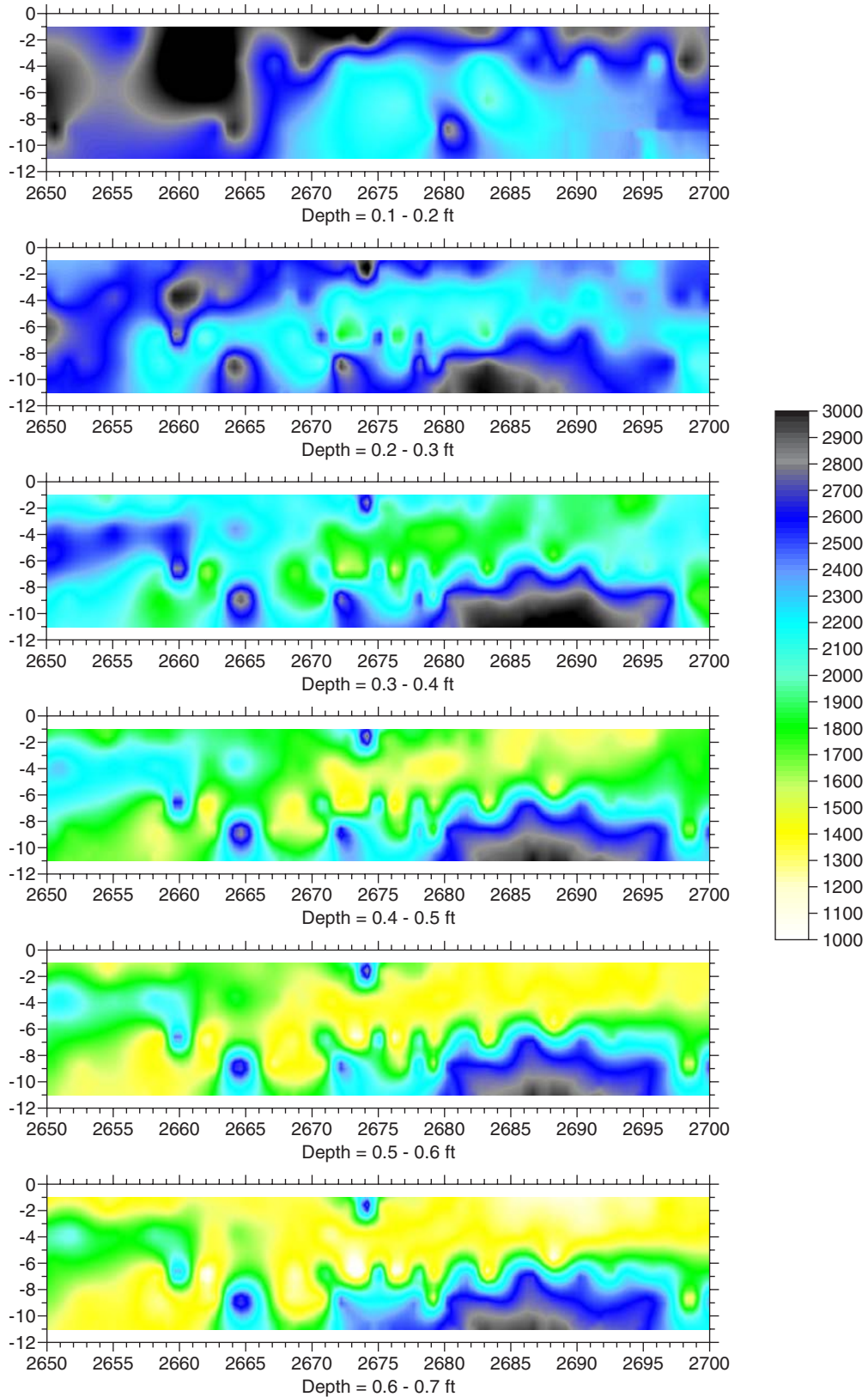
Figure 4.54. Section 2,650 to 2,700.
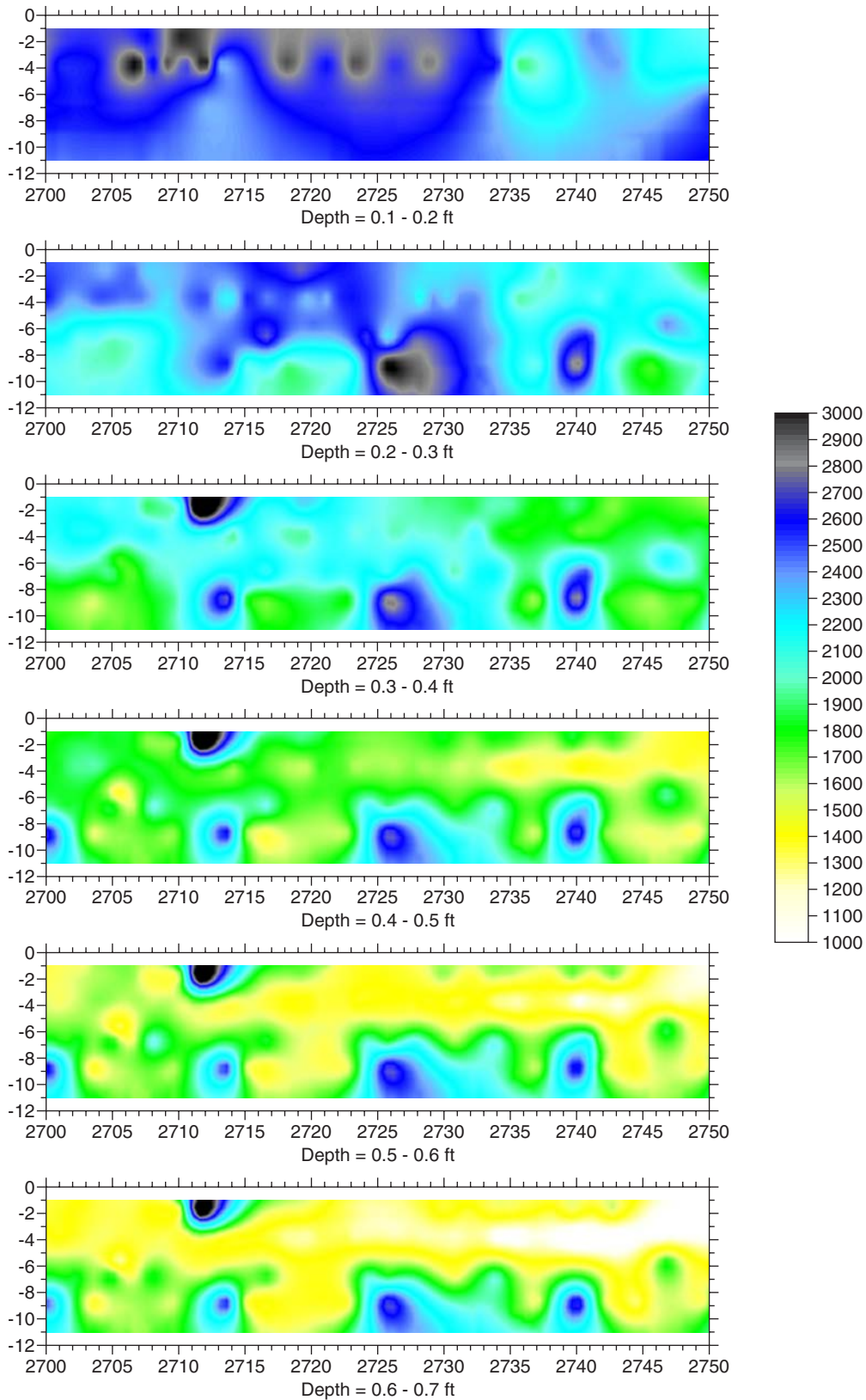
Figure 4.55. Section 2,700 to 2,750.
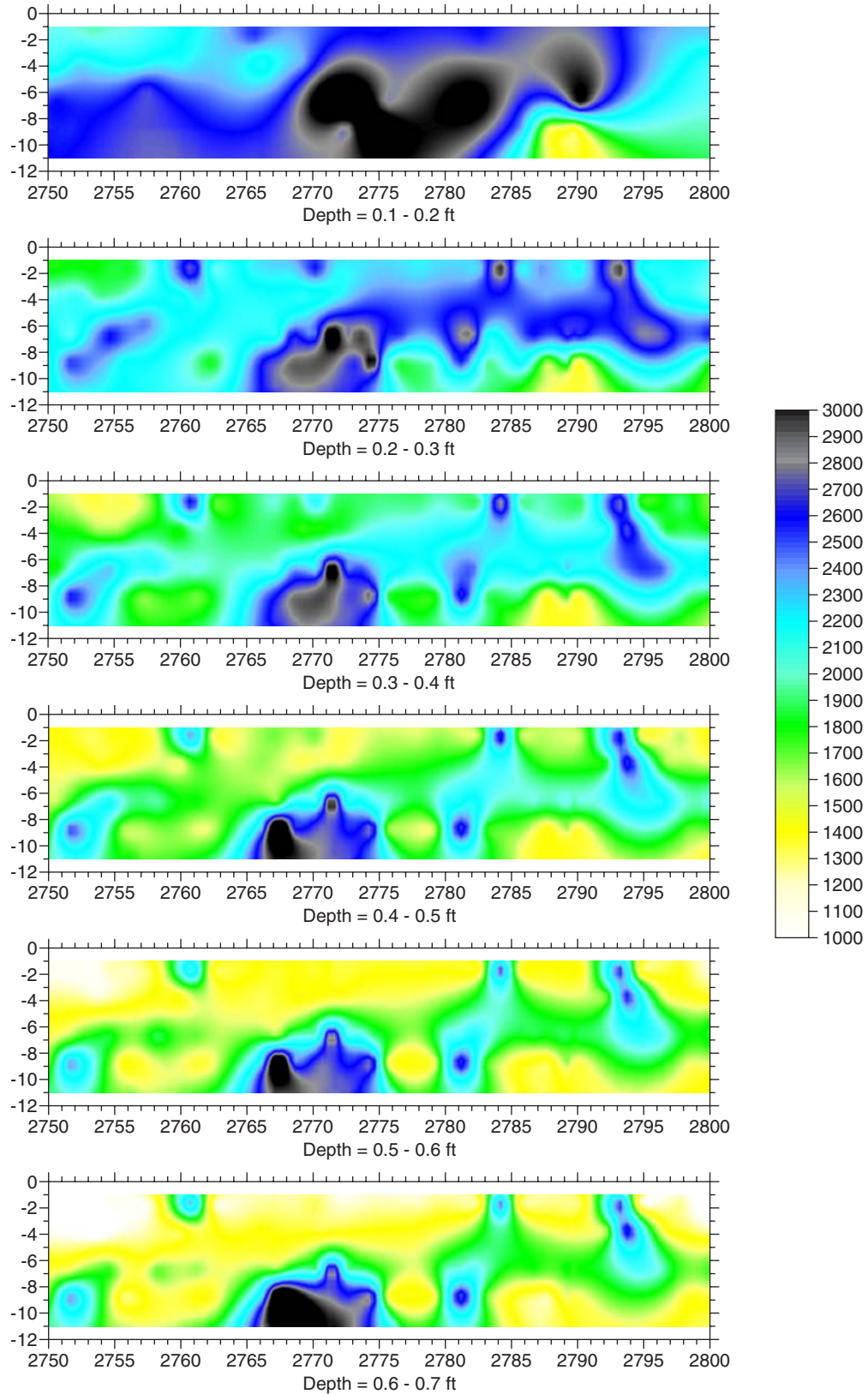
Figure 4.56. Section 2,750 to 2,800.
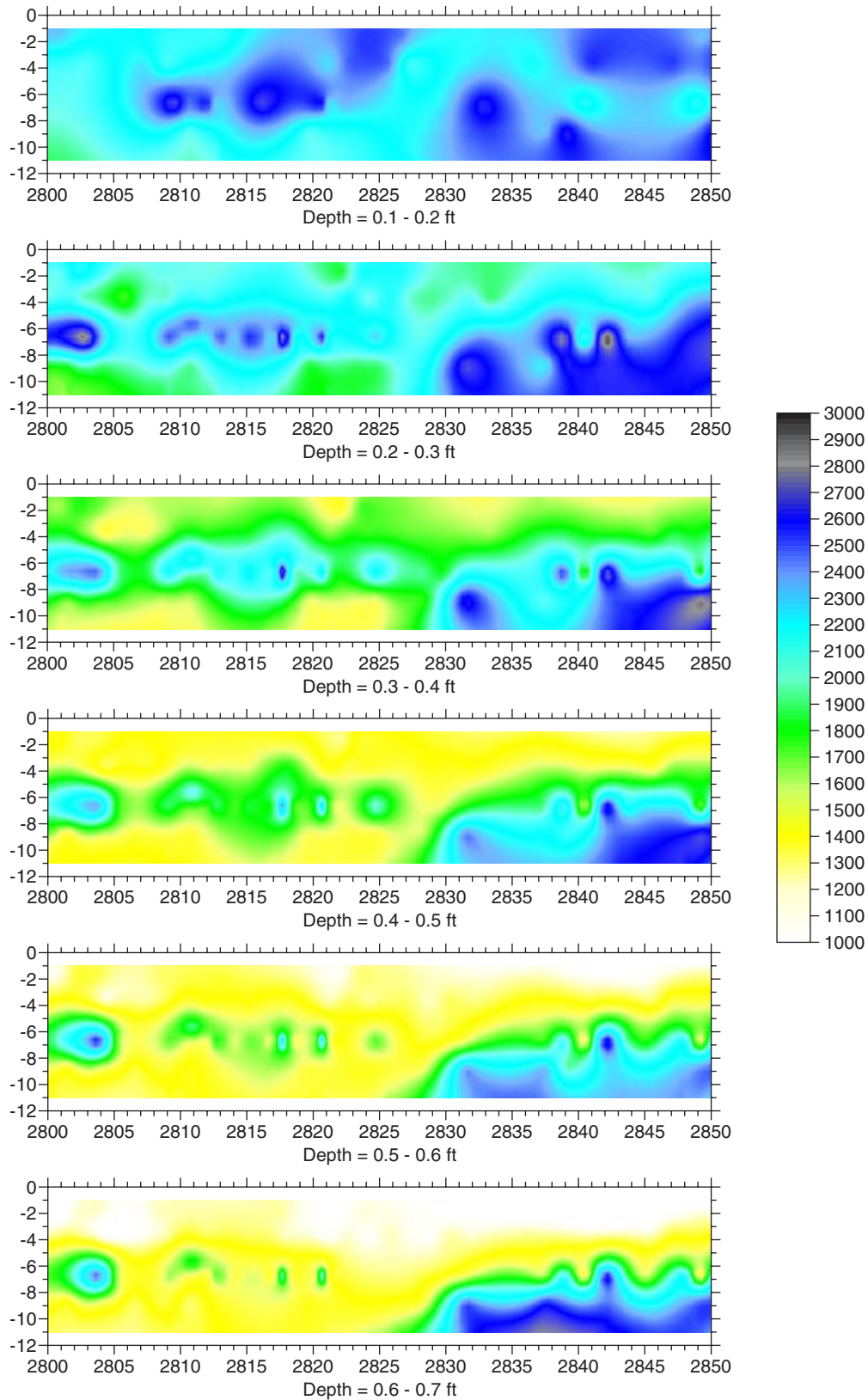
Figure 4.57. Section 2,800 to 2,850.
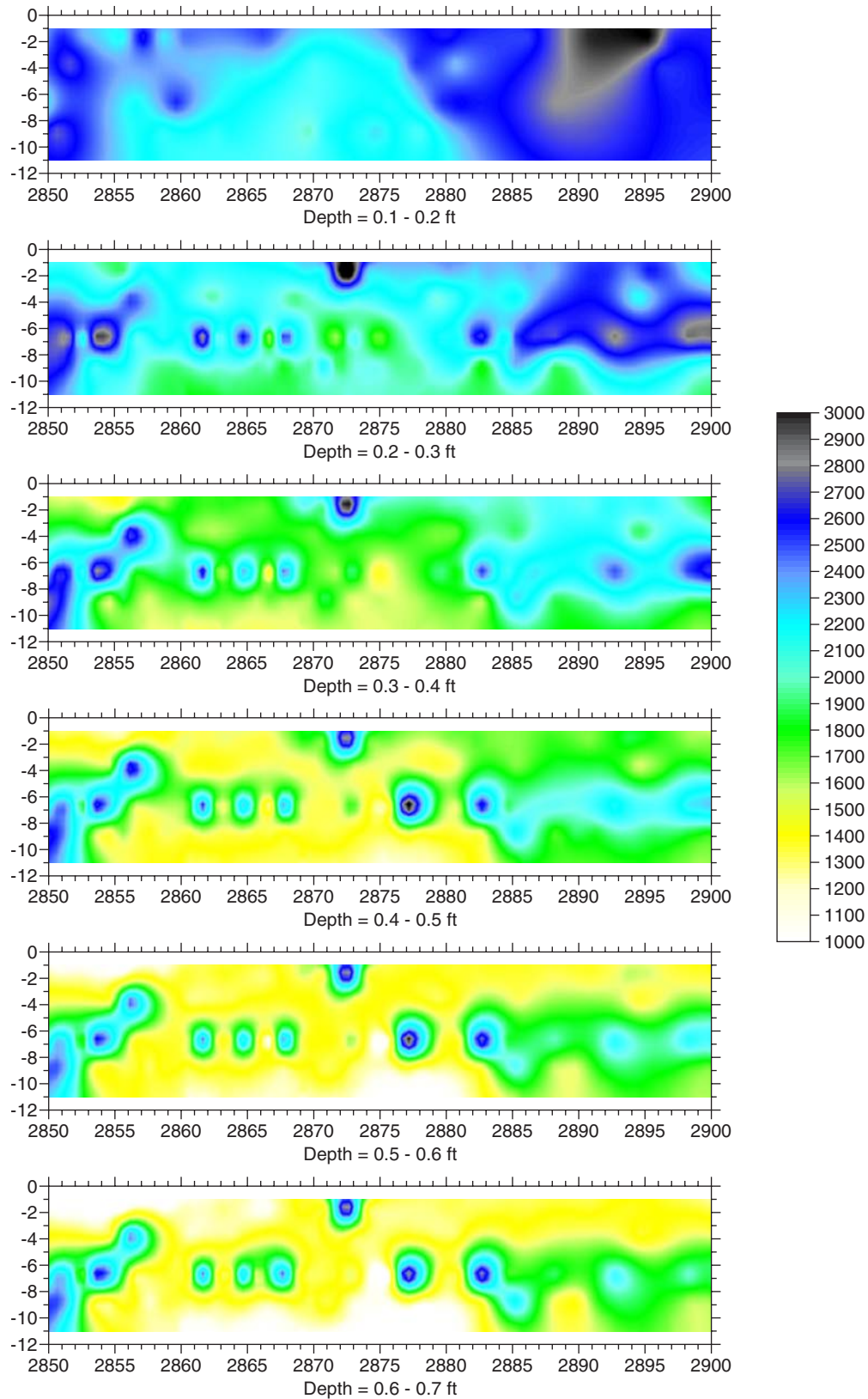
Figure 4.58. Section 2,850 to 2,900.
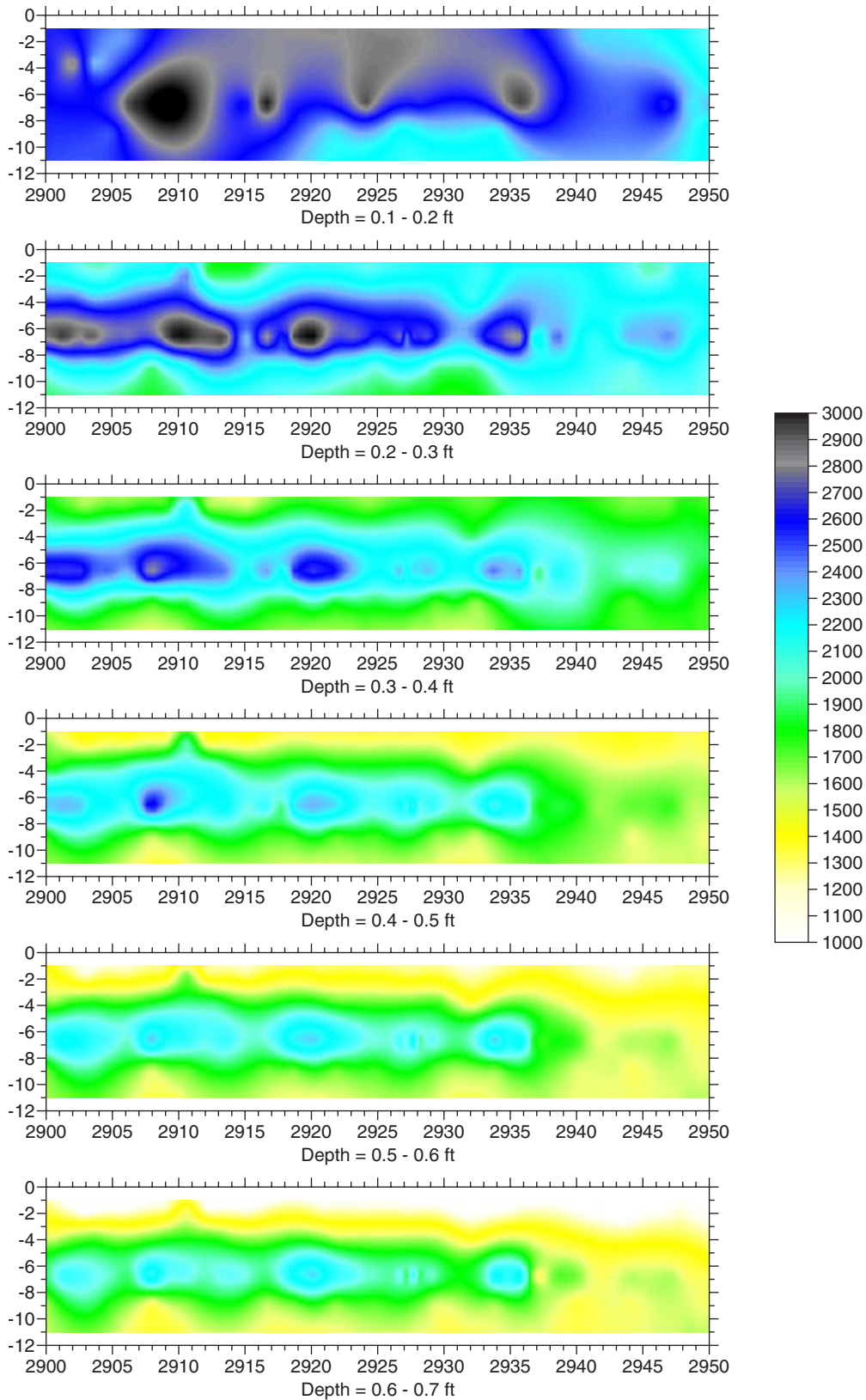
Figure 4.59. Section 2,900 to 2,950.
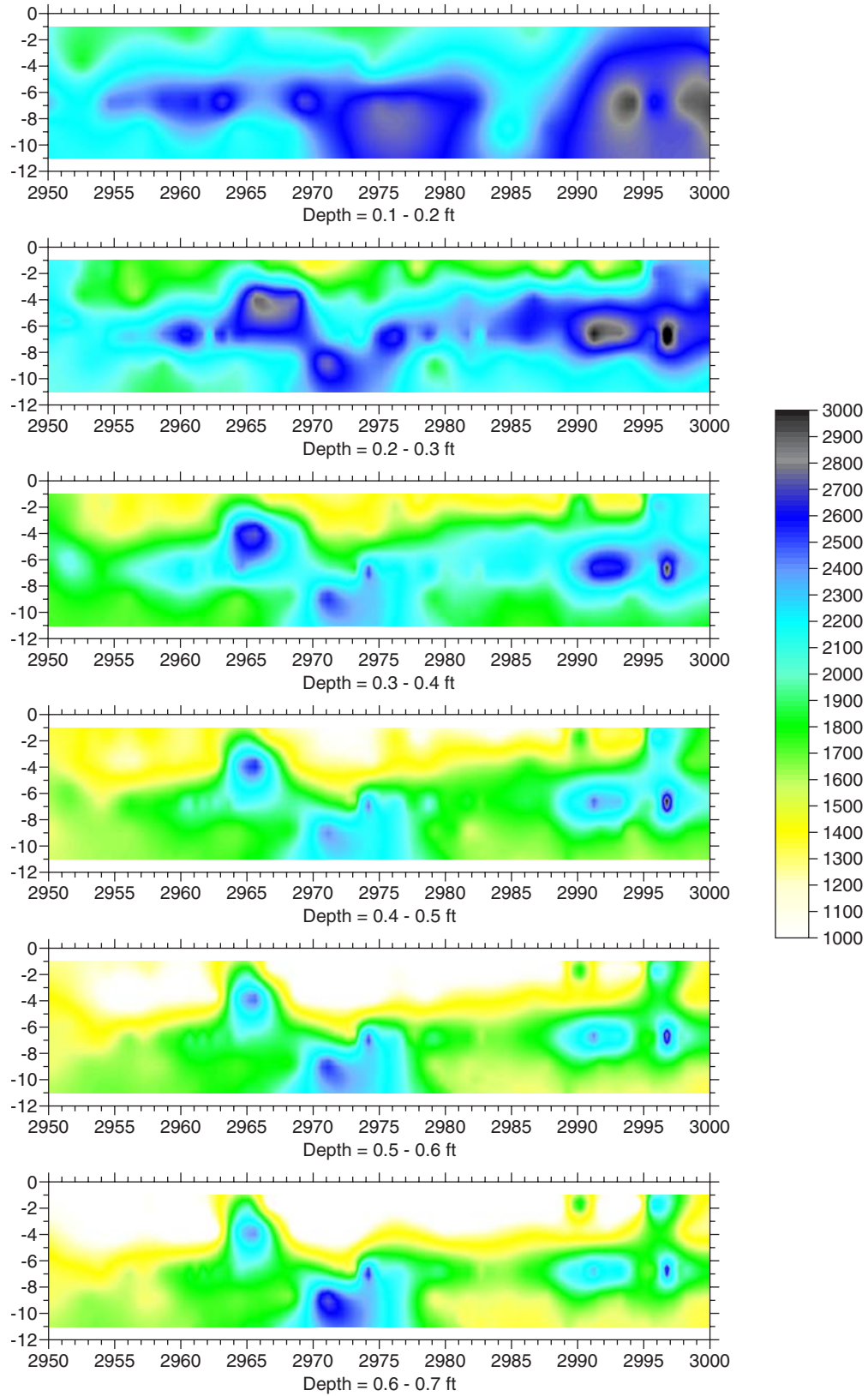
Figure 4.60. Section 2,950 to 3,000.
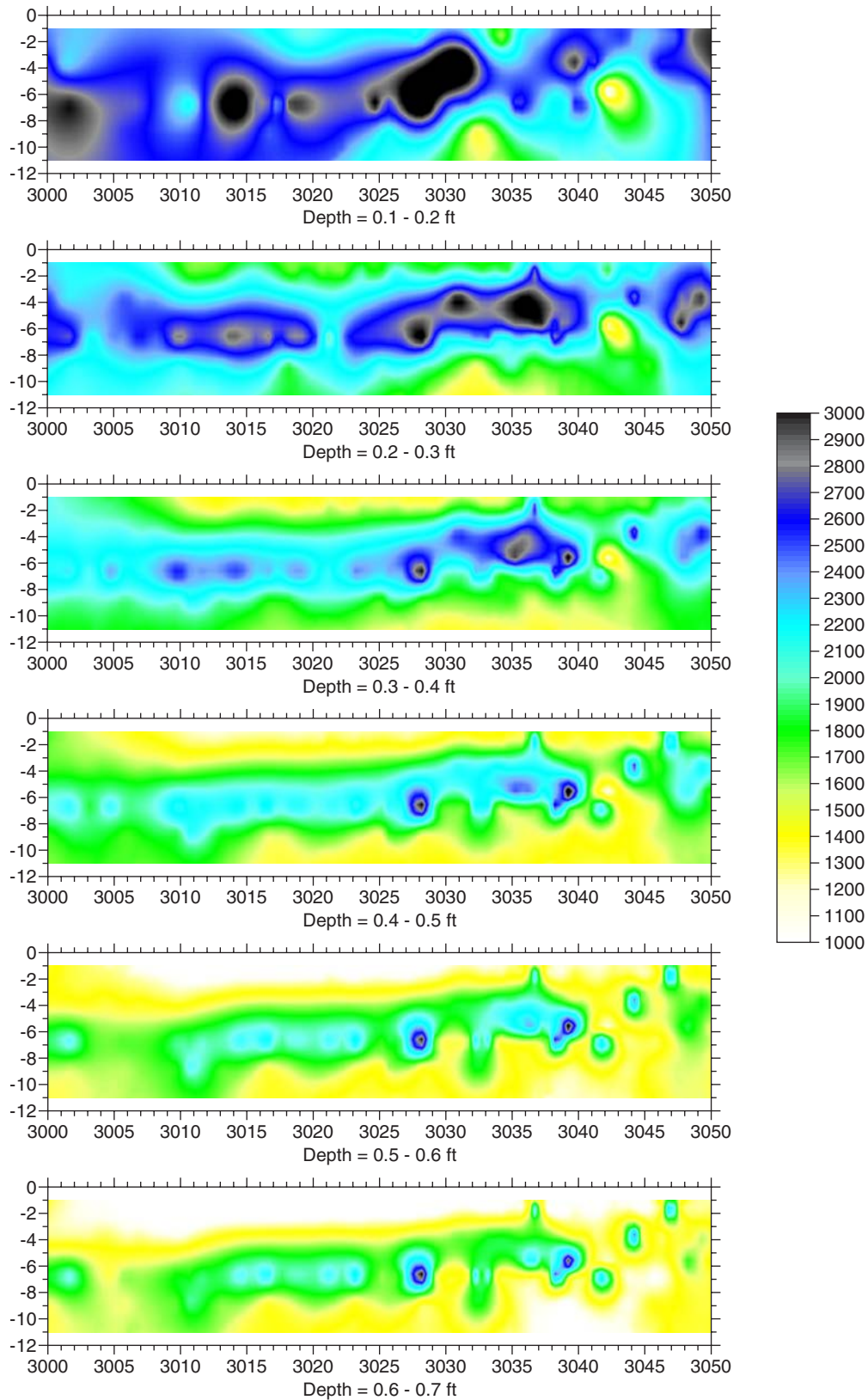
Figure 4.61. Section 3,000 to 3,050.
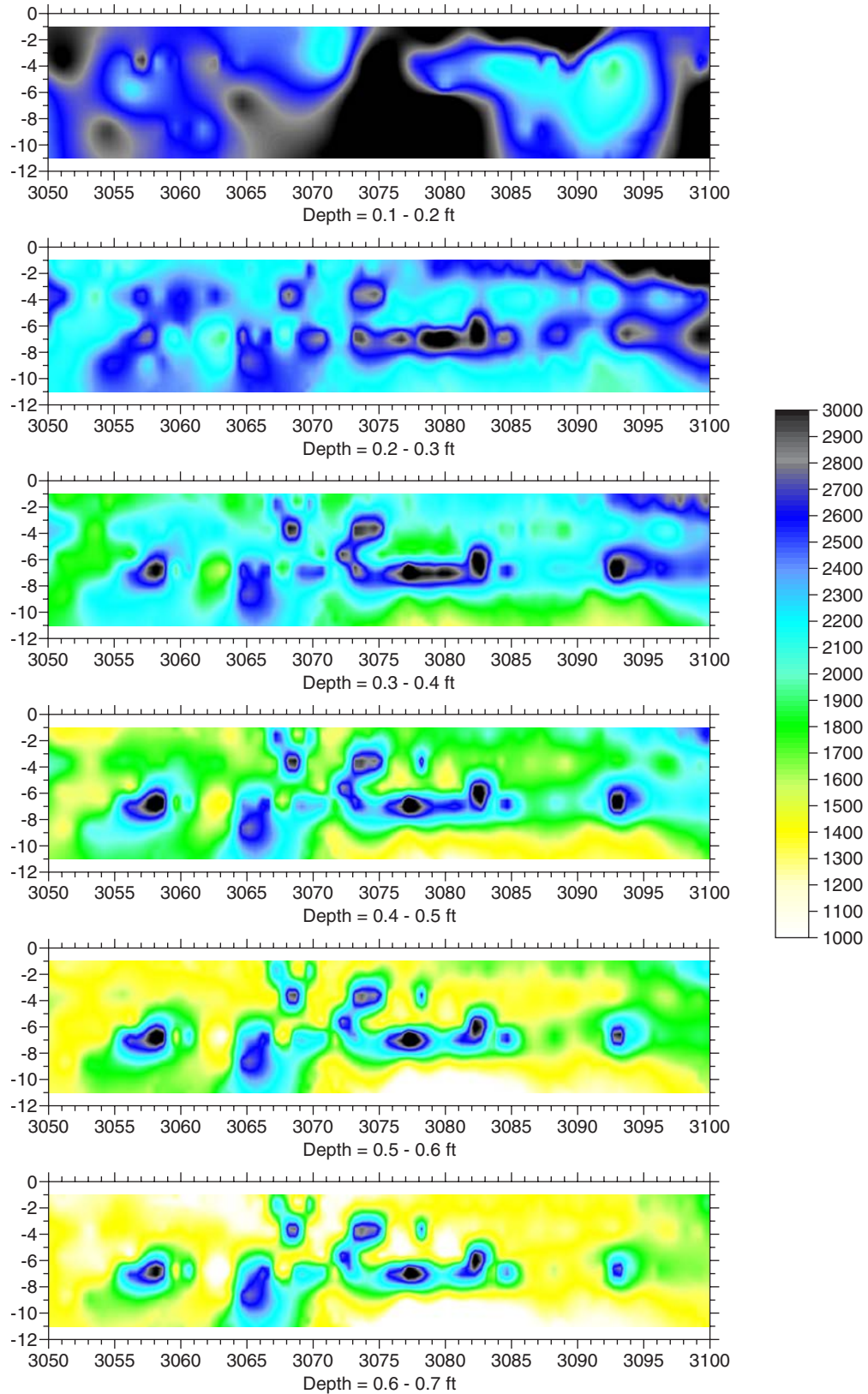
Figure 4.62. Section 3,050 to 3,100.
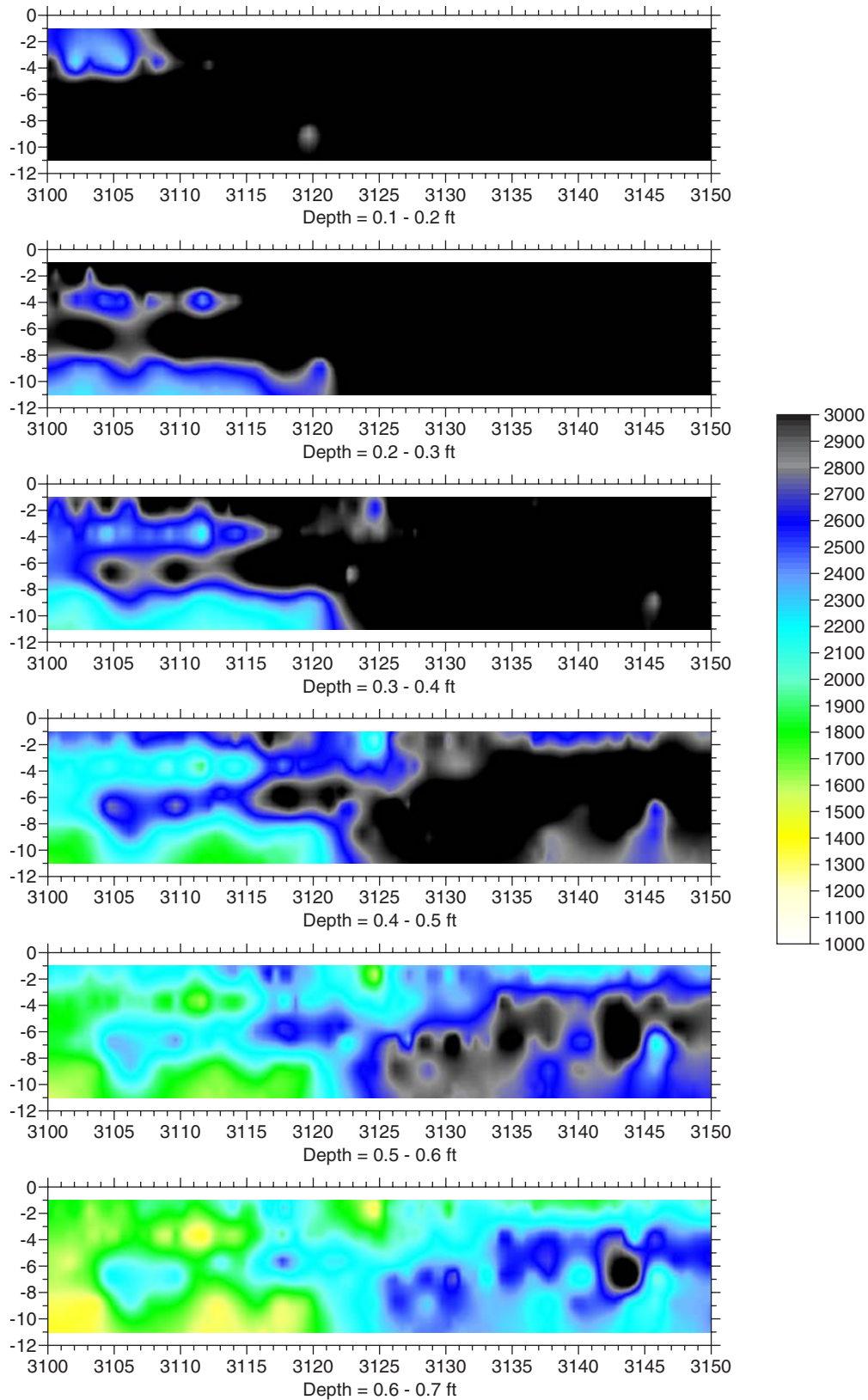
Figure 4.63. Section 3,100 to 3,150.
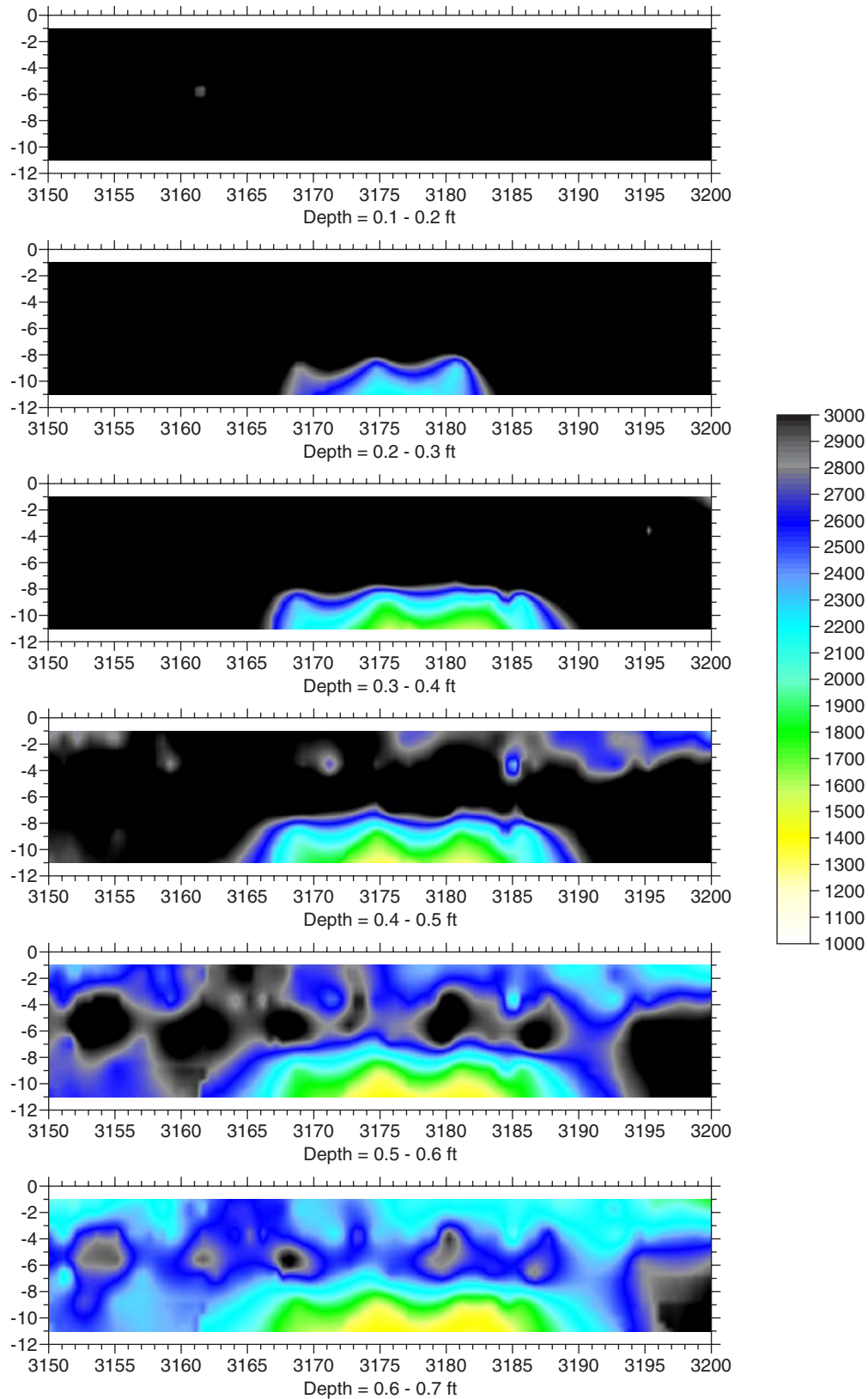
Figure 4.64. Section 3,150 to 3,200.
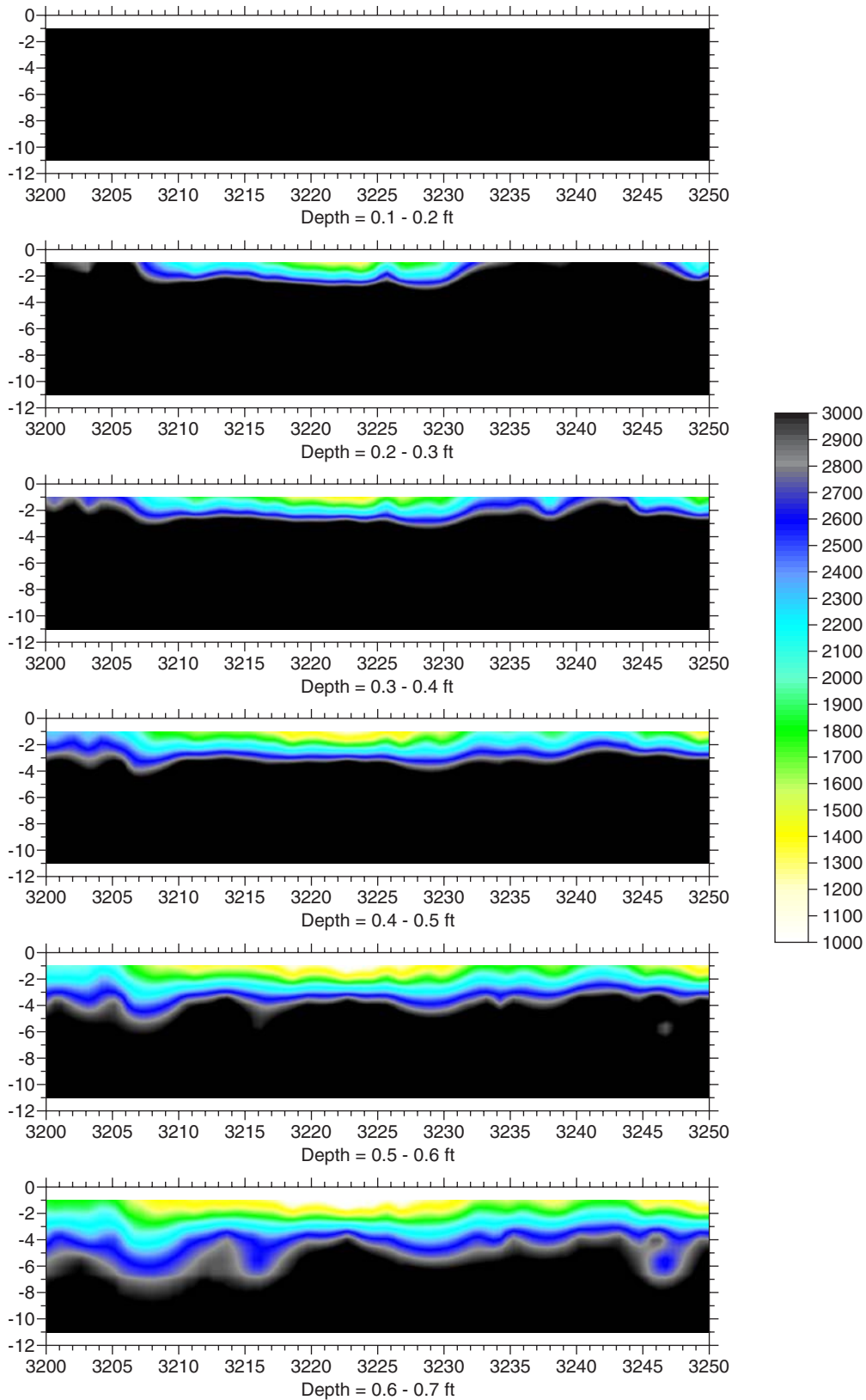
Figure 4.65. Section 3,200 to 3,250.
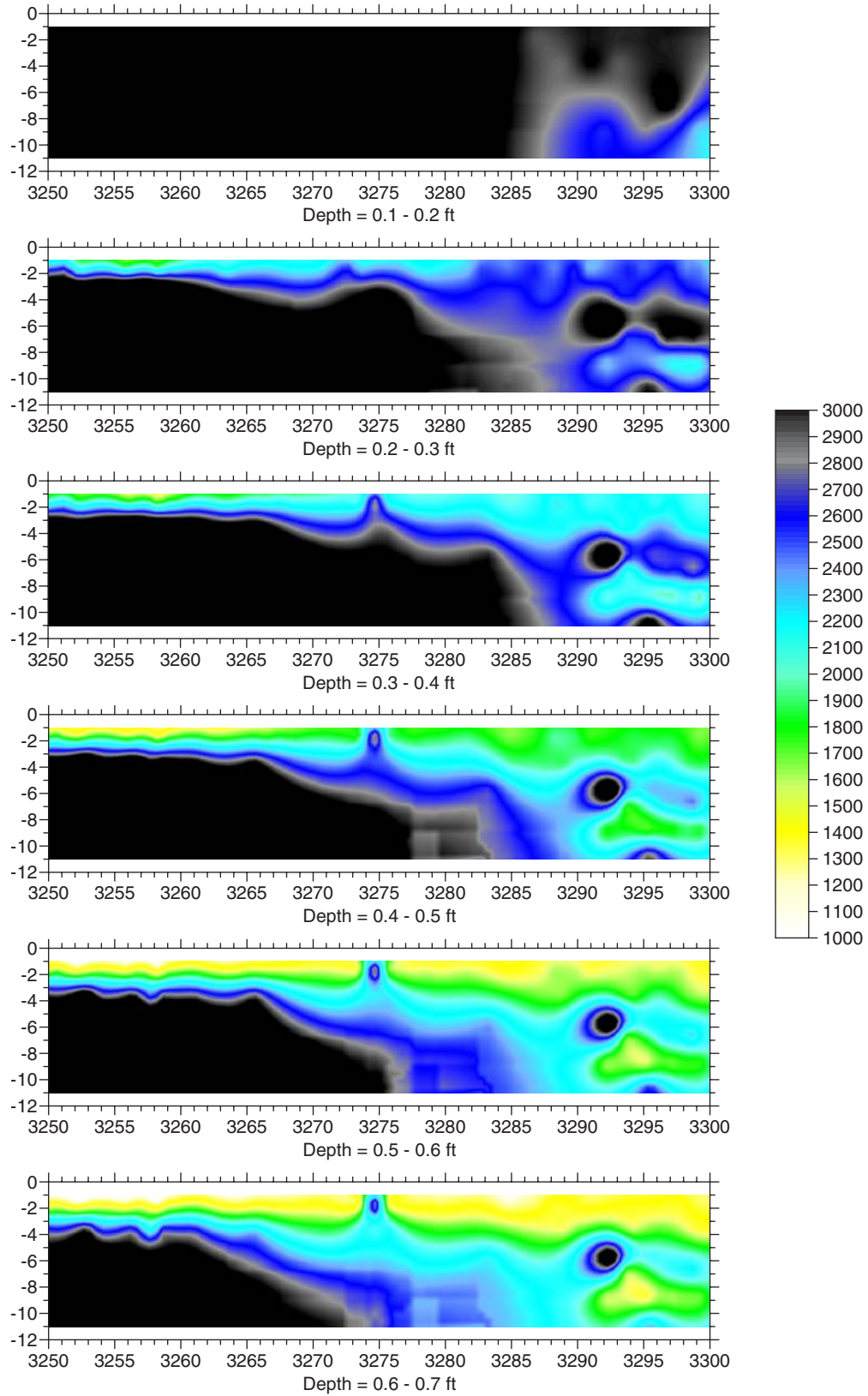
Figure 4.66. Section 3,250 to 3,300.
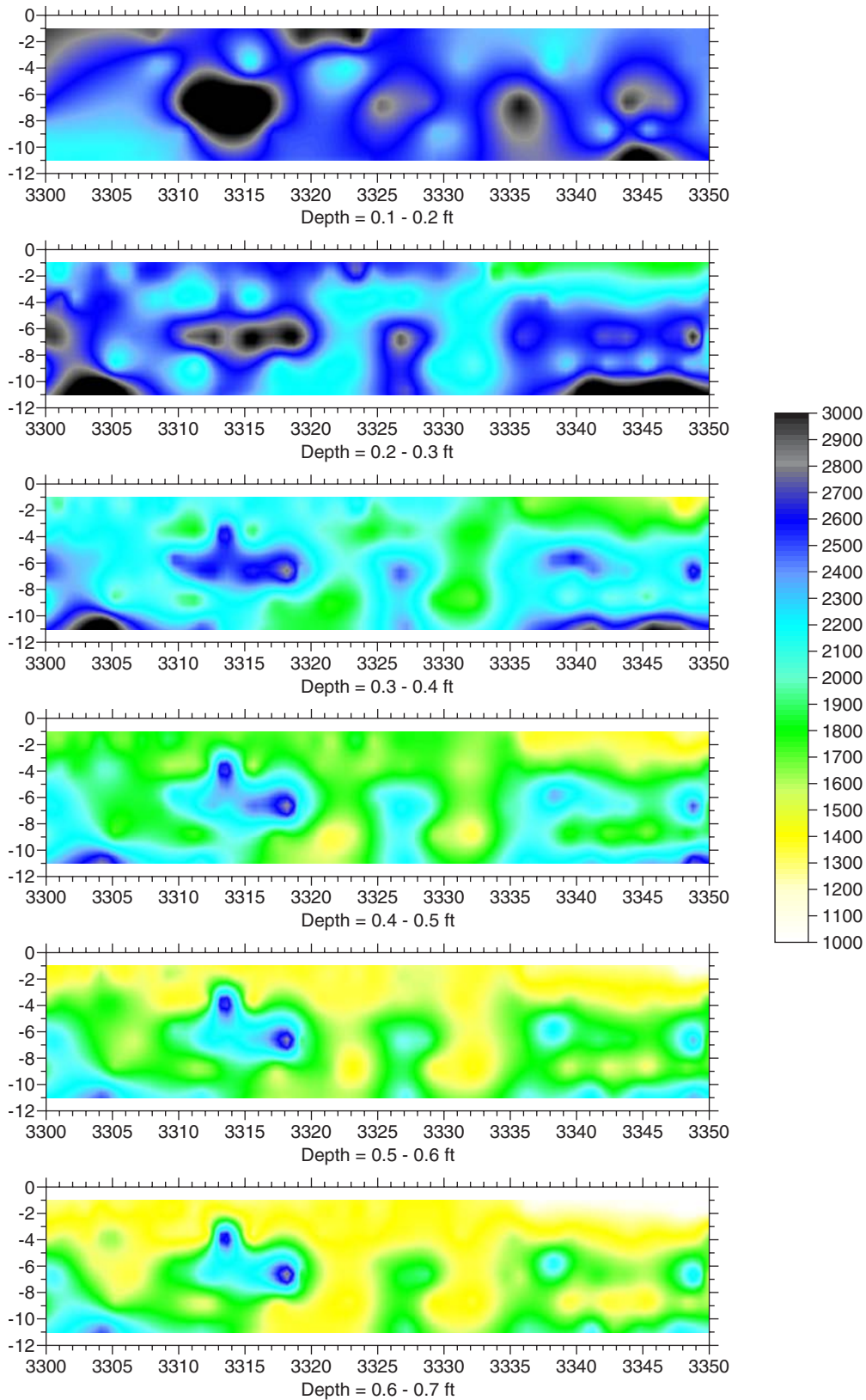
Figure 4.67. Section 3,300 to 3,350.

Figure 4.68. Section 3,350 to 3,400.

Figure 4.69. Section 3,400 to 3,450.
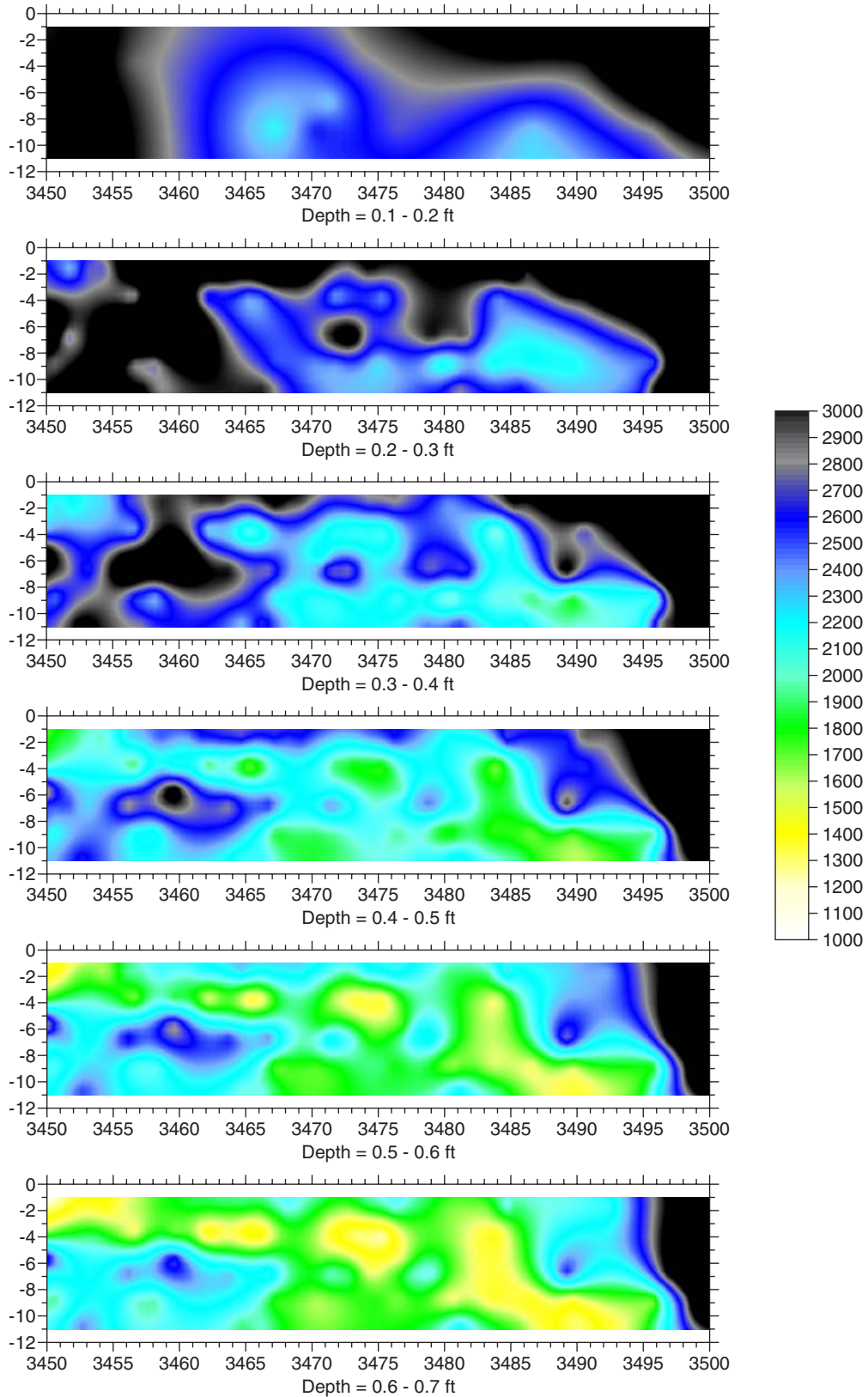
Figure 4.70. Section 3,450 to 3,500.
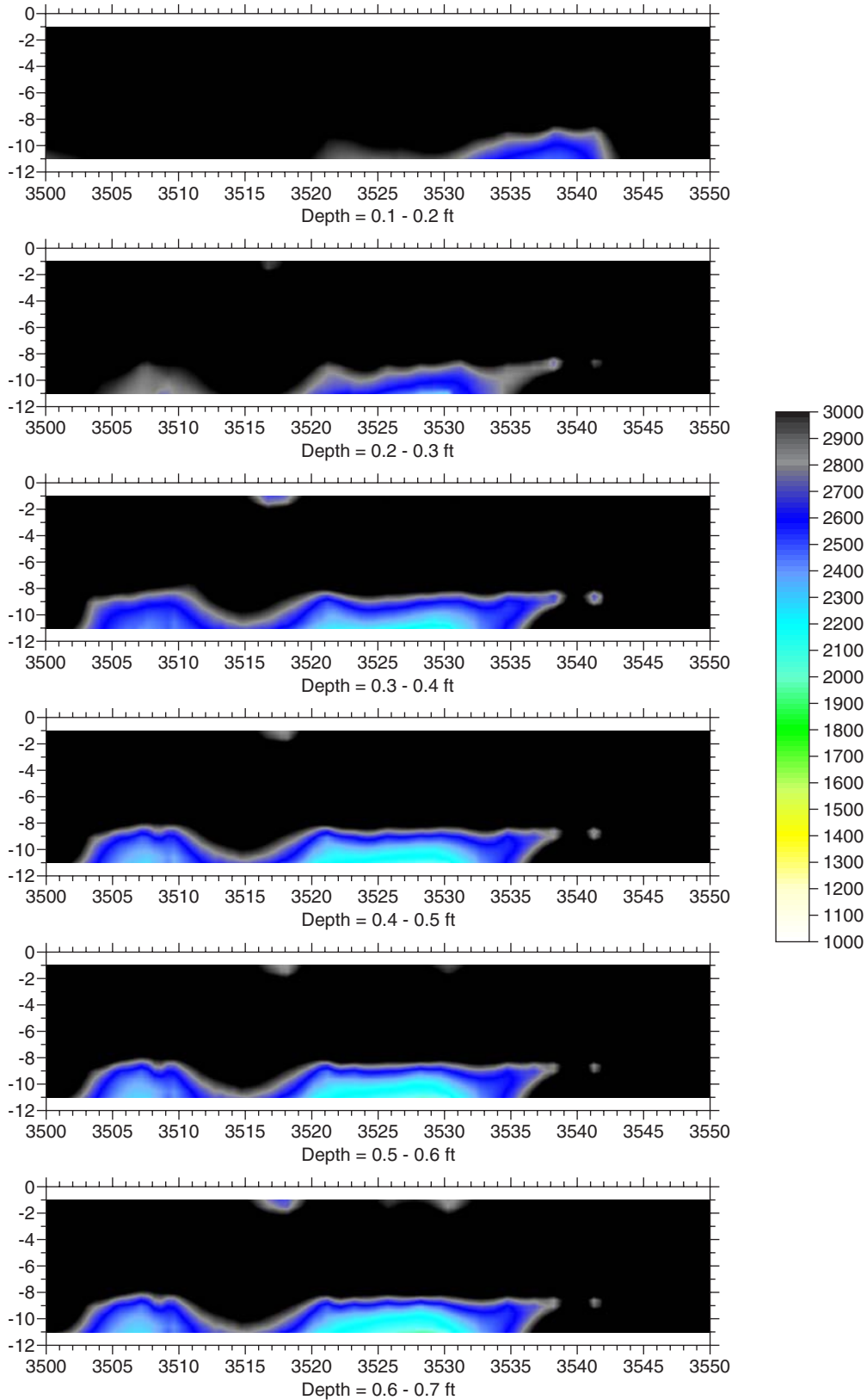
Figure 4.71. Section 3,500 to 3,550.
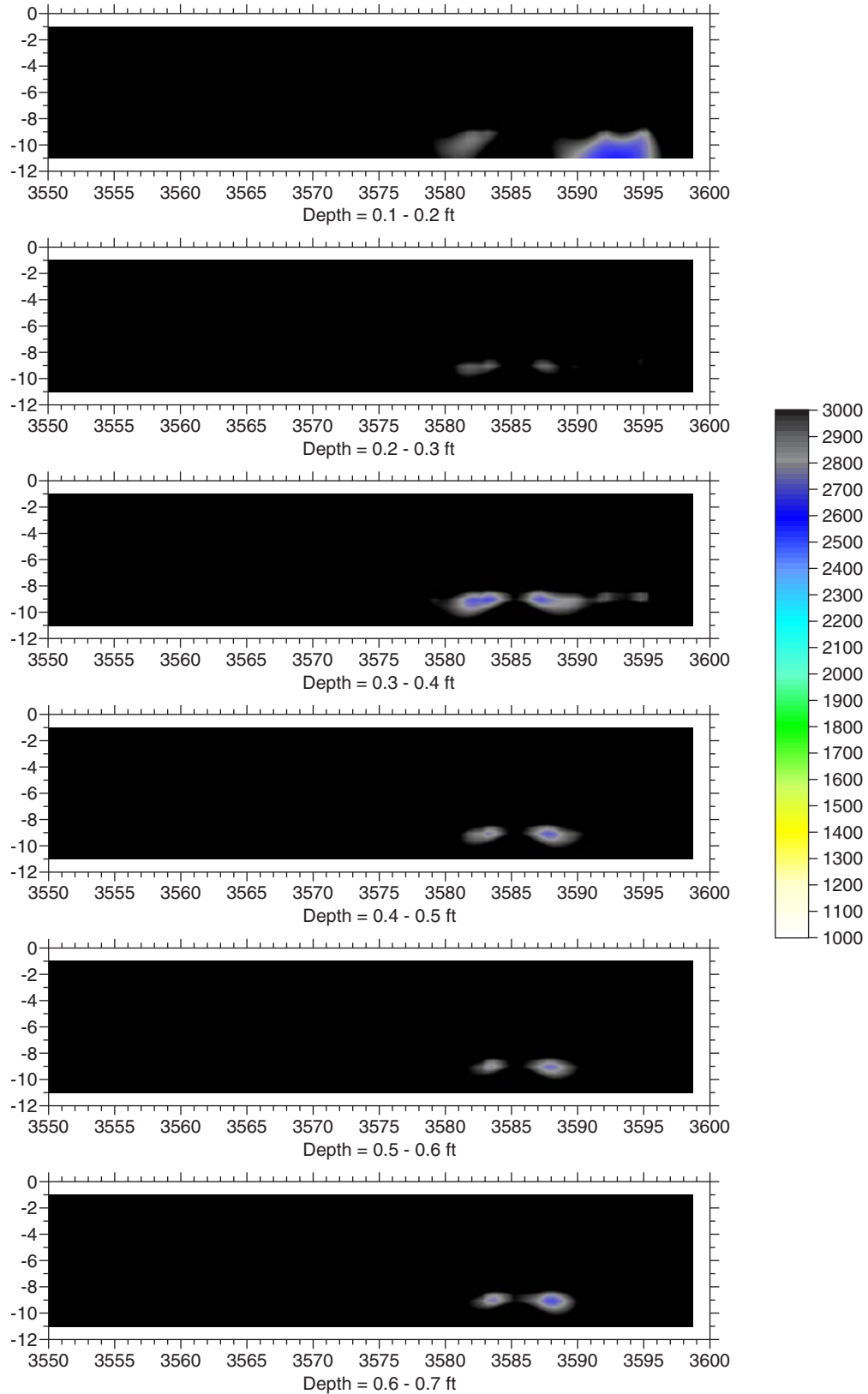
Figure 4.72. Section 3,550 to 3,600.

Related SHRP 2 Research

Nondestructive Testing to Identify Concrete Bridge Deck Deterioration (R06A)

Evaluating Applications of Field Spectroscopy Devices to Fingerprint Commonly Used Construction Materials (R06B)

Using Infrared and High-Speed Ground-Penetrating Radar for Uniformity Measurements on New HMA Layers (R06C)

Real-Time Smoothness Measurements on Portland Cement Concrete Pavements During Construction (R06E)

Assessment of Continuous Pavement Deflection Measuring Technologies (R06F)

Mapping Voids, Debonding, Delaminations, Moisture, and Other Defects Behind or Within Tunnel Linings (R06G)